SYNCHRONIZATION IN CDMA SYSTEMS

Lokesh Bheema Thiagarajan

(*B.Tech, Madras Institute of Technology, India*)

A THESIS SUBMITTED

FOR THE DEGREE OF DOCTOR OF PHILOSOPHY

DEPARTMENT OF ELECTRICAL AND COMPUTER ENGINEERING

NATIONAL UNIVERSITY OF SINGAPORE

2008

to my parents and my brother

Acknowledgements

I am very grateful to have A/Prof. Samir Attallah and Dr. Ying-Chang Liang as my supervisors. Their support and guidance have helped me a lot in pursuing my Ph.D immediately after my undergraduate studies. I wish to thank Dr. Karim Abed Meriam and Dr. Hongyi Fu for giving me their time to discuss my research work and for their collaboration.

I sincerely thank Dr. George Mathew who taught me Adaptive Signal Processing module through which I got a thorough understanding of signals, matrices and subspaces. I would like to thank Mr. Goh Thiam Pheng and Ms. Serene Oe of Wireless Communications lab, who provided help and support in carrying out my research. I express my heartfelt thanks to my friends, especially Dr. Zhang Qi, for lending me their time to discuss on research problems and for their invaluable friendship. I sincerely thank my seniors and my flat mates who made sure that I never felt lonely throughout my stay away from my family during my research. I express my sincere gratitude to National University of Singapore (NUS), for giving me the opportunity to do research and for supporting me financially through NUS Research Scholarship. My special thanks to Institute for Infocomm Research (I^2R) for accepting me as a student member and providing me with the opportunity to participate and discuss in talks given by eminent people from my field of research.

Contents

Summary

In this thesis, a subspace-based blind (non-data-aided) joint carrier frequency offset (CFO) and channel impulse response (CIR) estimator is proposed for uplink carrier frequency synchronization and channel estimation in direct-sequence code division multiple access (DS-CDMA), cyclic-prefix CDMA (CP-CDMA) and multi-carrier CDMA (MC-CDMA) systems. The proposed estimator is formulated by exploiting the orthogonality between the signal and noise subspaces.

The noise subspace used by the estimator is estimated from the received signal. Using the knowledge of the user's spreading code, the signal subspace for the desired user is obtained as a function of CFO and CIR parameters. Through matrix manipulations, the orthogonality between the signal and the noise subspaces can be expressed as a set of L linear equations equated to zero, where L denotes the length of CIR. In other words, if the CFO variable is equal to the user's true CFO value, then the desired user's CIR lies in the null space of a $(L \times L)$ positive semi-definite matrix. This $(L \times L)$ matrix is a function of CFO, noise subspace and desired user's spreading code. The determinant of the above $(L \times L)$ matrix is zero only when the CFO variable is equal to the desired user's true CFO value. Due to the presence of noise and use of finite precision, the determinant is not exactly zero at the desired user's true CFO value. By performing a one dimensional grid search for the CFO variable, the search point which minimizes the determinant of the above defined matrix is taken as the user's estimated CFO value. The CIR is estimated as the eigenvector associated with the minimum eigenvalue of the $(L \times L)$ matrix corresponding to the estimated CFO value.

Using asymptotic approximation for the user's angular CFO variable, a criterion for the selection of users' spreading codes is outlined to ensure that the CFO and CIR parameters are uniquely identifiable. The mean squared error (MSE) performance of the estimator is compared with Cramer-Rao lower bound (CRLB). The cost function used for CFO estimation is analyzed and is shown to be locally convex around the user's true CFO value. This knowledge is used to formulate a low-cost two-stage CFO estimator, where in the first stage a coarse grid search is performed to obtain an approximate CFO estimate. In the second stage, a finer CFO estimate is obtained by using Newton's algorithm initialized with the CFO estimate from the first stage. The convergence of Newton's algorithm is shown through computer simulations. The reduced computational complexity renders the two-stage estimator to be a practical solution for CFO estimation in uplink CDMA systems. The 'linearized' CFO estimator is shown to be unbiased and a theoretical MSE performance corresponding to CFO estimation is also derived. It is observed that the theoretical MSE overlaps with the CRLB. This implies that the proposed estimator can asymptotically achieve the CRLB.

List of Tables

List of Figures

List of Abbreviations

3G	third generation
4G	fourth generation
ACFO	angular carrier frequency offset
ADMM	approximate determinant minimization method
AWGN	additive white gaussian noise
B3G	beyond third generation
BER	bit error rate
BPSK	binary phase-shift keying
CDMA	code division multiple access
CFO	carrier frequency offset
CIR	channel impulse response
CP	cyclic prefix
CP-CDMA	cyclic prefix code division multiple access
CRLB	Cramer-Rao lower bound
DBPSK	differential binary phase-shift keying
DFT	discrete Fourier transform
DS-CDMA	direct sequence code division multiple access
ED	equalization and detection

EDMM	exact determinant minimization method
EVD	eigenvalue decomposition
FDMA	frequency division multiple access
FH-CDMA	frequency hopping code division multiple access
GEVPM	generalized eigenvalue problem method
GPS	global positioning system
HOS	higher order statistics
Hz	hertz
IB	interleaving block
IBI	inter block interference
ICI	inter carrier interference
IDFT	inverse discrete Fourier transform
IS-95	interim standard 95
ISI	inter symbol interference
MAI	multiple access interference
Mb/s	mega bits per second
MC-CDMA	multi-carrier code division multiple access
MC-DS-CDMA	multi-carrier direct-sequence code division multiple access
Mcps	mega chips per second
ML	maximum likelihood
MMSE	minimum mean squared error
MSE	mean squared error
OFDM	orthogonal frequency division multiplexing
P/S	parallel-to-serial
PAPR	peak-to-average power ratio

PLL	phase-locked loop
PN	phase noise
PSTN	public switched telephone network
QoS	quality of service
QPSK	quadrature phase-shift keying
RACE	reconfigurable ACFO and CIR estimator
RCP	remove cyclic prefix
S/P	serial-to-parallel
SB	spreading block
SCCP	single-carrier cyclic prefix
SDMA	spatial division multiple access
SFO	sampling frequency offset
SNR	signal to noise ratio
SS	spread spectrum
SVD	singular value decomposition
TB	transformation block
TH-CDMA	time hopping code division multiple access
TDMA	time division multiple access
VCO	voltage-controlled oscillator
WLAN	wireless local area network

List of Notations

$\mathbf{x}$	denotes column vector
$\mathbf{X}$	denotes matrix
$\mathcal{C}$	set of complex-valued scalars
$\mathcal{C}^N$	set of $(N \times 1)$ complex-valued vectors
$\mathbf{0}_{a \times b}$	$(a \times b)$ dimensional matrix with all elements equal to zero
$(.)^T$	transpose operator
$(.)^H$	conjugate transpose operator
$E[.]$	statistical expectation
$\mathbf{I}_N$	$(N \times N)$ identity matrix
$col(\mathbf{A})$	column space of matrix $\mathbf{A}$
$null(\mathbf{A})$	null space of matrix $\mathbf{A}$
$\star$	convolution operator
$\lfloor . \rfloor$	floor operator
$diag(\mathbf{a})$	returns a diagonal matrix with diagonal elements given by vector $\mathbf{a}$
$\mathbf{Z}_N(\phi)$	denotes $diag\left(\left[1, e^{j\phi}, e^{j2\phi}, \cdots, e^{j(N-1)\phi}\right]^T\right)$
$\mathbf{P}_N(\phi)$	denotes $diag\left(\left[e^{-j\frac{N-1}{2}\phi}, e^{-j\frac{N-3}{2}\phi}, \cdots, e^{j\frac{N-1}{2}\phi}\right]^T\right)$
$det(\mathbf{A})$	return determinant value of the square matrix $\mathbf{A}$
$\otimes$	Kronecker product

$\Vert . \Vert$	l_2-norm
$\odot$	Hadamard product
$\angle\alpha$	returns the phase value of complex scalar α
$\mathbf{T}_{cp}$	matrix to insert cyclic prefix
$\mathbf{R}_{cp}$	matrix to remove cyclic prefix
$rank(\mathbf{A})$	return rank of matrix $\mathbf{A}$
$\mathbf{W}_N$	N-point DFT matrix
$[\mathbf{x}]^{(l)}$	circular shifting the elements in vector $\mathbf{x}$ by l times
$[\mathbf{X}]^{(l)}$	circular shifting every column vector in $\mathbf{X}$ by l times
$(.)_r$	denotes real part of (.)
$(.)_i$	denotes imaginary part of (.)
$\circ$	circular convolution operator
$tr(\mathbf{A})$	returns trace of matrix $\mathbf{A}$
$adj(\mathbf{A})$	denotes adjoint of matrix $\mathbf{A}$
$\lceil . \rceil$	ceil operator
$\mathbf{A}(a:b, x:y)$	submatrix obtained from matrix $\mathbf{A}$ by extraction rows a to b and columns x to y
$\mathbf{A}(:, x)$	returns xth column vector of matrix $\mathbf{A}$
$\mathbf{A}(x, :)$	returns xth row vector of matrix $\mathbf{A}$
$[\mathbf{A}]_{x,y}$	returns the element in xth row and yth column of matrix $\mathbf{A}$

Chapter 1

Introduction

The radio communication link between mobile transceivers established by Marconi in 1897 [1] demonstrated that communications need not be limited to transceivers tethered by wires. In 1946, the first mobile telephone system was introduced to the public [2]. Since then, advances in wireless communication technology together with the realization of compact energy efficient digital and radio frequency circuits have made wireless transceivers available to about 50% of the world's population. The reduced implementation cost for wireless transceivers has resulted in ever growing numbers of users and their need for higher data rates and value added services lead to scarcity of available spectrum.

In order to reuse the available limited spectrum and cater for the geographically scattered users, the concept of cellular communication was introduced [1]. In cellular communication systems, the geographical area is divided into cells with small area. Every cell has a base station serving the users located within that particular cell. The base stations are connected to a mobile switching center. Further details on cellular communications can be found in [1] [3]. The transmissions in a cellular system can be classified as either uplink (reverse link) transmission or downlink (forward link) transmission [4]. In the uplink or reverse link transmission, the mobile terminal transmits its information to the base station. In the downlink or forward link, the base station transmits the data to the mobile terminals. A pictorial representation of a cellular system describing the uplink and downlink scenario is shown in Fig. 1.1. The following section outlines the multiple

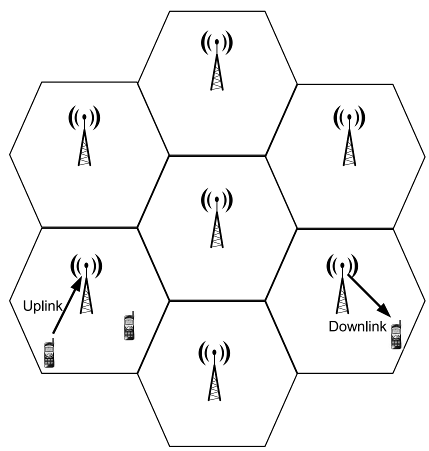

Fig. 1.1: Cellular System

access schemes developed to cater for the needs of the users' by efficiently using the available limited resources.

1.1 Multiple Access Schemes

Multiple access schemes enable sharing of the available finite spectrum resources among several mobile user terminals. It improves system capacity[1] and efficient spectrum utilization [1]. The major multiple access schemes available are [2] [5]:

1. FDMA – Frequency division multiple access
2. TDMA – Time division multiple access
3. CDMA – Code division multiple access
4. SDMA – Spatial division multiple access

or combination thereof.

The spectrum is shared among the users by assigning to each user an independent frequency band, time slot, spreading code or spatial signature.

FDMA

In a system with T users and available spectrum BHz, the spectrum is divided into narrow bands of bandwidth B/THz[2]. Every user is assigned to a specific frequency band. The concept of FDMA is pictorially illustrated in Fig. 1.2.

TDMA

The available spectrum is accessed by all users but each user can access the available spectrum only at specific time intervals. Fig. 1.3 illustrates TDMA

[1]The data rate with a certain quality of service (QoS) and the number of users supported by the system gives a measure for system capacity.

[2]The spectrum division need not be equal.

scheme.

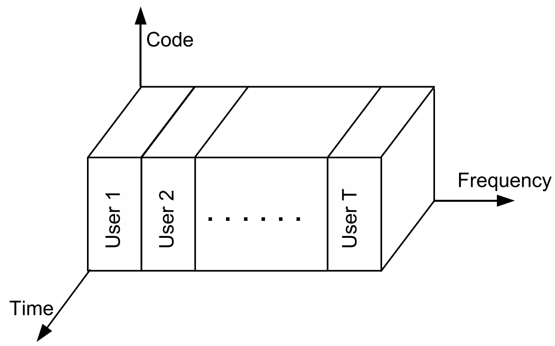

Fig. 1.2: FDMA

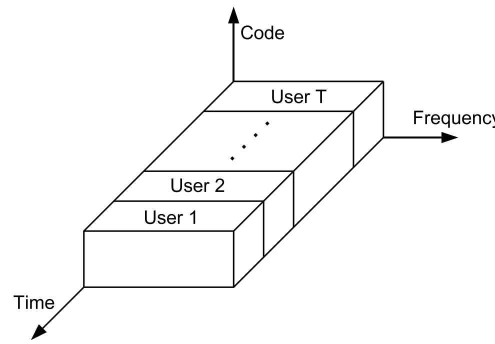

Fig. 1.3: TDMA

CDMA

The entire available spectrum is accessed by all users simultaneously at any point of time. The separation of users is done by spreading (encrypting) the user's data using a user specific spreading code. The pictorial illustration of CDMA concept is shown in Fig. 1.4.

SDMA

In SDMA, the spatial separation of users is exploited. Through the use of "smart" directional antennas the interference between the users is minimized. The separation of users using directional antennas is shown in Fig. 1.5.

A comparison of TDMA, FDMA and CDMA multiple access schemes is provided in [6]. TDMA and FDMA are limited by the available bandwidth, i.e., the number of users supported for a given bandwidth is fixed in TDMA and FDMA schemes. CDMA, on the other hand, is limited by multiple access interference

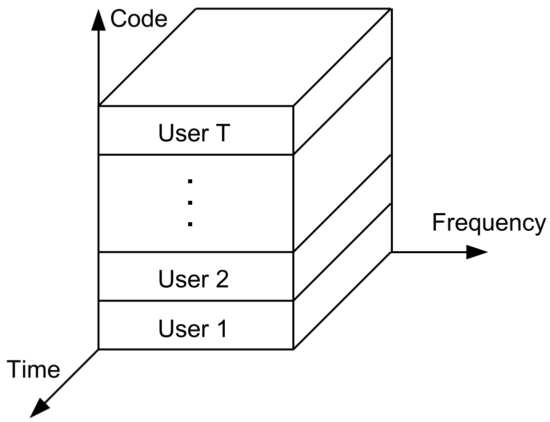

Fig. 1.4: CDMA

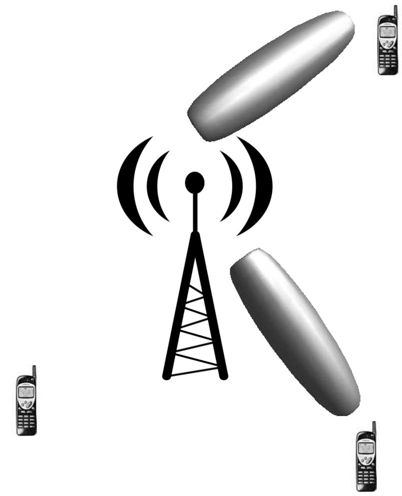

Fig. 1.5: SDMA

(MAI). As the number of users increases, the performance of the CDMA system degrades. Therefore, there is a trade-off between the number of users and the QoS that can be provided by the CDMA system. It is to be noted that, the capacity of CDMA systems can be improved [7] by substantially mitigating the effects of MAI [8]-[11] using the knowledge of the users' spreading codes and their associated multipath fading channel. The improved capacity, simultaneous spectrum sharing capability and inherent resistance to jamming, interception and multipath propagation effects [12] have led CDMA to be used in third generation (3G) standards [13] [14] and being proposed for fourth generation (4G) systems. Due to the above mentioned advantages, this thesis focuses on CDMA systems.

1.2 CDMA Systems

The basis of CDMA is spread-spectrum (SS) technology. SS is the joint outcome of developments in high-resolution radars, direction finding, guidance, interference rejection, jamming avoidance, information theory and secured communications [12] [15]. This technology was originally developed and used for military applications. In SS systems, a pseudo-random code is used to 'spread' the information signal to the allocated frequency bandwidth [16]. The spread signal can only be interpreted by that receiver which has the code used for spreading.

SS systems were first proposed for civilian mobile communications by Qualcomm Inc. in 1989 [12]. Each user's transmitter is allocated with a specific pseudo-random spreading code and the corresponding receiver has the same spreading code. Thus, the SS system was transformed into a multiuser wireless communication system. As the users were separated by means of user specific spreading codes, this multiple access technique was termed as CDMA. Based on the type of spreading technique used, CDMA systems can be classified as follows [16] [17]:

1. DS-CDMA – Direct-sequence CDMA
2. FH-CDMA – Frequency hopping CDMA
3. TH-CDMA – Time hopping CDMA
4. Hybrid CDMA
   (a) CP-CDMA – Cyclic-prefix CDMA
   (b) MC-CDMA – Multi-carrier CDMA
   (c) MC-DS-CDMA – Multi-carrier direct-sequence CDMA

In DS-CDMA, spreading code with bandwidth wider than that of the information signal is used to modulate the information signal directly. For FH-CDMA, the transmission bandwidth is divided into several frequency sub-bands. The spreading code is used to select the sub-band in which the information signal needs to be transmitted. The sub-band is periodically changed according to the spreading code. In TH-CDMA, the transmitted signal is rendered to occupy a large bandwidth by transmitting the information signal in short time bursts. The spreading code determines the start time of the short burst. Hybrid CDMA techniques are derived by combining one or more CDMA techniques with other transmission techniques. CP-CDMA is derived by combining DS-CDMA and cyclic prefixing technique. MC-CDMA is derived by combining CDMA and orthogonal frequency division multiplexing (OFDM) techniques together. CP-CDMA and MC-CDMA systems will be discussed in detail in our thesis. MC-DS-CDMA systems employ OFDM in combination with time domain spreading.

DS-CDMA based transmission is currently used in 3G systems. CP-CDMA systems are also considered for 3G and beyond 3G (B3G) systems [18]. Adaptive modulation based MC-CDMA systems are being proposed for fourth generation (4G) systems [19] in order to support 100Mb/s data rate [20]. Therefore, our research work mainly focuses on DS-CDMA, CP-CDMA and MC-CDMA systems which have the potential to become future wireless communication systems' air interfaces.

DS-CDMA

The user spreading code is a random sequence of values, usually $+1$ or -1. Gold sequences, m-sequences and Kasami sequences are some of the spreading codes used in DS-CDMA [16]. Let G denote the length of the spreading code. The spreading signal is obtained by modulating each of the G values in the code on to a chip-pulse. For example, Fig. 1.6 illustrates the spreading signal when the spreading code is $\{+1/\sqrt{5}, -1/\sqrt{5}, +1/\sqrt{5}, +1/\sqrt{5}, -1/\sqrt{5}\}$ and rectangular pulse of duration T_c is used as the chip-pulse. The modulation of data symbol using the

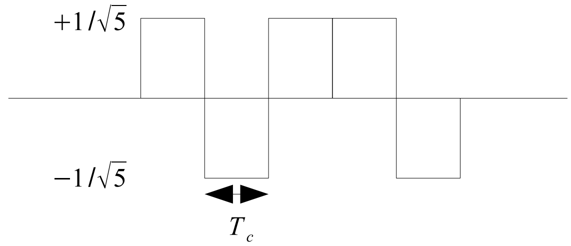

Fig. 1.6: Spreading signal.

spreading signal is shown in Fig. 1.7. The bandwidth of the spreading signal is

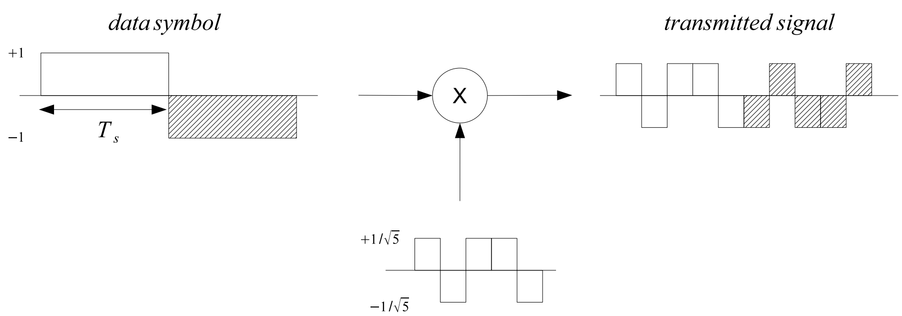

Fig. 1.7: DS-CDMA Transmitter.

$1/T_c$ Hz and that of the data signal is $1/T_s$ Hz. The bandwidth expansion factor defined as T_s/T_c is also equal to G and is called the system's spreading gain. The capacity, multiuser detection and bit error rate (BER) performance of DS-CDMA systems have been addressed in the literature, for example [8]-[11] [21]-[24].

CP-CDMA

CP-CDMA, first introduced in [25], is a hybrid of single-carrier cyclic prefix (SCCP) [26] [27] and DS-CDMA systems. That is, a cyclic prefix of suitable length is augmented to the signal obtained after modulating the data on to the spreading signal. The inter symbol interference (ISI) caused by the multipath fading channel can be eliminated by selecting the length of cyclic prefix to be greater than the delay spread of the multipath fading channel. After the removal of cyclic prefix at the receiver, the resulting channel matrix is circulant. This circulant channel matrix can be transformed into a diagonal matrix using discrete Fourier transform (DFT) and inverse discrete Fourier transform (IDFT) matrices [28]. The diagonal matrix renders a simple one tap frequency domain channel equalization for CP-CDMA systems. Detailed description of CP-CDMA system, retrieval of data from the received CP-CDMA signal, channel estimation and MAI cancelation have been presented in [29] [30].

MC-CDMA

The amalgamation of OFDM and CDMA systems led to the birth of MC-CDMA system [31], combining the benefits of both OFDM and CDMA. The fundamental principle of OFDM originates from [32] and the detailed description and analysis of OFDM system can be found in [33]-[39]. In an MC-CDMA system, the samples obtained after spreading the data symbols are transmitted on the orthogonal subcarriers instead of directly transmitting the data symbols as in OFDM. Though MC-CDMA systems reap the combined benefits from OFDM and CDMA, they also inherit the drawbacks in OFDM and CDMA. For example, MC-CDMA systems are sensitive to frequency offset, suffer from peak-to-average power ratio (PAPR) [40] [41] and their performance is limited due to inter carrier interference (ICI) and MAI.

In the following section, the types of synchronization in wireless communication systems and their significance are discussed.

1.3 Synchronization

Synchronization in any wireless communication system is essential for proper data transmission at the transmitter and proper data detection at the receiver [5]. The transmitter and receiver are said to be synchronized if they coordinate to operate in unison. Based on the system parameter in unison, synchronization can be broadly classified as follows:

1. Time synchronization – The transmitter and the receiver are said to be time synchronized if the receiver is able to identify the start of symbol in the received signal.

2. Frequency synchronization – If the local oscillators (carrier frequency oscillator and sampling frequency oscillator) at the transmitter and receiver have the same oscillation frequency then the transmitter and receiver are said to be frequency synchronized.

3. Carrier phase synchronization – If the carrier frequency oscillator at the transmitter and receiver have the same phase offset then the transmitter and receiver are said to be phase synchronized.

1.3.1 Time Synchronization

Time synchronization is essential in CDMA systems in order to identify the start of the transmitted symbol at the receiver. In this thesis, the uplink transmission in DS-CDMA, CP-CDMA and MC-CDMA systems are assumed to be quasi-time synchronous. In other words, the received signal from all users arrive at the base station within a fraction of the chip-pulse duration [42]. In IS-95 and CDMA2000 [13] standards for CDMA systems, time synchronization is achieved by using global positioning system (GPS) as an external time reference. The base stations are synchronized with the GPS clock and the mobile terminals align their timing to the base station with which they are associated [43]. As the users are located at different distances from base station, the users' transmitted signals may not reach the base station at the same time instant but can only reach within the chip-pulse duration resulting in quasi-time synchronization. Therefore, perfect time synchronization may not be possible in the uplink. Thus, assuming the uplink to be quasi-time synchronous is practically valid. In the rest of this thesis, quasi synchronous refers to quasi-time synchronous transmission.

1.3.2 Frequency Synchronization

Mismatch between the oscillation frequency of the oscillators at the transmitter and receiver could occur due to Doppler shift, crystal imperfections and environmental changes [44] [45]. This mismatch can be classified based on the oscillator with which the mismatch is associated as

1. Carrier frequency offset (CFO)
2. Sampling frequency offset (SFO)

1) CFO

The mismatch in the oscillation frequency of the carrier frequency oscillators at the transmitter and receiver leads to CFO. The CFO distorts the phase of the received signal samples. The data symbols cannot be detected properly at the receiver if the phase rotation introduced by the CFO is not corrected. In the uplink transmission, each user has an independent carrier frequency oscillator. After frequency down conversion at the receiver, the CFOs distorting the received signal corresponding to each user are independent. Therefore, the base station should compensate for each user's CFO individually [46] in order to properly detect the transmitted data. The base station has only one local oscillator and hence it is not possible to synchronize the base station to every independent user. Furthermore, the received signal in the uplink is a summation of all the users' transmitted signal and hence compensation for each individual user's CFO at the base station is not possible. However, the base station can estimate each user's CFO and provide this information to mobile terminals using the downlink transmission channel. The mobile terminals can then adjust their local oscillator's frequency to synchronize with the base station's local oscillator [44]. Even then, the frequency synchronization may not be accurate and each user signal component at base station will have a residual CFO. In this thesis, we addresses the problem of obtaining the residual CFO estimates at the base station using the received signal and *a priori* knowledge on signal structure.

2) SFO

The SFO is caused by the mismatch between the sampling clock at the transmitter and receiver. This mismatch could result in symbol window drift at the receiver leading to erroneous data detection. In the presence of CFO, the SFO induces phase rotation in the received samples [45]. The longer the length of the frame being transmitted, the more severe would be the effects of SFO [47]. In this thesis, we consider the absence of SFO. In other words, the SFO is considered to be too small that it does not have any notable impact on the system's performance for the given signal to noise ratio (SNR).

1.3.3 Carrier Phase Synchronization

The carrier frequency is controlled by a phase-locked loop (PLL) which consists of a voltage-controlled oscillator (VCO) [5]. The oscillation frequency is controlled by the voltage input to the VCO. The sinusoidal output from the VCO can be expressed as $e^{j2\pi f_c t+\theta(t)}$. The carrier frequency f_c is controlled by the voltage input and $\theta(t)$ is the phase offset or phase noise which varies with time. Using the power spectral density of the VCO output, the phase noise (PN) $\theta(t)$ can be modeled as a Wiener process or Gaussian process as shown in [48]. As PN is a random process, each symbol duration has a different set of PN samples. Hence the PN estimate for one symbol duration cannot be used for subsequent symbol duration. In [49], an iterative detector for OFDM system was proposed where the soft estimates for data symbols and PN were iteratively obtained using variational inference. We assume that the PN is much smaller than the CFO. Thus, we model the system in the absence of PN. Therefore, we estimate only the time-invariant parameters (parameters which remain unchanged for the entire frame duration).

1.4 Research Objective

Section 1.3 outlined the significance of synchronization in wireless communication systems. It also pointed out that our main focus in synchronization will be on CFO estimation without using pilot/training symbols. In the following, we logically formulate the research objective of this thesis.

In downlink scenario of any CDMA system, the base station is the only source for all the users' signals and hence the downlink transmission is time synchronized among users. The signal transmitted from the base station propagates through a multipath fading channel and reaches the mobile terminal. The mismatch in the oscillation frequency of the carrier frequency oscillators at the base station and mobile terminal induces CFO to all the users' signals received by the mobile terminal. The received signal at the mobile terminal is the aggregate of all users' signal convolved with a single multipath fading channel and phase rotated by a single CFO. In other words, there is only one pair of multipath fading channel and CFO to be estimated at the receiver in the downlink scenario. The mobile user in most cases is battery operated and hence has limited power. This constraint leads to use of simple pilot/training symbols based estimators for CFO and channel estimation. These estimators are called data-aided or pilot symbol assisted estimators.

In the uplink scenario, the transmitted signal from each user propagates through a multipath fading channel before reaching the base station. The received signal at the base station is the aggregate of each user's transmitted signal convolved with the multipath fading channel and phase rotated by CFO corresponding to that user. That is, every user in the uplink transmission has an independent pair of multipath fading channel to be equalized and CFO to be compensated. As the number of users increases, the parameters to be estimated also increases. Therefore, CFO and channel estimation in the downlink is simpler compared to uplink. Thus, estimating CFO and channel in uplink transmission is much more challenging.

The performance of DS-CDMA in the presence of Doppler shift and CFO was studied in [50]. In [50], the BER was observed to be significantly higher for large CFO even when the channel was estimated using pilot symbols. The effects of CFO on the performance of CP-CDMA systems are the same as that on DS-CDMA systems.

The core idea in OFDM systems is to transmit data over orthogonal subcarriers. The orthogonality of subcarriers leads to a simple one tap frequency domain channel equalization at the receiver. However, the presence of CFO destroys the orthogonality of the subcarriers [45] and hence the channel equalization cannot be done using a single tap equalizer. Furthermore, detecting the data symbols without compensating for the ICI caused by CFO in OFDM increases the system's BER. If N is the number of subcarriers in an OFDM system, then the BER performance of multi-carrier system was shown to be N times more sensitive to CFO than the single-carrier system [51]. The BER performance of OFDM system in the presence of CFO and multipath fading channel was analytically evaluated in [52]. This analytic BER expression (derived using the Gaussian approximation for ICI caused by CFO) confirmed the degradation in BER with the increase in CFO. Similar BER analysis done in [53] [54] also emphasized OFDM's sensitivity to CFO. The MC-CDMA system derived by combining OFDM and CDMA systems inherits the CFO sensitivity from OFDM. In the presence of CFO, MC-CDMA system suffers from both ICI and MAI (due to multiple users). The performance analysis carried out in [55]-[60] clearly shows that the CFO, if not properly compensated, increases the BER of MC-CDMA system. For proper detection, the multipath channel must also be equalized at the receiver [61] [62] and hence the receiver must obtain an accurate estimate for the channel. Thus, the estimation error in CFO and multipath fading channel estimates have a significant impact on the system's performance and hence the need for accurate CFO and channel estimator.

Assuming the absence of CFO, channel estimator for uplink DS-CDMA system was proposed in [63] using Kalman filter [64]. The Kalman filter requires an auto-regressive model for the channel and uses pilot symbols for the estimation. In scenarios where auto-regressive channel model was not available, [65] proposed a channel estimator based on least mean squares algorithm. Channel tracking was made possible in [65] by employing weighted least mean squares algorithm. A channel estimator similar to that in [65] was proposed for MC-CDMA uplink in [66]. The channel estimators in [67] [68] used pilot symbols to obtain the frequency domain channel estimates for MC-CDMA uplink. In [69], a unique channel estimator was proposed for uplink MC-CDMA system where only one pilot symbol per frame was used to obtain the initial channel estimate. The detected data symbols were used as pseudo pilots to get accurate channel estimate. For each symbol detection in the frame, the channel and data estimates corresponding to the previous symbol were used to construct the MAI and cancel it out from the current symbol. However, [69] assumes the absence of CFO and the initial channel estimate could be erroneous when the number of users is large. A similar type of channel estimator based on interference cancelation technique was proposed for CP-CDMA system in [70]. In the presence of CFO, channel and CFO estimator using pilot symbols has been proposed in [71] [72]. In [72], except the new user entering the uplink DS-CDMA system, the existing uplink users are assumed to be synchronized, i.e., the existing users have no CFO and their channel estimates are accurately known to the base station. Using the above assumption along with suitably constructed pilot symbols, a sub optimal linear unbiased estimator exploiting the correlation in the received signal was proposed to estimate the new user's CFO. A similar CFO estimator for uplink MC-CDMA system was proposed in [71]. The main drawback in above estimators is that the assumption of only one new user entering the system while the other existing users being synchronized may not be practical. As outlined earlier, the number of parameters to be estimated in the uplink is proportional to the number of users. Thus, the number of pilot symbols used for estimation increases with the increase in the number of users. The use of pilot symbols reduces system's throughput, power efficiency and utilization of allocated spectrum [73] [74]. Thus, there is an immense interest in the use of non-pilot based estimators for CFO and channel estimation. These estimators are called "blind" or "non-data-aided" estimators because the joint CFO and CIR estimation is done without transmitting any pilot/training symbols but using the received signal and the knowledge of signal structure.

Blind estimators are formulated based on any one of the following concepts:

1. Utilizing the orthogonality between the signal and noise subspace [75].

2. Exploiting certain structure in the signal (example virtual pilots) [76].

3. Using higher order statistics (HOS) [64] of the received signal.

Assuming the absence of CFO, blind channel estimators have been formulated for DS-CDMA systems in [77]-[82]. In [78], a blind channel estimator for uplink DS-CDMA system was proposed by matching the signal correlation statistics. Channel estimation using cumulant-based inverse filtering criteria, a HOS based estimator, was outlined in [79]. In [81], the channel estimator was formulated by exploiting the orthogonality between the signal subspace and noise subspace. A semi-blind channel estimator was developed in [82] by properly combining the cost functions for training based estimator and blind estimator. In [75], a blind channel estimator exploiting the subspace orthogonality concept was formulated for a generalized system model. These proposed blind channel estimators cannot be used in the presence of CFO.

In the presence of CFO, joint estimation of CFO and channel has been shown to be advantageous [83]. However, this joint estimation for CDMA systems has received much less attention [84] [85]. The blind joint CFO and channel estimator in [84] for DS-CDMA system was formulated based on orthogonality between the signal and noise subspaces. The orthogonal property of subspaces was used to convert the multiuser estimation problem into single user problems which can solved independently. The single user parameters were then estimated using polynomial matrix projection property. The polynomial matrix projection involved the computation of a polynomial matrix inverse. This rendered the estimator in [84] to be computationally demanding. In [85], the CFO was blindly estimated as a solution to generalized eigenvalue problem [86] and the channel was estimated as the eigenvector corresponding to minimum eigenvalue of a matrix. The cost function used in [85] was also derived based on the orthogonality between the signal and noise subspaces. The generalized eigenvalue problem method (GEVPM) based estimator was constructed using Taylor's series approximation for the complex sinusoid containing the CFO term in the cost function. As no matrix inversion was involved, the computation complexity was less in [85] when compared to that in [84]. However, the GEVPM based estimator can estimate only small CFO values as the Taylor's series approximation is accurate only for small CFO values.

Blind CFO estimators for OFDM system can be found in [87]-[90]. Most of the blind CFO estimators proposed for OFDM exploit the presence of virtual carriers also called null subcarriers [87] [89]. Virtual carriers or null subcarriers are the subcarriers of a multi-carrier system on which zeros are transmitted. CFO estimator formulated based on minimizing the ICI caused by CFO can be found in [90]. Assuming the transmitted data symbols to be from a circularly symmetric complex source, the CFO was blindly estimated in [91] by minimizing the kurtosis [92] of the received signal.

It is to be noted that OFDM is a single user system and hence there is no MAI, but MC-CDMA derived from OFDM and CDMA is a multiuser system where MAI is inevitable. The presence of MAI prevents the use of CFO estimators proposed for OFDM system to be used in MC-CDMA uplink. However, some of the blind CFO estimators proposed for OFDM system can be used for MC-CDMA downlink. Blind joint CFO and channel estimator for downlink transmission in MC-CDMA system has been formulated in [93]-[95]. There is very little study on joint CFO and channel estimation in the uplink transmission of MC-CDMA system. In [74], a blind CFO estimator was proposed for the uplink transmission in MC-CDMA system. However, [74] assumes the channel gains for all the subcarriers in the MC-CDMA system to be the same [88]. Thus, the assumption in [74] is not practically valid and hence the estimator cannot be applied in practical multipath fading channels. This justifies the need for a complete formulation of blind joint CFO and channel estimator for MC-CDMA uplink.

Therefore, the main objective of this thesis is to solve the problem of carrier frequency synchronization and channel estimation in the uplink transmission of DS-

CDMA, CP-CDMA and MC-CDMA systems by formulating a blind joint CFO and channel estimator. The main concern in any blind estimator is the identifiability of the estimates. The parameters are said to uniquely identified if the estimates are equal to their corresponding true values. In the absence of CFO, conditions to guarantee channel identifiability were discussed in [75]. Joint CFO and channel identifiability has not been studied in the literature for CDMA systems. In this thesis, we formulate the necessary conditions which asymptotically ensures the CFO and channel to be uniquely identifiable.

1.5 Contributions

In this thesis, a blind subspace-based joint CFO and channel estimator is proposed for the uplink transmission of DS-CDMA, CP-CDMA and MC-CDMA systems. The blind estimator is formulated by exploiting the orthogonality between the signal and noise subspaces. The CFO for the desired user is estimated by performing a one dimensional grid search with the objective of minimizing the determinant of some positive semi-definite matrix. The search point which minimizes the determinant is taken as the CFO estimate. The channel impulse response (CIR) is estimated as the eigenvector associated with the minimum eigenvalue of the positive semi-definite matrix corresponding to the estimated CFO value. This estimator is called exact determinant minimization method (EDMM) based estimator. To reduce the computational complexity, Taylor's series is used to approximate the positive semi-definite matrix in EDMM with a polynomial matrix. The coefficients of the polynomial matrix were computed only once before the start of the grid search. For each search point, only the polynomial matrix was evaluated.

This reduced the computational complexity when compared with EDMM based estimator. The above estimator is called approximate determinant minimization method (ADMM) based estimator. Through computer simulations, the proposed estimators (EDMM and ADMM) were shown to have better performance than the GEVPM based estimator.

Subspace-based joint CFO and CIR estimator for uplink transmission in CP-CDMA and MC-CDMA systems is formulated similar to the EDMM based estimator. The rich signal structure available in CP-CDMA and MC-CDMA systems was well exploited by the estimator. Through proper selection of spreading codes, the signal subspace dimension can always be guaranteed to be independent of the user's CFO and CIR values. To the authors' best knowledge, this result is not available in the literature. In any subspace-based estimator, the proof for identifiability of estimates is challenging. In the absence of CFO, the conditions to guarantee the identifiability of CIR estimates obtained from subspace-based estimators is available in the literature, see [75] [96]-[98] and references therein. To the authors' best knowledge, the identifiability conditions for joint CFO and CIR estimation are not available in the literature. In this thesis, it is shown that proper selection of users' spreading codes can asymptotically[3] guarantee the identifiability of CFO and CIR. Through computer simulations, the mean squared error (MSE) performance of the proposed estimator is shown to be close to Cramer-Rao lower bound (CRLB). Unlike the estimator in [74], the proposed estimator is formulated without assuming the channel gains of subcarriers to be equal. Besides, the estimator proposed is shown to outperform the one in [74].

The cost function used for CFO estimation is shown to be locally convex

[3]For high SNR and large spreading gain.

around the true CFO value. This knowledge is exploited by the proposed two-stage CFO estimator. In the first stage, a grid search with a large grid size is used to quickly lock into the local convexity region of the cost function. The coarse estimate from the first stage is used as the initial value for the Newton's algorithm in the second stage. The Newton's algorithm obtains the fine CFO estimate. This two-stage estimator has a low computational complexity when compared with EDMM based estimator and hence is a potential candidate for practical implementation. Using the first order perturbation analysis results for the noise subspace estimate, the proposed linearized estimator is shown to be unbiased. A theoretical MSE for the proposed linearized estimator is also derived and verified through computer simulations.

1.5.1 Publications

The contributions in this thesis have been published or accepted for publication as listed below:

Journals

[$J1$] S. Attallah, L. B. Thiagarajan, H. Fu and Y.-C. Liang, "Joint channel and carrier offset estimation for synchronous uplink CDMA systems," *IEEE Trans. Veh. Technol.*, vol. 56, pp. 2769-2774, Sept. 2007.

[$J2$] S. Attallah and L. B. Thiagarajan, "A comment on "Blind maximum likelihood CFO estimation for OFDM systems via polynomial rooting"", *IEEE Signal Process. Lett.*, vol. 14, pp. 291-291, April 2007.

[$J3$] L. B. Thiagarajan, Y.-C. Liang and S. Attallah, "Reconfigurable transceivers for wireless broadband access schemes," *IEEE Wireless Commun. Magazine*, vol. 14, no. 3, June 2007.

[$J4$] L. B. Thiagarajan, S. Attallah, K. Abed-Meraim, Y.-C. Liang and H. Fu, "Non-data-aided joint carrier frequency offset and channel estimator for uplink MC-CDMA systems," *accepted for publication in IEEE Trans. Signal Process. in 2008.*

Conferences

[$C1$] S. Attallah, L. B. Thiagarajan, H. Fu and Y.-C. Liang, "A joint carrier offset and channel estimation method for synchronous CDMA system," *in the Proc. ICASSP*, May 2006, pp. 597-600.

[$C2$] L. B. Thiagarajan, S. Attallah and Y.-C. Liang, "Two-stage frequency synchronization for uplink MC-CDMA system", *in Proc. WCNC*, Mar. 2007, pp. 2441-2445.

[$C3$] L. B. Thiagarajan, S. Attallah and Y.-C. Liang, "Blind channel estimation techniques for urban areas," *invited paper in Proc. SONDRA workshop*, France, April 2007.

[$C4$] L. B. Thiagarajan, S. Attallah, H. Fu and Y.-C. Liang, "Non-data-aided synchronization and channel estimation for asynchronous CDMA uplink," *in Proc. ICC'*07, June 2007, pp. 2906-2911.

[$C5$] L. B. Thiagarajan, Y.-C. Liang, and S. Attallah, "Low complexity iterative receiver for downlink MC-CDMA system in Doppler channels," *in Proc.* 67*th IEEE VTC*, May 2008, pp. 724-728.

[C6] L. B. Thiagarajan, S. Attallah, Y.-C. Liang, and K. Abed-Meraim, "Channel identifiability for blind subspace-based channel estimator in uplink MC-CDMA systems," *to appear in Proc. ICC 2008*, Beijing.

1.6 Thesis Outline

The outline of this thesis is as follows:

Chapter 2 outlines the concepts of vector space, subspace, properties of vector space and signal and noise subspaces for a generalized received signal. The methods used for the estimation of signal and noise subspaces are discussed. The first order perturbation analysis for the subspace estimates is also discussed.

In chapter 3, quasi-synchronous uplink system model for DS-CDMA system is presented. GEVPM and the proposed EDMM and ADMM based estimators are formulated. The computational complexity for the proposed estimator is compared with that of GEVPM. Using computer simulations, the performance of the proposed estimators is compared with that of GEVPM.

Chapter 4 and chapter 5 extend the formulation of EDMM based estimator to quasi-synchronous uplink transmission in CP-CDMA and MC-CDMA systems, respectively. The inherent signal structure in CP-CDMA and MC-CDMA systems are outlined. A criterion for the selection of spreading codes to guarantee the identifiability of CFO and channel estimates is constructed. The performance of the proposed estimator is obtained through computer simulations.

The cost function used for CFO estimation is shown to be locally convex around the true CFO value in chapter 6. Following this, a low complexity two-stage CFO estimator is presented and the computer simulation results show the convergence of the two-stage estimator.

In chapter 7, the proposed estimator is linearized for high SNR. Using first order perturbation analysis results for noise subspace estimate, the linearized estimator is shown to be unbiased and theoretical MSE performance corresponding to CFO estimation is also derived. The validity of the theoretical finding is verified through computer simulations. The perspective of this thesis and proposals for future research are given in Chapter 8.

Chapter 2

Signal Subspace and Noise Subspace

This chapter presents the mathematical preliminaries required to formulate the estimator. The definitions for signal subspace and noise subspace are provided using a generalized discrete time received signal. The properties of the above subspaces and methods available to estimate them are also discussed. The perturbation in signal subspace and noise subspace estimates is studied using first order perturbation analysis.

2.1 Vector Space

Let $\mathcal{V}$ be a set of $(N \times 1)$ vectors. Let $\mathbf{x}$, $\mathbf{y}$ and $\mathbf{z}$ be any three vectors from set $\mathcal{V}$. Let α, β and γ be complex-valued scalars, i.e., $\alpha, \beta, \gamma \in \mathcal{C}$; $\mathcal{C}$ denotes the complex plane. Set $\mathcal{V}$ is said to be a *vector space* over $\mathcal{C}^N$ if the vectors in $\mathcal{V}$ satisfy the following properties [99]-[101]:

Commutativity: $\mathbf{x}+\mathbf{y}=\mathbf{y}+\mathbf{x}$ for all $\mathbf{x},\mathbf{y}\in\mathcal{V}$.

Closed under Vector Addition: For all $\mathbf{x},\mathbf{y}\in\mathcal{V}$, $\mathbf{x}+\mathbf{y}\in\mathcal{V}$.

Associativity of Vector Addition: $(\mathbf{x}+\mathbf{y})+\mathbf{z}=\mathbf{x}+(\mathbf{y}+\mathbf{z})$ for all $\mathbf{x},\mathbf{y},\mathbf{z}\in\mathcal{V}$.

Existence of Additive Identity: For all $\mathbf{x}\in\mathcal{V}$, there exists a *zero vector*, $\mathbf{0}_{N\times 1}\in\mathcal{V}$, such that $\mathbf{x}+\mathbf{0}_{N\times 1}=\mathbf{0}_{N\times 1}+\mathbf{x}=\mathbf{x}$.

Existence of Additive Inverse: For all $\mathbf{x}\in\mathcal{V}$, there exists an *additive inverse vector*, $(-\mathbf{x})\in\mathcal{V}$, such that $\mathbf{x}+(-\mathbf{x})=(-\mathbf{x})+\mathbf{x}=\mathbf{0}_{N\times 1}$.

Closed under Scalar Multiplication: For any $\alpha\in\mathcal{C}$, $\alpha\mathbf{x}\in\mathcal{V}$ for all $\mathbf{x}\in\mathcal{V}$.

Associativity of Scalar Multiplication: For all $\mathbf{x}\in\mathcal{V}$ and $\alpha,\beta\in\mathcal{C}$, $(\alpha\beta)\mathbf{x}=\alpha(\beta\mathbf{x})$.

Existence of Scalar Multiplication Identity: $\alpha\mathbf{x}=\mathbf{x}\alpha=\mathbf{x}$ for all $\mathbf{x}\in\mathcal{V}$ and $\alpha=1\in\mathcal{C}$.

Distributive of Scalar Sum: For any $\mathbf{x}\in\mathcal{V}$ and scalars $\alpha,\beta\in\mathcal{C}$, $(\alpha+\beta)\mathbf{x}=\alpha\mathbf{x}+\beta\mathbf{x}$.

Distributive of Vector Sum: For all $\mathbf{x},\mathbf{y}\in\mathcal{V}$ and $\alpha\in\mathcal{C}$, $\alpha(\mathbf{x}+\mathbf{y})=\alpha\mathbf{x}+\alpha\mathbf{y}$.

2.1.1 Linear Independence

A set of non-zero vectors $\{\mathbf{x}_0, \mathbf{x}_1, \cdots, \mathbf{x}_{M-1}\} \in \mathcal{C}^N$ are said to be linearly independent if

$$\sum_{i=0}^{M-1} \alpha_i \mathbf{x}_i \;=\; \mathbf{0}_{N\times 1} \text{ iff } \alpha_i = 0 \text{ for } i = 0, 1, \cdots, M-1. \tag{2.1}$$

2.1.2 Basis of Vector Space

Basis of vector space is a set with minimum number of linearly independent vectors using which any vector in the vector space can be constructed. For example, the basis vectors for the vector space $\mathcal{C}^4$ are $[1,0,0,0]^T$, $[0,1,0,0]^T$, $[0,0,1,0]^T$ and $[0,0,0,1]^T$. Any vector $\mathbf{x} = [x_0, x_1, x_2, x_3]^T \in \mathcal{C}^4$ can be constructed by linearly combining the basis vectors as follows:

$$\begin{bmatrix} x_0 \\ x_1 \\ x_2 \\ x_3 \end{bmatrix} = x_0 \begin{bmatrix} 1 \\ 0 \\ 0 \\ 0 \end{bmatrix} + x_1 \begin{bmatrix} 0 \\ 1 \\ 0 \\ 0 \end{bmatrix} + x_2 \begin{bmatrix} 0 \\ 0 \\ 1 \\ 0 \end{bmatrix} + x_3 \begin{bmatrix} 0 \\ 0 \\ 0 \\ 1 \end{bmatrix}. \tag{2.2}$$

The basis of a vector space is not unique. That is, a vector space can have any number of basis, but the number of vectors in the basis remains the same for a vector space.

2.1.3 Subspace

Let $\{\mathbf{x}_0, \mathbf{x}_1, \cdots, \mathbf{x}_{M-1}\}$ be a set of $(N \times 1)$ vectors in vector space $\mathcal{C}^N$ and let $M < N$. The set of vectors generated by all possible linear combinations of vectors

$\{\mathbf{x}_0, \mathbf{x}_1, \cdots, \mathbf{x}_{M-1}\}$ is also a vector space and is called as *subspace*.

2.1.4 Dimension of Vector Space

The number of vectors in the basis of a vector space denotes the dimension of that vector space. Let $\mathcal{V}_1$ denote a subspace generated from basis vectors $\{\mathbf{x}_0, \mathbf{x}_1, \cdots, \mathbf{x}_{M-1}\}$. The $(N \times M)$ matrix $\mathbf{X}$ contains the basis vectors as shown below:

$$\mathbf{X} = [\mathbf{x}_0, \mathbf{x}_1, \cdots, \mathbf{x}_{M-1}]. \tag{2.3}$$

The dimension of subspace $\mathcal{V}_1$ is equal to the number of basis vectors which in turn is equal to the rank of matrix $\mathbf{X}$. Thus, subspace $\mathcal{V}_1$ is M dimensional.

2.2 Signal Subspace

Let the discrete time signal received, in the absence of noise, at the receiver be denoted by $(N \times 1)$ vector $\mathbf{r}(n)$. Let vector $\mathbf{r}(n)$ be expressed as

$$\mathbf{r}(n) = \sum_{i=0}^{\mathcal{S}-1} \mathbf{x}_i s_i(n), \tag{2.4}$$

where n denotes the time index, $s_i(n)$ denotes the transmitted data symbol and index i counts the number of independent data transmissions. Vector $\mathbf{x}_i \in \mathcal{C}^N$ and $\mathcal{S}$ depends on the system parameters, viz., number of users, multipath fading channel, transmission method etc. Let the vectors $\{\mathbf{x}_i\}_{i=0}^{\mathcal{S}-1}$ be assumed to be linearly independent and let $\mathcal{S} < N$. In the absence of noise, the received signal lies obviously in a subspace spanned by vectors $\{\mathbf{x}_i\}_{i=0}^{\mathcal{S}-1}$. This subspace is called

signal subspace. The dimension of signal subspace in (2.4) is $\mathcal{S}$. Equation (2.4) can be written as

$$\mathbf{r}(n) = \mathbf{X}\mathbf{s}(n), \tag{2.5}$$

where $(N \times \mathcal{S})$ matrix $\mathbf{X} = [\mathbf{x}_0, \mathbf{x}_1, \cdots, \mathbf{x}_{\mathcal{S}-1}]$ and vector $\mathbf{s}(n) = [s_0(n), s_1(n), \cdots, s_{\mathcal{S}-1}(n)]^T$. The autocorrelation matrix of the received signal is given by[1]

$$\begin{aligned} \mathbf{R} &= E\left[\mathbf{r}(n)\mathbf{r}^H(n)\right] && (2.6) \\ &= \mathbf{X}\, E\left[\mathbf{s}(n)\mathbf{s}^H(n)\right]\, \mathbf{X}^H. && (2.7) \end{aligned}$$

Assuming the data symbols to be uncorrelated, we have

$$E\left[\mathbf{s}(n)\mathbf{s}^H(n)\right] = \sigma_s^2 \mathbf{I}_{\mathcal{S}}, \tag{2.8}$$

where $E[|s_i(n)|^2] = \sigma_s^2$ denotes the symbol energy and $\mathbf{I}_{\mathcal{S}}$ denotes a $(\mathcal{S} \times \mathcal{S})$ identity matrix. Therefore, the autocorrelation matrix becomes

$$\mathbf{R} = \sigma_s^2 \mathbf{X}\mathbf{X}^H. \tag{2.9}$$

It can be easily verified that matrix $\mathbf{R}$ is of rank $\mathcal{S}$.

2.3 Additive Noise

The presence of additive noise is inevitable in any system. In our analysis, the additive noise is assumed to be a circularly symmetric white Gaussian random

[1] $E[.]$ denotes statistical expectation.

variable with zero mean. As the additive noise is white, proper care need to be taken at the receiver to bandlimit the noise before sampling. If the additive white noise is not bandlimited, then sampling would increase the noise power to infinity due to aliasing [115]. Let $(N \times 1)$ vector $\mathbf{v}(n)$ contain the additive white noise samples[2] for the nth symbol duration. The autocorrelation matrix for the additive white Gaussian noise (AWGN) vector is assumed to be

$$E\left[\mathbf{v}(n)\mathbf{v}^H(n)\right] = \sigma_n^2 \mathbf{I}_N, \tag{2.10}$$

where σ_n^2 denotes the noise variance. The autocorrelation matrix for $\mathbf{v}(n)$ in equation (2.10) is of full rank N. This implies that the AWGN vector $\mathbf{v}(n)$ can lie anywhere in $\mathcal{C}^N$ vector space.

In the presence of AWGN, the received signal is expressed as

$$\mathbf{r}(n) = \sum_{i=0}^{\mathcal{S}-1} \mathbf{x}_i s_i(n) + \mathbf{v}(n). \tag{2.11}$$

The autocorrelation matrix for the received signal in equation (2.11) is therefore

$$\begin{aligned} \mathbf{R} &= E\left[\mathbf{r}(n)\mathbf{r}^H(n)\right] \\ &= \sigma_s^2 \mathbf{X}\mathbf{X}^H + \sigma_n^2 \mathbf{I}_N. \end{aligned} \tag{2.12}$$

Equation (2.12) implies that, in the presence of AWGN the autocorrelation matrix $\mathbf{R}$ is of full rank N.

[2]Samples are obtained after properly bandlimiting the received signal.

2.4 Noise Subspace

The eigenvalue decomposition (EVD) [102] of the autocorrelation matrix $\mathbf{R}$ in equation (2.12) is given by

$$\mathbf{R} = \sigma_s^2 \mathbf{X}\mathbf{X}^H + \sigma_n^2 \mathbf{I}_N = [\mathbf{U}_s \mathbf{U}_n] \begin{bmatrix} (\sigma_s^2 + \sigma_n^2)\mathbf{I}_{\mathcal{S}} & \mathbf{0}_{\mathcal{S}\times(N-\mathcal{S})} \\ \mathbf{0}_{(N-\mathcal{S})\times\mathcal{S}} & \sigma_n^2 \mathbf{I}_{N-\mathcal{S}} \end{bmatrix} \begin{bmatrix} \mathbf{U}_s^H \\ \mathbf{U}_n^H \end{bmatrix}, \quad (2.13)$$

where $\mathbf{U}_s$ is a $(N \times \mathcal{S})$ matrix containing $\mathcal{S}$ eigenvectors of $\mathbf{R}$ corresponding to the largest eigenvalue $(\sigma_s^2 + \sigma_n^2)$, $\mathbf{U}_n$ is a $(N \times (N - \mathcal{S}))$ matrix containing $(N - \mathcal{S})$ eigenvectors of $\mathbf{R}$ corresponding to the smallest eigenvalue (σ_n^2). It is to be noted that, the number of significant eigenvalues (eigenvalues greater than σ_n^2) of $\mathbf{R}$ is equal to the dimension of the signal subspace.

The eigenvectors in $\mathbf{U}_s$ span the signal subspace, i.e., the signal component in $\mathbf{r}(n)$ can be obtained by linearly combining the column vectors of matrix $\mathbf{U}_s$. In other words,

$$\sum_{i=0}^{\mathcal{S}-1} \mathbf{x}_i s_i(n) \quad = \quad \mathbf{U}_s \mathbf{a}_s, \quad (2.14)$$

where vector $\mathbf{a}_s = [a_0, a_1, \cdots, a_{\mathcal{S}-1}]^T$ contains the coefficients for linearly combining the eigenvectors. The column vectors of matrix $\mathbf{U}_s$ are orthonormal and hence they form an orthonormal basis for the signal subspace.

***Column space / Span**: A set of vectors generated by all possible linear combinations of the column vectors of a matrix is called the column space or span of that matrix.*

Equation (2.14) implies that

$$\sum_{i=0}^{\mathcal{S}-1} \mathbf{x}_i s_i(n) \quad \in \quad col(\mathbf{U}_s). \tag{2.15}$$

Intersection Space*: Intersection space between column space of any two matrices* $\boldsymbol{A}$ *and* $\boldsymbol{B}$*, is a subspace which contains vectors lying in the column space of both matrices* $\boldsymbol{A}$ *and* $\boldsymbol{B}$*.*

The eigenvectors in $\mathbf{U}_n$ span a subspace called the ***noise subspace*** which is orthogonal to the signal subspace. The dimension of the noise subspace in our example is $(N-\mathcal{S})$. The column vectors of matrix $\mathbf{U}_n$ forms the orthonormal basis for the noise subspace. Some of the properties of the signal and noise subspaces are listed below:

$$\mathbf{U}_s\mathbf{U}_s^H + \mathbf{U}_n\mathbf{U}_n^H = \mathbf{I}_N \tag{2.16}$$

$$\mathbf{U}_s^H\mathbf{U}_n = \mathbf{0}_{\mathcal{S}\times(N-\mathcal{S})} \tag{2.17}$$

$$\mathbf{U}_n^H\mathbf{U}_s = \mathbf{0}_{(N-\mathcal{S})\times\mathcal{S}} \tag{2.18}$$

$$\mathbf{U}_n^H\mathbf{x}_i = \mathbf{0}_{(N-\mathcal{S})\times 1} \tag{2.19}$$

$$\mathbf{U}_n^H\left(\sum_{i=0}^{\mathcal{S}-1} \mathbf{x}_i s_i(n)\right) = \mathbf{0}_{(N-\mathcal{S})\times 1}. \tag{2.20}$$

The orthogonal property given in equations (2.19) and (2.20) will be used in the formulation of the estimator.

2.5 Subspace Estimation

Equation (2.13) shows that the signal and noise subspaces can be obtained by performing EVD on the autocorrelation matrix $\mathbf{R}$. The statistical expectation involved in the computation of $\mathbf{R}$ cannot be done using a single realization of $\mathbf{r}(n)$. Let the random vectors $\mathbf{s}(n)$ and $\mathbf{v}(n)$ be obtained from an ergodic random processes. This assumption aids in estimating the statistical expectation using time-average from a single realization [103], i.e.,

$$\sigma_n^2 \mathbf{I}_N = \lim_{B\to\infty} \frac{1}{B} \sum_{n=0}^{B-1} \mathbf{v}(n)\mathbf{v}^H(n) \tag{2.21}$$

$$\sigma_s^2 \mathbf{I}_{\mathcal{S}} = \lim_{B\to\infty} \frac{1}{B} \sum_{n=0}^{B-1} \mathbf{s}(n)\mathbf{s}^H(n) \tag{2.22}$$

$$\mathbf{R} = \lim_{B\to\infty} \frac{1}{B} \sum_{n=0}^{B-1} \mathbf{r}(n)\mathbf{r}^H(n), \tag{2.23}$$

where B denotes the number of sample vectors used to compute the time-average. Therefore, the signal and noise subspaces can be estimated by computing the EVD for the estimated autocorrelation matrix $\hat{\mathbf{R}}$ given by

$$\hat{\mathbf{R}} = \frac{1}{B} \sum_{n=0}^{B-1} \mathbf{r}(n)\mathbf{r}^H(n). \tag{2.24}$$

Singular Value Decomposition (SVD)

Let $\widetilde{\mathbf{\Phi}}$ be a $(N \times B)$ matrix constructed from the received signal vectors as

$$\widetilde{\mathbf{\Phi}} = \left[\mathbf{r}(0), \mathbf{r}(1), \cdots, \mathbf{r}(B-1)\right]. \tag{2.25}$$

Therefore we have,

$$\widetilde{\mathbf{\Phi}} \;=\; \mathbf{\Phi} + \mathbf{\Xi}, \tag{2.26}$$

where $\mathbf{\Phi}$ is a $(N \times B)$ matrix containing the received signal vectors in the absence of noise and the $(N \times B)$ matrix $\mathbf{\Xi}$ is given by $\mathbf{\Xi} = [\mathbf{v}(0), \mathbf{v}(1), \cdots, \mathbf{v}(B-1)]$. The SVD [104] of matrix $\mathbf{\Phi}$ is given by

$$\mathbf{\Phi} \;=\; \mathbf{U}\mathbf{\Sigma}\mathbf{V}^H, \tag{2.27}$$

where $\mathbf{U} = [\mathbf{U}_s, \mathbf{U}_n]$ is a $(N \times N)$ unitary matrix and $\mathbf{V}$ is a $(B \times B)$ unitary matrix. The $(N \times B)$ matrix $\mathbf{\Sigma}$ is of the form

$$\mathbf{\Sigma} \;=\; \left[\mathbf{\Lambda},\ \mathbf{0}_{N\times(B-N)}\right], \tag{2.28}$$

where $\mathbf{\Lambda}$ is a $(N \times N)$ diagonal matrix, which can be expressed as

$$\mathbf{\Lambda} \;=\; \begin{bmatrix} \sigma_s \mathbf{I}_{\mathcal{S}} & \mathbf{0}_{\mathcal{S}\times(N-\mathcal{S})} \\ \mathbf{0}_{(N-\mathcal{S})\times\mathcal{S}} & \mathbf{0}_{(N-\mathcal{S})\times(N-\mathcal{S})} \end{bmatrix}. \tag{2.29}$$

Equations (2.21) - (2.23) and (2.25) imply that, for large B the signal subspace and noise subspace can be estimated by computing the EVD for the estimated autocorrelation matrix $\hat{\mathbf{R}}$ or by computing the SVD for matrix $\widetilde{\mathbf{\Phi}}$. The above outlined methods are called **batch methods** as the estimation is done by using a batch of B received signal vectors simultaneously.

2.5.1 First Order Perturbation Analysis

In practice only a finite value for B is used and hence the estimated signal and noise subspaces are perturbed[3]. In other words, the SVD for $\widetilde{\mathbf{\Phi}}$ in (2.25) is given by

$$\begin{aligned}\widetilde{\mathbf{\Phi}} &= \widetilde{\mathbf{U}}\widetilde{\mathbf{\Sigma}}\widetilde{\mathbf{V}}^H &(2.30)\\ &= \left[\widetilde{\mathbf{U}}_s,\ \widetilde{\mathbf{U}}_n\right]\begin{bmatrix}\widetilde{\mathbf{\Sigma}}_s & \mathbf{0}_{\mathcal{S}\times(B-\mathcal{S})}\\ \mathbf{0}_{(N-\mathcal{S})\times\mathcal{S}} & \widetilde{\mathbf{\Sigma}}_n\end{bmatrix}\begin{bmatrix}\widetilde{\mathbf{V}}_s^H\\ \widetilde{\mathbf{V}}_n^H\end{bmatrix}, &(2.31)\end{aligned}$$

where $\widetilde{\mathbf{U}} = \left[\widetilde{\mathbf{U}}_s,\ \widetilde{\mathbf{U}}_n\right]$,

$$\widetilde{\mathbf{U}}_s = \mathbf{U}_s + \Delta\mathbf{U}_s \quad \text{and} \quad \widetilde{\mathbf{V}}_s = \mathbf{V}_s + \Delta\mathbf{V}_s \tag{2.32}$$

$$\widetilde{\mathbf{U}}_n = \mathbf{U}_n + \Delta\mathbf{U}_n \quad \text{and} \quad \widetilde{\mathbf{V}}_n = \mathbf{V}_n + \Delta\mathbf{V}_n, \tag{2.33}$$

where matrices $\Delta\mathbf{U}_s$, $\Delta\mathbf{U}_n$, $\Delta\mathbf{V}_s$ and $\Delta\mathbf{V}_n$ are the perturbations in the estimates for $\mathbf{U}_s$, $\mathbf{U}_n$, $\mathbf{V}_s$ and $\mathbf{V}_n$, respectively. Matrix $\widetilde{\mathbf{\Sigma}}_s$ is a $(\mathcal{S}\times\mathcal{S})$ diagonal matrix containing the $\mathcal{S}$ largest singular values of $\widetilde{\mathbf{\Phi}}$ and $\widetilde{\mathbf{\Sigma}}_n$ is a $((N-\mathcal{S})\times(B-\mathcal{S}))$ given by

$$\widetilde{\mathbf{\Sigma}}_n = \left[\widetilde{\mathbf{\Lambda}}_n,\ \mathbf{0}_{(N-\mathcal{S})\times(B-N)}\right], \tag{2.34}$$

where $\widetilde{\mathbf{\Lambda}}_n$ is a $((N-\mathcal{S})\times(N-\mathcal{S}))$ diagonal matrix containing the $(N-\mathcal{S})$ smallest singular values of $\widetilde{\mathbf{\Phi}}$. The column vectors of matrices $\widetilde{\mathbf{U}}_s$ and $\widetilde{\mathbf{U}}_n$ are the left singular vectors associated with the singular values in matrices $\widetilde{\mathbf{\Sigma}}_s$ and $\widetilde{\mathbf{\Sigma}}_n$, respectively.

[3]We assume that the dimension of signal and noise subspaces are know *a priori*.

Furthermore, it should be noted that

$$\widetilde{\mathbf{U}}_s^H \widetilde{\mathbf{U}}_s = \mathbf{I}_{\mathcal{S}} \quad \text{and} \quad \widetilde{\mathbf{U}}_n^H \widetilde{\mathbf{U}}_n = \mathbf{I}_{N-\mathcal{S}} \tag{2.35}$$

$$\widetilde{\mathbf{U}}_s^H \widetilde{\mathbf{U}}_n = \mathbf{0}_{(\mathcal{S}\times(N-\mathcal{S}))} \quad \text{and} \quad \widetilde{\mathbf{U}}_n^H \widetilde{\mathbf{U}}_s = \mathbf{0}_{(N-\mathcal{S})\times\mathcal{S}}. \tag{2.36}$$

The perturbation $\mathbf{\Xi}$ in $\widetilde{\mathbf{\Phi}}$ is transformed in a highly non-linear way by the SVD to produce the perturbed signal and noise subspaces [105]. At high SNR, a first order perturbation expansion can be used to derive expressions for $\Delta\mathbf{U}_s$ and $\Delta\mathbf{U}_n$ which are linear in $\mathbf{\Xi}$. This derivation presented in [105] is illustrated below.

Noise Subspace

Let us define matrix $\mathbf{Q}$ as

$$\mathbf{Q} \;=\; -\left(\widetilde{\mathbf{U}}_s^H \mathbf{U}_s\right)^{-1} \widetilde{\mathbf{U}}_s^H \mathbf{U}_n. \tag{2.37}$$

In the following we will show that the column vectors of matrix $(\mathbf{U}_n + \mathbf{U}_s\mathbf{Q})$ span the perturbed noise subspace $\widetilde{\mathbf{U}}_n$. The matrix product $\widetilde{\mathbf{U}}_s^H(\mathbf{U}_n + \mathbf{U}_s\mathbf{Q})$ is given by

$$\begin{aligned} \widetilde{\mathbf{U}}_s^H (\mathbf{U}_n + \mathbf{U}_s\mathbf{Q}) &= \widetilde{\mathbf{U}}_s^H \left(\mathbf{U}_n - \mathbf{U}_s \left(\widetilde{\mathbf{U}}_s^H \mathbf{U}_s\right)^{-1} \widetilde{\mathbf{U}}_s^H \mathbf{U}_n\right) \\ &= \widetilde{\mathbf{U}}_s^H \mathbf{U}_n - \widetilde{\mathbf{U}}_s^H \mathbf{U}_n \\ &= \mathbf{0}_{(\mathcal{S}\times(N-\mathcal{S}))}. \end{aligned} \tag{2.38}$$

Equation (2.38) implies that column vectors of matrix $(\mathbf{U}_n + \mathbf{U}_s\mathbf{Q})$ are orthogonal to the column vectors of matrix $\widetilde{\mathbf{U}}_s$. Therefore, the column vectors of matrix

$(\mathbf{U}_n + \mathbf{U}_s\mathbf{Q})$ span the perturbed noise subspace, i.e.,

$$col\left([\mathbf{U}_n + \mathbf{U}_s\mathbf{Q}]\right) \;=\; col\left(\widetilde{\mathbf{U}}_n\right). \tag{2.39}$$

Matrix $\mathbf{Q}$ given in (2.37) can be expressed as

$$\begin{aligned}\mathbf{Q} &= -\left[(\mathbf{U}_s + \Delta\mathbf{U}_s)^H \mathbf{U}_s\right]^{-1}\left[\mathbf{U}_s^H + (\Delta\mathbf{U}_s)^H\right]\mathbf{U}_n \\ &= -\left[\mathbf{I}_{\mathcal{S}} + (\Delta\mathbf{U}_s)^H\mathbf{U}_s\right]^{-1}(\Delta\mathbf{U}_s)^H\mathbf{U}_n. \end{aligned}\tag{2.40}$$

The perturbation in the signal subspace is of the order of $\boldsymbol{\Xi}$ [106]. Therefore, for high SNR the norm[4] of matrix $(\Delta\mathbf{U}_s)^H\mathbf{U}_s$ is small. Matrix $[\mathbf{I}_N + \mathbf{X}]^{-1}$ can be expressed as $\mathbf{I}_N - \mathbf{X} + \mathbf{X}^2 + \cdots$, when the elements of $\mathbf{X}$ are small. Thus, matrix $[\mathbf{I}_N + \mathbf{X}]^{-1}$ can be approximated as $[\mathbf{I}_N + \mathbf{X}]^{-1} \approx \mathbf{I}_N - \mathbf{X}$. Using the above result in (2.40) and considering only the first order terms, we obtain

$$\begin{aligned}\mathbf{Q} &\approx -\left(\mathbf{I}_{\mathcal{S}} - (\Delta\mathbf{U}_s)^H\mathbf{U}_s\right)(\Delta\mathbf{U}_s)^H\mathbf{U}_n \\ &= -(\Delta\mathbf{U}_s)^H\mathbf{U}_n. \end{aligned}\tag{2.41}$$

The equality in (2.41) is with respect to the first order term. Taking the norm on both sides of equation (2.41), we obtain

$$\|\mathbf{Q}\| \le \alpha\|\Delta\mathbf{U}_s\| \le \beta\|\boldsymbol{\Xi}\|, \tag{2.42}$$

[4]It could be any norm which satisfies $\|\mathbf{AB}\| \le \|\mathbf{A}\|\|\mathbf{B}\|$, for example, the Euclidean 2-norm or Frobenius norm.

where α and β are constants. Therefore, the norm of matrix $\mathbf{Q}$ is of the order of $\|\mathbf{\Xi}\|$. The matrix product $(\mathbf{U}_n + \mathbf{U}_s\mathbf{Q})^H (\mathbf{U}_n + \mathbf{U}_s\mathbf{Q})$ is given by

$$(\mathbf{U}_n + \mathbf{U}_s\mathbf{Q})^H (\mathbf{U}_n + \mathbf{U}_s\mathbf{Q}) \;\; = \;\; \mathbf{I}_{N-\mathcal{S}} + \mathbf{Q}^H\mathbf{Q}. \tag{2.43}$$

For high SNR, the second order term $\mathbf{Q}^H\mathbf{Q}$ can be omitted and hence we have

$$(\mathbf{U}_n + \mathbf{U}_s\mathbf{Q})^H (\mathbf{U}_n + \mathbf{U}_s\mathbf{Q}) \;\; = \;\; \mathbf{I}_{N-\mathcal{S}}. \tag{2.44}$$

Equation (2.44) implies that the columns vectors of matrix $(\mathbf{U}_n + \mathbf{U}_s\mathbf{Q})$ are orthonormal and hence

$$\widetilde{\mathbf{U}}_n \;\; = \;\; \mathbf{U}_n + \mathbf{U}_s\mathbf{Q}. \tag{2.45}$$

Thus, the perturbation in the estimated noise subspace is given by

$$\Delta\mathbf{U}_n \;\; = \;\; \mathbf{U}_s\mathbf{Q}. \tag{2.46}$$

As shown in (2.46), the perturbed right singular vectors $\widetilde{\mathbf{V}}_n$ can be expressed as

$$\widetilde{\mathbf{V}}_n = \mathbf{V}_n + \mathbf{V}_s\breve{\mathbf{Q}}, \tag{2.47}$$

where the norm of matrix $\breve{\mathbf{Q}}$ is of the order of $\|\mathbf{\Xi}\|$. Pre-multiplying $\widetilde{\mathbf{\Phi}}$ by $\widetilde{\mathbf{U}}_n = \mathbf{U}_n + \mathbf{U}_s\mathbf{Q}$, we obtain

$$(\mathbf{U}_n + \mathbf{U}_s\mathbf{Q})^H (\mathbf{\Phi} + \mathbf{\Xi}) \;\; = \;\; \widetilde{\mathbf{\Sigma}}_n\widetilde{\mathbf{V}}_n^H = \widetilde{\mathbf{\Sigma}}_n\left(\mathbf{V}_n + \mathbf{V}_s\breve{\mathbf{Q}}\right)^H. \tag{2.48}$$

It is known that $\mathbf{U}_n^H\boldsymbol{\Phi} = \mathbf{0}_{(N-\mathcal{S})\times B}$. Using this result in (2.48) and retaining only the first order terms, equation (2.48) can be simplified as

$$\mathbf{U}_n^H\boldsymbol{\Xi} + \mathbf{Q}^H\mathbf{U}_s^H\boldsymbol{\Phi} \quad = \quad \widetilde{\boldsymbol{\Sigma}}_n\mathbf{V}_n^H. \tag{2.49}$$

Post-multiplying (2.49) by $\mathbf{V}_s$ results in[5]

$$\mathbf{U}_n^H\boldsymbol{\Xi}\mathbf{V}_s + \mathbf{Q}^H\mathbf{U}_s^H\boldsymbol{\Sigma}_s \quad = \quad \mathbf{0}_{(N-\mathcal{S})\times\mathcal{S}}, \tag{2.50}$$

from which $\mathbf{Q}$ is obtained to be

$$\mathbf{Q} = -\boldsymbol{\Sigma}_s^{-1}\mathbf{V}_s^H\boldsymbol{\Xi}^H\mathbf{U}_n. \tag{2.51}$$

From equations (2.46) and (2.51), the perturbation in the noise subspace estimate is given by

$$\Delta\mathbf{U}_n = \mathbf{U}_n\mathbf{Q} = -\mathbf{U}_s\boldsymbol{\Sigma}_s^{-1}\mathbf{V}_s^H\boldsymbol{\Xi}^H\mathbf{U}_n. \tag{2.52}$$

Using the fact $\boldsymbol{\Phi} = \mathbf{U}_s\boldsymbol{\Sigma}_s\mathbf{V}_s^H$, the Moore-Penrose inverse of $\boldsymbol{\Phi}$ is computed as[6]

$$\boldsymbol{\Phi}^\dagger = \boldsymbol{\Phi}^H\left(\boldsymbol{\Phi}\boldsymbol{\Phi}^H\right)^{-1} = \mathbf{V}_s\boldsymbol{\Sigma}_s^{-1}\mathbf{U}_s^H. \tag{2.53}$$

[5]It should be noted that $\mathbf{V}_n^H\mathbf{V}_s = \mathbf{0}_{(B-\mathcal{S})\times\mathcal{S}}$ and $\boldsymbol{\Phi}\mathbf{V}_s = \boldsymbol{\Sigma}_s$.

[6]The Moore-Penrose or pseudo inverse of matrix $\mathbf{A}$ is denoted by $\mathbf{A}^\dagger$.

Substituting (2.53) into (2.52), we obtain the perturbation in the noise subspace estimate to be

$$\Delta\mathbf{U}_n = -\left(\boldsymbol{\Phi}^{\dagger}\right)^H \boldsymbol{\Xi}^H \mathbf{U}_n. \tag{2.54}$$

Note that, the perturbation in the noise subspace estimate is obtained in terms of the signal matrix $\boldsymbol{\Phi}$, noise matrix **Xi** and the true noise subspace $\mathbf{U}_n$.

Signal Subspace

Let us define matrix $\mathbf{P}$ as

$$\mathbf{P} \;=\; -\left(\widetilde{\mathbf{U}}_n^H \mathbf{U}_n\right)^{-1} \widetilde{\mathbf{U}}_n^H \mathbf{U}_s. \tag{2.55}$$

As in (2.38), it can shown that the column vectors of matrix $(\mathbf{U}_s + \mathbf{U}_n\mathbf{P})$ span the perturbed signal subspace. For high SNR, considering only the first order terms, it can be shown that

$$\widetilde{\mathbf{U}}_s \;=\; \mathbf{U}_s + \mathbf{U}_n\mathbf{P}. \tag{2.56}$$

Using the orthogonal property $\widetilde{\mathbf{U}}_n^H \widetilde{\mathbf{U}}_s = \mathbf{0}_{(N-\mathcal{S})\times\mathcal{S}}$, we note that

$$\begin{aligned}\mathbf{0}_{(N-\mathcal{S})\times\mathcal{S}} &= \left(\mathbf{U}_n + \mathbf{U}_s\mathbf{Q}\right)^H\left(\mathbf{U}_s + \mathbf{U}_n\mathbf{P}\right) \\ &= \mathbf{Q}^H + \mathbf{P}. \end{aligned}\tag{2.57}$$

Therefore, $\mathbf{P} = -\mathbf{Q}^H$ and the perturbation in the signal subspace estimate is obtained to be

$$\Delta\mathbf{U}_s = -\mathbf{U}_n\mathbf{Q}^H. \tag{2.58}$$

2.6 Summary

In this chapter, the definitions for vector space, subspace, dimension of subspace were given. The signal and noise subspaces were identified for a generalized discrete time received signal. Signal subspace and noise subspace properties and methods available for subspace estimation were also discussed. For high SNR, the perturbation in the noise subspace estimate was obtained in terms of the signal matrix $\mathbf{\Phi}$, noise matrix **Xi** and the true noise subspace $\mathbf{U}_n$. Thus, the derived expression for noise subspace perturbation can be used to evaluate the performance of algorithms using the noise subspace estimates.

Chapter 3

DS-CDMA System

Blind joint estimation of CFO and CIR for a desired user in the uplink of a DS-CDMA system is addressed in this chapter. The discrete time uplink received signal is formulated in the presence of CFO. Two subspace-based blind joint CFO and CIR estimation methods, namely exact determinant minimization method (EDMM) and approximate determinant minimization method (ADMM) are proposed. In [107], the generalized eigenvalue problem method (GEVPM) based joint CFO and CIR estimator [85] has been shown to be computationally less intensive than the estimator in [84]. In this chapter, the performance and computational complexity of the proposed methods are compared with the GEVPM based estimator. Computer simulation results are given to show that the proposed estimators have better performance than the GEVPM based estimator and have a wider CFO acquisition range [108].

3.1 System Model

Let there be T users in the uplink of a quasi-synchronous DS-CDMA system. Let $\mathbf{c}_i = [c_i(0), c_i(1), \cdots, c_i(G-1)]^T$ denote the ith user's spreading code with spreading gain $G > T$ and $c_i(k) \in \left\{-\frac{1}{\sqrt{G}}, +\frac{1}{\sqrt{G}}\right\}_{k=0}^{G-1}$. The ith user's transmitted signal during the nth symbol duration is given by

$$a_i(t) \;=\; \sum_{l=0}^{G-1} s_i(n)c_i(l)p(t - nT_s - lT_c) \quad t \in [nGT_c, (n+1)GT_c), \tag{3.1}$$

where $p(t)$ is the normalized chip-pulse shaping function [5], $s_i(n)$ denotes the ith user's data symbol transmitted during the nth symbol duration, T_c is the chip-pulse duration and T_s is the data symbol duration. The relationship between symbol duration and chip-pulse duration is $T_s = GT_c$.

The transmitted signal from each user propagates through an independent multipath fading channel and reaches the base station. The ith user's transmitted signal propagates through the multipath fading channel $\tilde{h}_i(t)$ and reaches the base station with residual CFO f_i. At the base station, the signal received from T users is given by

$$\tilde{y}(t) \;=\; \sum_{i=0}^{T-1} \left[\sum_n s_i(n)e^{j2\pi f_i t} \sum_{l=0}^{G-1} c_i(l)p(t - nGT_c - lT_c)\right] \star \tilde{h}_i(t) + \tilde{v}(t), \tag{3.2}$$

where $\tilde{v}(t)$ and $\star$ denotes the AWGN and convolution operation, respectively. The received signal is filtered using a bandlimiting filter $p_s(t)$ to prevent aliasing of noise during sampling. The received signal after band limiting is denoted by $\acute{y}(t)$ which can be expressed as

$$\acute{y}(t) = \sum_{i=0}^{T-1}\left[\sum_n s_i(n)e^{j2\pi f_i t}\sum_{l=0}^{G-1} c_i(l)p(t-nGT_c-lT_c)\right]\star\tilde{h}_i(t)\star p_s(t)+v(t), \tag{3.3}$$

where $v(t)=\tilde{v}(t)\star p_s(t)$. Let $\acute{h}_i(t)$ denote the ith user's composite multipath fading channel containing the combined effects of $p(t)$, $\tilde{h}_i(t)$ and $p_s(t)$, i.e.,

$$\acute{h}_i(t) = p(t)\star\tilde{h}_i(t)\star p_s(t). \tag{3.4}$$

Let the channel delay spread of $\acute{h}_i(t)$ be Δ_t for all users. Therefore, the effect of nth transmitted data symbol can be seen in the received signal during the time duration $[nGT_c, (n+1)GT_c+\Delta_t)$. The signal content in the duration $[(n+1)GT_c, (n+1)GT_c+\Delta_t)$ distorts the received signal corresponding to $(n+1)$th symbol duration. This distortion is called ISI. Substituting (3.4) into (3.3), we obtain

$$\acute{y}(t) = \sum_{i=0}^{T-1}\sum_n s_i(n)e^{j2\pi f_i t}\sum_{l=0}^{G-1} c_i(l)\acute{h}_i(t-nGT_c-lT_c)+v(t). \tag{3.5}$$

The composite channel $\acute{h}_i(t)$ can be modeled as a tapped delay line with L taps [4], where[1]

$$L = \left\lfloor\frac{\Delta_t}{T_c}\right\rfloor+1. \tag{3.6}$$

[1]Floor operator $\lfloor . \rfloor$ returns an integer value, such that $a-\lfloor a\rfloor \geq 0$.

The L taps are stacked to form a $(L \times 1)$ vector $\mathbf{h}_i$ given by

$$\mathbf{h}_i = \left[h_i(0), h_i(1), \cdots, h_i(L-1)\right]^T, \qquad (3.7)$$

where $h_i(n) = \acute{h}_i(t)|_{t=nT_c}$. Vector $\mathbf{h}_i$ contains the ith user's CIR and is assumed to have unit norm[2], i.e, $\mathbf{h}_i^H \mathbf{h}_i = 1$. The received signal is sampled at the rate $1/T_c$. The pth received sample during the nth symbol duration is given by

$$\begin{aligned} y(nG+p) &= \acute{y}(t)|_{t=nGT_c+pT_c} \\ &= \sum_{i=0}^{T-1} \sum_{n} s_i(n) e^{j(nG+p)\phi_i} \sum_{l=0}^{G-1} c_i(l) h_i(p-l) + v(nG+p), \end{aligned} \qquad (3.8)$$

where $\phi_i = 2\pi f_i T_c$ is the ith user's angular CFO (ACFO). The G samples of the received signal corresponding to the nth symbol duration are stacked to form a $(G \times 1)$ vector $\tilde{\mathbf{r}}(n)$ as

$$\tilde{\mathbf{r}}(n) = \left[y(nG+0), y(nG+1), \cdots, y(nG+G-1)\right]^T. \qquad (3.9)$$

Using (3.8), $\tilde{\mathbf{r}}(n)$ can be expressed as

$$\begin{aligned} \tilde{\mathbf{r}}(n) &= \sum_{i=0}^{T-1} s_i(n) e^{jnG\phi_i} \mathbf{Z}_G(\phi_i) \mathbf{B}_i \mathbf{h}_i \\ &+ \underbrace{\sum_{i=0}^{T-1} s_i(n-1) e^{j(n-1)G\phi_i} \mathbf{Z}_G(\phi_i) \acute{\mathbf{B}}_i \mathbf{h}_i}_{\text{ISI}} + \tilde{\mathbf{v}}(n), \end{aligned} \qquad (3.10)$$

where $\tilde{\mathbf{v}}(n) = \left[v(nG+0), v(nG+1), \cdots, v(nG+G-1)\right]^T$, $\mathbf{Z}_G(\phi_i) = diag([1, e^{j\phi_i},$

[2]Throughout out this thesis, the user's CIR is assumed to have unit norm.

$e^{j2\phi_i}, \cdots, e^{j(G-1)\phi_i}]^T$) and the $(N \times L)$ dimensional matrices $\mathbf{B}_i$ and $\acute{\mathbf{B}}_i$ are constructed using the ith user's spreading code. The $(G \times L)$ Toeplitz matrices $\mathbf{B}_i$ and $\acute{\mathbf{B}}_i$ are constructed as shown below:

$$\mathbf{B}_i = \left[\begin{matrix} c_i(0) & 0 & 0 & \cdots & 0 \\ c_i(1) & c_i(0) & 0 & \cdots & 0 \\ \vdots & \ddots & & & \vdots \\ c_i(L-2) & c_i(L-3) & \cdots & \cdots & 0 \\ c_i(L-1) & c_i(L-2) & c_i(L-3) & \cdots & c_i(0) \\ c_i(L) & c_i(L-1) & c_i(L-1) & \cdots & c_i(1) \\ \vdots & & \ddots & & \vdots \\ c_i(G-1) & c_i(G-2) & c_i(G-3) & \cdots & c_i(G-L) \end{matrix}\right] \begin{matrix} \uparrow \\ (L-1)\times L \\ \\ \downarrow \\ \uparrow \\ (G-L+1)\times L \\ \\ \downarrow \end{matrix} \tag{3.11}$$

$$\acute{\mathbf{B}}_i = \left[\begin{matrix} 0 & c_i(G-1) & c_i(G-2) & \cdots & c_i(G-L-1) \\ 0 & 0 & c_i(G-1) & \cdots & c_i(G-L-2) \\ \vdots & & \ddots & & \vdots \\ 0 & 0 & 0 & \cdots & c_i(G-1) \\ 0 & 0 & 0 & \cdots & 0 \\ \vdots & \ddots & & \ddots & \vdots \\ 0 & 0 & 0 & 0 & 0 \end{matrix}\right] \begin{matrix} \uparrow \\ (L-1)\times L \\ \\ \downarrow \\ \uparrow \\ (G-L+1)\times L \\ \downarrow . \end{matrix} \tag{3.12}$$

From (3.10), (3.11) and (3.12), it is observed that only the first $(L-1)$ elements of $\tilde{\mathbf{r}}(n)$ are distorted due to ISI. The presence of ISI is pictorially illustrated in

Fig. 3.1. Removing the first $(L-1)$ rows of matrix $\acute{\mathbf{B}}_i$ results in a zero matrix. Therefore, by discarding the first $(L-1)$ elements of $\tilde{\mathbf{r}}(n)$, we obtain $N = (G-L+1)$

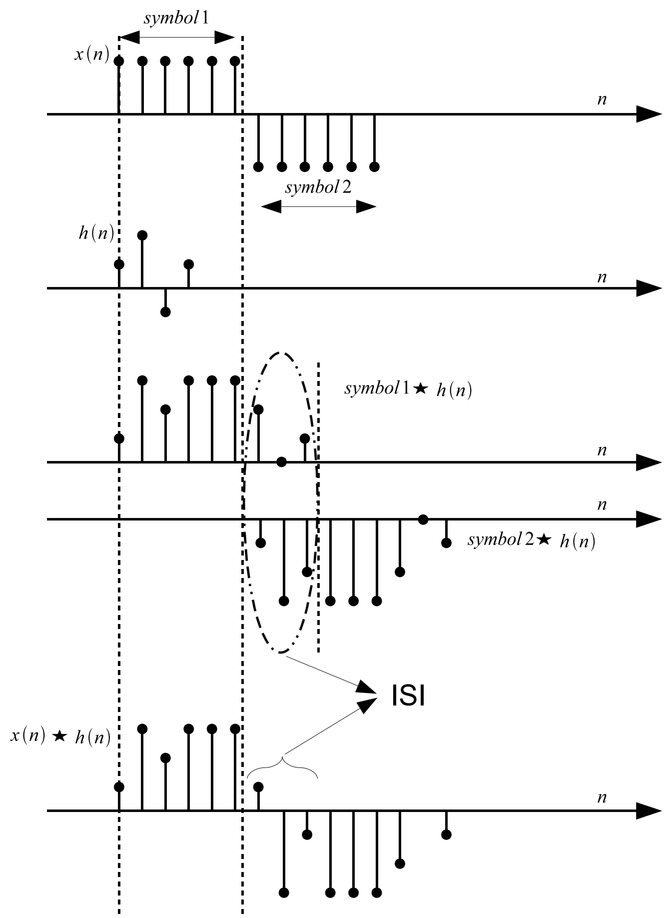

Fig. 3.1: Inter symbol interference.

ISI free samples for the nth symbol duration, i.e.,

$$\mathbf{r}(n) = [y(nG+L-1), y(nG+L), \cdots, y(nG+G-1)]^T \tag{3.13}$$

$$= \sum_{i=0}^{T-1} e^{(jnG+L-1)\phi_i} \mathbf{Z}_G(\phi_i) \widetilde{\mathbf{B}}_i \mathbf{h}_i s_i(n) + \mathbf{v}(n), \tag{3.14}$$

where $\mathbf{r}(n)$ is a $(N \times 1)$ vector, and $\mathbf{v}(n) = [v(nG+L-1), v(nG+L), \cdots, v(nG+G-1)]^T$. The $(N \times L)$ matrix $\widetilde{\mathbf{B}}_i$ is obtained by discarding the top $(L-1)$ row vectors from $\mathbf{B}_i$. It is assumed that $E[\mathbf{v}(n)\mathbf{v}^H(n)] = \sigma^2 \mathbf{I}_N$. The received samples in (3.14) are ISI free, but due to the presence of other users there is still MAI.

3.2 ACFO and CIR Estimation Problem

3.2.1 Objective

The objective is to estimate the ith user's ACFO and CIR values using only the received ISI free samples in $\mathbf{r}(n)$ and the knowledge of the user's spreading code. Thus, the estimator to be formulated is called *blind estimator* or *non-data-aided estimator*.

3.2.2 Assumptions

The following assumptions are necessary to ensure proper estimation of the desired user's ACFO and CIR.

AS1 : Vectors $\{\mathbf{Z}_G(\phi_i)\widetilde{\mathbf{B}}_i\mathbf{h}_i\}_{i=0}^{T-1}$ are linearly independent for any realization of $\mathbf{h}_i$ and any $\phi_i \in [-\pi, \pi)$.

Following the analysis in Section 2.2, it is observed that assumption **AS1** guarantees the signal subspace $(\mathbf{U}_s)$ dimension to be $\mathcal{S} = T$. Therefore, the dimension of noise subspace $(\mathbf{U}_n)$ is $(N - \mathcal{S})$. The $(N \times \mathcal{S})$ matrix $\mathbf{U}_s$ and $(N \times (N - \mathcal{S}))$

matrix $\mathbf{U}_n$ are estimated following the procedure stated in Section 2.5.

AS2 : The dimension of intersection space $col(\mathbf{U}_s)$ and $col(\mathbf{Z}_G(\phi)\widetilde{\mathbf{B}}_i)$ is 1 when $\phi = \phi_i$ and 0 when $\phi \neq \phi_i$ for $i = 0, 1, \cdots, T-1$. The basis for this intersection space is $\mathbf{Z}_G(\phi_i)\widetilde{\mathbf{B}}_i\mathbf{h}_i$.

Assumption **AS2** is essential to guarantee the identifiability of the estimated parameters (ACFO and CIR) [75].

3.2.3 Cost Function

The orthogonality between the signal and noise subspaces (see equation (2.19)) results in [84]

$$\mathbf{U}_n^H \mathbf{Z}_G(\phi_i)\widetilde{\mathbf{B}}_i\mathbf{h}_i = \mathbf{0}_{(N-\mathcal{S})\times 1}, \quad \text{for } i = 0, 1, \cdots, T-1, \tag{3.15}$$

Equation (3.15) can be written as

$$\mathbf{\Gamma}_i(\phi_i)\mathbf{h}_i = \mathbf{0}_{(N-\mathcal{S})\times 1} \quad \text{for } i = 0, 1, \cdots, T-1, \tag{3.16}$$

where

$$\mathbf{\Gamma}_i(\phi_i) = \mathbf{U}_n^H \mathbf{Z}_N(\phi_i)\widetilde{\mathbf{B}}_i, \tag{3.17}$$

is a $((N-\mathcal{S})\times L)$ matrix. In general, the equality in equation (3.16) is not satisfied due to the presence of noise and use of finite precision computations. Therefore, the ith user's cost function to minimize is obtained using the l_2-norm (not considering the trivial solution $\mathbf{h} = \mathbf{0}_{L\times 1}$) as:

$$\min_{\phi,\mathbf{h},\mathbf{h}\neq\mathbf{0}_{L\times 1}} J(\phi,\mathbf{h}) = \|\mathbf{\Gamma}_i(\phi)\mathbf{h}\|^2 = \mathbf{h}^H\mathbf{\Gamma}_i^H(\phi)\mathbf{\Gamma}_i(\phi)\mathbf{h}. \tag{3.18}$$

The cost function in (3.18) is a function of scalar ϕ and vector $\mathbf{h}$. The $\{\phi,\mathbf{h}\}$ which minimizes $J(\phi,\mathbf{h})$ is the ith user's estimated ACFO and CIR $\{\hat{\phi}_i,\hat{\mathbf{h}}_i\}$.

3.3 Generalized Eigenvalue Problem Method

The joint ACFO and CIR estimation problem is converted into a generalized eigenvalue problem [102] by using Taylor's series expansion for the complex exponential in the cost function [85]. The diagonal matrix $\mathbf{Z}_N(\phi)$ can be written as

$$\mathbf{Z}_N(\phi) \quad = \quad e^{j\frac{N-1}{2}\phi}\mathbf{P}_N(\phi), \tag{3.19}$$

where

$$\mathbf{P}_N(\phi) \quad = \quad diag\left(\left[e^{-j\frac{N-1}{2}\phi}, e^{-j\frac{N-3}{2}\phi}, \cdots, e^{j\frac{N-1}{2}\phi}\right]^T\right), \tag{3.20}$$

is a $(N\times N)$ diagonal matrix. Using Taylor's series expansion for the exponential terms in $\mathbf{P}_N(\phi)$, matrix $\mathbf{Z}_N(\phi)$ can be expressed as

$$\mathbf{Z}_N(\phi) \quad = \quad e^{j\frac{N-1}{2}\phi}\sum_{l=0}^{\infty}\frac{(j\phi)^l}{2^l l!}\mathbf{A}^l, \tag{3.21}$$

where

$$\mathbf{A} = diag\left([-(N-1), -(N-3), \cdots, (N-1)]^T\right). \quad (3.22)$$

To avoid singularity of matrix $\mathbf{A}$, G is selected such that $N = G - L + 1$ is an even integer. For small ACFO values, the series in (3.21) can be truncated. Thus, matrix $\mathbf{Z}_N(\phi)$ can be approximated by an rth order Taylor's series expansion as

$$\mathbf{Z}_N(\phi) \approx e^{j\frac{N-1}{2}\phi} \sum_{l=0}^{r} \frac{(j\phi)^l}{2^l l!} \mathbf{A}^l. \quad (3.23)$$

Substituting (3.23) into (3.18), the cost function is approximated as follows:

$$\begin{aligned} J(\phi, \mathbf{h}) &\approx \left\| \mathbf{U}_n^H \sum_{l=0}^{r} \frac{(j\phi)^l}{2^l l!} \mathbf{A}^n \widetilde{\mathbf{B}}_i \mathbf{h} \right\|^2 \\ &= \left(\sum_{k=0}^{r} \frac{(j\phi)^k}{2^k k!} \mathbf{U}_n^H \mathbf{A}^k \widetilde{\mathbf{B}}_i \mathbf{h} \right)^H \left(\sum_{l=0}^{r} \frac{(j\phi)^l}{2^l l!} \mathbf{U}_n^H \mathbf{A}^l \widetilde{\mathbf{B}}_i \mathbf{h} \right) \\ &= \sum_{k=0}^{r} \sum_{l=0}^{r} (-1)^k (j\phi)^{k+l} \mathbf{h}^H \mathbf{F}_{i,k}^H \mathbf{F}_{i,l} \mathbf{h}, \end{aligned} \quad (3.24)$$

where the $((N - \mathcal{S}) \times L)$ matrix $\mathbf{F}_{i,l}$ for the ith user is defined as

$$\mathbf{F}_{i,l} = \frac{\mathbf{U}_n^H \mathbf{A}^l \widetilde{\mathbf{B}}_i}{2^l l!} \quad \text{for } l = 0, 1, \cdots, r. \quad (3.25)$$

Let $\mathbf{E}_{i,l}$ denote a $(L \times L)$ Hermitian matrix given by

$$\mathbf{E}_{i,l} = (j)^l \sum_{m=0}^{l} (-1)^m \mathbf{F}_{i,m}^H \mathbf{F}_{i,l-m}, \quad (3.26)$$

for $l = 0, 1, \cdots, 2r$ and $i = 0, 1, \cdots, T-1$. Using (3.26), the cost function in (3.24) can be written as

$$J(\phi, \mathbf{h}) \approx \sum_{l=0}^{2r} \phi^l \mathbf{h}^H \mathbf{E}_{i,l} \mathbf{h}. \tag{3.27}$$

The ith user's ACFO and CIR can be estimated by minimizing the approximate cost function in (3.27). To find the parameters $\{\phi, \mathbf{h}\}$ which minimize the cost function, the partial derivative of the cost function w.r.t $\mathbf{h}$ is equated to zero, i.e.,

$$\mathbf{E}_{i,0}\mathbf{h} + \phi\mathbf{E}_{i,1}\mathbf{h} + \phi^2\mathbf{E}_{i,2}\mathbf{h} + \cdots + \phi^{2r}\mathbf{E}_{i,2r}\mathbf{h} \;\; = \;\; \mathbf{0}_{L\times 1}. \tag{3.28}$$

Equation (3.28) can be easily converted into a *generalized eigenvalue problem* which can be easily solved [102]. A set of $(2r+1)$ column vectors $\{\mathbf{a}_l\}_{l=0}^{2r}$ of dimension $(L \times 1)$ are defined as follows:

$$\mathbf{a}_0 = \mathbf{h} \quad \text{and} \quad \mathbf{a}_l = \phi\mathbf{a}_{l-1} \quad \text{for } l = 1, 2, \cdots 2r. \tag{3.29}$$

Substituting (3.29) into (3.28), we obtain

$$\mathbf{E}_{i,0}\mathbf{a}_0 + \mathbf{E}_{i,1}\mathbf{a}_1 + \mathbf{E}_{i,2}\mathbf{a}_2 + \cdots + \mathbf{E}_{i,2r}\mathbf{a}_{2r} \;\; = \;\; \mathbf{0}_{L\times 1}. \tag{3.30}$$

The $(L \times L)$ Hermitian matrix $\mathbf{E}_{i,2r}$ is assumed to be non-singular. Therefore, (3.30) can be rewritten as

$$\mathbf{a}_{2r} \;\; = \;\; -\left[\mathbf{E}_{i,2r}^{-1}\mathbf{E}_{i,0}\mathbf{a}_0 + \mathbf{E}_{i,2r}^{-1}\mathbf{E}_{i,1}\mathbf{a}_1 + \cdots + \mathbf{E}_{i,2r}^{-1}\mathbf{E}_{i,2r-1}\mathbf{a}_{2r-1}\right]. \tag{3.31}$$

Using the equations (3.31) and (3.29), a $(2rL \times 2rL)$ eigensystem is constructed as shown below:

$$\underbrace{\begin{bmatrix} \mathbf{0}_{L\times L} & \mathbf{I}_{L\times L} & \mathbf{0}_{L\times L} & \cdots & \mathbf{0}_{L\times L} \\ \mathbf{0}_{L\times L} & \mathbf{0}_{L\times L} & \mathbf{I}_{L\times L} & \cdots & \mathbf{0}_{L\times L} \\ \vdots & \vdots & \vdots & \ddots & \vdots \\ \mathbf{0}_{L\times L} & \mathbf{0}_{L\times L} & \mathbf{0}_{L\times L} & \cdots & \mathbf{I}_{L\times L} \\ -\mathbf{E}_{i,2r}^{-1}\mathbf{E}_{i,0} & -\mathbf{E}_{i,2r}^{-1}\mathbf{E}_{i,1} & -\mathbf{E}_{i,2r}^{-1}\mathbf{E}_{i,2} & \cdots & -\mathbf{E}_{i,2r}^{-1}\mathbf{E}_{i,2r-1} \end{bmatrix}}_{\text{sparse matrix}}$$

$$\times \begin{bmatrix} \mathbf{a}_0 \\ \mathbf{a}_1 \\ \vdots \\ \mathbf{a}_{2r-2} \\ \mathbf{a}_{2r-1} \end{bmatrix} = \phi \begin{bmatrix} \mathbf{a}_0 \\ \mathbf{a}_1 \\ \vdots \\ \mathbf{a}_{2r-2} \\ \mathbf{a}_{2r-1} \end{bmatrix}. \tag{3.32}$$

Using EVD, eigenvalues and eigenvectors of the sparse matrix in (3.32) are obtained. The ith user's estimated ACFO value ($\hat{\phi}_i$) is given by the real part of the minimum eigenvalue. Though, all the eigenvalue for the sparse matrix will solve (3.32), only the minimum eigenvalue is chosen as the Taylor's series is valid only for small ACFO values. The CIR is estimated by normalizing the $(L \times 1)$ vector containing the first L elements of the eigenvector corresponding to the minimum eigenvalue, i.e.,

$$\hat{\mathbf{h}}_i = \frac{\mathbf{a}_0}{\mathbf{a}_0^H \mathbf{a}_0}. \tag{3.33}$$

Thus, both ACFO and CIR are simultaneously estimated. As the method used for solving the generalized eigenvalue problem is used for ACFO and CIR estimation, the estimator is called GEVPM based estimator. The CIR is estimated as an eigenvector and hence there is always a scalar ambiguity associated with the estimate. This scalar ambiguity is explained in detail in Section 3.4.1. Table 3.1 lists the steps involved in GEVPM for ith user.

Table 3.1: Algorithm for GEVPM based estimator.

1	Estimate the noise subspace $\mathbf{U}_n$ from the received signal vectors $\{\mathbf{r}(n)\}_{n=0}^{B-1}$.
2	Construct the $(2rL \times 2rL)$ eigensystem for each user as shown in equation (3.32).
3	Compute the smallest eigenvalue $\hat{\phi}_i$ and the corresponding eigenvector of the sparse matrix constructed in step (3).
4	Estimate $\mathbf{h}_i$ by normalizing the $(L \times 1)$ vector containing the first L elements of the computed eigenvector.

3.4 Proposed Methods

3.4.1 Exact Determinant Minimization Method

Equation (3.16) implies that $\mathbf{h}_i$ lies in the null space of the matrix $\mathbf{\Gamma}_i(\phi_i)$, i.e.,

$$\mathbf{h}_i \in null\left(\mathbf{\Gamma}_i(\phi_i)\right). \tag{3.34}$$

Equation (3.34) holds, iff [109]

$$\mathbf{h}_i \in null\left(\mathbf{\Gamma}_i^H(\phi_i)\mathbf{\Gamma}_i(\phi_i)\right), \tag{3.35}$$

which implies that

$$\mathbf{\Gamma}_i^H(\phi_i)\mathbf{\Gamma}_i(\phi_i)\mathbf{h}_i \;\; = \;\; \mathbf{0}_{L\times 1}. \tag{3.36}$$

Therefore, the linear equations $\mathbf{\Gamma}_i(\phi_i)\mathbf{h}_i = \mathbf{0}$ and $\mathbf{\Gamma}_i^H(\phi_i)\mathbf{\Gamma}_i(\phi_i)\mathbf{h}_i = \mathbf{0}$ have the same solution for $\mathbf{h}_i$ [109]. In order to have a non-trivial solution for $\mathbf{h}_i$ ($\mathbf{h}_i \neq \mathbf{0}$), $\mathbf{\Gamma}_i^H(\phi_i)\mathbf{\Gamma}_i(\phi_i)$ must be a singular matrix, i.e.,

$$det\left(\mathbf{\Gamma}_i^H(\phi_i)\mathbf{\Gamma}_i(\phi_i)\right) \;\; = \;\; 0, \tag{3.37}$$

where $det(\mathbf{X})$ returns the determinant of matrix $\mathbf{X}$. Furthermore, it should be noted that $\mathbf{\Gamma}_i^H(\phi_i)\mathbf{\Gamma}_i(\phi_i)$ is a $(L \times L)$ positive semi-definite Hermitian matrix and hence its determinant is a real number greater than or equal to zero. Since matrix $\mathbf{\Gamma}_i^H(\phi_i)\mathbf{\Gamma}_i(\phi_i)$ is a function of ϕ_i, a simple grid search can be performed in the interval $[-\pi, \pi)$ and the search point ϕ which minimizes $det\left(\mathbf{\Gamma}_i^H(\phi)\mathbf{\Gamma}_i(\phi)\right)$ is the ith user's estimated ACFO value, i.e.,

$$\hat{\phi}_i \;\; = \;\; \arg\min_{\phi}\left\{det(\mathbf{\Gamma}_i^H(\phi)\mathbf{\Gamma}_i(\phi))\right\}. \tag{3.38}$$

Assumption **AS2** ensures that matrix $\mathbf{\Gamma}_i^H(\phi)\mathbf{\Gamma}_i(\phi)$ is rank deficient only when $\phi = \phi_i$. The grid search is performed using a suitable grid size v. Once the ACFO is estimated, the ith user's CIR is obtained as the eigenvector corresponding to the

Table 3.2: Algorithm for EDMM based estimator.

1	Estimate the noise subspace $\mathbf{U}_n$ from the received signal vectors $\{\mathbf{r}(n)\}_{n=0}^{B-1}$.
2	To estimate ϕ_i, perform a grid search in the interval $[-\pi, \pi)$ as follows: Initialization: Let $\hat{\phi}_i = -\pi$, $\phi = -\pi$ and $value = det\left(\mathbf{\Gamma}_i^H(\phi)\mathbf{\Gamma}_i(\phi)\right)$. a. $\phi = \phi + v$, if $\phi \geq \pi$ then goto step 3, else goto step 2b. b. $temp = det\left(\mathbf{\Gamma}_i^H(\phi)\mathbf{\Gamma}_i(\phi)\right)$. c. If $temp < value$ then $\hat{\phi}_i = \phi$ and $value = temp$, else goto step 2d. d. Goto step 2a.
3	Estimate $\mathbf{h}_i$ as the eigenvector corresponding to the minimum eigenvalue of the matrix $\mathbf{\Gamma}_i^H(\hat{\phi}_i)\mathbf{\Gamma}_i(\hat{\phi}_i)$.

minimum eigenvalue of matrix $\mathbf{\Gamma}_i^H(\hat{\phi}_i)\mathbf{\Gamma}_i(\hat{\phi}_i)$, i.e.,

$$\hat{\mathbf{h}}_i = \arg \min_{\mathbf{h}, \mathbf{h}^H\mathbf{h}=1} \left\{ \mathbf{h}^H \mathbf{\Gamma}_i^H(\hat{\phi}_i)\mathbf{\Gamma}_i(\hat{\phi}_i)\mathbf{h} \right\}. \tag{3.39}$$

The eigenvector corresponding to the minimum eigenvalue is chosen in order to minimize the cost function $J(\phi, \mathbf{h})$ in (3.18). It should be noted that $\mathbf{h} = \gamma\mathbf{h}_i$ lies in the null space of matrix $\mathbf{\Gamma}_i^H(\phi_i)\mathbf{\Gamma}_i(\phi_i)$, i.e., $\gamma\mathbf{h}_i \in null\left(\mathbf{\Gamma}_i^H(\hat{\phi}_i)\mathbf{\Gamma}_i(\hat{\phi}_i)\right)$ for any scalar $\gamma \in \mathcal{C}$. The unit norm constraint imposed on $\mathbf{h}$ implies that $\gamma = e^{j\zeta}$, where ζ is a real-valued scalar. Therefore, the estimated CIR is $\hat{\mathbf{h}}_i = e^{j\hat{\zeta}}\mathbf{h}_i$, where $\hat{\zeta}$ is unknown. This causes a scalar ambiguity in the estimated CIR. The scalar ambiguity problem could be circumvented by employing differential encoding at the transmitter and performing differential detection at the receiver.

In this method, no approximation is used for $\mathbf{Z}_N(\phi)$ matrix and the determinant of matrix $\mathbf{\Gamma}_i^H(\phi)\mathbf{\Gamma}_i(\phi)$ is minimized. Therefore, the estimator is called exact determinant minimization method (EDMM) based estimator and its algorithm is listed in Table 3.2.

3.4.2 Approximate Determinant Minimization Method

Our approximate determinant minimization method (ADMM) based estimator is the same as EDMM, except for matrix $\mathbf{\Gamma}_i^H(\phi)\mathbf{\Gamma}_i(\phi)$ being approximated using Taylor's series expansion. The main objective of ADMM is to reduce the computational complexity involved in the grid search. During the grid search in EDMM, the $(L \times L)$ matrix $\mathbf{\Gamma}_i^H(\phi)\mathbf{\Gamma}_i(\phi)$ needs to be computed for every search point ϕ. This involves $O(\mathfrak{s}(G^2L + L^3))$ number of complex multiplications where $\mathfrak{s}$ denotes the number of search points. To reduce the computational complexity, matrix $\mathbf{\Gamma}_i^H(\phi)\mathbf{\Gamma}_i(\phi)$ is approximated by a polynomial matrix as follows:

$$\mathbf{\Gamma}_i^H(\phi)\mathbf{\Gamma}_i(\phi) \approx \widetilde{\daleth}_i(\phi) = \mathbf{E}_{i,0} + \phi\mathbf{E}_{i,1} + \phi^2\mathbf{E}_{i,2} + \cdots + \phi^{2r}\mathbf{E}_{i,2r}. \tag{3.40}$$

The polynomial matrix in (3.40) is obtained using the rth order Taylor's series expansion for $\mathbf{Z}_N(\phi)$ as shown in Section 3.3. Matrices $\{\mathbf{E}_{i,l}\}_{l=0}^{2r}$ for $i = 0, 1, \cdots, T-1$ are computed before the search. Therefore, construction of $\mathbf{\Gamma}_i^H(\phi)\mathbf{\Gamma}_i(\phi)$ for each search point requires only $2rL^2$ number of multiplications which renders ADMM to be less computationally intensive than EDMM. However, prior knowledge about the interval over which the users' ACFO values are present is required to chose a suitable order r for the Taylor's series approximation. This prior knowledge can also be used to limit the search interval. For example, if $\phi_i \in [f_l, f_r]$, then the grid search can be done over the interval $[f_l, f_r]$. The CIR is estimated as the eigenvector corresponding to the minimum eigenvalue of matrix $\mathbf{\Gamma}_i^H(\hat{\phi}_i)\mathbf{\Gamma}_i(\hat{\phi}_i)$. Therefore, there is a scalar ambiguity associated with the estimated CIR as in GEVPM and EDMM based estimators. Table 3.3 lists the algorithm for the ith user's ADMM based estimator. To estimate a large ACFO, a higher order Taylor's series approximation is to be used.

Table 3.3: Algorithm for ADMM based estimator.

1	Estimate the noise subspace $\mathbf{U}_n$ from the received signal vectors $\{\mathbf{r}(n)\}_{n=0}^{B-1}$.
2	To estimate ϕ_i, perform a grid search in the range $[f_l, f_r]$ as follows: Initialization: Let $\hat{\phi}_i = f_l$, $\phi = f_l$ and $value = det\left(\widetilde{\beth}_i(\phi)\right)$. a. $\phi = \phi + v$, if $\phi > f_r$ then goto step 3, else goto step 2b. b. Compute $\widetilde{\beth}_i(\phi) = \sum_{l=0}^{2r} \phi^l \mathbf{E}_{i,l}$. c. $temp = det\left(\widetilde{\beth}_i(\phi)\right)$. d. If $temp < value$ then $\hat{\phi}_i = \phi$ and $value = temp$, else goto step 2e. e. Goto step 2a.
3	Estimate $\mathbf{h}_i$ as the eigenvector corresponding to the smallest eigenvalue of the matrix $\mathbf{\Gamma}_i^H(\hat{\phi}_i)\mathbf{\Gamma}_i(\hat{\phi}_i)$.

3.5 Computational Complexity Comparison

The computational complexity is analyzed only for the estimation of ACFO and CIR. The computational complexity involved in computing the noise subspace using any batch method is $O(N^3)$. However, the use of some adaptive algorithms for subspace estimation can reduce this computational complexity by one order [110]-[114].

GEVPM:

The computational complexity involved in constructing the $(2rL \times 2rL)$ eigensystem is approximately $O([(2r+1)(G^2L+L^3)])$ and computing the EVD for this eigensystem requires $O((2rL)^3)$ number of multiplications.

Li & Liu:

In order to compare the computational complexity, we also consider the estimator in [84] proposed by Li & Liu. Li & Liu jointly estimated the ACFO and CIR without using any pilots, but the estimator requires the computation of inverse of a polynomial matrix. The polynomial matrix is of dimension $(RL \times (N+R-1)(L-1))$, where $R > (N-1)(L-1)$. The computation of inverse requires $O((RL)^3)$ multiplications. The ACFO is estimated by searching the spectrum. This involves $O(\mathfrak{s}NL)$ multiplications, where $\mathfrak{s}$ denotes the number of search points. Estimating the CIR involves $O(NL^3+G^2)$ multiplications.

EDMM:

Each search point ϕ requires the computation of $(L \times L)$ matrix $\mathbf{\Gamma}_i^H(\phi)\mathbf{\Gamma}_i(\phi)$ and $det\left(\mathbf{\Gamma}_i^H(\phi)\mathbf{\Gamma}_i(\phi)\right)$. The determinant of a matrix is equal to the product of its eigenvalues. Thus, EVD can be used to compute the determinant during the grid search. EVD also computes the eigenvectors and hence the CIR estimate can be directly obtained from the computed eigenvectors. Therefore, the complete grid search requires $O(\mathfrak{s}(G^2L + 2L^3))$ multiplications, where $\mathfrak{s}$ denotes the number of search points.

ADMM:

The main difference between EDMM and ADMM resides in the computation of matrix $\mathbf{\Gamma}_i^H(\phi)\mathbf{\Gamma}_i(\phi)$. The computational complexity involved in the construction of matrices $\{\mathbf{E}_{i,l}\}_{l=0}^{2r}$ and $\widetilde{\daleth}_i(\phi)$ are $O([(2r+1)(G^2L+L^3)])$ and $O(2rL^2)$, respectively. For each search point, only matrix $\widetilde{\daleth}_i(\phi)$ is constructed and its determinant is computed. Thus, the computational complexity for the grid search over $\mathfrak{s}$ search points is $O(\mathfrak{s}(2rL^2 + L^3))$ which is relatively less when compared with the computational complexity for the grid search in EDMM.

The net computational complexity for all the above discussed methods are tabulated in Table 3.4. From Table 3.4, it is evident that the computation of

Table 3.4: Computational complexity comparison.

Estimator	Computational complexity
GEVPM	$O(N^3) + O\left([(2r+1)(G^2L + L^3)]\right) + O\left((2rL)^3\right)$
Li & Liu	$O(N^3) + O((RL)^3) + O(\mathfrak{s}NL) + O(NL^3 + G^2)$
EDMM	$O(N^3) + O\left(\mathfrak{s}(G^2L + 2L^3)\right)$
ADMM	$O(N^3) + O\left([(2r+1)(G^2L + L^3)]\right) + O\left(\mathfrak{s}(2rL^2 + L^3)\right)$

inverse for the polynomial matrix in Li & Liu's estimator renders it to be computational intensive. For small CFO values, r can be small. In this case, GEVPM has low-computational complexity compared to EDMM and ADMM based estimators. However, it will be later shown through computer simulations that EDMM and ADMM offer better performance than GEVPM.

3.6 Simulation Results

For computer simulations, a DS-CDMA system with spreading gain $G = 32$ and $T = 10$ users is considered. The number of received signal vectors used for subspace estimation is $B = 100$. The length of CIR for all users is assumed to be $L = 3$. The ith user's MSEs for ACFO and CIR estimates are computed as the mean of $\|\mathbf{h}_i - \hat{\mathbf{h}}_i\|^2$ and $(\phi_i - \hat{\phi}_i)^2$, respectively. The Cramer-Rao lower bound (CRLB) is computed as shown in Appendix A

Cost Function

Let $Y_\phi = det(\mathbf{\Gamma}_i^H(\phi)\mathbf{\Gamma}_i(\phi))$. Assuming the users' data symbols to be quadrature phase-shift keying (QPSK) modulated and SNR = 15dB, the plot of Y_ϕ for user $i = 0$ is given in Fig. 3.2. The cost function is plotted for four different cases, i.e., for $\phi_0 = -2.3$, $\phi_0 = -0.7$, $\phi_0 = 1$ and $\phi_0 = 2.1$. From Fig. 3.2, it is observed that the cost function of user $i = 0$ has a global minimum only at the user's true ACFO value.

EDMM vs GEVPM

The performance of GEVPM based estimator is compared with EDMM based estimator for two scenarios. In the first scenario, each user's ACFO value is assumed

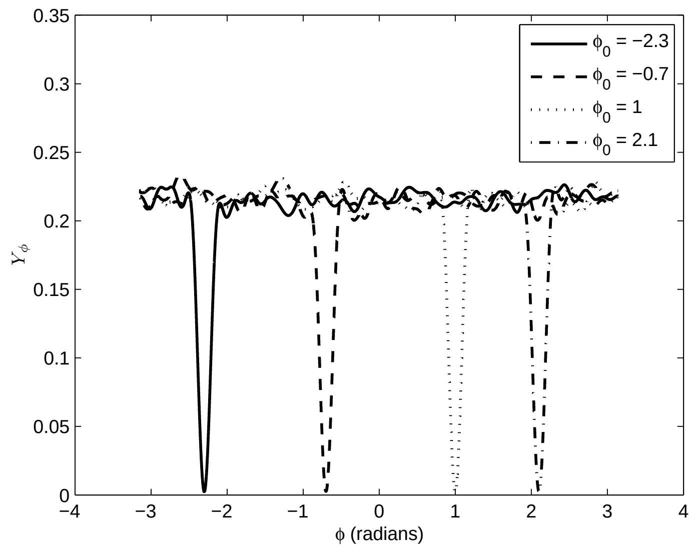

Fig. 3.2: Cost function for DS-CDMA system.

to be a random variable uniformly distributed over the interval $[-0.1, 0.1]$ and for the second scenario, the interval is assumed to be $[-0.2, 0.2]$. The ACFO value in the interval $[-\alpha, \alpha]$ corresponds to CFO of $\pm\alpha/(2\pi T_c)$Hz. Typically $1/T_c = 1.2288$ mega chips per second (Mcps) and hence the CFO is $\pm 1.9557\alpha 10^5$Hz. For a carrier frequency of 2GHz, the above CFO will correspond to $\pm 9.7785\alpha 10^{-3}\%$ of carrier frequency. Thus, when $\alpha = 0.2$, the CFO is $\pm 1.9557 \times 10^{-3}\%$ of 2Ghz which is 39KHz. This CFO value is typical in practical systems. The grid size for the grid search in EDMM is chosen to be $v = 0.001$. If a larger grid size is chosen, then the estimator may not be able to find the global minimum and hence the MSE performance will exhibit an error floor. If a finer grid size is chosen, then the number of search points will be large. This will increase the computational complexity of the estimator. Thus, an optimum grid size is to be chosen by prior

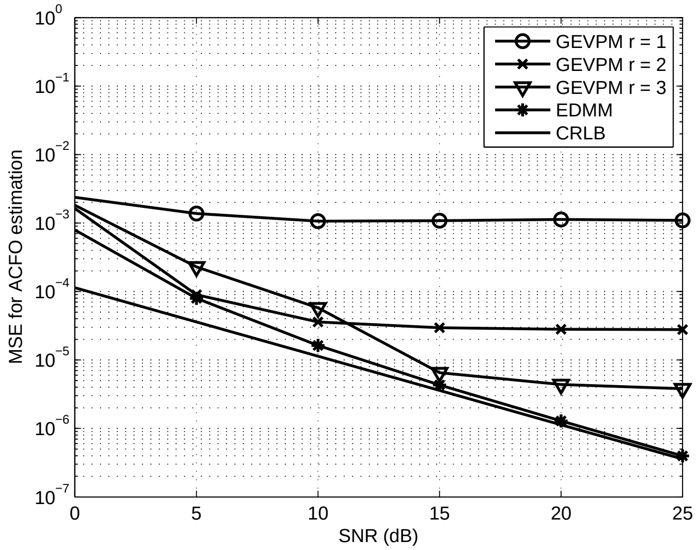

Fig. 3.3: EDMM vs GEVPM – ACFO estimation when $\{\phi_i \in [-0.1, 0.1]\}_{i=0}^{T-1}$.

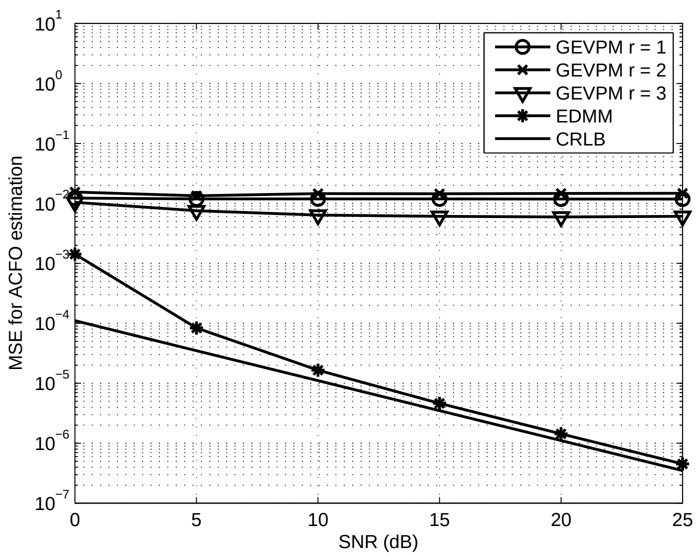

Fig. 3.4: EDMM vs GEVPM – ACFO estimation when $\{\phi_i \in [-0.2, 0.2]\}_{i=0}^{T-1}$.

experimentation and tradeoff between accuracy and computational complexity. As the users' ACFO values are in the interval $[-0.1, 0.1]$ and $[-0.2, 0.2]$ we select grid size $v = 0.001$ to have good estimation accuracy. The MSE for ACFO estimates obtained using GEVPM and EDMM based estimators for the above mentioned scenarios are shown in Fig. 3.3 and Fig. 3.4, respectively. The MSE for CIR estimates obtained using GEVPM and EDMM based estimators for the above mentioned scenarios are shown in Fig. 3.5 and Fig. 3.6, respectively. It is observed that the performance of EDMM is always better than GEVPM and is close to CRLB. This is due to the fact that EDMM uses no approximation. When the users' ACFO values are random variables uniformly distributed over the interval $[-0.1, 0.1]$, the performance of GEVPM based estimator can be improved using a higher order Taylor's series approximation. From Fig. 3.5 it is observed that GEVPM with $r = 3$ order Taylor's series approximation performs closer to EDMM. However, when the users' ACFO values are random variables uniformly distributed over the interval $[-0.2, 0.2]$, $r = 3$ order Taylor's series approximation may not be accurate and hence a larger value for r must be used.

In GEVPM, increasing r will render the sparse matrix in (3.32) even sparser which could lead to matrix ill-conditioning. Furthermore, the eigenvalues of the sparse matrix are in general complex values, whereas the parameter to be estimated is real-valued. Thus, increasing r may not improve the estimation accuracy. Therefore, GEVPM is not suitable to estimate large ACFO values. As there is no sparse matrix in EDMM, it does not suffer from any ill-conditioning. EDMM can estimate the user's ACFO value in the interval $[-\pi, \pi)$.

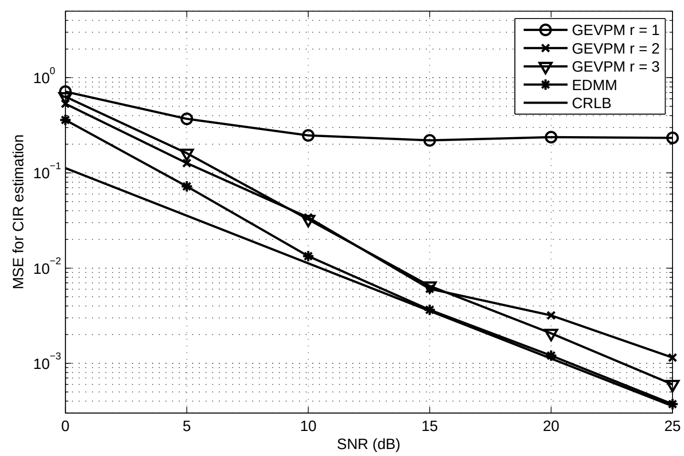

Fig. 3.5: EDMM vs GEVPM – CIR estimation when $\{\phi_i \in [-0.1, 0.1]\}_{i=0}^{T-1}$.

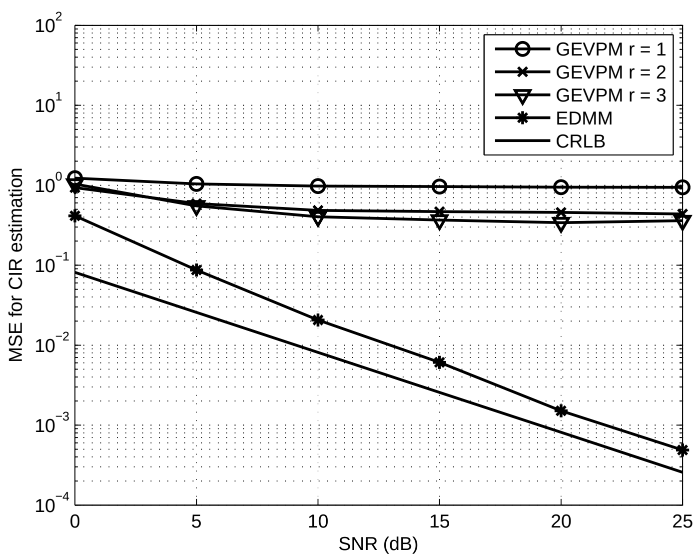

Fig. 3.6: EDMM vs GEVPM – CIR estimation when $\{\phi_i \in [-0.2, 0.2]\}_{i=0}^{T-1}$.

EDMM: In Presence of PN

The MSE performance of the proposed estimator in the presence of phase noise (PN) is obtained through computer simulations. We consider a Gaussian PN model as in [49]. In the presence of PN, the received signal at the base station is given by

$$\mathbf{r}(n) = \sum_{i=0}^{T-1} e^{(jnG+L-1)\phi_i} \dot{\mathbf{Z}}_N(n, \phi_i)\widetilde{\mathbf{B}}_i \mathbf{h}_i s_i(n) + \mathbf{v}(n), \tag{3.41}$$

where the $(N \times N)$ diagonal matrix is given by

$$\dot{\mathbf{Z}}_N(\phi_i) = diag\left(\left[e^{j\theta_i(nG+L-1)}, e^{j(\phi_i+\theta_i(nG+L))}, \cdots, e^{j((N-1)\phi_i+\theta_i(nG+G-1))}\right]^T\right). \tag{3.42}$$

Let $\theta_i(n) = [\theta_i(nG+L-1), \theta_i(nG+L), \theta_i(nG+L+1), \cdots, \theta_i(nG+G-1)]^T$. The element in the kth row and lth column of the Gaussian PN covariance matrix $\mathbf{R}_{\theta_i} = E[\theta_i(n)\theta_i^H(n)]$ is given by

$$\mathbf{R}_{\theta_i}(k,l) = \left(\frac{\pi\omega}{180}\right)^2 e^{-2\pi|k-l|\chi}, \tag{3.43}$$

where $\omega = 3$ and $\chi = 0.005$ were chosen for simulation [49]. Grid size of $v = 0.001$ is used for the grid search. The MSE for ACFO and CIR estimates obtained using EDMM are shown in Figs. 3.7 and 3.8, respectively. From the simulations results, it is observed that the PN does not affect the MSE at low SNR. At high SNR, the MSE for ACFO estimate obtained in the presence of PN, is higher that the MSE for ACFO estimate obtained in the absence of PN. This shows that the EDMM based estimator is not significantly affected by PN.

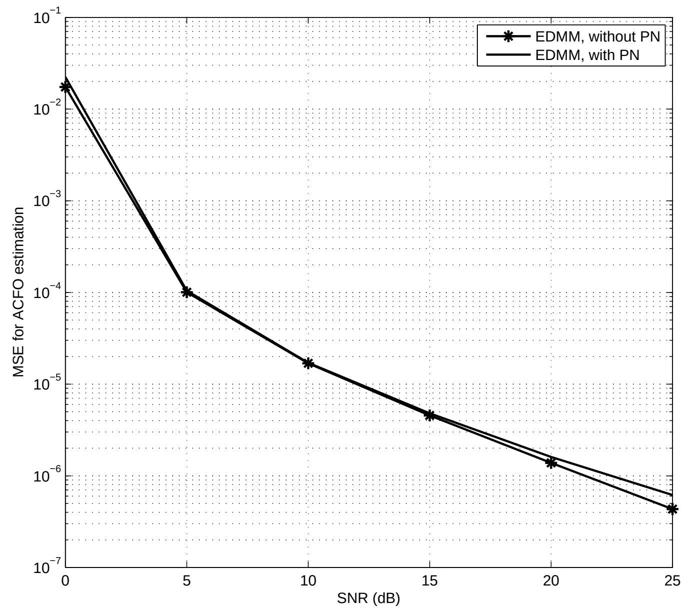

Fig. 3.7: EDMM: ACFO estimation when $\{\phi_i \in [-0.5, 0.5]\}_{i=0}^{T-1}$.

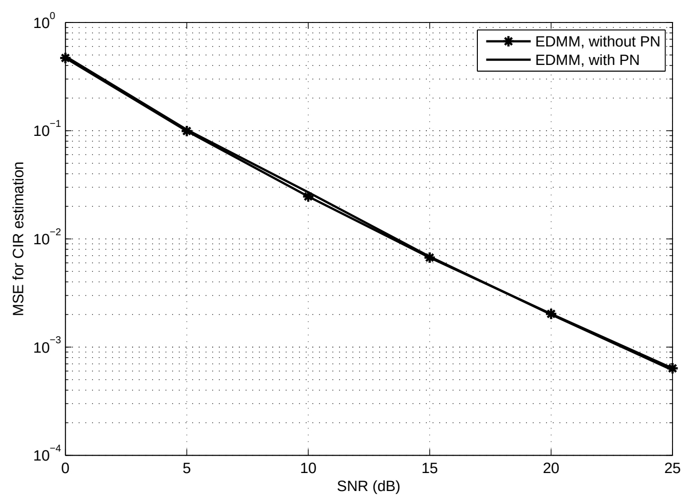

Fig. 3.8: EDMM: CIR estimation when $\{\phi_i \in [-0.5, 0.5]\}_{i=0}^{T-1}$.

ADMM vs GEVPM

The MSE performance of ADMM and GEVPM based estimators for ACFO and CIR estimation are compared in Fig. 3.9 and Fig. 3.10, respectively. The users' ACFO values are assumed to be random variables uniformly distributed over the interval $[-0.2, 0.2]$. The grid size used for the grid search in ADMM is $v = 0.001$. For a given order of Taylor's series approximation, ADMM performs better than

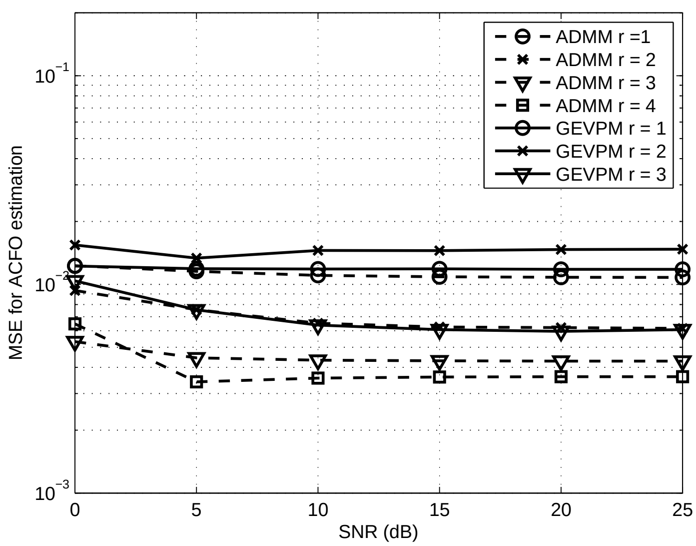

Fig. 3.9: ADMM vs GEVPM – ACFO estimation when $\{\phi_i \in [-0.2, 0.2]\}_{i=0}^{T-1}$.

GEVPM. Furthermore, large ACFO values can be estimated using ADMM by increasing the order of Taylor's series approximation. This is observed through the BER performance obtained through computer simulations. Unlike GEVPM, ADMM uses no sparse matrix and hence increasing r results in improving the performance of ADMM based estimator.

BER Performance

To clearly visualize the advantage of EDMM and ADMM over GEVPM, we investigate the effect of estimation error on BER performance through computer simulations. A subspace-based minimum mean squared error (MMSE) multiuser detector is formulated in Appendix B. The inevitable scalar phase ambiguity in the CIR estimate hinders coherent detection at the receiver. In order to overcome this problem, the transmitted data symbols are differentially encoded at the transmitter and differential detected at the receiver. In computer simulations, the users' data symbols are assumed to be differential BPSK (DBPSK) modulated. The BER performance of the estimator is compared with the ideal subspace-based MMSE multiuser detector, i.e., the multiuser detector (as in Appendix B) with knowledge of users' true ACFO and CIR values. The grid size used for the grid search in EDMM and ADMM is $v = 0.001$. The BER performance curves for GEVPM, ADMM and EDMM based estimators are shown in Fig. 3.11, Fig. 3.12 and Fig. 3.13, respectively. It is observed that the BER performance obtained using GEVPM is not close to the BER performance of the ideal detector as ϕ_i is relatively large for this method. Even increasing the order of Taylor's series approximation does not improve the BER performance. In Fig. 3.11, it can be seen that the BER performance for $r = 3$ is better than $r = 4$ and $r = 5$. This observation is attributed to the incapability of GEVPM to accurately estimate large ACFO for large value of r. In ADMM, the BER performance is observed to improve and approach the ideal detector's BER performance with increase in the order of Taylor's series approximation. Fig. 3.13, shows that the BER performance obtained using EDMM based estimator overlaps with the ideal detector's BER performance.

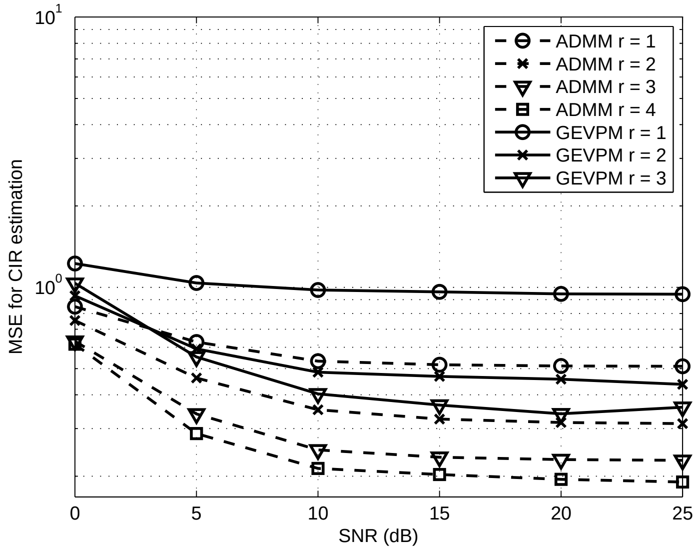

Fig. 3.10: ADMM vs GEVPM – CIR estimation when $\{\phi_i \in [-0.2, 0.2]\}_{i=0}^{T-1}$.

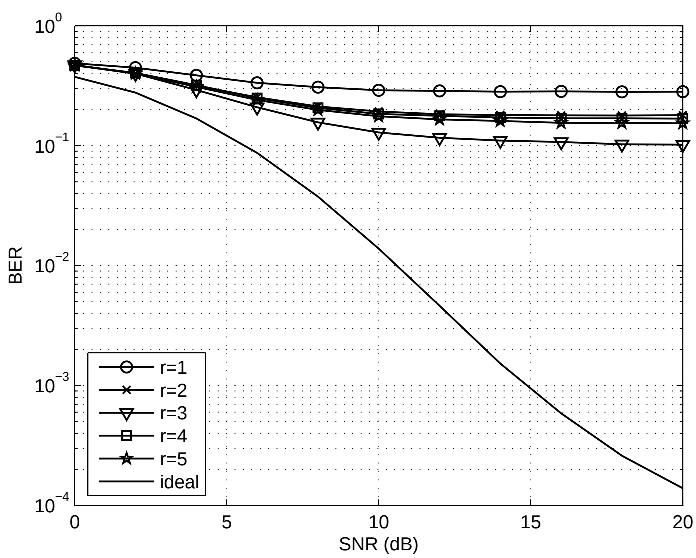

Fig. 3.11: BER performance for GEVPM when $\{\phi_i \in [-0.2, 0.2]\}_{i=0}^{T-1}$.

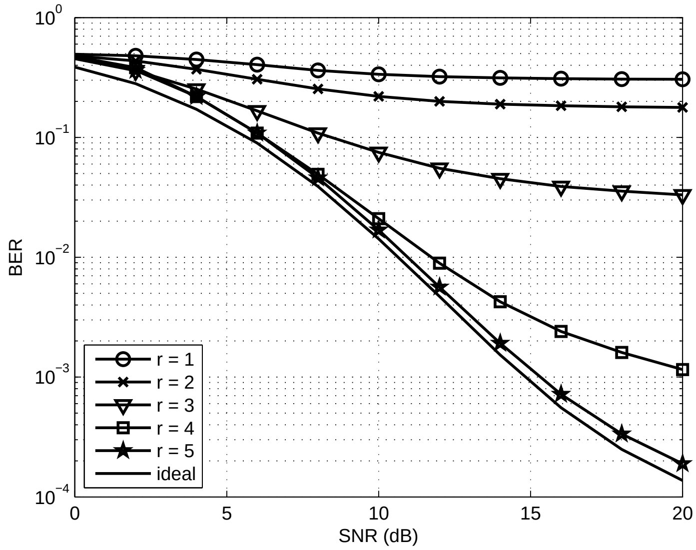

Fig. 3.12: BER performance for ADMM when $\{\phi_i \in [-0.2, 0.2]\}_{i=0}^{T-1}$.

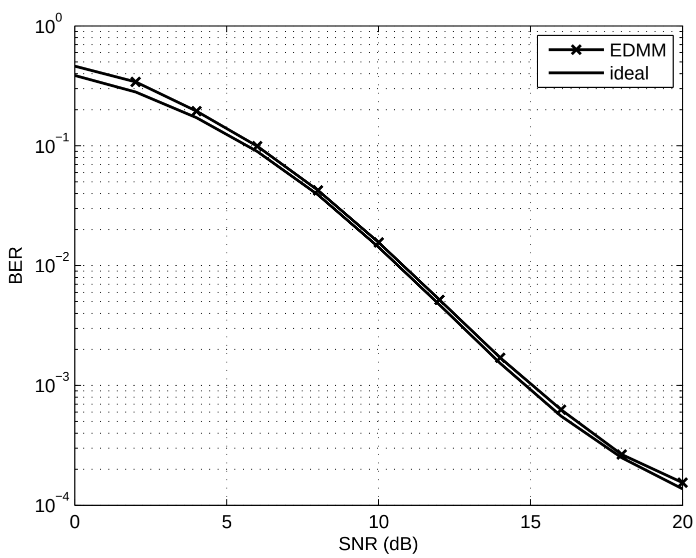

Fig. 3.13: BER performance for EDMM when $\{\phi_i \in [-0.5, 0.5]\}_{i=0}^{T-1}$.

Therefore, to estimate small ACFO values ADMM based estimator can be used and to estimate large ACFO values EDMM based estimator can be used. Note that, it is also possible to have a hybrid estimator where EDMM and ADMM based estimators are implemented in parallel. Depending on the *a priori* information available at the receiver, power limitation and computational complexity, the receiver can choose either one of the estimators for joint ACFO and CIR estimation.

3.7 Conclusion

In this chapter, the discrete time received signal in the uplink of a quasi-synchronous DS-CDMA system in the presence of CFO was systematically formulated. The existing GEVPM based estimator for joint ACFO and CIR estimation was outlined. Higher order Taylor's series approximation when used to estimate large ACFO values could result in ill-conditioning of the sparse matrix in GEVPM. Thus, GEVPM cannot be used for estimating large ACFO values. To overcome this problem, two subspace-based blind estimators, namely EDMM and ADMM, were proposed. EDMM and ADMM do not have any sparse matrix. The ACFO was estimated by minimizing the determinant of a small dimensional positive semi-definite matrix. EDMM employed no approximation and hence it could estimate large ACFO values, i.e., estimation could be done for $\phi_i \in [-\pi, \pi)$. ADMM used Taylor's series approximation in order to reduce the computational complexity of the grid search. Though ADMM used Taylor's series approximation, it offered better performance than GEVPM as there was no sparse matrix in ADMM. Furthermore, it was observed that performance of ADMM improved as the approximation order was increased. It should be noted that ACFO is estimated as the real part of an eigenvalue in GEVPM. This eigenvalue could be a complex number and hence the ACFO estimate may not be accurate. However, in the case of EDMM and ADMM, the ACFO is estimated through a search over real-valued search points. Thus, EDMM and ADMM based estimators give an accurate estimate for the ACFO.

Chapter 4

CP-CDMA System

In chapter 3, subspace-based blind joint ACFO and CIR estimators were proposed for the uplink transmission in DS-CDMA systems. These estimators used ISI free received samples for estimation. This motivates us in using techniques at the transmitter which can help the receiver to eliminate ISI. The use of cyclic prefix in OFDM system is known to eliminate ISI and leads to a low computational complexity channel equalizer at the receiver [33]. To exploit the benefits of cyclic prefix in single carrier systems, single carrier cyclic prefix (SCCP) system was proposed in the literature [26] [27]. CP-CDMA system is derived from SCCP and DS-CDMA systems. A DS-CDMA system which employs cyclic prefix is called CP-CDMA system. Unlike DS-CDMA, CP-CDMA can be configured for block transmission. In block transmission, the cyclic prefix is inserted for a block of data symbols instead of inserting for every data symbol. This improves the spectral efficiency as the redundant information being transmitted is reduced. In this chapter, the received signal in the uplink transmission of CP-CDMA system is analyzed in detail. The problem of ACFO and CIR estimation in CP-CDMA is solved by formulating an estimator similar to the EDMM based estimator proposed in chapter 3. Furthermore, a criterion for the selection of users' spreading codes to guarantee the identifiability of ACFO and CIR estimates is outlined. The performance of the proposed estimator is studied through computer simulations.

4.1 System Model

As in chapter 3, T denotes the number of users in the uplink transmission of a quasi-synchronous CP-CDMA system and the ith user's spreading code is assumed to be $\mathbf{c}_i = [c_i(0), c_i(1), \cdots, c_i(G-1)]^T$ with spreading gain $G > T$. For generalized treatment, block transmission is considered. Let Q denote the number of data symbols in the transmitted data block. At the transmitter, Q data symbols from each user are converted from serial to parallel form. This $(Q \times 1)$ vector forms the CP-CDMA data block. The data symbols in the block are spread by a user specific spreading code. The resulting $(N \times 1)$ vector $\mathbf{x}_i(n)$ obtained after spreading is given by

$$\mathbf{x}_i(n) = \mathbf{C}_i \mathbf{s}_i(n), \tag{4.1}$$

where $N = QG$ and $\mathbf{s}_i(n) = [s_i(nQ), s_i(nQ+1), \cdots, s_i(nQ+Q-1)]^T$ is the nth data block with $s_i(l)$ denoting the ith user's data symbol transmitted for the lth data symbol duration. The $(N \times Q)$ matrix $\mathbf{C}_i$ can be expressed as

$$\mathbf{C}_i = \mathbf{I}_Q \otimes \mathbf{c}_i, \tag{4.2}$$

where $\otimes$ denotes the Kronecker product. A cyclic prefix of length P is augmented to vector $\mathbf{x}_i(n)$ to obtain the $((N+P)\times 1)$ vector $\tilde{\mathbf{x}}_i(n) = [\tilde{x}_i(n(N+P)+0), \tilde{x}_i(n(N+P)+1), \cdots, \tilde{x}_i(n(N+P)+N+P-1)]^T$ as follows:

$$\tilde{\mathbf{x}}_i(n) \;=\; \mathbf{T}_{cp}\mathbf{x}_i(n), \tag{4.3}$$

where the $((N+P)\times N)$ cyclic prefix matrix $\mathbf{T}_{cp}$ is given by

$$\mathbf{T}_{cp} \;=\; \begin{bmatrix} \mathbf{I}_N(N-P+1:N,:) \\ \mathbf{I}_N \end{bmatrix}, \tag{4.4}$$

with $\mathbf{I}_N(N-P+1:N,:)$ denoting the last P row vectors of matrix $\mathbf{I}_N$. The elements of vector $\tilde{\mathbf{x}}_i(n)$ are converted from parallel to serial form, modulated onto normalized pulse shaping function $p(t)$ and transmitted through the channel. Let T_s and T_c denote the duration of the data symbol and the pulse shaping function, respectively. Therefore, the relationship between T_s and T_c is $QT_s = (N+P)T_c$. The ith user's transmitted signal corresponding to the nth data block is given by

$$a_i(t) \;=\; \sum_{l=0}^{N+P-1} \tilde{x}_i(n(N+P)+l)p(t-n(N+P)T_c - lT_c), \tag{4.5}$$

for $t \in [n(N+P)T_c, (n+1)(N+P)T_c)$. The block diagram of the CP-CDMA transmitter is shown in Fig. 4.1. The ith user's transmitted signal when $p(t)$ is a rectangular pulse of duration T_c, $\mathbf{c}_i = [+1,-1,+1,+1,-1]^T/\sqrt{5}$, $Q=2$, $N=10$, $P=2$ and data symbol is BPSK modulated is graphically shown in Fig. 4.2.

The transmitted signal from each user propagates through an independent multipath fading channel and reaches the base station with CFO f_i. Following the

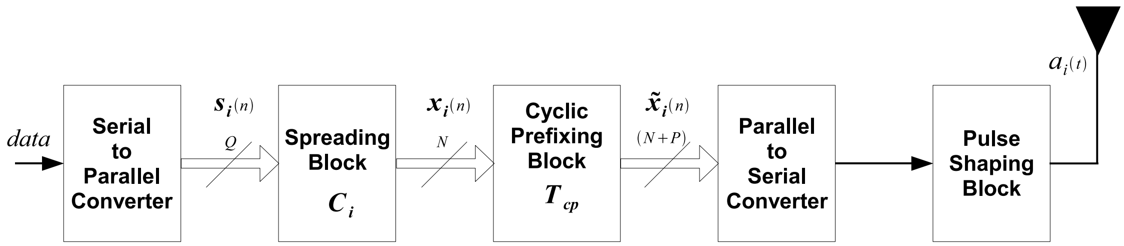

Fig. 4.1: CP-CDMA transmitter.

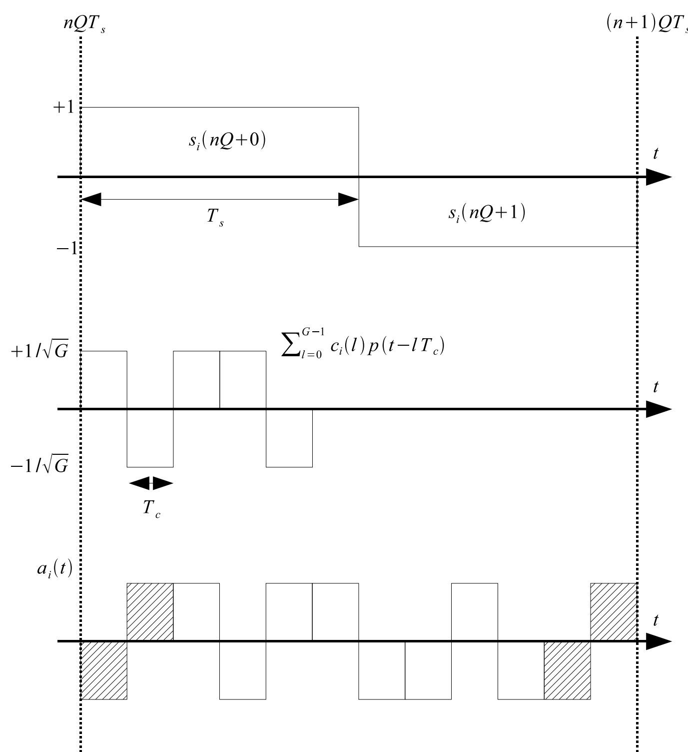

Fig. 4.2: Signal transmitted by ith user in CP-CDMA system.

steps illustrated in Section 3.1 of chapter 3, the signal received at the base station during the nth CP-CDMA symbol duration due to the presence of T users is given by[1]

$$\begin{aligned} y(n(N+P)+p) &= \sum_{i=0}^{T-1}\sum_{n} e^{j(n(N+P)+p)\phi_i} \sum_{l=0}^{N+P-1} \tilde{x}_i(n(N+P)+l)h_i(p-l) \\ &\quad +v(n(N+P)+p), \end{aligned} \tag{4.6}$$

where $h_i(n)$ and $\phi_i = 2\pi f_i T_c$ are the ith user's discrete time CIR and ACFO, respectively. The CIR for all users is assumed to have a maximum channel order of $L-1$. The $(L \times 1)$ CIR vector $\mathbf{h}_i$ is defined as

$$\mathbf{h}_i = \left[h_i(0), h_i(1), \cdots, h_i(L-1)\right]^T . \tag{4.7}$$

The multipath fading channel causes inter block interference (IBI), graphically illustrated in Fig. 4.3, where each transmitted block contains a cyclic prefix followed by Q data symbols. The $(N+P)$ samples corresponding to the nth CP-CDMA symbol duration are stacked to form $\tilde{\mathbf{r}}(n)$ as follows:

$$\tilde{\mathbf{r}}(n) = \left[y(n(N+P)), y(n(N+P)+1), \cdots, y(n(N+P)+N+P-1)\right]^T \tag{4.8}$$

[1] The received signal is sampled at rate $1/T_c$.

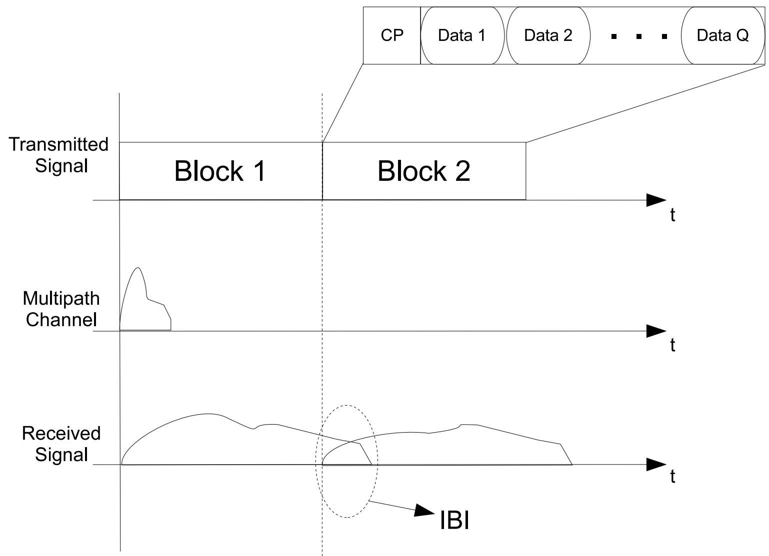

Fig. 4.3: Inter Block Interference.

$$\begin{aligned}
\tilde{\mathbf{r}}(n) &= \sum_{i=0}^{T-1} e^{jn(N+P)\phi_i}\mathbf{Z}_{N+P}(\phi_i)\widetilde{\mathbf{H}}_i\tilde{\mathbf{x}}_i(n) \\
&+ \underbrace{\sum_{i=0}^{T-1} e^{jn(N+P)\phi_i}\mathbf{Z}_{N+P}(\phi_i)\acute{\widetilde{\mathbf{H}}}_i\tilde{\mathbf{x}}_i(n-1)}_{\text{IBI}} + \tilde{\mathbf{v}}(n), \qquad (4.9)
\end{aligned}$$

where $\tilde{\mathbf{v}}(n) = [v(nG+0), v(nG+1), \cdots, v(n(N+P)+N+P-1)]^T$. Matrices $\widetilde{\mathbf{H}}_i$ and $\acute{\widetilde{\mathbf{H}}}_i$ are $((N+P)\times(N+P))$ dimensional Toeplitz matrices whose first column vectors are $[\mathbf{h}_i^T, \mathbf{0}_{(N+P-L)\times 1}]^T$ and $\mathbf{0}_{(N+P)\times 1}$, respectively and their first row vectors are $[h_i(0), \mathbf{0}_{1\times(N+P-1)}]$ and $[\mathbf{0}_{1\times(N+P-L+1)}, h_i(L-1), h_i(L-2), \cdots, h_i(1)]$, respectively. To obtain an IBI free received signal after the removal of the cyclic prefix, the length of the cyclic prefix P is chosen to be $L-1$. After removing the first P elements corresponding to the cyclic prefix, the resulting $(N\times 1)$ vector is given by

$$
\begin{aligned}
\mathbf{r}(n) &= \mathbf{R}_{cp}\tilde{\mathbf{r}}(n) \\
&= \sum_{i=0}^{T-1} e^{jn(N+P)\phi_i}\mathbf{R}_{cp}\mathbf{Z}_{N+P}(\phi_i)\widetilde{\mathbf{H}}_i\tilde{\mathbf{x}}_i(n) \\
&\quad + \underbrace{\sum_{i=0}^{T-1} e^{jn(N+P)\phi_i}\mathbf{R}_{cp}\mathbf{Z}_{N+P}(\phi_i)\acute{\widetilde{\mathbf{H}}}_i\tilde{\mathbf{x}}_i(n-1)}_{\text{IBI}} \; + \; \mathbf{R}_{cp}\tilde{\mathbf{v}}(n) \\
&= \sum_{i=0}^{T-1} e^{jn(N+P)\phi_i}\mathbf{R}_{cp}\mathbf{Z}_{N+P}(\phi_i)\widetilde{\mathbf{H}}_i\mathbf{T}_{cp}\mathbf{x}_i(n) + \mathbf{v}(n),
\end{aligned} \tag{4.10}
$$

where $\mathbf{v}(n) = \mathbf{R}_{cp}\tilde{\mathbf{v}}(n)$ and $\mathbf{R}_{cp}\mathbf{Z}_{N+P}(\phi_i)\acute{\widetilde{\mathbf{H}}}_i = e^{jP\phi_i}\mathbf{Z}_N(\phi_i)\mathbf{R}_{cp}\acute{\widetilde{\mathbf{H}}}_i = \mathbf{0}_{N\times(N+P)}$. It is assumed that $E\left[\mathbf{v}(n)\mathbf{v}^H(n)\right] = \sigma^2\mathbf{I}_N$. Equation (4.10) can be further simplified as

$$
\begin{aligned}
\mathbf{r}(n) &= \sum_{i=0}^{T-1} e^{j(n(N+P)+P)\phi_i}\mathbf{Z}_N(\phi_i)\mathbf{R}_{cp}\widetilde{\mathbf{H}}_i\mathbf{T}_{cp}\mathbf{x}_i(n) + \mathbf{v}(n) \\
&= \sum_{i=0}^{T-1} e^{j(n(N+P)+P)\phi_i}\mathbf{Z}_N(\phi_i)\mathbf{H}_i\mathbf{x}_i(n) + \mathbf{v}(n) \qquad (4.11) \\
&= \sum_{i=0}^{T-1} e^{j(n(N+P)+P)\phi_i}\mathbf{Z}_N(\phi_i)\mathbf{H}_i\mathbf{C}_i\mathbf{s}_i(n) + \mathbf{v}(n), \qquad (4.12)
\end{aligned}
$$

where $\mathbf{H}_i = \mathbf{R}_{cp}\widetilde{\mathbf{H}}_i\mathbf{T}_{cp}$ is a $(N \times N)$ circulant channel matrix [28] whose first column vector is given by $[\mathbf{h}_i^T, \mathbf{0}_{(N-L)\times 1}]$. An example illustrating the structure of the various matrices involved in a CP-CDMA system is given in Appendix C. It should be noted that the received signal vector in (4.12) is free from IBI. The objective is to estimate the ith user's ACFO and CIR using (4.12) and knowledge of user spreading code.

4.2 CP-CDMA Signal Structure

Let $\mathbf{b}_{i,k}$ denote the kth column vector of matrix $\mathbf{C}_i$. The circulant channel matrix $\mathbf{H}_i$ multiplying the vector $\mathbf{b}_{i,k}$ can be expressed as

$$\mathbf{H}_i\mathbf{b}_{i,k} = \widetilde{\mathbf{B}}_{i,k}\mathbf{h}_i \quad \text{for } k = 0, 1, \cdots, Q-1, \tag{4.13}$$

where $\widetilde{\mathbf{B}}_{i,k}$ is a $(N \times L)$ Toeplitz matrix whose first column vector and first row vector are $\mathbf{b}_{i,k}$ and $[b_{i,k}(0), b_{i,k}(N-1), \cdots, b_{i,k}(N-L+1)]$, respectively. The lth element in vector $\mathbf{b}_{i,k}$ is denoted by $b_{i,k}(l)$ for $l = 0, 1, \cdots, N-1$. Using (4.13), the received signal vector in (4.12) can be written as

$$\mathbf{r}(n) = \sum_{i=0}^{T-1}\sum_{k=0}^{Q-1} e^{j(n(N+P)+P)\phi_i}\mathbf{Z}_N(\phi_i)\widetilde{\mathbf{B}}_{i,k}\mathbf{h}_i s_i(nQ+k) + \mathbf{v}(n). \tag{4.14}$$

Observing equation(4.14), it is noted that the received signal corresponding to the ith user lies in the column space spanned by vectors $\left\{\mathbf{Z}_N(\phi_i)\widetilde{\mathbf{B}}_{i,k}\mathbf{h}_i\right\}_{k=0}^{Q-1}$. Thus, the dimension of the subspace spanned by the received signal corresponding to the ith user is given by rank of $(N \times Q)$ matrix $\mathbf{Z}_N(\phi_i)\left[\widetilde{\mathbf{B}}_{i,0}\mathbf{h}_i, \widetilde{\mathbf{B}}_{i,1}\mathbf{h}_i, \cdots, \widetilde{\mathbf{B}}_{i,Q-1}\mathbf{h}_i\right]$. Matrix $\mathbf{Z}_N(\phi_i)$ is unitary and hence

$$rank\left(\mathbf{Z}_N(\phi_i)\left[\widetilde{\mathbf{B}}_{i,0}\mathbf{h}_i, \cdots, \widetilde{\mathbf{B}}_{i,Q-1}\mathbf{h}_i\right]\right) = rank\left(\left[\widetilde{\mathbf{B}}_{i,0}\mathbf{h}_i, \cdots, \widetilde{\mathbf{B}}_{i,Q-1}\mathbf{h}_i\right]\right). \tag{4.15}$$

Let the spreading code of every user be assumed to satisfy the following assumption:

AS1 : The DFT of $(N \times 1)$ vector $\mathbf{b}_{i,0}$ does not have any zero element for $i = 0, 1, \cdots, T-1$.

Assumption **AS1**[2] implies that the $(N \times 1)$ vector $\mathbf{W}_N \mathbf{b}_{i,k}$ does not have any zero element for $k = 1, 2, \cdots, Q-1$ and $i = 0, 1, \cdots, T-1$.

***Lemma* 4.1.** If the $(N \times 1)$ vector $\mathbf{W}_N \mathbf{b}_{i,k}$ does not have any zero element, then the $(N \times QL)$ matrix $\breve{\mathbf{B}}_i = \left[\widetilde{\mathbf{B}}_{i,0}, \widetilde{\mathbf{B}}_{i,1}, \cdots, \widetilde{\mathbf{B}}_{i,Q-1}\right]$ is of full rank QL, provided that $N > QL$.

Proof: *The column vectors of matrix $\breve{\boldsymbol{B}}_i$ are obtained by circular shifting the column vector $\boldsymbol{b}_{i,k}$. Let $\boldsymbol{\Theta}_{i,k}$ denote a $(N \times N)$ circulant matrix with $\boldsymbol{b}_{i,k}$ as the first column vector, i.e.,*

$$\boldsymbol{\Theta}_{i,k} = \left[[\boldsymbol{b}_{i,k}]^{(0)}, [\boldsymbol{b}_{i,k}]^{(1)}, \cdots, [\boldsymbol{b}_{i,k}]^{(N-1)}\right], \tag{4.16}$$

where $[\boldsymbol{a}]^{(l)}$ denotes the vector obtained by circularly shifting vector $\boldsymbol{a}$ by l times. A single circular shift comprises of moving the last element of the column vector to the first. Thus, matrix $\breve{\boldsymbol{B}}_i$ contains a subset of column vectors from matrix $\boldsymbol{\Theta}_{i,k}$. If $Q = 3$, $L = 2$, $G = 4$ and $\boldsymbol{c}_i = [a_0, a_1, a_2, a_3]^T$ then, the $(N \times QL)$ matrix $\breve{\boldsymbol{B}}_i$ is

[2] It should be noted that the Fourier transform of $\mathbf{b}_{i,0}$ at frequency points $\{2\pi k/N\}_{k=0}^{N-1}$ only are assumed to be non-zero.

given by

$$\breve{\boldsymbol{B}}_i = \begin{bmatrix} a_0 & a_1 & a_2 & a_3 & 0 & 0 & 0 & 0 & 0 & 0 & 0 & 0 \\ 0 & a_0 & a_1 & a_2 & a_3 & 0 & 0 & 0 & 0 & 0 & 0 & 0 \\ 0 & 0 & 0 & 0 & a_0 & a_1 & a_2 & a_3 & 0 & 0 & 0 & 0 \\ 0 & 0 & 0 & 0 & 0 & a_0 & a_1 & a_2 & a_3 & 0 & 0 & 0 \\ 0 & 0 & 0 & 0 & 0 & 0 & 0 & 0 & a_0 & a_1 & a_2 & a_3 \\ a_3 & 0 & 0 & 0 & 0 & 0 & 0 & 0 & 0 & a_0 & a_1 & a_2 \end{bmatrix}^T . \quad (4.17)$$

The above example clearly illustrates that matrix $\breve{\boldsymbol{B}}_i$ *can be constructed by selecting a set of* QL *column vectors from* $\boldsymbol{\Theta}_{i,k}$.

Using the circulant matrix property, $\boldsymbol{\Theta}_{i,k}$ *can be transformed into a diagonal matrix as shown below*

$$\boldsymbol{W}_N \boldsymbol{\Theta}_{i,k} \boldsymbol{W}_N^H = \boldsymbol{\Lambda}_{i,k}, \quad (4.18)$$

where

$$\boldsymbol{\Lambda}_{i,k} = diag(\boldsymbol{W}_N \boldsymbol{b}_{i,k}). \quad (4.19)$$

As $\boldsymbol{W}_N$ *and* $\boldsymbol{W}_N^H$ *are unitary matrices,* $rank(\boldsymbol{\Theta}_{i,k}) = rank(\boldsymbol{\Lambda}_{i,k})$. *It should be noted that vector* $\boldsymbol{W}_N \boldsymbol{b}_{i,k}$ *does not have any element equal to zero. Therefore,* $rank(\boldsymbol{\Lambda}_{i,k}) = rank(\boldsymbol{\Theta}_{i,k}) = N$. *As matrix* $\boldsymbol{\Theta}_{i,k}$ *is of full rank* N*, the column vectors of* $\boldsymbol{\Theta}_{i,k}$ *are linearly independent. Therefore, matrix* $\breve{\boldsymbol{B}}_i$ *is of full rank* QL *for* $i = 0, 1, \cdots, T-1$. □

Lemma 4.1 implies that each user's signal subspace is Q dimensional and independent of the user's ACFO and CIR values. It also implies that the transformation $\mathbf{H}_i\mathbf{b}_{i,k} = \widetilde{\mathbf{B}}_{i,k}\mathbf{h}_i$ is unique, i.e.,

$$\mathbf{H}_i\mathbf{b}_{i,k} \quad = \quad \widetilde{\mathbf{B}}_{i,k}\mathbf{x} \quad \text{iff } \mathbf{x} = \mathbf{h}_i. \tag{4.20}$$

4.3 Blind Subspace-based Estimator

4.3.1 Assumptions

The following assumptions, similar to that made in chapter 3, are used in the formulation of the estimator.

AS2 : Column vectors $\{\{\mathbf{Z}_N(\phi_i)\widetilde{\mathbf{B}}_{i,k}\mathbf{h}_i\}_{k=0}^{Q-1}\}_{i=0}^{T-1}$ are linearly independent for any realization of $\mathbf{h}_i$ and any $\phi_i \in [-\pi, \pi)$.

Assumption **AS2** implies that the dimension of signal subspace ($\mathbf{U}_s$) is[3] $\mathcal{S} = QT$. Thus, the dimension of noise subspace ($\mathbf{U}_n$) is $(N - \mathcal{S})$. The $(N \times \mathcal{S})$ matrix $\mathbf{U}_s$ and $(N \times (N - \mathcal{S}))$ matrix $\mathbf{U}_n$ are estimated following the procedure stated in Section 2.5.

The orthogonality between the signal and noise subspaces results in

$$\mathbf{U}_n^H\mathbf{Z}_N(\phi_i)\widetilde{\mathbf{B}}_{i,k}\mathbf{h}_i \quad = \quad \mathbf{0}_{(N-\mathcal{S})\times 1}, \tag{4.21}$$

[3] It should be noted that $N > QT$ since $N = QG$ and $G > T$.

for $k = 0, 1, \cdots, Q-1$ and $i = 0, 1, \cdots, T-1$. Equation (4.21) can be written as

$$\begin{aligned} \boldsymbol{\Psi}\widetilde{\mathbf{Z}}(\phi_i)\mathbf{D}_i\mathbf{h}_i &= \mathbf{0}_{Q(N-\mathcal{S})\times 1}, && (4.22)\\ \boldsymbol{\Gamma}_i(\phi_i)\mathbf{h}_i &= \mathbf{0}_{Q(N-\mathcal{S})\times 1}, && (4.23)\end{aligned}$$

where

$$\begin{aligned} \boldsymbol{\Psi} &= \mathbf{I}_Q \otimes \mathbf{U}_n^H, && (4.24)\\ \widetilde{\mathbf{Z}}(\phi_i) &= \mathbf{I}_Q \otimes \mathbf{Z}_N(\phi_i), && (4.25)\\ \mathbf{D}_i &= \left[\widetilde{\mathbf{B}}_{i,0}^T, \widetilde{\mathbf{B}}_{i,1}^T, \cdots, \widetilde{\mathbf{B}}_{i,Q-1}^T\right]^T, && (4.26)\\ \boldsymbol{\Gamma}_i(\phi_i) &= \boldsymbol{\Psi}\widetilde{\mathbf{Z}}(\phi_i)\mathbf{D}_i. && (4.27)\end{aligned}$$

Equation (4.23) is used to obtain the cost function for the estimator. The following assumption is made in order to establish the uniqueness of the estimated parameters (ACFO and CIR) using (4.23).

AS3 : The dimension of intersection space between $col(\mathbf{I}_Q \otimes \mathbf{U}_s)$ and $col\left(\widetilde{\mathbf{Z}}(\phi)\mathbf{D}_i\mathbf{h}_i\right)$ is 1 when $\phi = \phi_i$ and 0 when $\phi \neq \phi_i$ for $i = 0, 1, \cdots, T-1$.

Assumption **AS3** and the full rank property of $(QN \times L)$ matrix[4] $\mathbf{D}_i$ ensures that equation (4.23) has a unique and non trivial solution for ϕ_i and $\mathbf{h}_i$.

[4]Using Lemma 4.1, matrix $\mathbf{D}_i$ can be proved to be a full rank matrix.

4.3.2 ACFO and CIR Estimator

Using (4.23), the cost function to minimize is given by

$$\min_{\phi,\mathbf{h},\mathbf{h}\neq\mathbf{0}_{L\times 1}} J(\phi,\mathbf{h}) \;=\; \|\boldsymbol{\Gamma}_i(\phi)\mathbf{h}\|^2 = \mathbf{h}^H\boldsymbol{\Gamma}_i^H(\phi)\boldsymbol{\Gamma}_i(\phi)\mathbf{h}. \tag{4.28}$$

The estimator for CP-CDMA system is formulated following the steps given for EDMM in Section 3.4.1. The ith user's ACFO is estimated as follows:

$$\hat{\phi}_i \;=\; \arg\min_{\phi}\left\{det\left(\boldsymbol{\Gamma}_i^H(\phi)\boldsymbol{\Gamma}_i(\phi)\right)\right\}. \tag{4.29}$$

That is, the search point $\phi \in [-\pi,\pi)$ which minimizes $det\left(\boldsymbol{\Gamma}_i^H(\phi)\boldsymbol{\Gamma}_i(\phi)\right)$ is the estimated ACFO. Assumption **AS3** ensures that matrix $\boldsymbol{\Gamma}_i^H(\phi)\boldsymbol{\Gamma}_i(\phi)$ is rank deficient only when $\phi=\phi_i$ and $\mathbf{h}_i \in null\left(\boldsymbol{\Gamma}_i^H(\phi_i)\boldsymbol{\Gamma}_i(\phi_i)\right)$. The grid search is performed over the interval $[-\pi,\pi)$ using a suitable grid size v. The ith user's CIR is estimated as the eigenvector corresponding to the minimum eigenvalue of the $(L\times L)$ positive semi-definite Hermitian matrix $\boldsymbol{\Gamma}_i^H(\hat{\phi}_i)\boldsymbol{\Gamma}_i(\hat{\phi}_i)$, i.e,

$$\hat{\mathbf{h}}_i \;=\; \arg\min_{\mathbf{h},\mathbf{h}^H\mathbf{h}=1}\left\{\mathbf{h}^H\boldsymbol{\Gamma}_i^H(\hat{\phi}_i)\boldsymbol{\Gamma}_i(\hat{\phi}_i)\mathbf{h}\right\}. \tag{4.30}$$

As in Section 3.4.2, ADMM based ACFO and CIR estimator for CP-CDMA system can be formulated to reduce the computational complexity.

4.4 ACFO and CIR Identifiability

The crux of the proposed estimator lies in the equation

$$\mathbf{\Psi}\widetilde{\mathbf{Z}}(\phi)\mathbf{D}_i\mathbf{h} \;=\; \mathbf{0}_{Q(N-\mathcal{S})\times 1}, \tag{4.31}$$

where ϕ and $\mathbf{h}$ are the parameters to be estimated. For the ith user's ACFO and CIR estimates to be identified uniquely, it is required to have $\widetilde{\mathbf{Z}}(\phi)\mathbf{D}_i\mathbf{h} \in null(\mathbf{\Psi})$ iff $\phi = \phi_i$ and[5] $\mathbf{h} = e^{j\zeta}\mathbf{h}_i$ where ζ is a real-valued scalar. To the authors' knowledge, only identifiability of CIR estimate in the absence of ACFO is reported in the literature (e.g. [75]). The uniqueness of CIR estimate is established in [75] by assuming the intersection space between $col(\mathbf{D}_i)$ and $col(\mathbf{I}_Q \otimes \mathbf{U}_s)$ to be of dimension one. Details about construction of matrix $\mathbf{D}_i$ were not addressed. Furthermore, the identifiability of estimates in joint ACFO and CIR estimation has not been addressed so far. In the following, the selection of spreading codes to ensure unique identifiability of ACFO and CIR estimates is outlined. It is to be noted that the dimension of intersection space between $col(\widetilde{\mathbf{Z}}(\phi)\mathbf{D}_i)$ and $col(\mathbf{I}_Q \otimes \mathbf{U}_s)$ is not assumed to be one, but practically feasible constraints are imposed on the users' spreading codes to ensure the dimension of intersection space to be one.

Let matrix $\daleth_i$ be a $(QN \times L(T+1))$ matrix defined as

$$\daleth_i \;=\; \left[\widetilde{\mathbf{Z}}(\phi)\mathbf{D}_i, \widetilde{\mathbf{Z}}(\phi_0)\mathbf{D}_0, \widetilde{\mathbf{Z}}(\phi_1)\mathbf{D}_1, \cdots, \widetilde{\mathbf{Z}}(\phi_{T-1})\mathbf{D}_{T-1}\right], \tag{4.32}$$

for $i = 0, 1, \cdots, T-1$. For the ACFO and CIR estimates to be unique, matrix $\daleth_i$ should be of rank $L(T+1)$ when $\phi \neq \phi_i$ and of rank LT when[6] $\phi = \phi_i$. If the

[5]This implies that $det\left(\mathbf{\Gamma}_i^H(\phi)\mathbf{\Gamma}_i(\phi)\right) = 0$ iff $\phi = \phi_i$.
[6]Therefore, it is necessary to have $QN \geq L(T+1)$.

above rank condition is satisfied then assumption **AS5** is valid. Matrix $\daleth_i$ can be expressed as

$$\daleth_i = \left[\widetilde{\mathbf{G}}_{i,0}^T, \widetilde{\mathbf{G}}_{i,1}^T, \cdots, \widetilde{\mathbf{G}}_{i,Q-1}^T\right]^T, \tag{4.33}$$

for $i = 0, 1, \cdots, T-1$ where the $(N \times L(T+1))$ matrix $\widetilde{\mathbf{G}}_{i,k}$ for $k = 0, 1, \cdots, Q-1$ is given by

$$\widetilde{\mathbf{G}}_{i,k} = \left[\mathbf{Z}_N(\phi)\widetilde{\mathbf{B}}_{i,k},\ \mathbf{G}_k\right]. \tag{4.34}$$

The $(N \times LT)$ matrix $\mathbf{G}_k$ in (4.34) for $k = 0, 1, \cdots, Q-1$ is constructed as follows:

$$\mathbf{G}_k = \left[\mathbf{Z}_N(\phi_0)\widetilde{\mathbf{B}}_{0,k}, \mathbf{Z}_N(\phi_1)\widetilde{\mathbf{B}}_{1,k}, \cdots, \mathbf{Z}_N(\phi_{T-1})\widetilde{\mathbf{B}}_{T-1,k}\right]. \tag{4.35}$$

Matrix $\daleth_i$ will be of full rank $L(T+1)$ if matrix $\widetilde{\mathbf{G}}_{i,k}$ is of full rank $L(T+1)$ for any $k \in [0, Q-1]$ and all possible combinations of $\{\phi, \phi_0, \phi_1, \cdots, \phi_{T-1}\} \in [-\pi, \pi)$. Without loss of generality, let $i = 0$ be the desired user. Therefore, for the $i = 0$ user's ACFO and CIR estimates to be uniquely identified it is sufficient to have matrix $\widetilde{\mathbf{G}}_{0,0}$ to be of full rank $L(T+1)$ for all possible combinations of $\{\phi, \phi_0, \phi_1, \cdots, \phi_{T-1}\} \in [-\pi, \pi)$. Matrix $\widetilde{\mathbf{G}}_{0,0}$ depends only on the users' spreading codes, ϕ and $\{\phi_i\}_{i=0}^{T-1}$. As ϕ and ϕ_i can take any real value from the interval $[-\pi, \pi)$, verifying the rank of matrix $\widetilde{\mathbf{G}}_{0,0}$ for all possible values of ϕ and $\{\phi_i\}_{i=0}^{T-1}$ is not possible. Therefore, the following approximation is used to render the above verification feasible. The ith user's ACFO (ϕ_i) can be expressed as

$$\phi_i = \frac{2\pi l_i}{N} + \delta_i, \tag{4.36}$$

where it is assumed that N is even and integer $l_i \in [-N/2, N/2-1]$ for $i = 0, 1, \cdots, T-1$. As N increases, $\delta_i \to 0$ and hence matrix $\mathbf{Z}(\phi_i)$ can be approximated as

$$\mathbf{Z}_N(\phi_i) \;\approx\; \mathbf{Z}_N(2\pi l_i/N), \tag{4.37}$$

because $\mathbf{Z}(\delta_i) \to \mathbf{I}_N$ as $\delta_i \to 0$. Similarly, matrix $\mathbf{Z}_N(\phi)$ is approximated as

$$\mathbf{Z}_N(\phi) \;\approx\; \mathbf{Z}_N(2\pi l/N), \tag{4.38}$$

where $l \in [-N/2, N/2-1]$. Using (4.37) and (4.38), matrix $\widetilde{\mathbf{G}}_{0,0}$ can be expressed as

$$\widetilde{\mathbf{G}}_{0,0} \approx \left[\mathbf{Z}_N(2\pi l/N)\widetilde{\mathbf{B}}_{i,0}, \mathbf{Z}_N(2\pi l_0/N)\tilde{\mathbf{B}}_{0,0}, \cdots, \mathbf{Z}_N(2\pi l_{T-1}/N)\tilde{\mathbf{B}}_{T-1,0}\right]. \tag{4.39}$$

The user spreading codes are chosen such that matrix $\widetilde{\mathbf{G}}_{0,0}$, constructed using (4.39), is of rank $L(T+1)$ for all combinations of $\{l, l_0, l_1, \cdots, l_{T-1}\} \in [-N/2, N/2-1]$ except when $l = l_0$ where $rank\left(\widetilde{\mathbf{G}}_{0,0}\right) = LT$. Since $\mathbf{Z}_N(2\pi l/N)$ is a unitary matrix, it can be factored out without altering the rank of $\widetilde{\mathbf{G}}_{0,0}$ as

$$\widetilde{\mathbf{G}}_{0,0} \approx \left[\widetilde{\mathbf{B}}_{i,0}, \mathbf{Z}_N(2\pi p_0/N)\tilde{\mathbf{B}}_{0,0}, \cdots, \mathbf{Z}_N(2\pi p_{T-1}/N)\tilde{\mathbf{B}}_{T-1,0}\right], \tag{4.40}$$

where $\{p_i = l_i - l\}_{i=0}^{T-1}$ and $\{p_0, p_1, \cdots, p_{T-1}\} \in [-N/2, N/2-1]$. Therefore, it is sufficient to construct matrix $\widetilde{\mathbf{G}}_{0,0}$ (as given in (4.40)) to be of full rank $L(T+1)$ for all possible combinations of $\{p_0, p_1, \cdots, p_{T-1}\} \in [-N/2, N/2-1]$ except for $p_0 = 0$ where $rank\left(\widetilde{\mathbf{G}}_{0,0}\right) = LT$. The condition $p_0 = 0$ implies that $l_0 - l = 0$, i.e., the estimated ACFO is the desired user's true ACFO value.

For example, let the spreading gain be $G = 32$, $Q = 2$ (therefore $N = 64$), number of users $T = 4$ and length of CIR be $L = 3$. The rank of the (64×15) dimensional matrix $\widetilde{\mathbf{G}}_{0,0}$ for all possible combinations of $\{p_0, p_1, p_2, p_3\}$ (except $p_0 = 0$) is plotted in Fig. 4.4. Fig. 4.4 confirms that $\widetilde{\mathbf{G}}_{0,0}$ is full rank for all possible combinations of $\{p_0, p_1, p_2, p_3\}$ (except $p_0 = 0$). This shows that, there are spreading codes in practice which satisfy assumption **AS3**.

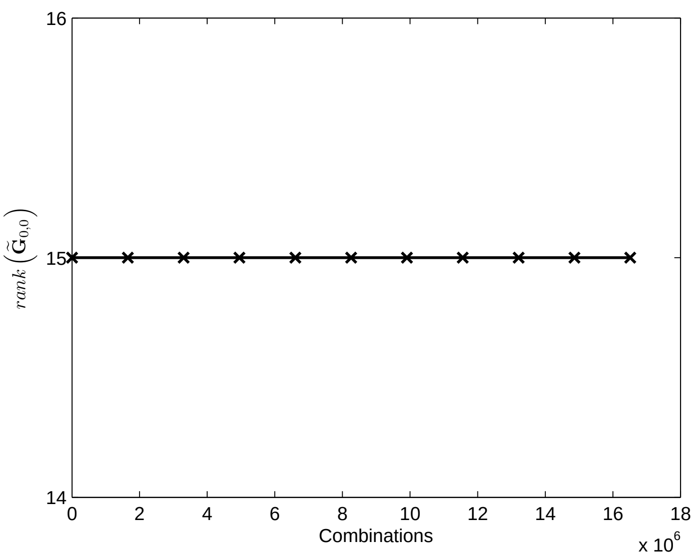

Fig. 4.4: Full rank of matrix $\widetilde{\mathbf{G}}_{0,0}$.

The conditions so far imposed on N are $Q(N - \mathcal{S}) \geq L$, $N \geq LQT$ and $QN \geq L(T+1)$. Therefore, $N = QG$ should be selected such that[7]

$$G \;\geq\; max\left\{\left\lceil \frac{L + \mathcal{S}Q}{Q^2} \right\rceil, LT, \left\lceil \frac{L}{Q^2}(T+1) \right\rceil\right\}. \tag{4.41}$$

[7]Ceiling operator $\lceil . \rceil$: $\lceil a \rceil$ returns the smallest integer, such that $\lceil a \rceil - a \geq 0$.

4.5 Simulation Results

For computer simulations, a CP-CDMA system with spreading gain $G = 32$ and $T = 5$ users is considered. The number of data symbols transmitted in a block is $Q = 2$ and hence $N = QG = 64$. The length of CIR for all users is assumed to be $L = 3$ and the cyclic prefix length is $P = 2$. The users' data symbols are assumed to be QPSK modulated. A set of $B = 100$ received signal vectors are used for subspace estimation. Without loss of generality, $i = 0$ user is considered as the desired user. The ith user's MSEs for ACFO and CIR estimates are computed as the mean of $\|\mathbf{h}_i - \hat{\mathbf{h}}_i\|^2$ and $(\phi_i - \hat{\phi}_i)^2$, respectively.

Cost Function

Let $Y_\phi = det(\mathbf{\Gamma}_i^H(\phi)\mathbf{\Gamma}_i(\phi))$. The plot of Y_ϕ for $i = 0$ user is given in Fig. 3.2. The SNR is set to 15dB. The cost function is plotted for four different cases, i.e., for $\phi_0 = -2.3$, $\phi_0 = -0.7$, $\phi_0 = 1$ and $\phi_0 = 2.1$. From Fig. 3.2, it is observed that the $i = 0$ user's cost function has a global minimum only at the user's true ACFO value.

MSE Performance

The users' ACFO values are assumed to be a uniformly distributed random variable in the interval $[-0.5, 0.5]$. The ACFO value within the interval $[-0.5, 0.5]$ corresponds to a frequency offset of $\pm 4.8892 \times 10^{-3}\%$ of the carrier frequency 2GHz. The CRLB is computed as shown in Appendix A. The MSE for ACFO estimate obtained using the proposed estimator is shown in Fig. 4.6 for different grid sizes v. In Fig. 4.6, an error floor is observed for $v = 0.01$. This is due to the use of

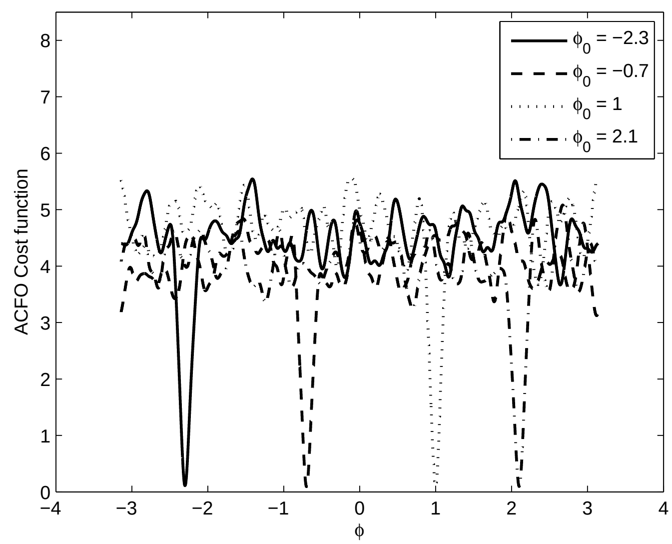

Fig. 4.5: Cost function for CP-CDMA system.

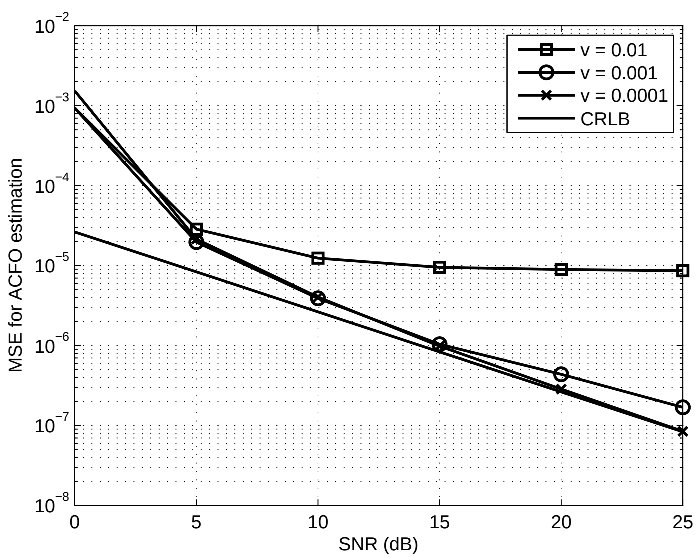

Fig. 4.6: MSE for ACFO estimation when $\{\phi_i \in [-0.5, 0.5]\}_{i=0}^{T-1}$.

large grid size. As v is reduced, the performance gets closer to the CRLB. The MSE curves for CIR estimation corresponding to different grid sizes used for the grid search are given in Fig. 4.7. It is observed that the MSE corresponding to CIR estimation gets closer to the CRLB as the grid size is reduced.

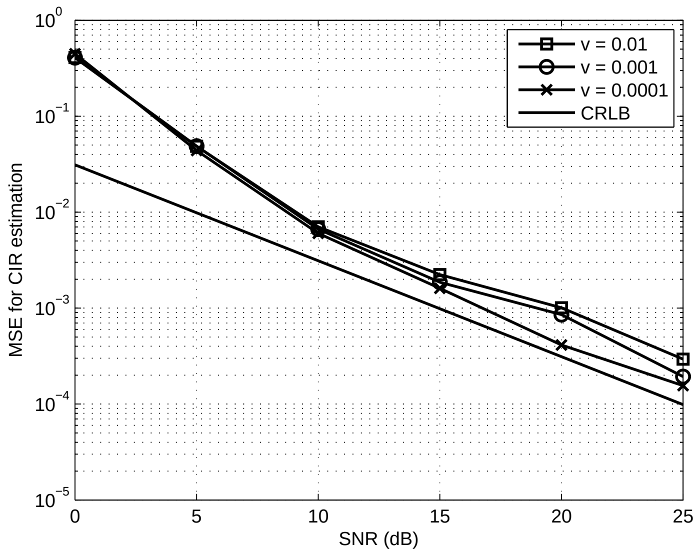

Fig. 4.7: MSE for CIR estimation when $\{\phi_i \in [-0.5, 0.5]\}_{i=0}^{T-1}$.

In Presence of PN

The MSE performance of the proposed estimator in the presence of PN is obtained through computer simulations. We consider a Gaussian PN model as in [49]. In the presence of PN, the received signal at the base station is given by

$$\mathbf{r}(n) = \sum_{i=0}^{T-1} \sum_{k=0}^{Q-1} e^{(jn(N+P)+P)\phi_i} \dot{\mathbf{Z}}_N(n, \phi_i) \widetilde{\mathbf{B}}_{i,k} \mathbf{h}_i s_i(nQ+k) + \mathbf{v}(n), \tag{4.42}$$

where the $(N \times N)$ diagonal matrix is given by

$$\dot{\mathbf{Z}}_N(n,\phi_i) = diag\left(\left[e^{j\theta_i(nG+L-1)}, e^{j(\phi_i+\theta_i(nG+L))}, \cdots, e^{j((N-1)\phi_i+\theta_i(nG+G-1))}\right]^T\right). \tag{4.43}$$

Let $\theta_i(n) = [\theta_i(nG+L-1), \theta_i(nG+L), \theta_i(nG+L+1), \cdots, \theta_i(nG+G-1)]^T$. The element in the pth row and qth column of the Gaussian PN covariance matrix $\mathbf{R}_{\theta_i} = E[\theta_i(n)\theta_i^H(n)]$ is given by

$$\mathbf{R}_{\theta_i}(p,q) = \left(\frac{\pi\omega}{180}\right)^2 e^{-2\pi|p-q|\chi}, \tag{4.44}$$

where $\omega = 3$ and $\chi = 0.005$ were chosen for simulation [49]. A grid size of $\upsilon = 0.0001$ is used for the grid search. Each user's ACFO value is assumed to be in the interval $[-0.5, 0.5]$. The MSE for ACFO and CIR estimates obtained using EDMM are shown in Figs. 4.8 and 4.9, respectively. From the simulations results, it is observed that the PN does not affect the MSE at low SNR. At high SNR, the MSE for ACFO and CIR estimates obtained in the presence of PN, is higher than the MSE for ACFO and CIR estimates obtained in the absence of PN. Thus, the proposed estimator is not significantly affected by PN.

MSE vs Users

We compare the MSE for ACFO and CIR estimates obtained using EDMM for different number of users and different length of CIR. For simulation we consider $G = 32$, $Q = 2$ and users ACFO in the interval $[-0.5, 0.5]$. Grid size $\upsilon = 0.0001$ is used for the grid search. Figs. 4.10 and 4.11 shows the MSE for ACFO and CIR estimates, respectively. As the number of users is increased, it is observed that the

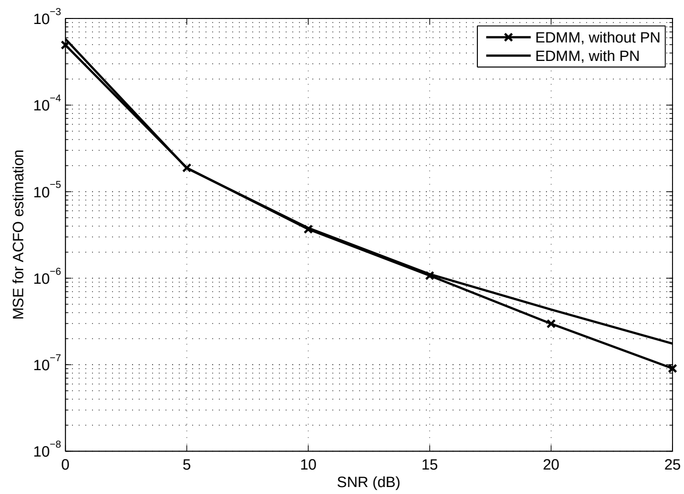

Fig. 4.8: ACFO estimation when $\{\phi_i \in [-0.5, 0.5]\}_{i=0}^{T-1}$.

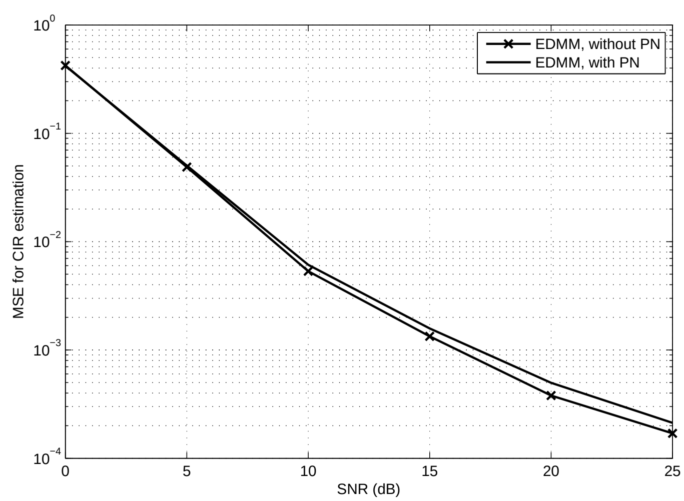

Fig. 4.9: CIR estimation when $\{\phi_i \in [-0.5, 0.5]\}_{i=0}^{T-1}$.

MSE increases. This is due to the increase in MAI. Furthermore, it is observed that the performance of EDMM based estimator gracefully degrades with the increase in the number of users. Note that when $T > 10$ and $L = 5$, the spreading gain does not satisfy the inequality in (4.41). In this case, though the estimator performs well, the identifiability of the estimates is yet to be proved when the inequality in (4.41) is not satisfied and the grid search is on the interval $[-0.5, 0.5]$.

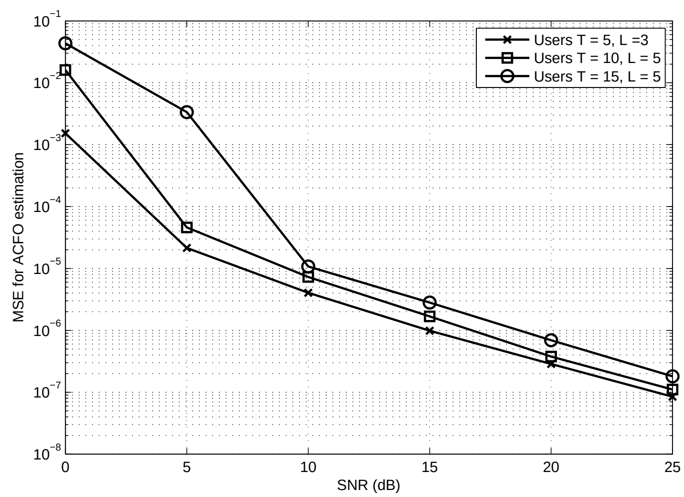

Fig. 4.10: ACFO estimation when $\{\phi_i \in [-0.5, 0.5]\}_{i=0}^{T-1}$.

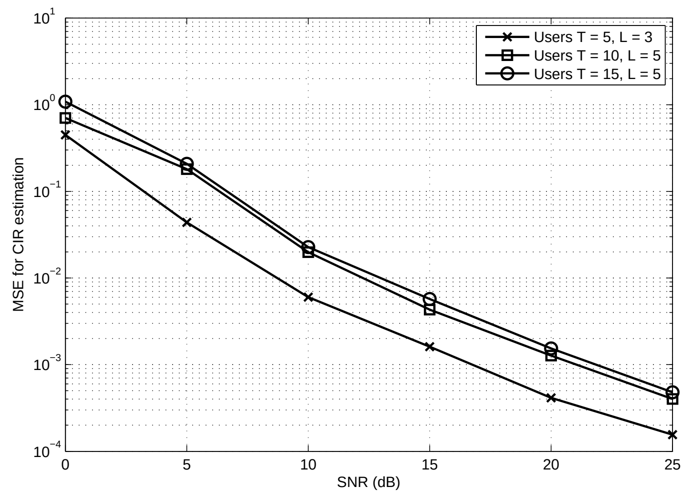

Fig. 4.11: CIR estimation when $\{\phi_i \in [-0.5, 0.5]\}_{i=0}^{T-1}$.

4.6 Conclusion

In this chapter, EDMM based estimator was formulated for jointly estimating ACFO and CIR in the uplink transmission of CP-CDMA system. The dimension of each user's signal subspace was shown to be independent of the user's ACFO and CIR values, if the DFT of user spreading codes did not have any nulls. Furthermore, a criterion for selection of users' spreading codes was formulated to asymptotically guarantee the identifiability of ACFO and CIR estimates. Through computer simulations, the MSE performance of the proposed estimator was shown to be close to CRLB.

Chapter 5

MC-CDMA System

In chapter 3 and chapter 4, subspace-based blind joint ACFO and CIR estimator was formulated for multiuser CDMA systems where the spreading was done in time domain. In this chapter, a subspace-based blind joint ACFO and CIR estimator is formulated for MC-CDMA system where the spreading is done in the frequency domain. MC-CDMA system is a hybrid of OFDM and CDMA systems. To leverage the benefits from both OFDM and CDMA, accurate carrier frequency synchronization and CIR estimation is essential. The formulation of the joint ACFO and CIR estimator is similar to that done in chapter 3 and chapter 4. The received signal in the uplink transmission of MC-CDMA system is analyzed and is shown that the inherent signal structure can guarantee the dimension of each user's signal subspace to be independent of the user's ACFO and CIR values. The dissimilarities between CP-CDMA and MC-CDMA systems are also highlighted in this chapter. The estimator in [74] proposed for blind ACFO estimation in uplink MC-CDMA system is shown to be unsuitable for frequency selective multipath fading channels whereas our estimator is shown to perform well in both frequency selective and frequency flat fading channels. Furthermore, a criterion for the selection of users' spreading codes is outlined to guarantee the identifiability of the estimates. The performance of the proposed estimator for MC-CDMA uplink is studied through computer simulations.

5.1 System Model

A generalized MC-CDMA system with T users in the uplink is considered. The uplink transmission is assumed to be quasi-synchronous. As in CP-CDMA, $\mathbf{c}_i = [c_i(0), c_i(1), \cdots, c_i(G-1)]^T$ denotes the ith user's spreading code with spreading gain $G > T$ and Q denotes the maximum number of data symbols in a data block. Let Q_i denote the number of data symbols in the ith user's data block, where $Q_i \leq Q$. At the ith user's transmitter, Q_i data symbols are converted from serial to parallel form and appended with $(Q - Q_i)$ number of zeros to form a $(Q \times 1)$ vector $\mathbf{s}_i(n)$ given by

$$\mathbf{s}_i(n) = [s_i(nQ_i), s_i(nQ_i+1), \cdots, s_i(nQ_i+Q_i-1), \mathbf{0}_{1\times(Q-Q_i)}]^T, \tag{5.1}$$

where $s_i(nQ_i + k)$ denotes the ith user's kth data symbol transmitted during nth data block. In this chapter, we assume one data block to contain Q data symbols, i.e., $Q_i = Q$ for $i = 0, 1, \cdots, T-1$. The $(Q \times 1)$ vector $\mathbf{s}_i(n)$ is spread using user specific spreading code as follows:

$$\breve{\mathbf{x}}_i(n) = \mathbf{C}_i \mathbf{s}_i(n), \tag{5.2}$$

where the $(N \times Q)$ code matrix $\mathbf{C}_i = \mathbf{I}_Q \otimes \mathbf{c}_i$. Users with high data rate requirements can be supported by assigning more than one spreading code to them. The N elements of vector $\check{\mathbf{x}}_i(n)$ needs to be suitably modulated onto N orthogonal subcarriers[1]. The N subcarriers are divided into Q groups such that each group has G subcarriers. Let $\{f_m^{(q)}; 0 \leq m \leq G-1\}$ denote the indices of the subcarriers in the qth group, where $0 \leq q \leq Q-1$. The subcarriers in each group are uniformly spaced over the available bandwidth, thus creating frequency diversity. The subcarrier indices for the qth group are given by $f_m^{(q)} = mQ + q$ where $m = 0, 1, \cdots, G-1$ [66]. For example, the subcarrier grouping for $G = 4$ and $Q = 4$ ($N = QG = 16$) is pictorially illustrated in Fig. 5.1. The G elements in

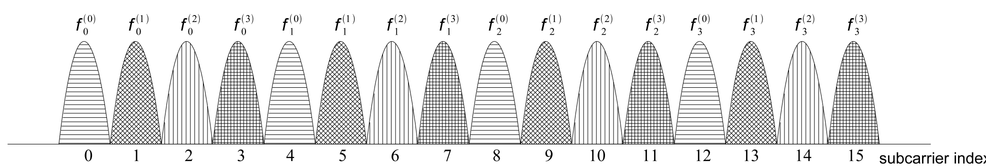

Fig. 5.1: Subcarrier grouping.

vector $\tilde{\mathbf{x}}_i(n)$ corresponding to the data symbol $s_i(nQ+q)$ are modulated onto the G subcarriers in qth group whose indices are $f_m^{(q)}$. In other words, the elements $c_i(0)s_i(nQ+q), c_i(1)s_i(nQ+q), \cdots, c_i(G-2)s_i(nQ+q)$ and $c_i(G-1)s_i(nQ+q)$ are modulated onto the subcarriers with indices $q, Q+q, 2Q+q, \cdots, (G-2)Q+q$ and $(G-1)Q+q$, respectively for $q = 1, 2, \cdots, Q-1$. The subcarrier assignment is done by the $(N \times N)$ interleaving matrix $\mathbf{\Pi}$. Matrix $\mathbf{\Pi}$ is obtained by permuting

[1]The number of subcarriers in the MC-CDMA system is $N = QG$.

row (or column) vectors of matrix $\mathbf{I}_N$ such that

$$\mathbf{\Pi}^H\mathbf{\Pi} = \mathbf{\Pi}\mathbf{\Pi}^H = \mathbf{I}_N. \tag{5.3}$$

The N elements of the vector obtained after interleaving are modulated onto N subcarriers by the N-point IDFT processor. The ith user's $(N \times 1)$ signal vector after N-point IDFT computation is given by

$$\mathbf{x}_i(n) \;\; = \;\; \mathbf{W}_N^H\mathbf{\Pi}\mathbf{C}_i\mathbf{s}_i(n), \tag{5.4}$$

where $\mathbf{W}_N$ denotes the N-point discrete Fourier transform (DFT) matrix. A cyclic prefix of length P is augmented to $\mathbf{x}_i(n)$ as in chapter 4 and the resulting $((N + P) \times 1)$ column vector $\tilde{\mathbf{x}}_i(n)$ is given by

$$\tilde{\mathbf{x}}_i(n) \;\; = \;\; \mathbf{T}_{cp}\mathbf{x}_i(n). \tag{5.5}$$

At the ith user's transmitter, the transmission after obtaining $\tilde{\mathbf{x}}_i(n)$ is same as that in CP-CDMA transmitter described in chapter 4. The block diagram for ith user's MC-CDMA transmitter is illustrated in Fig. 5.2. As in chapters 3 and 4, the maximum length of the composite CIR for all users is assumed to be L and the ith user's CIR is denoted by

$$\mathbf{h}_i \;\; = \;\; [h_i(0), h_i(1), \cdots, h_i(L-1)]^T. \tag{5.6}$$

Therefore, the length of the cyclic prefix is chosen to be $P = L - 1$ so that the IBI is eliminated after the removal of the cyclic prefix at the receiver. Let ϕ_i denote the

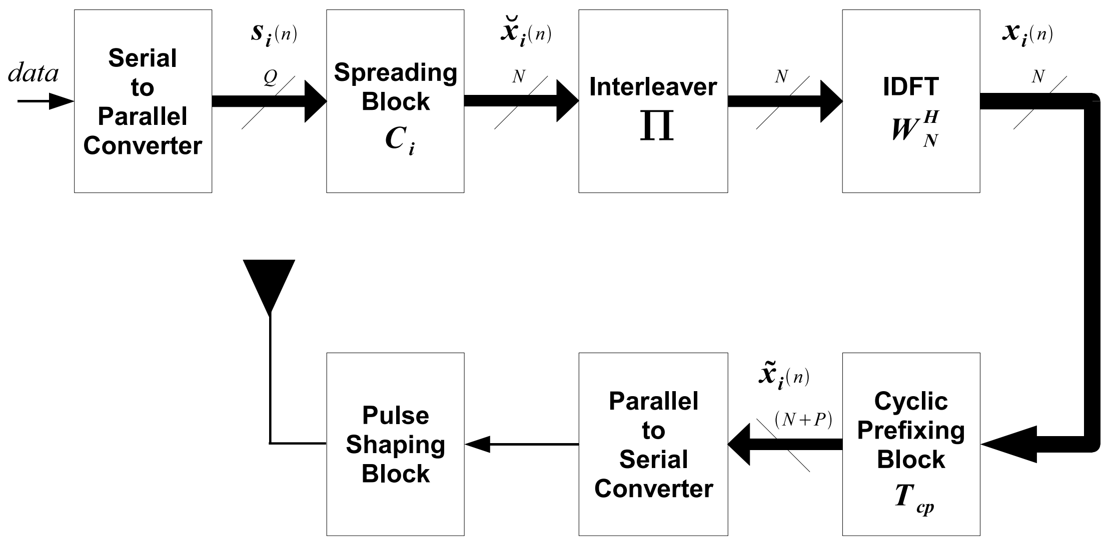

Fig. 5.2: MC-CDMA Transmitter.

ith user's ACFO. Following the steps in Section 4.1, the $(N \times 1)$ vector obtained due to the presence of T users, after the removal of the cyclic prefix at the receiver is given by (see equation (4.11))

$$\begin{aligned} \mathbf{r}(n) &= \sum_{i=0}^{T-1} e^{j(n(N+P)+P)\phi_i} \mathbf{Z}_N(\phi_i)\mathbf{H}_i\mathbf{x}_i(n) + \mathbf{v}(n) \\ &= \sum_{i=0}^{T-1} e^{j(n(N+P)+P)\phi_i} \mathbf{Z}_N(\phi_i)\mathbf{H}_i\mathbf{W}_N^H \mathbf{\Pi}\mathbf{C}_i\mathbf{s}_i(n) + \mathbf{v}(n), \end{aligned} \tag{5.7}$$

where $\mathbf{H}_i$ is the $(N \times N)$ circulant channel matrix whose first column vector is $[\mathbf{h}_i^T, \mathbf{0}_{1\times(N-L)}]^T$. It is assumed that $E[\mathbf{v}(n)\mathbf{v}^H(n)] = \sigma^2\mathbf{I}_N$. The objective is to estimate the ith user's ACFO and CIR by using only the received signal and the knowledge of the desired user's spreading code.

5.2 CP-CDMA and MC-CDMA Dissimilarity

Both CP-CDMA and MC-CDMA can support block transmission and use spreading codes for identifying the users. They use cyclic prefix to eliminate IBI and aid for a simple frequency domain channel equalization at the receiver. However, there exists key dissimilarities between CP-CDMA and MC-CDMA systems. Interleaving and IDFT computation are performed in MC-CDMA system whereas in CP-CDMA there are no such operations.

5.2.1 Frequency Spectrum

In the absence of CFO, the received signal obtained after the removal of cyclic prefix is given by

$$\begin{aligned}
\text{CP-CDMA:} \quad \mathbf{r}(n) &= \sum_{i=0}^{T-1} \mathbf{H}_i \mathbf{C}_i \mathbf{s}_i(n) + \mathbf{v}(n), && (5.8)\\
\text{MC-CDMA:} \quad \mathbf{r}(n) &= \sum_{i=0}^{T-1} \mathbf{H}_i \mathbf{W}_N^H \mathbf{\Pi} \mathbf{C}_i \mathbf{s}_i(n) + \mathbf{v}(n). && (5.9)
\end{aligned}$$

Computing the DFT for the received signal in (5.8) and (5.9), we obtain

$$\begin{aligned}
\text{CP-CDMA:} \quad \mathbf{W}_N \mathbf{r}(n) &= \sum_{i=0}^{T-1} \mathbf{\Lambda}_i \mathbf{W}_N \mathbf{C}_i \mathbf{s}_i(n) + \mathbf{W}_N \mathbf{v}(n), && (5.10)\\
\text{MC-CDMA:} \quad \mathbf{W}_N \mathbf{r}(n) &= \sum_{i=0}^{T-1} \mathbf{\Lambda}_i \mathbf{\Pi} \mathbf{C}_i \mathbf{s}_i(n) + \mathbf{W}_N \mathbf{v}(n) && (5.11)\\
&= \sum_{i=0}^{T-1} \widetilde{\mathbf{\Lambda}}_i \mathbf{C}_i \mathbf{s}_i(n) + \mathbf{W}_N \mathbf{v}(n), && (5.12)
\end{aligned}$$

where $\mathbf{\Lambda}_i = \mathbf{W}_N \mathbf{H}_i \mathbf{W}_N^H$ is a $(N \times N)$ diagonal matrix and $\widetilde{\mathbf{\Lambda}}_i = \mathbf{\Lambda}_i \mathbf{\Pi}$. The N-point DFT of the ith user's CIR forms the N diagonal elements of $\mathbf{\Lambda}_i$. In other words, the available bandwidth is divided into N orthogonal subbands. The l diagonal element of matrix $\mathbf{\Lambda}_i$ is denoted by $\lambda_{i,l}$ for $l = 0, 1, \cdots, N-1$. Let $\mathbf{g}_i(n) = \mathbf{W}_N \mathbf{C}_i \mathbf{s}_i(n)$ and $g_{i,l}(n)$ for $l = 0, 1, \cdots, N-1$ denote the lth element of vector $\mathbf{g}_i(n)$. Observing equation (5.10) we can note that, the Q data symbols are not separated and each subband has contributions from all the Q data symbols in the data block. This is due to the presence of DFT matrix $\mathbf{W}_N$ in (5.10). However in MC-CDMA, (5.12) implies that each subband carries the spread signal corresponding to only one specific data symbol in the data block. In other words, the CP-CDMA signal has intra block interference whereas MC-CDMA signal has no intra block interference. This is clearly illustrated by Fig. 5.3 for $G = 4$ and $Q = 2$. The different shades used for MC-CDMA in Fig. 5.3 denotes the subcarrier grouping scheme outlined in Section 5.1.

5.2.2 Signal Structure

Let $\mathbf{b}_{i,k}$ denote the kth column vector of $(N \times Q)$ matrix $\mathbf{W}_N^H \mathbf{\Pi} \mathbf{C}_i$ for $k = 0, 1, \cdots, Q-1$. As in chapter 4, the multiplication $\mathbf{H}_i \mathbf{b}_{i,k}$ can be expressed as

$$\mathbf{H}_i \mathbf{b}_{i,k} = \widetilde{\mathbf{B}}_{i,k} \mathbf{h}_i, \tag{5.13}$$

and the received signal vector $\mathbf{r}(n)$ can be rewritten using (5.13) as

$$\mathbf{r}(n) = \sum_{i=0}^{T-1} \sum_{k=0}^{Q-1} e^{j(n(N+P)+P)\phi_i} \mathbf{Z}_N(\phi_i) \widetilde{\mathbf{B}}_{i,k} \mathbf{h}_i s_i(nQ+k) + \mathbf{v}(n), \tag{5.14}$$

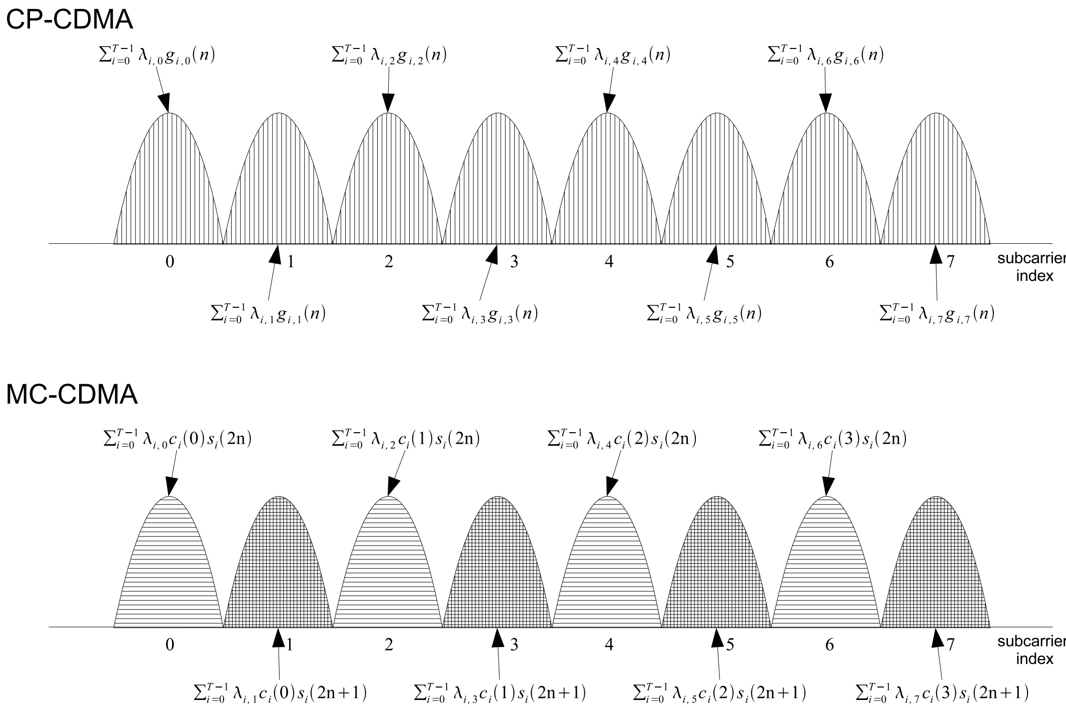

Fig. 5.3: CP-CDMA and MC-CDMA Frequency Spectrum.

where $\widetilde{\mathbf{B}}_{i,k}$ is a $(N\times L)$ Toeplitz matrix with $\mathbf{b}_{i,k}$ and $[b_{i,k}(0), b_{i,k}(N-1), \cdots, b_{i,k}(N-L+1)]$ as first column vector and first row vector, respectively. The key differences between the structure of matrix $\widetilde{\mathbf{B}}_{i,k}$ for CP-CDMA and MC-CDMA systems are outlined in this section.

5.2.2.1 Rank of $\widetilde{\mathbf{B}}_{i,k}$:

In chapter 4, assumption **AS3** was used to ensure that matrix $\widetilde{\mathbf{B}}_{i,k}$ is of full rank in CP-CDMA system. In MC-CDMA, $\widetilde{\mathbf{B}}_{i,k}$ can be proved to be of full rank without using any assumption.

***Lemma* 5.1.** The $(N \times L)$ matrix $\widetilde{\mathbf{B}}_{i,k}$ is of full rank L for any selection of the user's spreading code.

Proof: *Let $\mathbf{\Theta}_{i,k}$ be a $(N \times N)$ circulant matrix, whose first column vector is $\boldsymbol{b}_{i,k}$, i.e.,*

$$\mathbf{\Theta}_{i,k} = \left[[\boldsymbol{b}_{i,k}]^{(0)}, [\boldsymbol{b}_{i,k}]^{(1)}, \cdots, [\boldsymbol{b}_{i,k}]^{(N-1)}\right], \tag{5.15}$$

where $[\boldsymbol{b}_{i,k}]^{(l)}$ denotes the vector obtained by circular shifting the elements of $\boldsymbol{b}_{i,k}$ by l times. It is observed that, matrix $\widetilde{\boldsymbol{B}}_{i,k}$ can be obtained as the first L column vectors of matrix $\mathbf{\Theta}_{i,k}$ as follows:

$$\widetilde{\boldsymbol{B}}_{i,k} = \mathbf{\Theta}_{i,k}(:, 1 : L), \tag{5.16}$$

where $\mathbf{\Theta}_{i,k}(:, 1 : L)$ is a $(N \times L)$ matrix containing the first L column vectors of $\mathbf{\Theta}_{i,k}$. Using the circulant matrix property [28], $\mathbf{\Theta}_{i,k}$ can be expressed as

$$\mathbf{\Theta}_{i,k} = \boldsymbol{W}_N^H \mathbf{\Lambda}_{i,k} \boldsymbol{W}_N, \tag{5.17}$$

where $\mathbf{\Lambda}_{i,k}$ is a $(N \times N)$ diagonal matrix whose non-zero elements are given by the DFT of the column vector $\boldsymbol{b}_{i,k}$, i.e.,

$$\mathbf{\Lambda}_{i,k} = diag(\tilde{\boldsymbol{d}}_{i,k}), \tag{5.18}$$

where $\tilde{\boldsymbol{d}}_{i,k}$ denotes the kth column vector of $(N \times Q)$ matrix $\mathbf{\Pi}\,\boldsymbol{C}_i$ for $k = 0, 1, \cdots, Q-1$. Rank of $\mathbf{\Theta}_{i,k}$ is equal to rank of $\mathbf{\Lambda}_{i,k}$ which in turn is equal to the number of *non-zero elements in vector* $\tilde{\boldsymbol{d}}_{i,k}$ *which is* G*. Thus rank of* $\boldsymbol{\Theta}_{i,k}$ *is* G*. The following example outlines the above result.*

Let $G = 4$ *and* $Q = 2$*, therefore* $N = 8$*. Let* $\boldsymbol{c}_i = [c_i(0), c_i(1), c_i(2), c_i(3)]^T$*. The* $(N \times Q)$ *matrix* $\boldsymbol{\Pi}\boldsymbol{C}_i$ *for this example is*

$$\boldsymbol{\Pi}\boldsymbol{C}_i = \begin{bmatrix} c_i(0) & 0 & c_i(1) & 0 & c_i(2) & 0 & c_i(3) & 0 \\ 0 & c_i(0) & 0 & c_i(1) & 0 & c_i(2) & 0 & c_i(3) \end{bmatrix}^T . \quad (5.19)$$

From (5.19), it can be clearly seen that vector $\{\tilde{\boldsymbol{d}}_{i,k}\}_{k=0}^{Q-1}$ *has* $G = 4$ *non-zero elements. Hence the rank of matrix* $\boldsymbol{\Lambda}_{i,k}$ *(in turn the rank of* $\boldsymbol{\Theta}_{i,k}$*) is* $G = 4$*.*

The interleaving done at the transmitter results in the presence of $Q-1$ *zeros between every non-zero element in* $\tilde{\boldsymbol{d}}_{i,k}$ *causing an interpolation effect [115]. Using the Fourier transform property it can be shown that*

$$[\boldsymbol{b}_{i,k}]^{(qG)} = \boldsymbol{b}_{i,k}, \quad (5.20)$$

where q *is any integer. Therefore, the column vectors of* $\boldsymbol{\Theta}_{i,k}$ *with column indices* $\{l, G+l, 2G+l, \cdots, (Q-1)G+l\}_{l=0}^{G-1}$ *are all identical. As matrix* $\boldsymbol{\Theta}_{i,k}$ *is of rank* G*, the first* G *column vectors of* $\boldsymbol{\Theta}_{i,k}$ *must be linearly independent. Thus matrix* $\widetilde{\boldsymbol{B}}_{i,k}$*, which contains only the first* L $(L << G)$ *column vectors of* $\boldsymbol{\Theta}_{i,k}$*, is of full rank* L *for any* $\boldsymbol{c}_i$*.* □

Lemma 5.1 implies that the transformation $\mathbf{H}_i\mathbf{b}_{i,k} = \widetilde{\mathbf{B}}_{i,k}\mathbf{h}_i$ is unique, i.e.,

$$\mathbf{H}_i\mathbf{b}_{i,k} = \widetilde{\mathbf{B}}_{i,k}\mathbf{x} \quad \text{iff } \mathbf{x} = \mathbf{h}_i. \quad (5.21)$$

5.2.2.2 Orthonormal Basis for ith User's Signal Subspace:

In CP-CDMA, the i user's signal subspace is spanned by the basis vectors $\{\widetilde{\mathbf{B}}_{i,k}\mathbf{h}_i\}_{k=0}^{Q-1}$. These basis vectors are not orthogonal. However, the basis vectors $\{\widetilde{\mathbf{B}}_{i,k}\mathbf{h}_i\}_{k=0}^{Q-1}$ in MC-CDMA system are orthogonal by construction. This property is explained below in detail.

***Lemma* 5.2.** The column vectors of matrices $\{\widetilde{\mathbf{B}}_{i,k}\}_{k=0}^{Q-1}$ corresponding to the ith user span orthogonal subspaces for any selection of the user spreading code $\mathbf{c}_i$.

Proof: *Using (5.16), the column vectors of matrix $\widetilde{\boldsymbol{B}}_{i,k}$ can be represented as*

$$\widetilde{\boldsymbol{B}}_{i,k} \;=\; [[\boldsymbol{b}_{i,k}]^{(0)},\ [\boldsymbol{b}_{i,k}]^{(1)},\ [\boldsymbol{b}_{i,k}]^{(2)}, \cdots, [\boldsymbol{b}_{i,k}]^{(L-1)}]. \tag{5.22}$$

By definition, vectors $\boldsymbol{b}_{i,k}$ and $\tilde{\boldsymbol{d}}_{i,k}$ are related as follows:

$$\boldsymbol{b}_{i,k} \;=\; \boldsymbol{W}_N^H \tilde{\boldsymbol{d}}_{i,k}. \tag{5.23}$$

Using (5.23) in (5.22), it can be shown that [115]

$$\boldsymbol{W}_N \widetilde{\boldsymbol{B}}_{i,k} = \left[\boldsymbol{Z}_N(0)\,\tilde{\boldsymbol{d}}_{i,k}, \boldsymbol{Z}_N\left(-\frac{2\pi}{N}\right)\tilde{\boldsymbol{d}}_{i,k}, \cdots, \boldsymbol{Z}_N\left(-\frac{2\pi(L-1)}{N}\right)\tilde{\boldsymbol{d}}_{i,k}\right]. \tag{5.24}$$

For a given user i, the column vectors $\{\tilde{\boldsymbol{d}}_{i,k}\}_{k=0}^{Q-1}$ are orthogonal by construction. This orthogonality arises from the location of the non-zero elements, i.e., for a non-zero element located at position p of vector $\tilde{\boldsymbol{d}}_{i,l}$, the element at the pth position for the other $(Q-1)$ column vectors $\{\tilde{\boldsymbol{d}}_{i,k}\}_{k=0,k\neq l}^{Q-1}$ is zero for $l = 0, 1, \cdots, Q-1$. The above structure of $\tilde{\boldsymbol{d}}_{i,k}$ is explicitly shown in (5.19) and therefore, for ith user

$$\tilde{\boldsymbol{d}}_{i,k}^H \tilde{\boldsymbol{d}}_{i,l} \;=\; 0, \tag{5.25}$$

for $k = 0, 1, \cdots, Q-1$, $k \neq l$ *and* $l \in [0, Q-1]$. *The placement of zero elements in vectors obtained by right multiplying the diagonal matrices* $\boldsymbol{Z}_N(-2\pi l/N)$ *with* $\tilde{\boldsymbol{d}}_{i,k}$ *is unaltered. Therefore, for a given user* i, *we have*

$$\left(\boldsymbol{Z}_N\left(-\frac{2\pi r}{N}\right)\tilde{\boldsymbol{d}}_{i,k}\right)^H \boldsymbol{Z}_N\left(-\frac{2\pi s}{N}\right)\tilde{\boldsymbol{d}}_{i,l} \quad = \quad 0, \tag{5.26}$$

for $k \neq l$ *and* $0 \leq r, s \leq L-1$. *Using (5.24) and (5.26), it can be deduced that, for a given user* i

$$\begin{aligned} (\boldsymbol{W}_N \widetilde{\boldsymbol{B}}_{i,k})^H \boldsymbol{W}_N \widetilde{\boldsymbol{B}}_{i,l} &= \mathbf{0}, \\ \widetilde{\boldsymbol{B}}_{i,k}^H \widetilde{\boldsymbol{B}}_{i,l} &= 0, \end{aligned} \tag{5.27}$$

for $k \neq l$ *and* $0 \leq k, l \leq Q-1$. *It is to be noted that if* $k = l$ *in (5.27), then for any user* i

$$\widetilde{\boldsymbol{B}}_{i,k}^H \widetilde{\boldsymbol{B}}_{i,k} \quad = \quad \boldsymbol{I}_L. \tag{5.28}$$

Equations (5.27) and (5.28) imply that the column vectors of matrices $\{\widetilde{\boldsymbol{B}}_{i,k}\}_{k=0}^{Q-1}$ *span orthogonal subspaces*[2] *for any selection of spreading code* $\boldsymbol{c}_i$. $\square$

Lemma 5.2 implies that the column vectors $\{\widetilde{\mathbf{B}}_{i,k}\mathbf{h}_i\}_{k=0}^{Q-1}$ in MC-CDMA are orthonormal for any selection of spreading code $\mathbf{c}_i$ and CIR $\mathbf{h}_i$ ($\mathbf{h}_i^H\mathbf{h}_i = 1$). Following the proof of Lemma 5.2, another observation to be noted is that, for any user i and user j ($i \neq j$), the column space of matrices $\widetilde{\mathbf{B}}_{j,l}$ and $\{\widetilde{\mathbf{B}}_{i,k}\}_{k=0,k\neq l}^{Q-1}$ are orthogonal for $0 \leq l \leq Q-1$ and $\{i, j\} \in [0, T-1]$. The above orthogonal signal structure is not available in CP-CDMA system.

[2] The L column vectors of matrix $\widetilde{\mathbf{B}}_{i,k}$ are only linearly independent and not orthogonal.

From the received signal $\mathbf{r}(n)$ in (5.14), it is inferred that the ith user's received signal component lies in the subspace spanned by the column vector of matrix $\mathbf{Z}_N(\phi_i)\left[\widetilde{\mathbf{B}}_{i,0}\mathbf{h}_i, \widetilde{\mathbf{B}}_{i,1}\mathbf{h}_i, \cdots, \widetilde{\mathbf{B}}_{i,Q-1}\mathbf{h}_i\right]$. Lemma 5.1 and Lemma 5.2 imply that the dimension of the subspace spanned by the ith user's signal subspace is[3] Q and it is independent of the user's spreading code $\mathbf{c}_i$, CIR $\mathbf{h}_i$ ($\mathbf{h}_i \neq \mathbf{0}_{L\times 1}$) and ACFO ϕ_i. Furthermore, the data block size for each user in MC-CDMA system can be different but in CP-CDMA system the user's data block size is fixed. This feature in MC-CDMA aids in supporting users with different data rate requirements.

5.3 Blind Subspace-based Estimator

Let $\mathbf{D}_i$ denote a $(QN \times L)$ matrix defined as follows:

$$\mathbf{D}_i = \left[\widetilde{\mathbf{B}}_{i,0}^T, \widetilde{\mathbf{B}}_{i,1}^T, \cdots, \widetilde{\mathbf{B}}_{i,Q-1}^T\right]^T, \tag{5.29}$$

for $i = 0, 1, \cdots, T-1$. The following assumptions are made for the formulation of the estimator.

AS1 : Column vectors $\{\{\mathbf{Z}_N(\phi_i)\widetilde{\mathbf{B}}_{i,k}\mathbf{h}_i\}_{k=0}^{Q-1}\}_{i=0}^{T-1}$ are linearly independent for any realization of $\mathbf{h}_i$ and $\phi_i \in [-\pi, \pi)$.

AS2 : The intersection space between $col(\mathbf{I}_Q \otimes \mathbf{U}_s)$ and $col(\widetilde{\mathbf{Z}}(\phi)\mathbf{D}_i\mathbf{h}_i)$ is of dimension 1 when $\phi = \phi_i$ and 0 when $\phi \neq \phi_i$ for $i = 0, 1, \cdots, T-1$.

[3]If the ith user transmits only Q_i data symbols in one MC-CDMA symbol duration then the corresponding user's received signal subspace is Q_i dimensional.

Following the steps as in Section 4.3, the ith user's cost function to be minimized is given by

$$\min_{\phi,\mathbf{h},\mathbf{h}\neq\mathbf{0}_{L\times 1}} J(\phi,\mathbf{h}) = \|\mathbf{\Gamma}_i(\phi)\mathbf{h}\|^2 = \mathbf{h}^H\mathbf{\Gamma}_i^H(\phi)\mathbf{\Gamma}_i(\phi)\mathbf{h}, \tag{5.30}$$

where

$$\mathbf{\Gamma}_i(\phi) = \mathbf{\Psi}\widetilde{\mathbf{Z}}(\phi)\mathbf{D}_i, \tag{5.31}$$

$$\mathbf{\Psi} = \mathbf{I}_Q \otimes \mathbf{U}_n^H, \tag{5.32}$$

$$\widetilde{\mathbf{Z}}(\phi_i) = \mathbf{I}_Q \otimes \mathbf{Z}_N(\phi_i). \tag{5.33}$$

Lemma 5.1 implies that matrix $\mathbf{D}_i$ is of full rank QL. The ACFO and CIR estimates are obtained as follows:

$$\hat{\phi}_i = \arg\min_{\phi} \left\{ det\left(\mathbf{\Gamma}_i^H(\phi)\mathbf{\Gamma}_i(\phi)\right)\right\}, \tag{5.34}$$

$$\hat{\mathbf{h}}_i = \arg\min_{\mathbf{h},\mathbf{h}^H\mathbf{h}=1} \left\{\mathbf{h}^H\mathbf{\Gamma}_i^H(\hat{\phi}_i)\mathbf{\Gamma}_i(\hat{\phi}_i)\mathbf{h}\right\}. \tag{5.35}$$

Assumption **AS2** guarantees that the ith users ACFO and CIR estimates are uniquely identified. The ACFO is estimated by performing a grid search over the interval $[-\pi,\pi)$ with a suitable grid size v. To reduce the computational complexity, ADMM based ACFO and CIR estimator can be formulated for MC-CDMA system following the steps in Section 3.4.2.

5.4 Tureli's Estimator

Tureli's estimator [74] considers a special case in the uplink transmission of MC-CDMA system. The number of data symbols in the data block is $Q = 1$ and the subcarriers are assumed to have same frequency response [88], i.e, $\lambda_{i,0} = \lambda_{i,1} = \cdots = \lambda_{i,N-1}$. The received signal in [74], according to the notations used in this thesis is given by

$$\mathbf{r}(n) = \sum_{i=0}^{T-1} \mathbf{Z}_N(\phi_i)\mathbf{W}_N^H \mathbf{a}_i s_i(n) + \mathbf{v}(n), \tag{5.36}$$

where

$$\mathbf{a}_i = \mathbf{W}_N \mathbf{H}_i \mathbf{W}_N^H \mathbf{c}_i \tag{5.37}$$

and $s_i(n)$ is the ith user's data symbol transmitted during the nth MC-CDMA symbol duration. Equation (5.36) implies that the ith user received signal lies in the span of $\mathbf{Z}(\phi_i)\mathbf{W}_N^H\mathbf{a}_i$. Thus the orthogonality between the signal and noise subspaces leads to

$$\mathbf{U}_n^H \mathbf{Z}_N(\phi_i)\mathbf{W}_N^H \mathbf{a}_i = \mathbf{0}. \tag{5.38}$$

However, the condition used in [74] (see equation (11) in [74]) is

$$\mathbf{U}_n^H \mathbf{Z}_N(\phi_i)\mathbf{W}_N^H \mathbf{c}_i = \mathbf{0}. \tag{5.39}$$

For frequency selective multipath fading channels, it can be clearly seen that column space of vectors $\mathbf{Z}_N(\phi_i)\mathbf{W}_N^H\mathbf{a}_i$ and $\mathbf{Z}_N(\phi_i)\mathbf{W}_N^H\mathbf{c}_i$ are different and hence using

(5.39) to estimate the ACFO in frequency selective multipath fading channels is not possible. Furthermore, equation (5.39) implies that

$$\mathbf{a}_i = \mathbf{c}_i \quad \text{iff} \quad \mathbf{H}_i = \mathbf{I}_N. \tag{5.40}$$

Thus the estimator in [74] assumes that the circulant channel matrix $\mathbf{H}_i = \mathbf{I}_N$ for all users and therefore it cannot be used in frequency selective multipath fading channels.

5.4.1 Computational Complexity

The prosed estimator and the estimator in [74] have the same computational complexity for flat fading channels where $L = 1$. In frequency selective fading channels, the proposed estimator has higher computational complexity due to the computation of the determinant of $(L \times L)$ matrix for each search point, where $L > 1$. Tureli's estimator [74] has the same computational complexity as that for $L = 1$ case. This is because, Tureli's estimator ignores the frequency selective fading channel and still treats the channel to be a frequency flat fading channel.

5.5 ACFO and CIR Identifiability

The blind estimator proposed for the ith user in CP-CDMA and MC-CDMA systems is constructed from the linear equation

$$\boldsymbol{\Psi}\widetilde{\mathbf{Z}}(\phi_i)\mathbf{D}_i\mathbf{h}_i \quad = \quad \mathbf{0}_{Q(N-\mathcal{S})\times 1}. \tag{5.41}$$

Therefore, the identifiability conditions derived for CP-CDMA system also hold for MC-CDMA system. In Section 4.4, ACFO and CIR identifiability were asymptotically guaranteed for the ith user in CP-CDMA system by selecting the spreading codes such that the $(N \times L(T+1))$ matrix $\widetilde{\mathbf{G}}_{0,0}$ given by

$$\widetilde{\mathbf{G}}_{0,0} \approx \left[\widetilde{\mathbf{B}}_{i,0}, \mathbf{Z}_N(2\pi p_0/N)\widetilde{\mathbf{B}}_{0,0}, \mathbf{Z}_N(2\pi p_1/N)\widetilde{\mathbf{B}}_{1,0}, \cdots, \mathbf{Z}_N(2\pi p_{T-1}/N)\widetilde{\mathbf{B}}_{T-1,0}\right], \tag{5.42}$$

for $\{p_0, p_1, \cdots, p_{T-1}\} \in [-N/2, N/2-1]$ satisfies the rank requirement. The rank requirement is as follows:

$$\begin{aligned} rank\left(\widetilde{\mathbf{G}}_{0,0}\right) &= L(T+1) \quad \text{for } \{p_0, p_1, \cdots, p_{T-1}\} \in [-N/2, N/2-1] \text{ and } p_i \neq 0 \\ rank\left(\widetilde{\mathbf{G}}_{0,0}\right) &= LT \qquad\qquad \text{for } \{p_0, p_1, \cdots, p_{T-1}\} \in [-N/2, N/2-1] \text{ and } p_i = 0. \end{aligned} \tag{5.43}$$

The rank requirement in (5.43) also holds for ensuring ACFO and CIR identifiability in MC-CDMA system. Thus, the user spreading codes are chosen such that (5.43) is satisfied.

For example, let the spreading gain be $G = 32$, $Q = 2$ (therefore $N = 64$), number of users $T = 4$ and length of CIR be $L = 3$. The rank of (64×15) dimensional matrix $\widetilde{\mathbf{G}}_{0,0}$ for all possible combinations of $\{p_0, p_1, p_2, p_3\}$ (except $p_0 = 0$) is plotted in Fig. 5.4. Fig. 5.4 confirms that $\widetilde{\mathbf{G}}_{0,0}$ is full rank for all possible combinations of $\{p_0, p_1, p_2, p_3\}$ (except $p_0 = 0$). This confirms that, there are spreading codes in practice which satisfy assumption **AS2**.

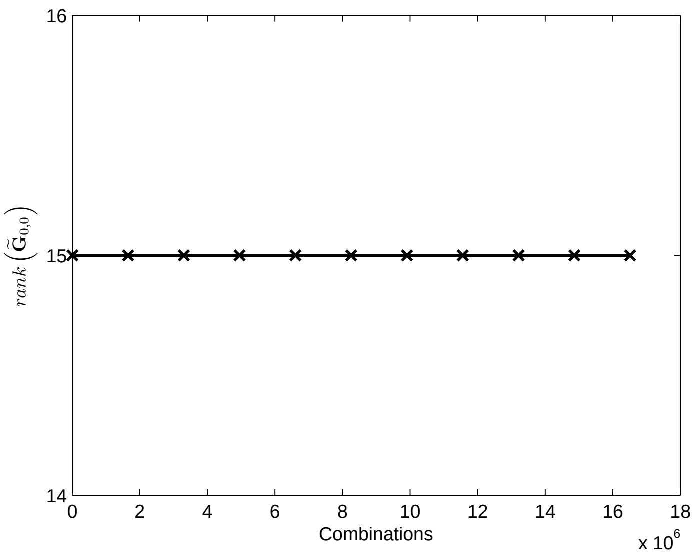

Fig. 5.4: Full rank of matrix $\widetilde{\boldsymbol{G}}_{0,0}$.

5.6 Signal Subspace and Spreading Codes

In CP-CDMA system, the selection of spreading codes can ensure the identifiability of ACFO and CIR estimates provided assumption **AS1** is satisfied. In other words, the signal subspace should be QT dimensional for any combination of users' ACFOs and CIRs. In the following, we show that the selection of spreading codes according to the rank requirement in (5.43) ensures the signal subspace to be QT dimensional for any combination of users' ACFOs and CIRs.

Let us define a $(N \times LT)$ matrix as

$$\mathbf{G}_k = \left[\breve{\mathbf{M}}_{0,k}, \breve{\mathbf{M}}_{1,k}, \cdots, \breve{\mathbf{M}}_{T-1,k}\right] \quad \text{for } k = 0, 1, \cdots, Q-1, \tag{5.44}$$

where

$$\breve{\mathbf{M}}_{i,k} \;\; = \;\; \mathbf{Z}_N(\phi_i)\widetilde{\mathbf{B}}_{i,k}, \tag{5.45}$$

for $k = 0, 1, \cdots, Q-1$ and $i = 0, 1, \cdots, T-1$. Assumption **AS1** states that the column vectors $\left\{\left\{\mathbf{Z}_N(\phi_i)\widetilde{\mathbf{B}}_{i,k}\mathbf{h}_i\right\}_{k=0}^{Q-1}\right\}_{i=0}^{T-1}$ are linearly independent for any choice of $\{\phi_i\}_{i=0}^{T-1} \in [-\pi, \pi)$ and CIR $\{\mathbf{h}_i\}_{i=0}^{T-1}$. The above column vectors will be linearly independent for any realization of users CIRs, if the $(N \times LQT)$ matrix $\mathbf{M}$ given by

$$\mathbf{M} \;\; = \;\; \left[\mathbf{G}_0, \mathbf{G}_1, \cdots, \mathbf{G}_{Q-1}\right], \tag{5.46}$$

is of full column rank[4] LQT for all combinations of $\{\phi_0, \phi_1, \cdots, \phi_{T-1}\} \in [-\pi, \pi)$. The following lemma will help us in finding the relationship between matrices $\mathbf{G}_0$ and $\{\mathbf{G}_k\}_{k=1}^{Q-1}$.

***Lemma* 5.3.** For a given user i, matrices $\{\widetilde{\mathbf{B}}_{i,k}\}_{k=1}^{Q-1}$ and $\widetilde{\mathbf{B}}_{i,0}$ are related as follows:

$$\widetilde{\mathbf{B}}_{i,k} \;\; = \;\; \mathbf{Z}_N\left(2\pi k/N\right)\; \widetilde{\mathbf{B}}_{i,0}\; \mathbf{Z}_L(-2\pi/N),$$

for $k = 1, 2, \cdots, Q_1$.

Proof: *Equation (5.23) can also be written as*

$$\boldsymbol{b}_{i,k} \;\; = \;\; \boldsymbol{W}_N^H[\tilde{\boldsymbol{d}}_{i,0}]^{(k)}. \tag{5.47}$$

The circular shifting operation can be expressed using circular convolution operation

[4]It is assumed that $N > LQT$.

as follows:

$$[\tilde{\boldsymbol{d}}_{i,0}]^{(k)} = \boldsymbol{I}_N(:,k) \circ \tilde{\boldsymbol{d}}_{i,0}, \tag{5.48}$$

where $\boldsymbol{I}_N(:,k)$ *denotes the* k*th column vector of matrix* $\boldsymbol{I}_N$ *and* $\circ$ *denotes the circular convolution operator. Substituting (5.48) into (5.47), vector* $\boldsymbol{b}_{i,k}$ *can be expressed as*

$$\begin{aligned}\boldsymbol{b}_{i,k} &= \boldsymbol{W}_N^H \left(\boldsymbol{I}_N(:,k) \circ \tilde{\boldsymbol{d}}_{i,0}\right) \\ &= \left[\boldsymbol{W}_N^H \boldsymbol{I}_N(:,k)\right] \odot \left[\boldsymbol{W}_N^H \tilde{\boldsymbol{d}}_{i,0}\right] \quad \textit{(where } \odot \textit{ denotes Hadamard product)} \\ &= \boldsymbol{Z}_N\left(2\pi k/N\right) \boldsymbol{b}_{i,0}. \end{aligned} \tag{5.49}$$

Using (5.49), it can be proved that the column vectors obtained by circularly shifting $\boldsymbol{b}_{i,k}$ *can be written as*

$$[\boldsymbol{b}_{i,k}]^{(l)} = \boldsymbol{Z}_N\left(2\pi k/N\right)[\boldsymbol{b}_{i,0}]^{(l)} e^{-2\pi l/N}, \quad \textit{for } l = 0, 1, \cdots, N-1. \tag{5.50}$$

Thus, matrix $\{\widetilde{\boldsymbol{B}}_{i,k}\}_{k=1}^{Q-1}$ *and* $\widetilde{\boldsymbol{B}}_{i,0}$ *are related as follows:*

$$\begin{aligned}\widetilde{\boldsymbol{B}}_{i,k} &= \left[[\boldsymbol{b}_{i,k}]^{(0)}, [\boldsymbol{b}_{i,k}]^{(1)}, \cdots, [\boldsymbol{b}_{i,k}]^{(L-1)}\right] \\ &= \boldsymbol{Z}_N\left(2\pi k/N\right)\ \widetilde{\boldsymbol{B}}_{i,0}\ \boldsymbol{Z}_L(-2\pi/N), \end{aligned} \tag{5.51}$$

for $k = 1, 2, \cdots, Q-1$. □

Using Lemma 5.3, it can be proved that

$$\mathbf{G}_k = \mathbf{Z}_N(2\pi k/N)\ \mathbf{G}_0\left(\mathbf{I}_T \otimes \mathbf{Z}_L(-2\pi/N)\right), \tag{5.52}$$

for $k = 1, 2, \cdots, Q-1$. Equation (5.52) implies that

$$col\,(\mathbf{G}_k) \;=\; col\,(\mathbf{Z}_N(2\pi k/N)\,\mathbf{G}_0) \quad \text{for } k = 1, 2, \cdots, Q-1, \tag{5.53}$$

and hence if $\mathbf{G}_0$ is of full rank LT then each of the matrices $\{\mathbf{G}_k\}_{k=1}^{Q-1}$ are of full rank LT. Let $\mathbf{M}_c$ be a $(N \times LQT)$ matrix defined as

$$\mathbf{M}_c \;=\; [\mathbf{G}_0,\ \mathbf{Z}_N(2\pi/N)\mathbf{G}_0, \cdots, \mathbf{Z}_N(2\pi(Q-1)/N)\mathbf{G}_0]\,. \tag{5.54}$$

From equations (5.53) and (5.54), it is inferred that the column vectors of matrices $\mathbf{M}$ and $\mathbf{M}_c$ span the same column space. Thus, if matrix $\mathbf{M}_c$ is full rank then matrix $\mathbf{M}$ also has full rank. Assuming N to be large such that $\{\phi_i = 2\pi p_i/N\}_{i=0}^{T-1}$, the $(N \times LT)$ matrix $\mathbf{G}_0$ can be approximated as

$$\mathbf{G}_0 \approx \left[\mathbf{Z}_N\left(\frac{2\pi p_0}{N}\right)\widetilde{\mathbf{B}}_{0,0},\ \mathbf{Z}_N\left(\frac{2\pi p_1}{N}\right)\widetilde{\mathbf{B}}_{1,0}, \cdots, \mathbf{Z}_N\left(\frac{2\pi p_{T-1}}{N}\right)\widetilde{\mathbf{B}}_{T-1,0}\right], \tag{5.55}$$

where $\{p_0, p_1, \cdots, p_{T-1}\} \in [-N/2, N/2-1]$.

The selection of users' spreading codes ensures that matrix $\mathbf{G}_0$ in (5.55) is of full rank LT for $\{p_0, p_1, \cdots, p_{T-1}\} \in [-N/2, N/2-1]$ (see equation (5.43), where $\mathbf{G}_{0,0} = \left[\widetilde{\mathbf{B}}_{i,0},\ \mathbf{G}_0\right]$). Equation (5.55) implies that

$$\mathbf{W}_N\mathbf{G}_0 \;\approx\; \left[\left[\mathbf{W}_N\widetilde{\mathbf{B}}_{0,0}\right]^{(p_0)}, \left[\mathbf{W}_N\widetilde{\mathbf{B}}_{1,0}\right]^{(p_1)}, \cdots, \left[\mathbf{W}_N\widetilde{\mathbf{B}}_{T-1,0}\right]^{(p_{T-1})}\right]. \tag{5.56}$$

Matrix $\mathbf{W}_N\mathbf{M}_c$ can be approximated using (5.56) as follows:

$$\mathbf{W}_N\mathbf{M}_c \;\approx\; \left[[\mathbf{W}_N\mathbf{G}_0]^{(0)}, [\mathbf{W}_N\mathbf{G}_0]^{(1)}, \cdots, [\mathbf{W}_N\mathbf{G}_0]^{(Q-1)}\right]. \tag{5.57}$$

Using the fact that the $(N \times LT)$ matrix $\mathbf{G}_0$ is of full rank LT for $\{p_0, p_1, \cdots, p_{T-1}\} \in [-N/2, N/2-1]$, matrix $\mathbf{M}_c$ can be proved to be of full rank LQT (see Appendix D). Therefore, assumption **AS1** is satisfied by proper selection of users' spreading codes in MC-CDMA system. Thus, the signal subspace is QT dimensional for any combination of users' ACFOs and CIRs.

5.7 Simulation Results

A MC-CDMA system having spreading gain of $G = 32$, block size $Q = 2$, number of subcarriers $N = QG = 64$, $T = 5$ users and the data symbols being QPSK modulated is simulated. The maximum length of CIR for all users is $L = 3$. The noise subspace is estimated using $B = 100$ received signal vectors. The ith user's normalized MSE for ACFO estimate is computed as the mean of $(\phi_i - \hat{\phi}_i)^2/(2\pi/N)^2$ and the MSE for the CIR estimate is computed as the mean of $\|\mathbf{h}_i - \hat{\mathbf{h}}_i\|^2$. The CRLB is computed as shown in Appendix A. Without loss of generality $i = 0$ user is considered as the desired user.

Cost Function

The plot of $Y_\phi = det(\mathbf{\Gamma}_i^H(\phi)\mathbf{\Gamma}_i(\phi))$ for $i = 0$ user is given in Fig. 5.5. The cost function is plotted for four different cases, i.e., for $\phi_0 = -2.3$, $\phi_0 = -0.7$, $\phi_0 = 1$ and $\phi_0 = 2.1$. The SNR is set to 15dB. From Fig. 5.5, it is observed that the $i = 0$ user's cost function has a global minimum only at the user's true ACFO value.

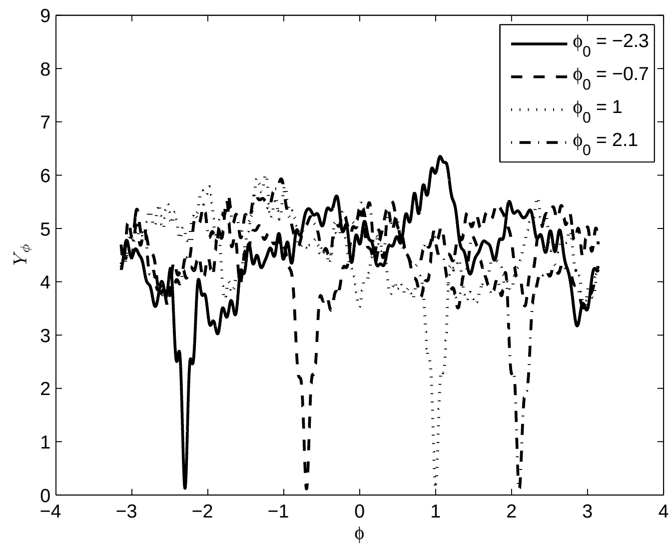

Fig. 5.5: Cost function for MC-CDMA system.

Proposed Estimator

The ACFO for each user is assumed to be a random variable uniformly distributed over the interval $[-0.5, 0.5]$. The grid search is limited to the interval $[-0.5, 0.5]$ by assuming that the receiver has prior knowledge of the interval over which the users' ACFO values are distributed. The MSE curves for ACFO estimation corresponding to grid sizes $v = 0.01$ (coarse), $v = 0.001$, $v = 0.0001$ are given in Fig. 5.6. It is evident from Fig. 5.6 that the estimation accuracy improves by reducing the grid size. Once the ACFO is estimated, the CIR is estimated as the eigenvector corresponding to the minimum eigenvalue of the matrix in (5.35). The MSE curves for CIR estimation corresponding to different grid sizes are given in Fig. 5.7, where it can be observed that the MSE curves for $v = 0.001$ and $v = 0.0001$ overlap. When v is reduced, the ACFO estimation error is also reduced, i.e., $\hat{\phi}_i = \phi_i + \delta$ where $\delta \to 0$, therefore $e^{j\hat{\phi}_i} \approx e^{j\phi_i}$. Thus, the MSE curves for CIR estimation corresponding to small grid sizes overlap. Furthermore, the MSE curves obtained for ACFO and CIR estimation get closer to the CRLB as the grid size v is reduced.

Comparison with Tureli's Estimator

The parameters used to compare the proposed estimator's MSE performance with Tureli's estimator in [74] are $G = 32$, $Q = 1$, ($N = QG = 32$) and $T = 5$ users. The data symbols are assumed to be QPSK modulated. The MSE performances for multipath frequency selective fading channel and flat fading channel are shown in Fig. 5.8. For flat fading, the length of CIR is one ($L = 1$). For frequency selective fading, the length of CIR is assumed to be $L = 3$. The users' ACFO values are assumed to be uniformly distributed over the interval $[-0.5, 0.5]$. It is observed that, for $L = 1$ both the proposed and Tureli's estimators have similar MSE performance. However, Tureli's estimator hits an error floor when $L = 3$ thereby confirming that it is not suitable for frequency selective multipath fading channels. The proposed estimator's MSE for $L = 3$ is identical to that for $L = 1$. Therefore, the proposed estimator is suitable for both frequency selective and frequency flat fading channels.

In Presence of PN

The MSE performance of the proposed estimator in the presence of PN is obtained through computer simulations. We consider a Gaussian PN model as in

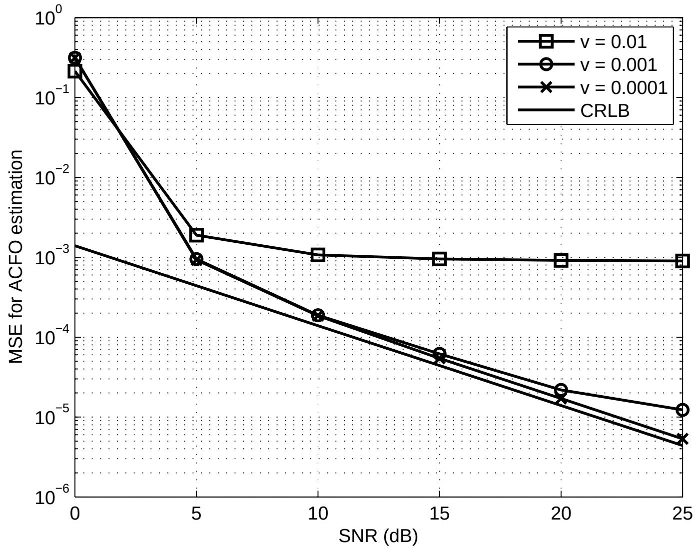

Fig. 5.6: MSE for ACFO estimation when $\phi_i \in [-0.5, 0.5]$.

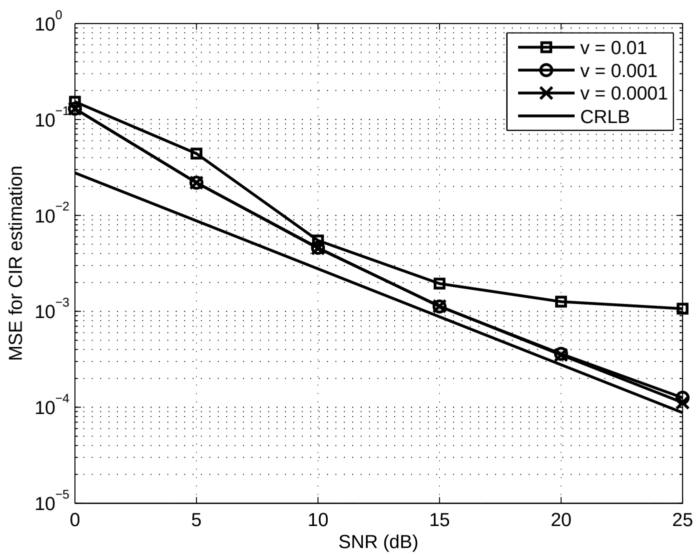

Fig. 5.7: MSE for CIR estimation when $\phi_i \in [-0.5, 0.5]$.

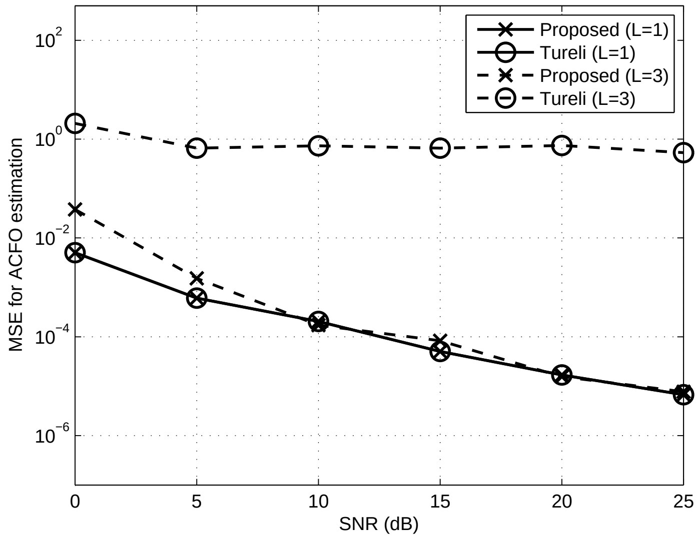

Fig. 5.8: Comparison with Tureli's ACFO estimator.

[49]. In the presence of PN, the received signal at the base station is given by

$$\mathbf{r}(n) = \sum_{i=0}^{T-1}\sum_{k=0}^{Q-1} e^{(jn(N+P)+P)\phi_i}\dot{\mathbf{Z}}_N(n,\phi_i)\widetilde{\mathbf{B}}_{i,k}\mathbf{h}_i s_i(nQ+k) + \mathbf{v}(n), \tag{5.58}$$

where the $(N \times N)$ diagonal matrix is given by

$$\dot{\mathbf{Z}}_N(n,\phi_i) = diag\left(\left[e^{j\theta_i(nG+L-1)}, e^{j(\phi_i+\theta_i(nG+L))}, \cdots, e^{j((N-1)\phi_i+\theta_i(nG+G-1))}\right]^T\right). \tag{5.59}$$

Let $\theta_i(n) = [\theta_i(nG+L-1), \theta_i(nG+L), \theta_i(nG+L+1), \cdots, \theta_i(nG+G-1)]^T$. The element in the pth row and qth column of the Gaussian PN covariance matrix $\mathbf{R}_{\theta_i} = E[\theta_i(n)\theta_i^H(n)]$ is given by

$$\mathbf{R}_{\theta_i}(p,q) = \left(\frac{\pi\omega}{180}\right)^2 e^{-2\pi|p-q|\chi}, \tag{5.60}$$

where $\omega = 3$ and $\chi = 0.005$ were chosen for simulation [49]. The MSE for ACFO and CIR estimates obtained using EDMM are shown in Figs. 5.9 and 5.10, respectively. From the simulations results, it is observed that the PN does not affect the MSE at low SNR. At high SNR, the MSE for ACFO and CIR estimates obtained in the presence of PN, is higher than the MSE for ACFO and CIR estimates obtained in the absence of PN. Thus, the proposed estimator is not significantly affected by PN.

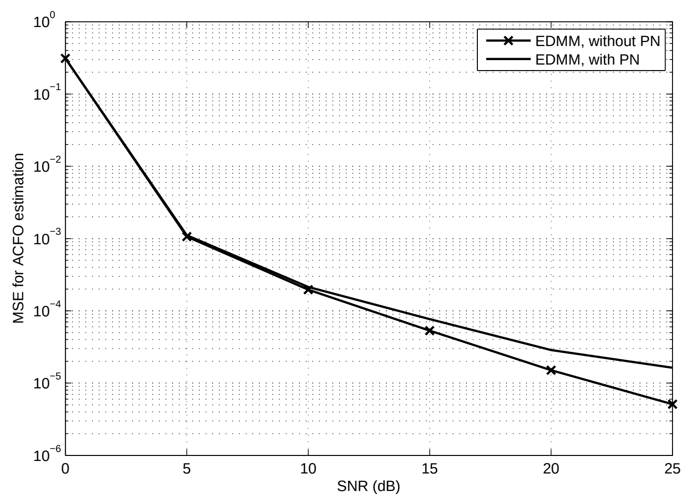

Fig. 5.9: ACFO estimation when $\{\phi_i \in [-0.5, 0.5]\}_{i=0}^{T-1}$.

MSE vs Users

We compare the MSE for ACFO and CIR estimates obtained using EDMM for different number of users. For simulation we consider $G = 32$, $Q = 2$, $L = 3$ and users ACFO in the interval $[-0.5, 0.5]$. Grid size $v = 0.0001$ is used for the grid search. Figs. 5.11 and 5.12 shows the MSE for ACFO and CIR estimates,

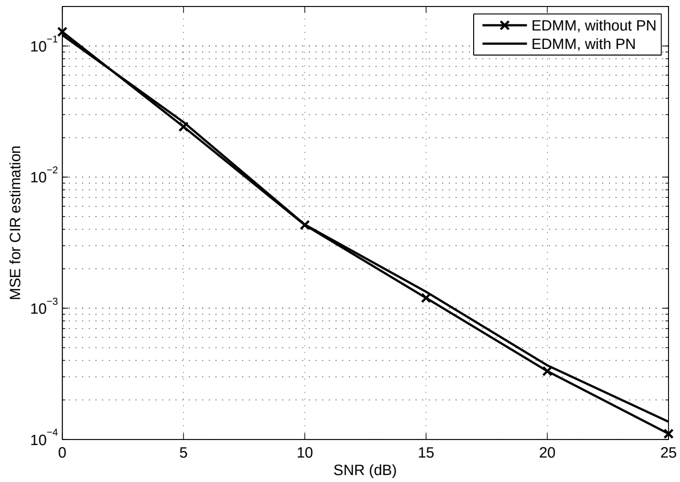

Fig. 5.10: CIR estimation when $\{\phi_i \in [-0.5, 0.5]\}_{i=0}^{T-1}$.

respectively. As the number of users is increased, it is observed that the MSE increases. This is due to the increase in MAI. Furthermore, it is observed that the performance of EDMM based estimator gracefully degrades with the increase in the number of users. Note that when $T > 10$, the spreading gain does not satisfy the inequality in (4.41). In this case, though the estimator performs well, the identifiability of the estimates is yet to be proved when the inequality in (4.41) is not satisfied and the grid search is on the interval $[-0.5, 0.5]$.

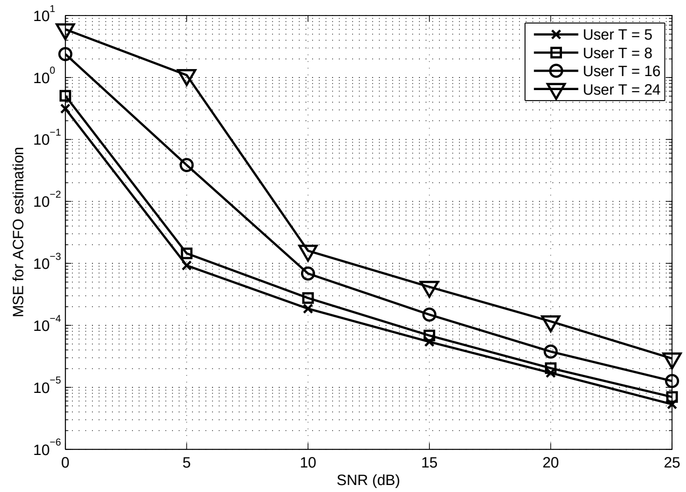

Fig. 5.11: ACFO estimation when $\{\phi_i \in [-0.5, 0.5]\}_{i=0}^{T-1}$.

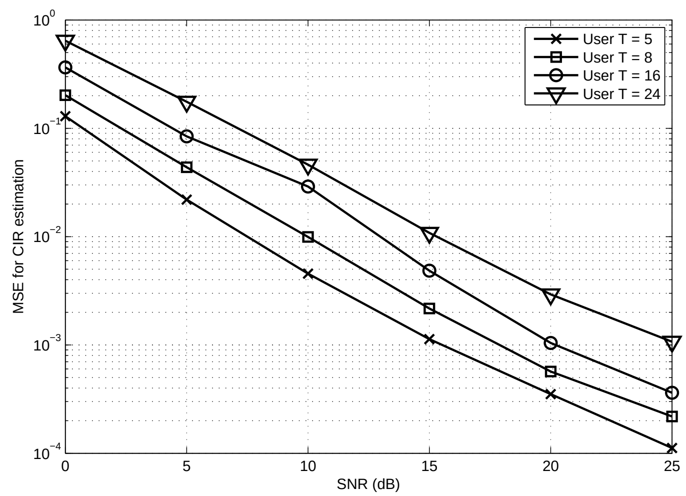

Fig. 5.12: CIR estimation when $\{\phi_i \in [-0.5, 0.5]\}_{i=0}^{T-1}$.

5.8 Conclusion

In this chapter, the differences between CP-CDMA and MC-CDMA systems were clearly outlined. The $(N \times L)$ matrices $\left\{\{\widetilde{\mathbf{B}}_{i,k}\}_{k=0}^{Q-1}\right\}_{i=0}^{T-1}$ were shown to be of full rank L without imposing any constraint on the user spreading code. Though the formulation of the blind joint ACFO and CIR estimator for MC-CDMA system is similar to that for CP-CDMA system, the matrix constructions in CP-CDMA and MC-CDMA are different. The existing ACFO estimator for uplink MC-CDMA system formulated by Tureli et. al. was shown to be applicable only in flat fading channels and cannot be used in frequency selection multipath fading channels. The proposed estimator's performance was compared with the existing Tureli's estimator. In flat fading channels, both the proposed and Tureli's estimators were observed to have similar performance. In frequency selective multipath fading channels, Tureli's estimator could not estimate the ACFO, whereas the proposed estimator could accurately estimate the user's ACFO value. Thus the proposed estimator can be used in both flat fading and frequency selective multipath fading channels. In DS-CDMA and CP-CDMA systems, the signal subspace dimensionality was assumed to be T and QT, respectively. In this chapter, it was shown that if the users' spreading codes were properly chosen for MC-CDMA system then the signal subspace is QT dimensional for any combination of users' ACFOs and CIRs. For small grid size v, the MSE performances for ACFO and CIR estimation obtained through computer simulations were observed to be close to CRLB.

Chapter 6

Two-Stage ACFO Estimator

In chapter 3, chapter 4 and chapter 5, EDMM based estimator using a grid search is used to estimate the desired user's ACFO. A grid search over the interval $[-\pi, \pi)$ with grid size $v = 0.0001$ involves searching 62831 points. For each search point, the determinant of a $(L \times L)$ matrix is to be computed. This computation requires $O(L^3)$ multiplications. Therefore, as L increases the computational complexity of the proposed estimator increases drastically. Prior knowledge about users' ACFO can be used to truncate the search interval. However, this truncation in the search interval does not provide significant reduction in the computational complexity in absolute sense. For example, if the desired user's ACFO is a random variable uniformly distributed over the interval $[-0.5, 0.5]$, then the grid search can be done over the interval $[-0.5, 0.5]$. For the above scenario, if the grid size is $v = 0.0001$ then the number of search points to be searched is 10001. Thus, it is evident that employing a fine grid search based estimator for ACFO estimation is computationally demanding. Hence the analysis of the cost function is essential to formulate a less computationally intensive ACFO estimator. In this chapter, the cost function used for ACFO estimation in DS-CDMA, CP-CDMA and MC-CDMA systems is shown to be locally convex. Using this knowledge, the grid search method used for ACFO estimation is improved. A coarse grid search is performed to obtain a coarse ACFO estimate for the desired user. This estimate is then used as the initial value for the Newton's algorithm which converges to give a finer ACFO estimate for the desired user.

6.1 Generalized Received Signal

The following description of vector $\mathbf{r}(n)$ allows us to represent the received signal vector in the uplink transmission of DS-CDMA, CP-CDMA and MC-CDMA systems. The $(N \times 1)$ vector $\mathbf{r}(n)$ is given by

$$\mathbf{r}(n) = \sum_{i=0}^{T-1} e^{j(n(N+P)+P)\phi_i} \mathbf{Z}_N(\phi_i)\breve{\mathbf{B}}_i \left(\mathbf{I}_Q \otimes \mathbf{h}_i\right) \mathbf{s}_i(n) + \mathbf{v}(n). \tag{6.1}$$

The data block size for DS-CDMA system is $Q = 1$. For DS-CDMA system $N = G - L + 1$ but for CP-CDMA and MC-CDMA systems $N = QG$. The parameter P for DS-CDMA, CP-CDMA and MC-CDMA systems is $P = L - 1$. For DS-CDMA, $\breve{\mathbf{B}}_i$ is a $(N \times L)$ dimensional matrix given by $\breve{\mathbf{B}}_i = \widetilde{\mathbf{B}}_i$. For CP-CDMA and MC-CDMA, $\breve{\mathbf{B}}_i$ is a $(N \times QL)$ matrix given by $\breve{\mathbf{B}}_i = [\widetilde{\mathbf{B}}_{i,0}, \widetilde{\mathbf{B}}_{i,1}, \cdots, \widetilde{\mathbf{B}}_{i,Q-1}]$. In the above mentioned systems, the ACFO is estimated by minimizing the determinant of the $(L \times L)$ matrix $\daleth_i(\phi) = \mathbf{\Gamma}_i^H(\phi)\mathbf{\Gamma}_i(\phi)$ where

$$\mathbf{\Gamma}_i(\phi) = \mathbf{\Psi}\widetilde{\mathbf{Z}}(\phi)\mathbf{D}_i. \tag{6.2}$$

Matrix $\boldsymbol{\Psi} = \mathbf{I}_Q \otimes \mathbf{U}_n^H$ and $\widetilde{\mathbf{Z}}(\phi) = \mathbf{I}_Q \otimes \mathbf{Z}_N(\phi)$. Matrix $\mathbf{D}_i$ is $(N \times L)$ dimensional for DS-CDMA system and is given by $\mathbf{D}_i = \widetilde{\mathbf{B}}_i$. For CP-CDMA and MC-CDMA systems, $\mathbf{D}_i$ is a $(QN \times L)$ dimensional matrix constructed as $\mathbf{D}_i = \left[\widetilde{\mathbf{B}}_{i,0}^T, \widetilde{\mathbf{B}}_{i,1}^T, \cdots, \widetilde{\mathbf{B}}_{i,Q-1}^T\right]^T$.

6.2 Matrix $\widetilde{\mathbf{Z}}(\phi)$

The $(QN \times QN)$ dimensional diagonal matrix $\widetilde{\mathbf{Z}}(\phi)$ can be written as

$$\widetilde{\mathbf{Z}}(\phi) \;=\; \mathbf{I}_Q \otimes e^{j\frac{N-1}{2}\phi}\mathbf{Z}_a(\phi), \tag{6.3}$$

where

$$\mathbf{Z}_a(\phi) \;=\; diag\left(\left[e^{-j\frac{N-1}{2}\phi},\; e^{-j\frac{N-3}{2}\phi}, \cdots, e^{j\frac{N-1}{2}\phi}\right]^T\right). \tag{6.4}$$

For the ith user's estimator, matrix $\mathbf{Z}_a(\phi)$ can be approximated using first order Taylor's series expansion as follows:

$$\mathbf{Z}_a(\phi) \;\approx\; \mathbf{Z}_a(\phi_i) + \frac{j(\phi-\phi_i)}{2}\mathbf{Z}_a(\phi_i)\mathbf{A}, \tag{6.5}$$

where

$$\mathbf{A} \;=\; diag\left([-(N-1),\; -(N-3), \cdots, (N-1)]^T\right). \tag{6.6}$$

The singularity of matrix $\mathbf{A}$ is circumvented by choosing N to be an even integer. Substituting (6.5) into (6.3), matrix $\widetilde{\mathbf{Z}}(\phi)$ is approximated as

$$\widetilde{\mathbf{Z}}(\phi) \approx e^{j\frac{N-1}{2}\phi}\left(\bar{\mathbf{Z}}_{a,i} + \frac{j(\phi-\phi_i)}{2}\bar{\mathbf{Z}}_{a,i}\bar{\mathbf{A}}\right), \tag{6.7}$$

where

$$\bar{\mathbf{A}} = \mathbf{I}_Q \otimes \mathbf{A}, \tag{6.8}$$

$$\bar{\mathbf{Z}}_{a,i} = \mathbf{I}_Q \otimes \mathbf{Z}_a(\phi_i). \tag{6.9}$$

6.3 Cost Function for ACFO Estimation

The grid search based ACFO estimator is given by

$$\hat{\phi}_i = \arg\min_{\phi}\left\{det\left(\mathbf{\Gamma}_i^H(\phi)\mathbf{\Gamma}_i(\phi)\right)\right\}. \tag{6.10}$$

Let $\daleth_i(\phi) = \mathbf{\Gamma}_i^H(\phi)\mathbf{\Gamma}_i(\phi)$ and hence

$$\daleth_i(\phi) = \mathbf{D}_i^H\widetilde{\mathbf{Z}}^H(\phi)\mathbf{\Psi}^H\mathbf{\Psi}\widetilde{\mathbf{Z}}(\phi)\mathbf{D}_i. \tag{6.11}$$

Let $Y_\phi = det(\daleth_i(\phi))$, thus the objective is to analyze the function Y_ϕ. Substituting (6.7) into (6.11), an approximation for matrix $\daleth_i(\phi)$ is obtained as follows:

$$\daleth_i(\phi) \approx \widetilde{\daleth}_i(\phi) = \mathbf{K}_0 + (\phi-\phi_i)\mathbf{K}_1 + (\phi-\phi_i)^2\mathbf{K}_2, \tag{6.12}$$

where[1]

$$\begin{aligned}
\mathbf{K}_0 &= \mathbf{D}_i^H \bar{\mathbf{Z}}_{a,i}^H \boldsymbol{\Psi}^H \boldsymbol{\Psi} \bar{\mathbf{Z}}_{a,i} \mathbf{D}_i, && (6.13)\\
\mathbf{K}_1 &= j\left[\mathbf{D}_i^H \bar{\mathbf{Z}}_{a,i}^H \boldsymbol{\Psi}^H \boldsymbol{\Psi} \bar{\mathbf{Z}}_{a,i} \bar{\mathbf{A}} \mathbf{D}_i - \mathbf{D}_i^H \bar{\mathbf{A}}^H \bar{\mathbf{Z}}_{a,i}^H \boldsymbol{\Psi}^H \boldsymbol{\Psi} \bar{\mathbf{Z}}_{a,i} \mathbf{D}_i\right]/2, && (6.14)\\
\mathbf{K}_2 &= \left[\mathbf{D}_i^H \bar{\mathbf{A}}^H \bar{\mathbf{Z}}_{a,i}^H \boldsymbol{\Psi}^H \boldsymbol{\Psi} \bar{\mathbf{Z}}_{a,i} \bar{\mathbf{A}} \mathbf{D}_i\right]/4. && (6.15)
\end{aligned}$$

Matrices $\mathbf{K}_0$, $\mathbf{K}_1$ and $\mathbf{K}_2$ are $(L \times L)$ dimensional Hermitian matrices, where $\mathbf{K}_0$ and $\mathbf{K}_2$ are positive semi-definite. The approximation in (6.12) is valid for small values of ϕ around ϕ_i, and hence Y_ϕ can be approximated with $\tilde{Y}_\phi$ as follows:

$$Y_\phi \approx \tilde{Y}_\phi = det\left(\widetilde{\beth}_i(\phi)\right). \tag{6.16}$$

The first derivative of $\tilde{Y}_\phi$ w.r.t ϕ is given by [116]

$$\frac{\partial \tilde{Y}_\phi}{\partial \phi} = tr\left(adj(\widetilde{\beth}_i(\phi))\frac{\partial \widetilde{\beth}_i(\phi)}{\partial \phi}\right), \tag{6.17}$$

where $adj(\widetilde{\beth}_i(\phi))$ denotes the adjoint of matrix $\widetilde{\beth}_i(\phi)$. It can be shown that (see Appendix E),

$$adj(\widetilde{\beth}_i(\phi)) \approx \mathbf{F}_0 + (\phi - \phi_i)\mathbf{F}_1 + (\phi - \phi_i)^2 \mathbf{F}_2. \tag{6.18}$$

Matrices $\mathbf{F}_0$ and $\mathbf{F}_2$ are $(L \times L)$ positive semi-definite Hermitian matrices and $\mathbf{F}_1$ is a $(L \times L)$ Hermitian matrix. Substituting (6.18) into (6.17), the first derivative

[1]For notational convenience, the user index i is not tagged to matrices $\mathbf{K}_0$, $\mathbf{K}_1$ and $\mathbf{K}_2$.

of $\tilde{Y}_\phi$ is simplified to

$$\begin{aligned}\frac{\partial \tilde{Y}_\phi}{\partial \phi} &= tr(\mathbf{F}_0\mathbf{K}_1) + (\phi - \phi_i)tr(\mathbf{F}_1\mathbf{K}_1 + 2\mathbf{F}_0\mathbf{K}_2) \\ &\quad + (\phi - \phi_i)^2 tr(\mathbf{F}_2\mathbf{K}_1 + 2\mathbf{F}_1\mathbf{K}_2) + 2(\phi - \phi_i)^3 tr(\mathbf{F}_2\mathbf{K}_2). \end{aligned} \tag{6.19}$$

Therefore, the value of the first derivative of $\tilde{Y}_\phi$ at $\phi = \phi_i$ is

$$\left.\frac{\partial \tilde{Y}_\phi}{\partial \phi}\right|_{\phi=\phi_i} = tr(\mathbf{F}_0\mathbf{K}_1) \tag{6.20}$$

where $\mathbf{F}_0 = adj(\mathbf{K}_0)$. As $\mathbf{K}_0 = \mathbf{D}_i^H \bar{\mathbf{Z}}_{a,i}^H \mathbf{\Psi}^H \mathbf{\Psi} \bar{\mathbf{Z}}_{a,i} \mathbf{D}_i$, it can easily be verified that $\mathbf{K}_0\mathbf{h}_i = \mathbf{0}_{L\times 1}$ and $\mathbf{h}_i \neq \mathbf{0}_{L\times 1}$. Therefore, $\mathbf{h}_i \in null(\mathbf{K}_0)$ and hence

$$rank(\mathbf{K}_0) < L. \tag{6.21}$$

If $\mathbf{X}$ is a $(L \times L)$ matrix, then the adjoint of $\mathbf{X}$ exists iff $rank(\mathbf{X}) \geq L - 1$, else $adj(\mathbf{X}) = \mathbf{0}_{L\times L}$ [116]. The asymptotic constraint on the users' spreading codes ensures that $rank(\mathbf{K}_0) = L - 1$ for CP-CDMA and MC-CDMA systems. Assumption **AS2** in chapter 3 implies that $rank(\mathbf{K}_0) = L - 1$ for DS-CDMA system. Thus,

$$adj(\mathbf{K}_0) = \alpha \mathbf{h}_i \mathbf{h}_i^H, \tag{6.22}$$

where α is the product of the non-zero eigenvalues of $\mathbf{K}_0$ [116]. Substituting (6.22) into (6.20), the first derivative of $\tilde{Y}_\phi$ at $\phi = \phi_i$ is

$$\left.\frac{\partial \tilde{Y}_\phi}{\partial \phi}\right|_{\phi=\phi_i} = tr\left(\mathbf{F}_0 \mathbf{K}_1\right),$$

$$\left.\frac{\partial \tilde{Y}_\phi}{\partial \phi}\right|_{\phi=\phi_i} = \alpha \mathbf{h}_i^H \mathbf{K}_1 \mathbf{h}_i = 0, \tag{6.23}$$

since $\mathbf{\Psi}\bar{\mathbf{Z}}_{a,i}\mathbf{D}_i\mathbf{h}_i = \mathbf{0}_{Q(N-\mathcal{S})\times 1}$. Therefore, the first derivative of $\tilde{Y}_\phi$ w.r.t ϕ is zero at $\phi = \phi_i$. To prove that $\tilde{Y}_\phi$ is convex, the second derivative of $\tilde{Y}_\phi$ must be shown to be positive.

6.4 Second Derivative of $\tilde{Y}_\phi$

It is necessary to show that the second derivative of the cost function around the true ACFO value is positive, so that the Newton's algorithm can converge and remain stable [119]. Therefore, it is essential to check whether the second derivative of the cost function is positive in the interval around the true ACFO value where the first order Taylor's series approximation holds good.

The determinant of matrix $\tilde{\beth}_i(\phi)$ can also be expressed as [116]

$$det(\tilde{\beth}_i(\phi))L = L\,\tilde{Y}_\phi = tr\left(adj(\tilde{\beth}_i(\phi))\tilde{\beth}_i(\phi)\right). \tag{6.24}$$

Therefore,

$$\begin{aligned} L\,\tilde{Y}_\phi &= tr(\mathbf{F}_0\mathbf{K}_0) + (\phi-\phi_i)tr(\mathbf{F}_1\mathbf{K}_0 + \mathbf{F}_0\mathbf{K}_1) + (\phi-\phi_i)^2 tr(\mathbf{F}_2\mathbf{K}_0 + \mathbf{F}_1\mathbf{K}_1 + \mathbf{F}_0\mathbf{K}_2) \\ &\quad + (\phi-\phi_i)^3 tr(\mathbf{F}_1\mathbf{K}_2 + \mathbf{F}_2\mathbf{K}_1) + (\phi-\phi_i)^4 tr(\mathbf{F}_2\mathbf{K}_2). \end{aligned} \tag{6.25}$$

The first derivative of $L\,\tilde{Y}_\phi$ is given by

$$\begin{aligned} L\,\frac{\partial\tilde{Y}_\phi}{\partial\phi} &= tr(\mathbf{F}_1\mathbf{K}_0 + \mathbf{F}_0\mathbf{K}_1) + 2(\phi-\phi_i)tr(\mathbf{F}_2\mathbf{K}_0 + \mathbf{F}_1\mathbf{K}_1 + \mathbf{F}_0\mathbf{K}_2) \\ &\quad + 3(\phi-\phi_i)^2 tr(\mathbf{F}_1\mathbf{K}_2 + \mathbf{F}_2\mathbf{K}_1) + 4(\phi-\phi_i)^3 tr(\mathbf{F}_2\mathbf{K}_2). \end{aligned} \tag{6.26}$$

By multiplying equation (6.19) with L and equating it to (6.26), the following results are derived:

$$tr(\mathbf{F}_2\mathbf{K}_2) = 0 \quad \text{and} \quad tr(\mathbf{F}_1\mathbf{K}_0) = 0. \tag{6.27}$$

Note that, the $(L\times L)$ matrices $\mathbf{K}_0+(\phi-\phi_i)\mathbf{K}_1+(\phi-\phi_i)^2\mathbf{K}_2$ and $\mathbf{F}_0+(\phi-\phi_i)\mathbf{F}_1+(\phi-\phi_i)^2\mathbf{F}_2$ are positive semi-definite for any real value ϕ, i.e., $-\infty \leq \phi \leq \infty$ (refer to equation (E.3) in Appendix E).

***Lemma* 6.1.** If $\mathbf{A}$ and $\mathbf{B}$ are two $(L\times L)$ positive semi-definite Hermitian matrices then $tr(\mathbf{AB}) \geq 0$. [118]

Therefore, Lemma 6.1 implies that

$$\begin{aligned} tr\left(\left[\mathbf{F}_0 + (\phi-\phi_i)\mathbf{F}_1 + (\phi-\phi_i)^2\mathbf{F}_2\right]\mathbf{K}_2\right) &\geq 0, \\ tr\left(\mathbf{F}_2\left[\mathbf{K}_0 + (\phi-\phi_i)\mathbf{K}_1 + (\phi-\phi_i)^2\mathbf{K}_2\right]\right) &\geq 0, \end{aligned} \tag{6.28}$$

for $-\infty \leq \phi \leq \infty$. Using (6.27) in (6.28), we obtain

$$tr(\mathbf{F}_0\mathbf{K}_2) + (\phi - \phi_i) tr(\mathbf{F}_1\mathbf{K}_2) \geq 0, \tag{6.29}$$

$$tr(\mathbf{F}_2\mathbf{K}_0) + (\phi - \phi_i) tr(\mathbf{F}_2\mathbf{K}_1) \geq 0, \tag{6.30}$$

for $-\infty \leq \phi \leq \infty$. Lemma 6.1 implies that $tr(\mathbf{F}_0\mathbf{K}_2) \geq 0$ and $tr(\mathbf{F}_2\mathbf{K}_0) \geq 0$. Therefore, equations (6.29) and (6.30) will hold for any value of ϕ only if $tr(\mathbf{F}_1\mathbf{K}_2) = tr(\mathbf{F}_2\mathbf{K}_1) = 0$. Thus, $L\,\tilde{Y}_\phi$ in (6.25) is given by

$$L\,\tilde{Y}_\phi = tr(\mathbf{F}_0\mathbf{K}_0) + (\phi - \phi_i)^2 tr(\mathbf{F}_2\mathbf{K}_0 + \mathbf{F}_1\mathbf{K}_1 + \mathbf{F}_0\mathbf{K}_2). \tag{6.31}$$

It is known that $\tilde{Y}_\phi \geq 0$ for $-\infty \leq \phi \leq \infty$, therefore the discriminant of the quadratic equation in (6.31) should be negative or zero, i.e.,

$$-4\,tr(\mathbf{F}_0\mathbf{K}_0)\,tr(\mathbf{F}_2\mathbf{K}_0 + \mathbf{F}_1\mathbf{K}_1 + \mathbf{F}_0\mathbf{K}_2) \leq 0. \tag{6.32}$$

Lemma 6.1 implies that $tr(\mathbf{F}_0\mathbf{K}_0) \geq 0$ and hence

$$tr(\mathbf{F}_2\mathbf{K}_0 + \mathbf{F}_1\mathbf{K}_1 + \mathbf{F}_0\mathbf{K}_2) \geq 0. \tag{6.33}$$

The second derivative of $\tilde{Y}_\phi$ computed from (6.31) is given by

$$L\,\frac{\partial^2 \tilde{Y}_\phi}{\partial \phi^2} = 2\,tr(\mathbf{F}_2\mathbf{K}_0 + \mathbf{F}_1\mathbf{K}_1 + \mathbf{F}_0\mathbf{K}_2). \tag{6.34}$$

Combining the results in equations (6.33) and (6.34), we can deduce that

$$\frac{\partial^2 \tilde{Y}_\phi}{\partial \phi^2} \geq 0. \tag{6.35}$$

Therefore, the second derivative of $\tilde{Y}_\phi$ is shown to be greater than or equal to zero. Hence, the cost function is convex in the interval around the user's true ACFO value where the first order Taylor's series approximation is valid.

6.5 Two-Stage ACFO Estimator

The cost function Y_ϕ is non-quadratic, so Newton's algorithm cannot be used directly without proper initialization as it might lock into a local minimum. A commonly used approach in numerical methods is to do a coarse search to obtain an initial value close to the global minimum and then use Newton's algorithm to obtain a finer estimate. Convergence and stability of Newton's algorithm has been extensively studied in the literature. For example, [119] shows that for non-quadratic cost functions, local convexity around the global minimum of the cost function is essential for the algorithm to remain stable at the minimum point. Thus it is essential to show that Y_ϕ is locally convex around the true ACFO value. Section 6.3 and Section 6.4 shows that Y_ϕ is locally convex around the true ACFO value.

The use of coarse search can significantly reduce the computational complexity. Prior experimentation and simulations can be used to find a suitable grid size (v) for the coarse search, such that the probability of not locking into the local convexity region is minimized. The grid search can be done just once and then Newton's algorithm can be used to track the variations in the ACFO value exploiting the local convexity. Table 6.1 lists the algorithm for the ith user's two-stage ACFO estimator where $\aleph$ is the number of iterations and $\phi_{i,l}$ is the ith user's ACFO estimate during the lth iteration. In order to compute the second derivative of Y_ϕ, the first derivative of $adj(\beth_i(\phi))$ is required. This can be approximated as follows:

$$\frac{\partial adj(\beth_i(\phi))}{\partial \phi} \approx \frac{adj(\beth_i(\phi)) - adj(\beth_i(\phi - \Delta))}{\Delta}, \tag{6.36}$$

where Δ is a very small constant.

6.6 Computational Complexity

In analyzing the computational complexity, we count only the number of multiplications involved. The computational complexity analysis is done for both EDMM based estimator and the two-stage estimator after the computation of noise subspace projection matrix, i.e., $\mathbf{U}_n \mathbf{U}_n^H$.

EDMM Based Estimator

In a linear search based estimator, for each search point the matrix $\beth_i(\phi)$ needs to be constructed and its determinant evaluated. The number of multiplications involved to construct the $(L \times L)$ matrix $\beth_i(\phi)$ is $O(Q(2N^2(L+1))$. The determinant of $\beth_i(\phi)$ can be evaluated by computing the eigenvalue decomposition (EVD) and taking the product of the eigenvalues. The EVD also gives the eigenvectors and hence there is no computation involved in CIR estimation. The number of multiplications required for computing EVD of a $(L \times L)$ matrix is $O(L^3)$. Therefore, if the grid search has $\mathfrak{s}$ search points, then the computational complexity is

Table 6.1: Algorithm for two-stage ACFO estimator.

	Stage 1
1a.	Compute $Y_\phi = det(\gimel_i(\phi))$ for $\phi = \frac{k\pi}{N}$ where $-N/2 \le k \le N/2-1$.
1b.	Select ϕ value for which Y_ϕ has minimum value and assign it to $\hat{\phi}_i$. Goto Stage 2.
	Stage 2
2a.	Initialize $\phi_{i,0} = \hat{\phi}_i$, $l = 1$ and compute $Y_{\phi_{i,0}}$.
2b.	If $l > \aleph$, then stop else goto step 2c.
2c.	Compute $\left.\frac{\partial Y_\phi}{\partial \phi}\right\|_{\phi=\phi_{i,l-1}}$ and $\left.\frac{\partial^2 Y_\phi}{\partial \phi^2}\right\|_{\phi=\phi_{i,l-1}}$.
2d.	Compute $\theta = \phi_{i,l-1} - \mu \frac{\left.\frac{\partial Y_\phi}{\partial \phi}\right\|_{\phi=\phi_{i,l-1}}}{\left.\frac{\partial^2 Y_\phi}{\partial \phi^2}\right\|_{\phi=\phi_{i,l-1}}}$ and $Y_\theta = det(\gimel_i(\theta))$.
2e.	If $Y_\theta \le Y_{\phi_{i,l-1}}$, then $\phi_{i,l} = \theta$ else $\phi_{i,l} = \phi_{i,l-1}$.
2f.	$l = l + 1$ and goto step 2b.

$O\left(\mathfrak{s}\left[Q(2N^2(L+1)) + L^3\right]\right)$.

Two-Stage Estimator

In the first stage of the two-stage estimator a linear search is performed for $2N$ points and hence the computational complexity for the first stage is $O(N[Q(2N^2(L+1)) + L^3])$. In the second stage, the first and second derivatives of the ACFO cost function Y_ϕ needs to be computed. The number of multiplications involved in computing the first derivative is $O(Q(2N^2(L+1)+N)+3L^3+2L^2-L)$. The second derivative is computed using two first derivatives, therefore the computational complexity involved in computing the first and second derivatives is $O([Q(2N^2(L+1)+N)+3L^3+2L^2-L])$. If the Newton algorithm has $\aleph$ iterations, then the computational complexity for the second stage is $O(\aleph[Q(2N^2(L+1)+N)+3L^3+2L^2-L])$.

The computational complexity of the estimators are summarized in Table II. It should be noted that the Newton's algorithm converges in a few iterations. Therefore, the two-stage estimator is computationally less intensive when compared with EDMM based estimator using a fine grid search.

Table 6.2: Computational complexity.

Estimator	Computational Complexity
Linear Search Based	$O\left(\mathfrak{s}\left[Q(2N^2(L+1)) + L^3\right]\right)$
Two-Stage Estimator	
a) First Stage	$O\left(N\left[Q(2N^2(L+1)) + L^3\right]\right)$
b) Second Stage	$O(\aleph\left[Q(2N^2(L+1)+N) + 3L^3 + 2L^2 - L\right])$

6.7 Simulation Results

The simulation parameters described in chapters 3, 4 and 5 for DS-CDMA, CP-CDMA and MC-CDMA systems, respectively are used here. Without loss of generality, $i = 0$ user is considered to be the desired user. The plot of Y_ϕ and $\tilde{Y}_\phi$ for DS-CDMA, CP-CDMA and MC-CDMA systems with SNR = 15dB are shown in Figs. 6.1, 6.2 and 6.3, respectively. It is observed that the cost function Y_ϕ is locally convex in the interval around the desired user's true ACFO value and $\tilde{Y}_\phi$ approximates Y_ϕ in this interval.

The MSE performance for ACFO estimation obtained using the two-stage estimator is compared with that obtained using EDMM based estimator in Figs. 6.4, 6.5 and 6.6 corresponding to DS-CDMA, CP-CDMA and MC-CDMA systems, respectively. Each user's ACFO is assumed to be a random variable uniformly distributed over the interval $[-0.5, 0.5]$. The grid size used for the fine search in EDMM is $v = 0.0001$. The grid size used for the coarse search in the first stage is π/N. For the Newton's algorithm in the second stage, the step size used is $\mu = 0.7$,

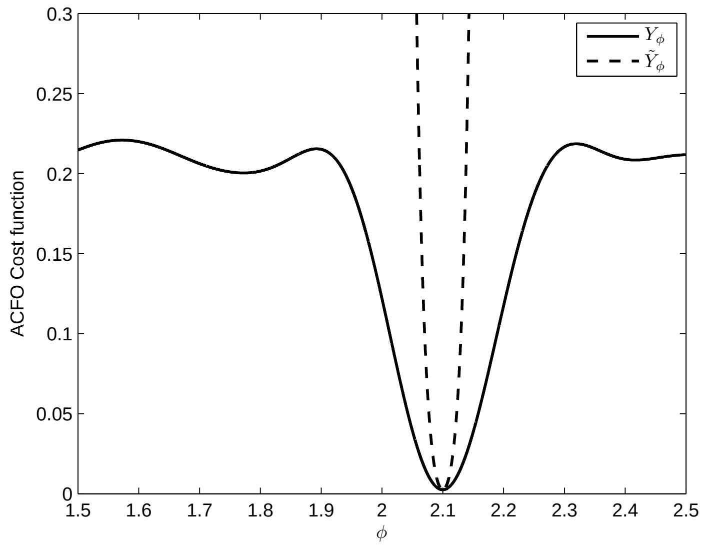

Fig. 6.1: DS-CDMA sytem with $\phi_0 = 2.1$.

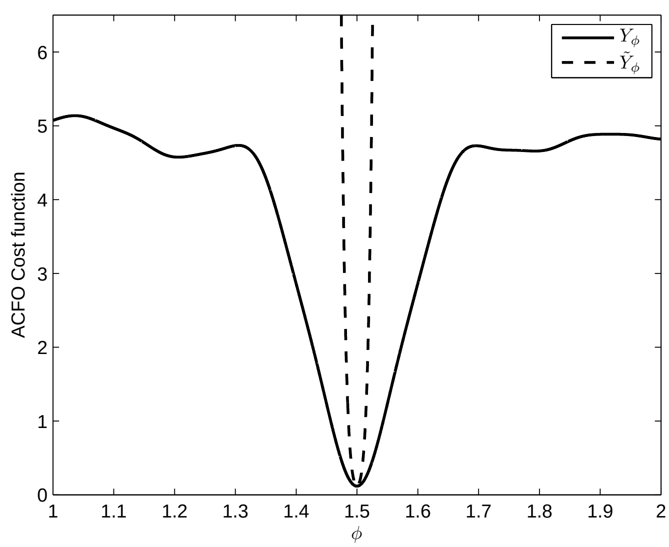

Fig. 6.2: CP-CDMA sytem with $\phi_0 = 1.5$.

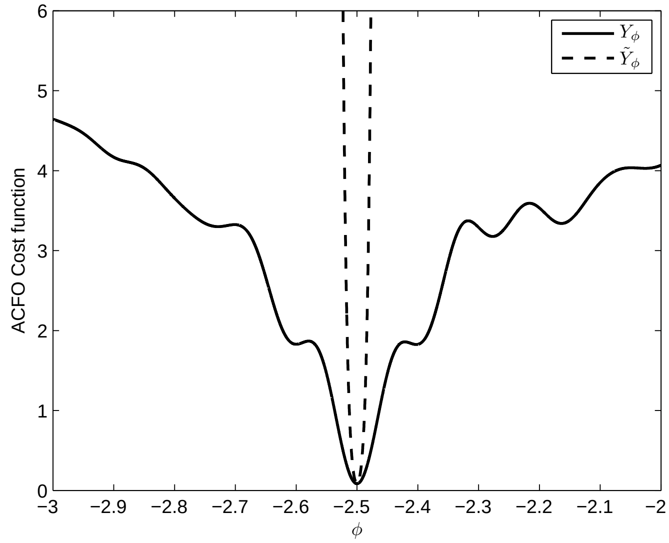

Fig. 6.3: MC-CDMA sytem with $\phi_0 = -2.5$.

number of iterations is $\aleph = 100$ and $\Delta = 0.01$ is used for computing the derivative for the adjoint of matrix $\beth_i(\phi)$. For MC-CDMA, the MSE for ACFO estimate is normalized to the subcarrier spacing. It is observed that the MSE for ACFO estimate obtained after first stage hits a error floor. This is due to the large grid size used in the coarse search. The two-stage estimator's ACFO MSE performance is observed to be identical to that of EDMM. This observation also confirms the convergence of Newton's algorithm in the second stage. The plot of normalized MSE for ACFO estimate versus iteration for MC-CDMA system is shown in Fig. 6.7 where it is observed that the Newton's algorithm converges within 5 iterations. Similar observations were also noted for DS-CDMA and CP-CDMA systems.

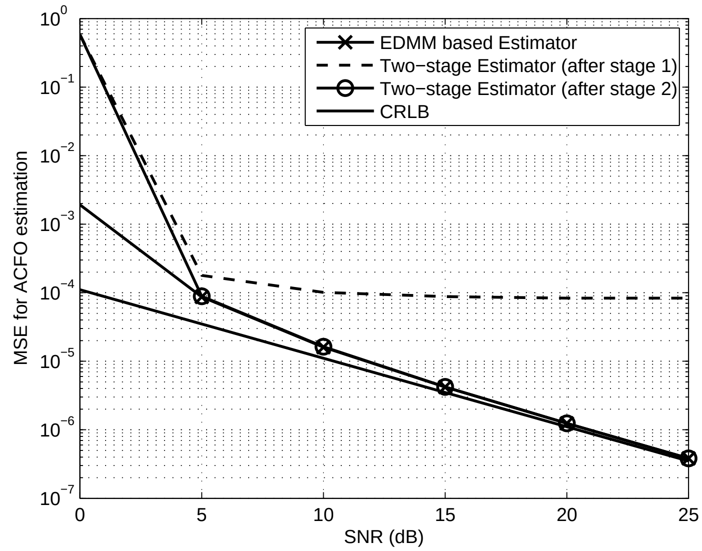

Fig. 6.4: Two-stage ACFO estimator for DS-CDMA sytem.

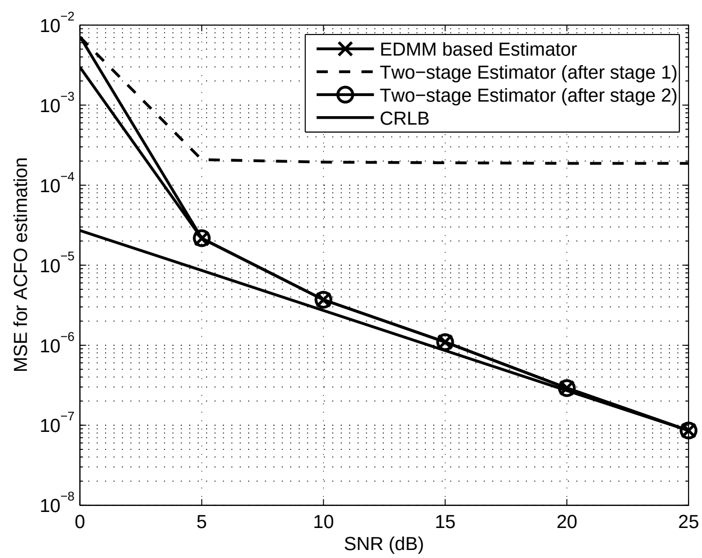

Fig. 6.5: Two-stage ACFO estimator for CP-CDMA sytem.

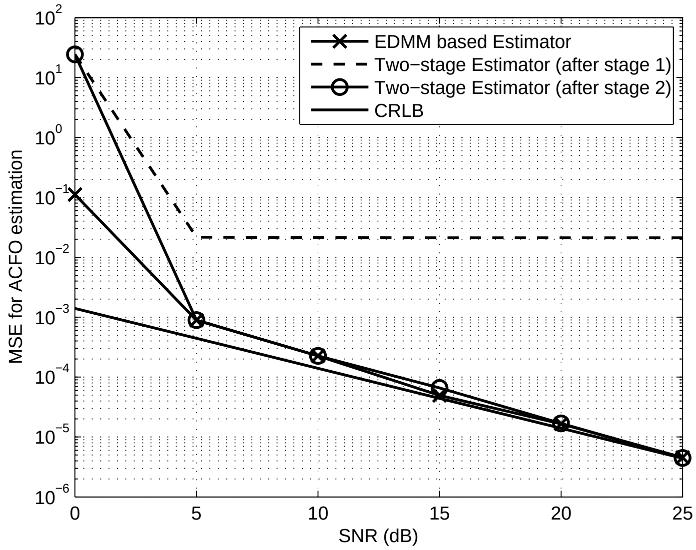

Fig. 6.6: Two-stage ACFO estimator for MC-CDMA sytem.

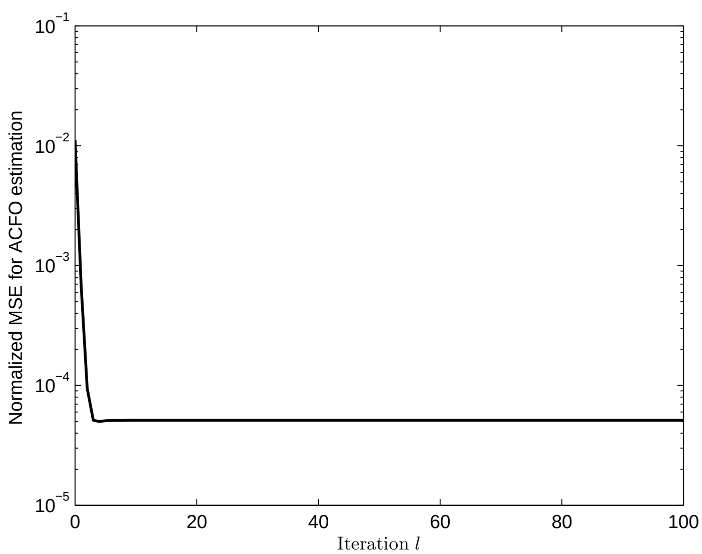

Fig. 6.7: Convergence of Newton's algorithm for MC-CDMA system when $SNR = 15dB$.

6.8 Conclusion

In this chapter, EDMM based estimator using a fine grid search was shown to be computationally demanding as the length of CIR increases. To reduce the computational complexity without compromising for performance degradation, the cost function used for ACFO estimation was analyzed and shown to be locally convex around the true ACFO value. Taking advantage of the cost function's local convexity, a two-stage ACFO estimator was proposed. In the first stage, a coarse grid search was used to obtain a coarse ACFO estimate. This coarse estimate was used as the initial value for the Newton's algorithm in the second second stage. Due to local convexity, the Newton's algorithm converged and a fine estimate for the ACFO was obtained. Through computer simulations, the two-stage estimator and the EDMM based estimator were shown to have almost the same MSE performance. The proposed two-stage ACFO estimator can also be considered to be a feasible solution for tracking small variations in the user's ACFO value during data transmissions.

Chapter 7

Asymptotic Unbiasedness and Theoretical MSE for ACFO Estimation

The objective of this chapter is to analytically evaluate the sensitivity of the estimator proposed in chapter 3, chapter 4 and chapter 5 to AWGN. Due to the presence of noise, the noise subspace estimation is not accurate and there will always be a perturbation in the noise subspace estimate [81]. Using Taylor's series, the ACFO estimator can be linearized as shown in [89]. Using the first order perturbation analysis for the noise subspace estimate given in chapter 2, the 'linearized' estimator is shown to be asymptotically unbiased. Theoretical MSE performance corresponding to ACFO estimation is also derived. The theoretical findings are verified through computer simulations.

7.1 Generalized Received Signal

The following description of vector $\mathbf{r}(n)$ allows to represent the received signal vector in the uplink transmission of DS-CDMA, CP-CDMA and MC-CDMA systems. The $(N \times 1)$ vector $\mathbf{r}(n)$ is given by

$$\mathbf{r}(n) \;=\; \sum_{i=0}^{T-1} e^{j(n(N+P)+P)\phi_i}\mathbf{Z}_N(\phi_i)\breve{\mathbf{B}}_i\left(\mathbf{I}_Q \otimes \mathbf{h}_i\right)\mathbf{s}_i(n) + \mathbf{v}(n). \tag{7.1}$$

The size of data block for DS-CDMA system is $Q = 1$. For DS-CDMA system $N = G - L + 1$ but for CP-CDMA and MC-CDMA systems $N = QG$. The parameter P for DS-CDMA/CP-CDMA/MC-CDMA system is $P = L - 1$. Matrix $\breve{\mathbf{B}}_i = \widetilde{\mathbf{B}}_i$ for DS-CDMA and $\breve{\mathbf{B}}_i = [\widetilde{\mathbf{B}}_{i,0}, \widetilde{\mathbf{B}}_{i,1}, \cdots, \widetilde{\mathbf{B}}_{i,Q-1}]$ for CP-CDMA/MC-CDMA. The $(L \times L)$ matrix $\sqsupset_i(\phi)$ is defined as $\sqsupset_i(\phi) = \mathbf{\Gamma}_i^H(\phi)\mathbf{\Gamma}_i(\phi)$, where $\mathbf{\Gamma}_i(\phi) = \mathbf{\Psi}\widetilde{\mathbf{Z}}(\phi)\mathbf{D}_i$. Matrix $\mathbf{\Psi} = \mathbf{I}_Q \otimes \mathbf{U}_n^H$ and $\widetilde{\mathbf{Z}}(\phi) = \mathbf{I}_Q \otimes \mathbf{Z}_N(\phi)$. Matrix $\mathbf{D}_i = \widetilde{\mathbf{B}}_i$ for DS-CDMA system and $\mathbf{D}_i = [\widetilde{\mathbf{B}}_{i,0}^T, \widetilde{\mathbf{B}}_{i,1}^T, \cdots, \widetilde{\mathbf{B}}_{i,Q-1}^T]^T$ for CP-CDMA/MC-CDMA system.

7.2 Unbiasedness

At high SNR, the perturbation in the ith user's ACFO estimate can be expressed as [89]

$$\Delta\phi_i \;=\; -\frac{\left.\frac{\partial Y_\phi}{\partial \phi}\right|_{\phi=\phi_i}}{\left.\frac{\partial^2 Y_\phi}{\partial \phi^2}\right|_{\phi=\phi_i}}, \tag{7.2}$$

where $Y_\phi = det(\daleth_i(\phi))$. Equation (7.2) can be written as

$$\Delta\phi_i = -\frac{tr\left(adj(\daleth_i(\phi_i))\left.\frac{\partial\,\daleth_i(\phi)}{\partial\phi}\right|_{\phi=\phi_i}\right)}{tr\left(adj(\daleth_i(\phi_i))\left.\frac{\partial^2\daleth_i(\phi)}{\partial\phi^2}\right|_{\phi=\phi_i}\right)+tr\left(\left.\frac{\partial\,adj(\daleth_i(\phi))}{\partial\phi}\right|_{\phi=\phi_i}\left.\frac{\partial\,\daleth_i(\phi)}{\partial\phi}\right|_{\phi=\phi_i}\right)}. \tag{7.3}$$

For values of ϕ around the true ACFO value ϕ_i, $adj(\daleth_i(\phi))$ can be approximated using (6.22) as follows[1]:

$$adj(\daleth_i(\phi)) \approx adj(\mathbf{K}_0) = \xi\mathbf{h}_i\mathbf{h}_i^H \tag{7.4}$$

for ϕ around ϕ_i, where $\mathbf{K}_0$ is defined in chapter 6 equation (6.13). Thus, $tr\left(adj(\daleth_i(\phi_i))\left.\frac{\partial^2\daleth_i(\phi)}{\partial\phi^2}\right|_{\phi=\phi_i}\right)$ is more dominant than $tr\left(\left.\left[\frac{\partial adj(\daleth_i(\phi))}{\partial\phi}\frac{\partial\daleth_i(\phi)}{\partial\phi}\right]\right|_{\phi=\phi_i}\right)$ for values of ϕ around ϕ_i. Substituting (7.4) into (7.3) and using the above observation, $\Delta\phi_i$ can be expressed as

$$\Delta\phi_i \approx -\frac{\mathbf{h}_i^H\left.\frac{\partial\,\daleth_i(\phi)}{\partial\phi}\right|_{\phi=\phi_i}\mathbf{h}_i}{\mathbf{h}_i^H\left.\frac{\partial^2\daleth_i(\phi)}{\partial\phi^2}\right|_{\phi=\phi_i}\mathbf{h}_i}. \tag{7.5}$$

Let *num* and *den* denote the numerator and denominator in (7.5), respectively. The B received vectors used for subspace estimation are stacked to form $(N \times B)$ matrix $\widetilde{\mathbf{\Phi}} = [\mathbf{r}(0), \mathbf{r}(1), \cdots, \mathbf{r}(B-1)]$. Matrix $\widetilde{\mathbf{\Phi}}$ can be expressed as

$$\widetilde{\mathbf{\Phi}} = \mathbf{\Phi} + \mathbf{\Xi}, \tag{7.6}$$

[1] The scalar ξ is the product of non-zero eigenvalues of matrix $\mathbf{K}_0$.

where $\boldsymbol{\Xi} = [\mathbf{v}(0), \mathbf{v}(1), \cdots, \mathbf{v}(B-1)]$ and $\boldsymbol{\Phi}$ is a $(N \times B)$ matrix containing the received vectors in the absence of noise. Due to the presence of noise the estimated noise subspace is perturbed, i.e,

$$\widehat{\mathbf{U}}_n = \mathbf{U}_n + \Delta\mathbf{U}_n, \tag{7.7}$$

where $\widehat{\mathbf{U}}_n$ is the noise subspace estimate and $\Delta\mathbf{U}_n$ is the perturbation in the noise subspace estimate. Using the first order perturbation analysis result, the perturbation in the noise subspace estimate can be expressed as (see equation (2.52) in Section 2.5.1)

$$\Delta\mathbf{U}_n = -\left(\boldsymbol{\Phi}^{\dagger}\right)^H \boldsymbol{\Xi}^H \mathbf{U}_n. \tag{7.8}$$

Let $\widehat{\boldsymbol{\Psi}}$ be a $(Q(N-\mathcal{S}) \times QN)$ matrix denoting the estimate of $\boldsymbol{\Psi}$ where $\boldsymbol{\Psi} = \mathbf{I}_Q \otimes \mathbf{U}_n^H$, i.e.,

$$\widehat{\boldsymbol{\Psi}} = \boldsymbol{\Psi} + \Delta\boldsymbol{\Psi}, \tag{7.9}$$

where $\Delta\boldsymbol{\Psi}$ is the perturbation in the estimate of $\boldsymbol{\Psi}$. Substituting (7.8) in (7.9), $\Delta\boldsymbol{\Psi}$ can be expressed as

$$\Delta\boldsymbol{\Psi} = \mathbf{I}_Q \otimes (\Delta\mathbf{U}_n)^H. \tag{7.10}$$

In the presence of perturbation in the noise subspace estimate, matrix $\sqsupset_i(\phi)$ is obtained as

$$\sqsupset_i(\phi) \;=\; \mathbf{D}_i^H \widetilde{\mathbf{Z}}^H(\phi) \widehat{\mathbf{\Psi}}^H \widehat{\mathbf{\Psi}} \widetilde{\mathbf{Z}}(\phi) \mathbf{D}_i. \tag{7.11}$$

Substituting (7.9) into (7.11) and retaining only the first order terms, *num* and *den* are obtained as follows:

$$\begin{aligned} num &= j\mathbf{h}_i^H \mathbf{D}_i^H \widetilde{\mathbf{Z}}^H(\phi_i)(\Delta\mathbf{\Psi})^H \mathbf{\Psi} \bar{\mathbf{A}} \widetilde{\mathbf{Z}}(\phi_i) \mathbf{D}_i \mathbf{h}_i \\ &\quad - j\mathbf{h}_i^H \mathbf{D}_i^H \widetilde{\mathbf{Z}}^H(\phi_i) \bar{\mathbf{A}} \mathbf{\Psi}^H (\Delta\mathbf{\Psi}) \widetilde{\mathbf{Z}}(\phi_i) \mathbf{D}_i \mathbf{h}_i, \qquad (7.12) \\ den &= 2\mathbf{h}_i^H \mathbf{D}_i^H \widetilde{\mathbf{Z}}^H(\phi_i) \bar{\mathbf{A}} \widehat{\mathbf{\Psi}}^H \widehat{\mathbf{\Psi}} \bar{\mathbf{A}} \widetilde{\mathbf{Z}}(\phi_i) \mathbf{D}_i \mathbf{h}_i \\ &\quad - \mathbf{h}_i^H \mathbf{D}_i^H \widetilde{\mathbf{Z}}^H(\phi_i)(\Delta\mathbf{\Psi})^H \mathbf{\Psi} \bar{\mathbf{A}}^2 \widetilde{\mathbf{Z}}(\phi_i) \mathbf{D}_i \mathbf{h}_i \\ &\quad - \mathbf{h}_i^H \mathbf{D}_i^H \widetilde{\mathbf{Z}}^H(\phi_i) \bar{\mathbf{A}}^2 \mathbf{\Psi}^H (\Delta\mathbf{\Psi}) \widetilde{\mathbf{Z}}(\phi_i) \mathbf{D}_i \mathbf{h}_i, \qquad (7.13) \end{aligned}$$

where

$$\begin{aligned} \bar{\mathbf{A}} &= \mathbf{I}_Q \otimes \widetilde{\mathbf{A}}, \qquad (7.14) \\ \widetilde{\mathbf{A}} &= diag\left([0, 1, \cdots, N-1]^T\right). \qquad (7.15) \end{aligned}$$

For high SNR, *den* can be approximated, independently of noise, as

$$den \;\approx\; 2\, \mathbf{h}_i^H \mathbf{D}_i^H \widetilde{\mathbf{Z}}^H(\phi_i) \bar{\mathbf{A}} \mathbf{\Psi}^H \mathbf{\Psi} \bar{\mathbf{A}} \widetilde{\mathbf{Z}}(\phi_i) \mathbf{D}_i \mathbf{h}_i. \tag{7.16}$$

As $\Delta\mathbf{\Psi}$ contains the noise terms which have zero mean, we have $E[\Delta\mathbf{\Psi}] = \mathbf{0}_{Q(N-\mathcal{S})\times QN}$. Therefore $E[num] = 0$ and hence

$$E[\Delta\phi_i] = \frac{E(num)}{den} = 0. \tag{7.17}$$

Thus, the linearized estimator has been shown to be unbiased for high SNR.

7.3 Theoretical MSE for ACFO Estimation

Let $\mathbf{w}_i = \widetilde{\mathbf{Z}}(\phi_i)\mathbf{D}_i\mathbf{h}_i$ and $\mathbf{V} = j(\Delta\mathbf{\Psi})^H\mathbf{\Psi}\bar{\mathbf{A}}$, therefore for high SNR

$$\begin{aligned} den &\approx 2\,\mathbf{w}_i^H\bar{\mathbf{A}}\mathbf{\Psi}^H\mathbf{\Psi}\bar{\mathbf{A}}\mathbf{w}_i, && (7.18)\\ num &= \mathbf{w}_i^H\mathbf{V}\mathbf{w}_i + \mathbf{w}_i^H\mathbf{V}^H\mathbf{w}_i \\ &= \alpha + \alpha^*, && (7.19) \end{aligned}$$

where $\alpha = \mathbf{w}_i^H\mathbf{V}\mathbf{w}_i$. The MSE for the ith user's ACFO estimate is given by

$$E\left[(\Delta\phi_i)^2\right] = \frac{E\left[num^2\right]}{den^2}. \tag{7.20}$$

Equation (7.19) implies that

$$E\left[num^2\right] = E\left[2\alpha\alpha^*\right] + E\left[(\alpha)^2 + (\alpha^*)^2\right]. \tag{7.21}$$

Let the complex scalar α be expressed in polar coordinates as

$$\alpha = \beta e^{j\theta}, \tag{7.22}$$

where β is a positive real number and $\theta \in [-\pi, \pi)$. It should be noted that

$$\begin{aligned}
\alpha &= \mathbf{w}_i^H \mathbf{V} \mathbf{w}_i \\
&= -j \ \mathbf{w}_i \left[\mathbf{I}_Q \otimes \left(\left(\boldsymbol{\Phi}^{\dagger} \right)^H \boldsymbol{\Xi}^H \mathbf{U}_n \mathbf{U}_n^H \right) \right] \bar{\mathbf{A}} \mathbf{w}_i, \qquad (7.23)
\end{aligned}$$

where $(B \times N)$ matrix $\boldsymbol{\Xi}$ contains AWGN samples. Therefore, α is a Gaussian random variable with mean zero. This implies that β is a Rayleigh distributed random variable and θ is a uniformly distributed random variable over the interval $[-\pi, \pi)$. Furthermore, β and θ are independent. Using this finding, $E\left[(\alpha)^2 + (\alpha^*)^2\right]$ is obtained as follows:

$$\begin{aligned}
E\left[(\alpha)^2 + (\alpha^*)^2\right] &= E\left[\beta^2 \left(e^{j2\theta} + e^{-j2\theta}\right)\right] \\
&= E\left[\beta^2\right] \ E\left[\left(e^{j2\theta} + e^{-j2\theta}\right)\right] \\
&= E\left[\beta^2\right] \ E\left[cos(2\theta)\right] \\
&= 0. \qquad (7.24)
\end{aligned}$$

Substituting (7.24) into (7.21), we obtain

$$E\left[num^2\right] = 2 \ E\left[\alpha\alpha^*\right]. \qquad (7.25)$$

Therefore, the ith user's theoretical MSE is

$$\begin{aligned}
E\left[(\Delta\phi_i)^2\right] &= \frac{2\ E\left[\alpha\alpha^*\right]}{4\ \left(\mathbf{w}_i^H\bar{\mathbf{A}}\mathbf{\Psi}^H\mathbf{\Psi}\bar{\mathbf{A}}\mathbf{w}_i\right)^2} \\
&= \frac{E\left[\mathbf{w}_i^H\mathbf{V}\mathbf{w}_i\mathbf{w}_i^H\mathbf{V}^H\mathbf{w}_i\right]}{2\ \left(\mathbf{w}_i^H\bar{\mathbf{A}}\mathbf{\Psi}^H\mathbf{\Psi}\bar{\mathbf{A}}\mathbf{w}_i\right)^2} \\
&= \frac{E\left[\mathbf{w}_i^H(\Delta\mathbf{\Psi})^H\mathbf{\Psi}\bar{\mathbf{A}}\mathbf{w}_i\mathbf{w}_i^H\bar{\mathbf{A}}\mathbf{\Psi}^H(\Delta\mathbf{\Psi})\mathbf{w}_i\right]}{2\ \left(\mathbf{w}_i^H\bar{\mathbf{A}}\mathbf{\Psi}^H\mathbf{\Psi}\bar{\mathbf{A}}\mathbf{w}_i\right)^2} \\
&= \frac{E\left[\ tr\left(\mathbf{\Psi}\bar{\mathbf{A}}\mathbf{w}_i\mathbf{w}_i^H\bar{\mathbf{A}}\mathbf{\Psi}^H(\Delta\mathbf{\Psi})\mathbf{w}_i\mathbf{w}_i^H(\Delta\mathbf{\Psi})^H\right)\right]}{2\ \left(\mathbf{w}_i^H\bar{\mathbf{A}}\mathbf{\Psi}^H\mathbf{\Psi}\bar{\mathbf{A}}\mathbf{w}_i\right)^2} \\
&= \frac{tr\left(\mathbf{\Psi}\bar{\mathbf{A}}\mathbf{w}_i\mathbf{w}_i^H\bar{\mathbf{A}}\mathbf{\Psi}^H\ E\left[(\Delta\mathbf{\Psi})\mathbf{w}_i\mathbf{w}_i^H(\Delta\mathbf{\Psi})^H\right]\right)}{2\ \left(\mathbf{w}_i^H\bar{\mathbf{A}}\mathbf{\Psi}^H\mathbf{\Psi}\bar{\mathbf{A}}\mathbf{w}_i\right)^2}. \qquad (7.26)
\end{aligned}$$

Combining (7.8) and (7.10), $\Delta\mathbf{\Psi}$ can be expressed as

$$\Delta\mathbf{\Psi} = -\left(\mathbf{I}_Q\otimes\bar{\mathbf{\Xi}}\right)\ \left(\mathbf{I}_Q\otimes\mathbf{\Phi}^\dagger\right), \qquad (7.27)$$

where $\bar{\mathbf{\Xi}} = \mathbf{U}_n^H\mathbf{\Xi}$. It should be noted that

$$\begin{aligned}
\left(\mathbf{I}_Q\otimes\mathbf{\Phi}^\dagger\right)\mathbf{w}_i &= \Big[\left(\mathbf{\Phi}^\dagger\mathbf{Z}_N(\phi_i)\widetilde{\mathbf{B}}_{i,0}\mathbf{h}_i\right)^T, \left(\mathbf{\Phi}^\dagger\mathbf{Z}_N(\phi_i)\widetilde{\mathbf{B}}_{i,1}\mathbf{h}_i\right)^T, \cdots, \\
&\qquad \cdots, \left(\mathbf{\Phi}^\dagger\mathbf{Z}_N(\phi_i)\widetilde{\mathbf{B}}_{i,Q-1}\mathbf{h}_i\right)^T\Big]^T \\
&= \left[\mathbf{g}_{i,0}^T, \mathbf{g}_{i,1}^T, \cdots, \mathbf{g}_{i,Q-1}^T\right]^T, \qquad (7.28)
\end{aligned}$$

where $\mathbf{g}_{i,k}$ is $(B \times 1)$ vector given by

$$\mathbf{g}_{i,k} = \mathbf{\Phi}^{\dagger}\mathbf{Z}_N(\phi_i)\widetilde{\mathbf{B}}_{i,k}\mathbf{h}_i, \tag{7.29}$$

for $k = 0, 1, \cdots, Q-1$. The $(Q(N-\mathcal{S}) \times QB)$ matrix $\left(\mathbf{I}_Q \otimes \bar{\mathbf{\Xi}}\right)$ can be written as[2]

$$\left(\mathbf{I}_Q \otimes \bar{\mathbf{\Xi}}\right) = \left[\left(\mathbf{I}_Q(:,1) \otimes \bar{\mathbf{\Xi}}\right), \left(\mathbf{I}_Q(:,2) \otimes \bar{\mathbf{\Xi}}\right), \cdots, \left(\mathbf{I}_Q(:,Q) \otimes \bar{\mathbf{\Xi}}\right)\right], \tag{7.30}$$

where $(Q(N-\mathcal{S}) \times B)$ matrix $\left(\mathbf{I}_Q(:,k) \otimes \bar{\mathbf{\Xi}}\right)$ for $k = 0, 1, \cdots, Q-1$ is given by

$$\begin{aligned}\mathbf{I}_Q(:,k) \otimes \bar{\mathbf{\Xi}} &= \left[\left\{\mathbf{I}_Q(:,k) \otimes \bar{\mathbf{\Xi}}(:,1)\right\}, \left\{\mathbf{I}_Q(:,k) \otimes \bar{\mathbf{\Xi}}(:,2)\right\}, \cdots,\right. \\ &\qquad \left.\cdots, \left\{\mathbf{I}_Q(:,k) \otimes \bar{\mathbf{\Xi}}(:,B)\right\}\right]. \end{aligned} \tag{7.31}$$

Using equations (7.28), (7.29), (7.30) and (7.31), the $(Q(N-\mathcal{S}) \times 1)$ vector $(\Delta\mathbf{\Psi})\mathbf{w}_i$ can be expressed as

$$\begin{aligned}(\Delta\mathbf{\Psi})\mathbf{w}_i &= -\left(\mathbf{I}_Q \otimes \bar{\mathbf{\Xi}}\right)\left(\mathbf{I}_Q \otimes \mathbf{\Phi}^{\dagger}\right)\left[\mathbf{g}_{i,0}^T, \mathbf{g}_{i,1}^T, \cdots, \mathbf{g}_{i,Q-1}^T\right]^T \\ &= -\sum_{k=0}^{Q-1}\sum_{n=1}^{B} [\mathbf{g}_{i,k}]_{(1,n)} \quad \left[\mathbf{I}_Q(:,k) \otimes \bar{\mathbf{\Xi}}(:,n)\right], \end{aligned} \tag{7.32}$$

where $[\mathbf{g}_{i,k}]_{(1,n)}$ denotes the nth element of vector $\mathbf{g}_{i,k}$. Let $\bar{\mathbf{e}}_{k,n}$ be a $(Q(N-\mathcal{S}) \times 1)$ vector defined as

$$\bar{\mathbf{e}}_{k,n} = \mathbf{I}_Q(:,k) \otimes \bar{\mathbf{\Xi}}(:,n), \tag{7.33}$$

[2]For any matrix $\mathbf{A}$, $\mathbf{A}(:,k)$ denotes the kth column vector of $\mathbf{A}$.

for $k = 0, 1, \cdots, Q-1$ and $n = 1, 2, \cdots, B$. Using equations (7.32) and (7.33), $E\left[(\Delta\boldsymbol{\Psi})\mathbf{w}_i\mathbf{w}_i^H(\Delta\boldsymbol{\Psi})^H\right]$ is found to be

$$E\left[(\Delta\boldsymbol{\Psi})\mathbf{w}_i\mathbf{w}_i^H(\Delta\boldsymbol{\Psi})^H\right] = \sum_{k=0}^{Q-1}\sum_{n=0}^{B-1}\sum_{\acute{k}=0}^{Q-1}\sum_{\acute{n}=0}^{B-1} [\mathbf{g}_{i,k}]_{(1,n)} \left([\mathbf{g}_{i,\acute{k}}]_{(1,\acute{n})}\right)^* E\left[\bar{\mathbf{e}}_{k,n}\bar{\mathbf{e}}_{\acute{k},\acute{n}}^H\right]. \tag{7.34}$$

The elements of matrix $\bar{\boldsymbol{\Xi}}$ are Gaussian random variables with zero mean and variance σ^2 and hence

$$E\left[\bar{\mathbf{e}}_{k,n}\bar{\mathbf{e}}_{\acute{k},\acute{n}}^H\right] = \sigma^2\left[\mathbf{T}_{k,\acute{k}} \otimes \mathbf{I}_{N-\mathcal{S}}\right]\delta_{n,\acute{n}}, \tag{7.35}$$

where $\mathbf{T}_{k,\acute{k}}$ is a $(Q \times Q)$ matrix with all its elements equal to zero except for the element in kth row and $\acute{k}$th column being 1. The delta function $\delta_{n,\acute{n}} = 1$ iff $n = \acute{n}$ and 0 otherwise. Substituting (7.35) into (7.34), we obtain

$$E\left[(\Delta\boldsymbol{\Psi})\mathbf{w}_i\mathbf{w}_i^H(\Delta\boldsymbol{\Psi})^H\right] = \sum_{k=0}^{Q-1}\sum_{\acute{k}=0}^{Q-1}\sum_{n=0}^{B-1} \sigma^2\left[\mathbf{T}_{k,\acute{k}} \otimes \mathbf{I}_{N-\mathcal{S}}\right][\mathbf{g}_{i,k}]_{(1,n)}\left([\mathbf{g}_{i,\acute{k}}]_{(1,n)}\right)^*,$$

$$E\left[(\Delta\boldsymbol{\Psi})\mathbf{w}_i\mathbf{w}_i^H(\Delta\boldsymbol{\Psi})^H\right] = \sum_{k=0}^{Q-1}\sum_{\acute{k}=0}^{Q-1} \sigma^2\left[\mathbf{T}_{k,\acute{k}} \otimes \mathbf{I}_{N-\mathcal{S}}\right]\mathbf{g}_{i,\acute{k}}^H\mathbf{g}_{i,k}. \tag{7.36}$$

The scalar $\mathbf{g}_{i,\acute{k}}^H\mathbf{g}_{i,k}$ is given by

$$\mathbf{g}_{i,\acute{k}}^H\mathbf{g}_{i,k} = \mathbf{h}_i^H\widetilde{\mathbf{B}}_{i,\acute{k}}^H\mathbf{Z}_N^H(\phi_i)\left(\boldsymbol{\Phi}^\dagger\right)^H\boldsymbol{\Phi}^\dagger\mathbf{Z}_N(\phi_i)\widetilde{\mathbf{B}}_{i,k}\mathbf{h}_i. \tag{7.37}$$

The $(N \times N)$ matrix $\left(\boldsymbol{\Phi}^\dagger\right)^H\boldsymbol{\Phi}^\dagger$ is equal to $\left(\boldsymbol{\Phi}\boldsymbol{\Phi}^H\right)^{-1}$. Using the weak law of large numbers, it can be shown that [75]

$$\mathbf{\Phi}\mathbf{\Phi}^H \rightarrow B\mathbf{I}_N, \tag{7.38}$$

in probability. Therefore, equation (7.37) is simplified to

$$\mathbf{g}_{i,\acute{k}}^H \mathbf{g}_{i,k} \;\; = \;\; \frac{1}{B}\, \mathbf{h}_i^H \widetilde{\mathbf{B}}_{i,\acute{k}}^H \widetilde{\mathbf{B}}_{i,k} \mathbf{h}_i. \tag{7.39}$$

The data block size (Q) is 1 in DS-CDMA systems and hence

$$E\left[(\Delta\mathbf{\Psi})\mathbf{w}_i\mathbf{w}_i^H(\Delta\mathbf{\Psi})^H\right] \;\; \approx \;\; \frac{\sigma^2}{B}\, \mathbf{I}_{N-\mathcal{S}}. \tag{7.40}$$

For MC-CDMA systems we have

$$\widetilde{\mathbf{B}}_{i,\acute{k}}^H \widetilde{\mathbf{B}}_{i,k} \;\; = \;\; \mathbf{I}_L \; \delta_{k,\acute{k}}. \tag{7.41}$$

For CP-CDMA system, using the structure of $\widetilde{\mathbf{B}}_{i,k}$ it can be shown that

$$\widetilde{\mathbf{B}}_{i,\acute{k}}^H \widetilde{\mathbf{B}}_{i,k} \;\; \approx \;\; \mathbf{I}_L \; \delta_{k,\acute{k}}. \tag{7.42}$$

Thus, for CP-CDMA and MC-CDMA systems $E\left[(\Delta\mathbf{\Psi})\mathbf{w}_i\mathbf{w}_i^H(\Delta\mathbf{\Psi})^H\right]$ is given by

$$E\left[(\Delta\mathbf{\Psi})\mathbf{w}_i\mathbf{w}_i^H(\Delta\mathbf{\Psi})^H\right] \;\; = \;\; \frac{\sigma^2}{B}\, \mathbf{I}_{Q(N-\mathcal{S})}. \tag{7.43}$$

Using (7.41) and (7.43), $E\left[(\Delta\phi_i)^2\right]$ in (7.26) is simplified to

$$
\begin{aligned}
E\left[(\Delta\phi_i)^2\right] &= \frac{\sigma^2}{2B}\frac{tr\left(\boldsymbol{\Psi}\bar{\mathbf{A}}\mathbf{w}_i\mathbf{w}_i^H\bar{\mathbf{A}}\boldsymbol{\Psi}^H\right)}{\left(\mathbf{w}_i^H\bar{\mathbf{A}}\boldsymbol{\Psi}^H\boldsymbol{\Psi}\bar{\mathbf{A}}\mathbf{w}_i\right)^2} \\
&= \frac{\sigma^2}{2B}\frac{1}{\mathbf{w}_i^H\bar{\mathbf{A}}\boldsymbol{\Psi}^H\boldsymbol{\Psi}\bar{\mathbf{A}}\mathbf{w}_i} \\
&= \frac{\sigma^2}{2B}\frac{1}{\sum_{k=0}^{Q-1}\mathbf{h}_i^H\widetilde{\mathbf{B}}_{i,k}^H\mathbf{A}\mathbf{Z}_N^H(\phi_i)\mathbf{U}_n\mathbf{U}_n^H\mathbf{Z}_N(\phi_i)\mathbf{A}\widetilde{\mathbf{B}}_{i,k}\mathbf{h}_i\boldsymbol{\Psi}\bar{\mathbf{A}}\mathbf{w}_i} \\
&= \frac{\sigma^2}{2B}\frac{1}{\sum_{k=0}^{Q-1}\mathbf{h}_i^H\widetilde{\mathbf{B}}_{i,k}^H\mathbf{A}\mathbf{Z}_N^H(\phi_i)\left[\mathbf{I}_N-\mathbf{U}_s\mathbf{U}_s^H\right]\mathbf{Z}_N(\phi_i)\mathbf{A}\widetilde{\mathbf{B}}_{i,k}\mathbf{h}_i\boldsymbol{\Psi}\bar{\mathbf{A}}\mathbf{w}_i} \\
&= \frac{\sigma^2}{2B}\frac{1}{\sum_{k=0}^{Q-1}\mathbf{h}_i^H\widetilde{\mathbf{B}}_{i,k}^H\mathbf{A}^2\widetilde{\mathbf{B}}_{i,k}\mathbf{h}_i-\sum_{k=0}^{Q-1}\mathbf{h}_i^H\widetilde{\mathbf{B}}_{i,k}^H\mathbf{A}\widetilde{\mathbf{U}}_s\widetilde{\mathbf{U}}_s^H\mathbf{A}\widetilde{\mathbf{B}}_{i,k}\mathbf{h}_i}, \qquad (7.44)
\end{aligned}
$$

where $\widetilde{\mathbf{U}}_s\widetilde{\mathbf{U}}_s^H = \mathbf{Z}_N^H(\phi_i)\mathbf{U}_s\mathbf{U}_s^H\mathbf{Z}_N(\phi_i)$ is the signal subspace projection matrix when the users ACFO values are $\{0, \phi_1-\phi_0, \phi_2-\phi_0, \cdots, \phi_{T-1}-\phi_0\}$, i.e., if ith user is the desired user then $\widetilde{\mathbf{U}}_s\widetilde{\mathbf{U}}_s^H$ is the signal subspace projection matrix when users ACFO values are $\{\phi_0-\phi_i, \cdots, \phi_{i-1}-\phi_i, 0, \phi_{i+1}-\phi_i, \cdots, \phi_{T-1}-\phi_i\}$.

7.4 Simulation Results

The DS-CDMA, CP-CDMA and MC-CDMA system parameters used for computer simulations in chapter 3, chapter 4 and chapter 5 are considered here. EDMM based ACFO estimator with grid size $\upsilon = 0.0001$ is used in the above systems.

Unbiasedness

The plot of $E[\hat{\phi}_i]$ is shown for DS-CDMA, CP-CDMA and MC-CDMA systems. Without loss of generality, $i = 0$ user is considered to be the desired user. For each value of ϕ_0 in the interval $[-0.5, 0.5]$, $E[\hat{\phi}_0]$ is obtained through computer simulation. The plot of $E[\hat{\phi}_0]$ vs ϕ_0 for SNR = 0dB, SNR = 5dB and SNR = 15dB are shown in Figs. 7.1, 7.2 and 7.3, respectively. For SNR = 0dB, it is observed that the estimator is biased, but as the SNR is increased, the estimator becomes unbiased. This phenomenon is evident from Figs. 7.2 and 7.3.

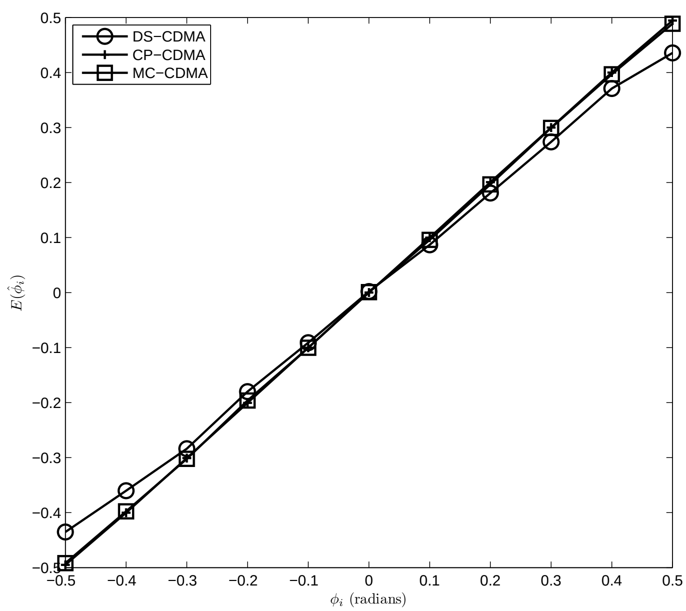

Fig. 7.1: Unbiasedness of the proposed linearized ACFO estimator for SNR = 0dB.

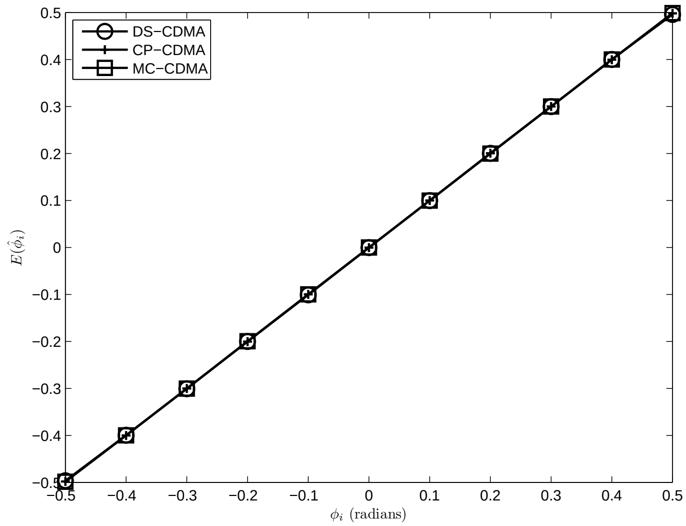

Fig. 7.2: Unbiasedness of the proposed linearized ACFO estimator for SNR = 5dB.

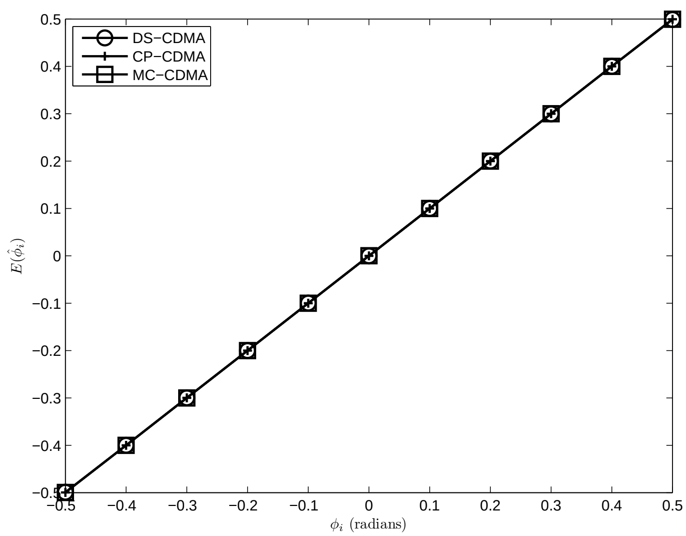

Fig. 7.3: Unbiasedness of the proposed linearized ACFO estimator for SNR = 15dB.

Theoretical MSE

Using (7.44), the theoretical MSE is computed for the proposed estimator. Each user's ACFO value is assumed to be a uniformly distributed random variable over the interval $[-0.5, 0.5]$. Without loss of generality, $i = 0$ user is considered as the desired user. The plot of the theoretical MSE with the estimator's MSE performance and CRLB for DS-CDMA, CP-CDMA and MC-CDMA systems are shown in Figs. 7.4, 7.5 and 7.6, respectively. These plots confirm the validity of the expression derived for the theoretical MSE. For MC-CDMA system, the theoretical MSE is normalized to the subcarrier spacing, i.e., $E[(\Delta\phi_0)^2]/(2\pi/N)^2$. The theoretical MSE is observed to overlap with the CRLB for high SNR. This shows that the proposed estimator asymptotically hits the CRLB.

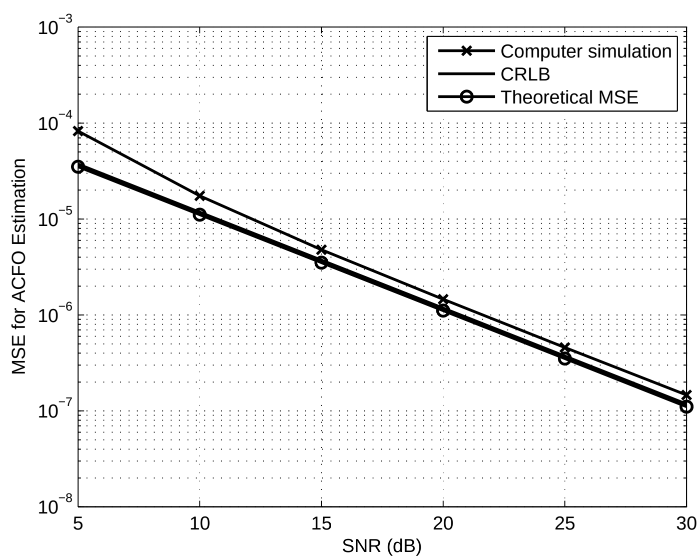

Fig. 7.4: Theoretical MSE performance for DS-CDMA system.

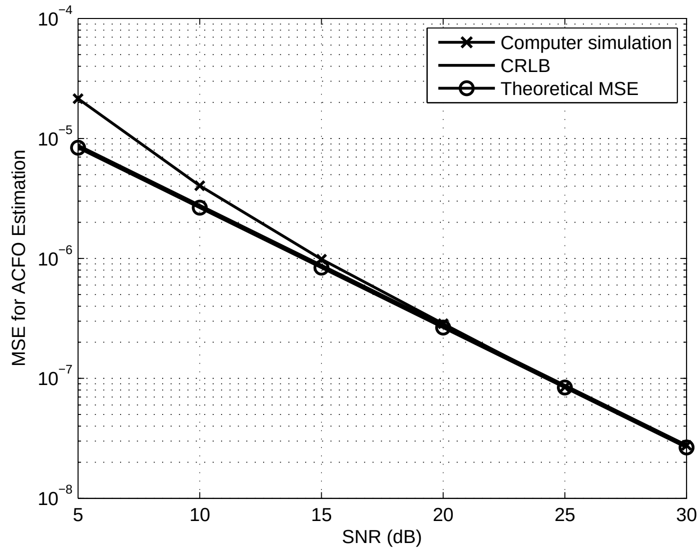

Fig. 7.5: Theoretical MSE performance for CP-CDMA system.

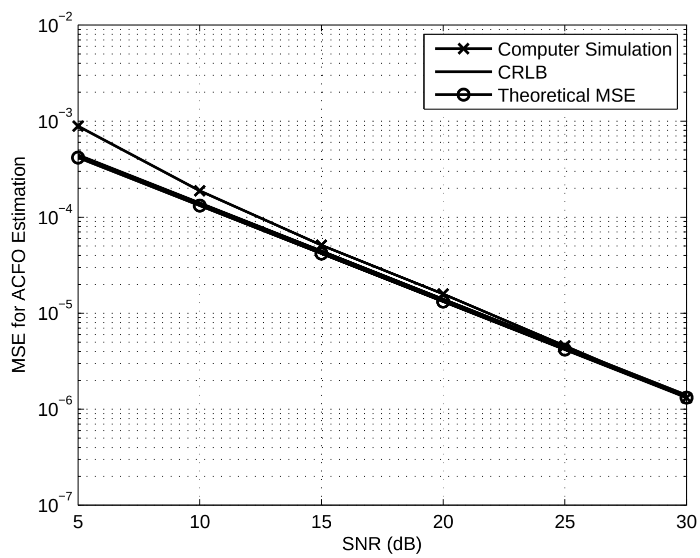

Fig. 7.6: Theoretical MSE performance for MC-CDMA system.

7.5 Conclusion

In this chapter the proposed estimator for DS-CDMA, CP-CDMA and MC-CDMA systems was linearized using Taylor's series approximation. Using the first order perturbation analysis results for noise subspace estimate, the linearized estimator was shown to be unbiased. For high SNR, the theoretical MSE performance corresponding to ACFO estimation was also derived. The theoretical findings were verified through computer simulations. From computer simulations result, it was observed that the theoretical MSE overlaps with the CRLB for high SNR. This shows that the proposed estimator asymptotically attains the CRLB.

Chapter 8

Perspective and Future Research

8.1 Perspective

In this thesis, the problem of carrier frequency synchronization in the uplink transmission of DS-CDMA, CP-CDMA and MC-CDMA systems has been addressed. The users' CFO estimates required for carrier frequency synchronization are obtained from the proposed subspace-based blind joint ACFO and CIR estimator.

The GEVPM based estimator for joint ACFO and CIR estimation in uplink transmission of DS-CDMA system has been shown to be not suitable for estimating large ACFO values. To overcome this problem, EDMM based estimator was proposed to estimate the desired user's ACFO value in the interval $[-\pi, \pi)$. The EDMM based estimator used a one dimensional grid search, where for each search point a $(L \times L)$ matrix needs to be constructed and the determinant for the same needs to be computed. The $(L \times L)$ matrix for each search point was obtained by multiplying $(L \times (N - \mathcal{S}))$ matrix with $((N - \mathcal{S}) \times L)$ matrix. This rendered the EDMM based estimator to be computationally intensive. To reduce the computational complexity, ADMM based estimator was proposed. In ADMM, the $(L \times L)$ matrix was approximated using a polynomial matrix. The coefficient matrices of the polynomial matrix were computed only once before the start of the grid search. For each search point in ADMM, only the polynomial matrix was computed. This approach in ADMM significantly reduced the computational complexity involved in the grid search.

EDMM based estimator for joint ACFO and CIR estimation was also formulated for CP-CDMA and MC-CDMA systems. The received signal in CP-CDMA and MC-CDMA systems had a unique structure which was exploited in developing a criterion for the selection of users' spreading codes. This selection criterion was shown to asymptotically guarantee the identifiability of the estimates. Furthermore, the dimension of the signal subspace was shown to be independent of the users' ACFO and CIR values if the spreading codes were selected according to the formulated criterion. The MSE performance of the proposed estimator obtained through computer simulations was observed to be close to CRLB.

Though the ADMM based estimator reduced the computational complexity, it was only suitable to estimate small ACFO values because of the Taylor's series approximation. Even with ADMM, the number of search points to be searched were high and hence the grid search was computationally demanding. To further reduce the computational complexity, the cost function used by estimator was studied. It was shown to be locally convex around the desired user's true ACFO value. Local convexity at the global minimum of a cost function is necessary for Newton's algorithm to converge to the global minimum and remain stable. The local convexity of the ACFO cost function led to the formulation of a two-stage ACFO estimator. In the first stage a coarse grid search was performed to obtain a coarse ACFO estimate for the desired user. This coarse ACFO estimate was used as the initial value for the Newton's algorithm in the second stage which converged to the desired user's true ACFO value. This two-stage ACFO estimator was shown to have low computational complexity when compared with EDMM and hence can be considered as a practical solution for ACFO estimation in CDMA systems.

For high SNR values, the proposed ACFO estimator was linearized as shown in [89]. Using first order perturbation analysis for the noise subspace estimate, the linearized estimator was asymptotically shown to be unbiased. Furthermore, theoretical MSE performance corresponding to ACFO estimation was also derived and verified through computer simulations.

In summary, a subspace-based blind joint ACFO and CIR estimator was proposed and analyzed for the uplink transmission in DS-CDMA, CP-CDMA and MC-CDMA systems which are being used in 3G systems (DS-CDMA) and being considered for B3G systems (CP-CDMA and MC-CDMA).

8.2 Proposals for Future Research

It is to be noted that the estimator proposed for DS-CDMA, CP-CDMA and MC-CDMA systems are based on the orthogonality between the signal and noise subspaces. Therefore, a reconfigurable transceiver can be proposed to support the above three systems. A prototype reconfigurable transceiver is proposed in [120] assuming perfect channel knowledge and absence of CFO. Future wireless communication will be based on the concept of coexistence of several wireless communication systems. Thus, the need for a reconfigurable transceiver supporting different air interfaces is inevitable. Fourth generation and future wireless communication systems are expected to allow users to have telephony, wireless internet and other applications anytime and anywhere. The main objective for 4G systems is to provide seamless mobility for users. For example, say users A and B work in same office. At home, user A receives a call on his mobile from B's public switched telephone network (PSTN) terminal at the office. User B requests A to send some classified files. Mobile user A should be able to seamlessly transfer the call to his laptop and simultaneously use the wireless local area network (WLAN) to remotely log into A's office desktop. Then A can search for the files and send the files to B using the same call interface. If need arises, a video chat may also be initiated during the conversation by either user A or user B. In this example, user A simultaneously uses the cellular mobile network and WLAN. That is, user A's laptop should be able to support both cellular mobile network and WLAN. This example clearly justifies the need for a reconfigurable transceiver in 4G systems. Our proposed estimator is best suited for the software radio platform because:

1) It has the right structure to be implemented as a reconfigurable transceiver to support OFDM, DS-CDMA, CP-CDMA and MC-CDMA systems which could be used in 4G systems.

2) The proposed estimator is the only blind estimator which could jointly estimate the ACFO and CIR in uplink MC-CDMA system.

The block diagrams for the reconfigurable transceiver supporting OFDM, DS-CDMA, CP-CDMA and MC-CDMA systems are shown in Fig. 8.1 and Fig. 8.2, respectively. For illustration, OFDM system with N subcarriers and cyclic prefix length of P is considered in the following.

Reconfigurable Transmitter

The transmitter consists of spreading (SB), serial-to-parallel (S/P), interleaving (IB), transformation (TB), cyclic prefixing (CP), parallel-to-serial (P/S) and pulse shaping blocks. Except for pulse shaping block, rest of the blocks in the transmitter are parameterized. By choosing suitable parameters for the blocks, the transmitter can be configured to be a OFDM or DS-CDMA or CP-CDMA or MC-CDMA transmitter. SB block spreads the input data symbols using a spreading code with spreading gain x_1. S/P converts x_2 number of input samples from serial form to parallel form. The IB is parameterized by matrix $\mathbf{A}_1$. IB interleaves the elements in the input vector, i.e., if the input vector is $\mathbf{b}$ then the output from IB is $\mathbf{A}_1\mathbf{b}$. If $\mathbf{A}_1$ is an identity matrix, then there is no interleaving operation. Matrix $\mathbf{A}_2$ parameterizes the transformation block. TB is used to compute N-point IDFT of the input vector, i.e., $\mathbf{A}_2 = \mathbf{W}_N^H$ for OFDM and MC-CDMA systems and $\mathbf{A}_2$ is an identity matrix for DS-CDMA and CP-CDMA systems. CP block is parameterized by matrix $\mathbf{A}_3$. Matrix $\mathbf{A}_3 = \mathbf{T}_{cp}$ for realizing OFDM or CP-CDMA or MC-CDMA transmitter and $\mathbf{A}_3$ is an identity matrix for realizing DS-CDMA transmitter. P/S converts x_3 number of parallel input samples into serial output samples. Table 8.1 tabulates the values for x_1, x_2, x_3, $\mathbf{A}_1$, $\mathbf{A}_2$ and $\mathbf{A}_3$ for realizing the transmitter for OFDM, DS-CDMA, CP-CDMA and MC-CDMA systems using the reconfigurable transmitter in Fig. 8.1.

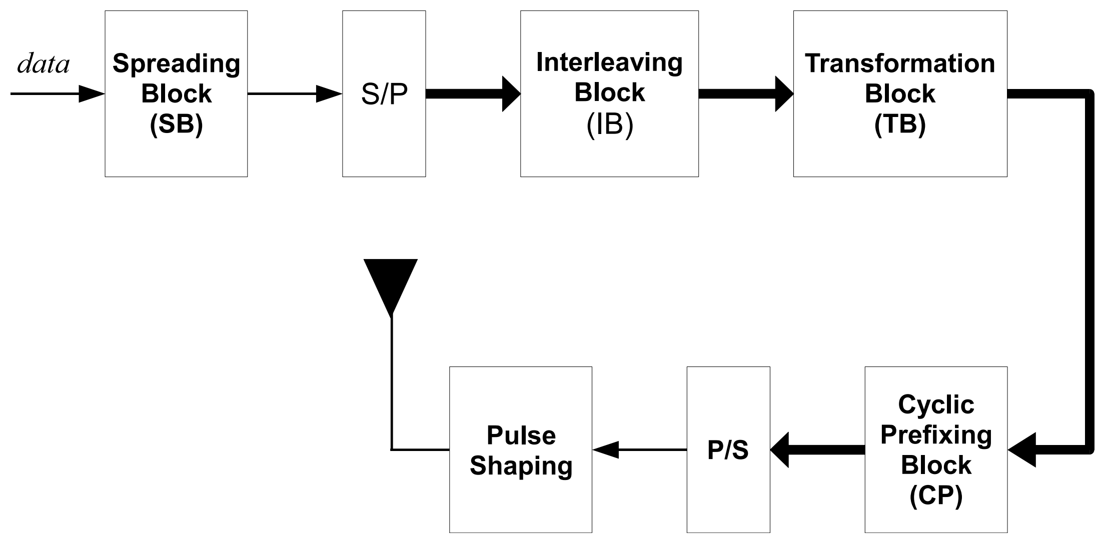

Fig. 8.1: Reconfigurable transmitter.

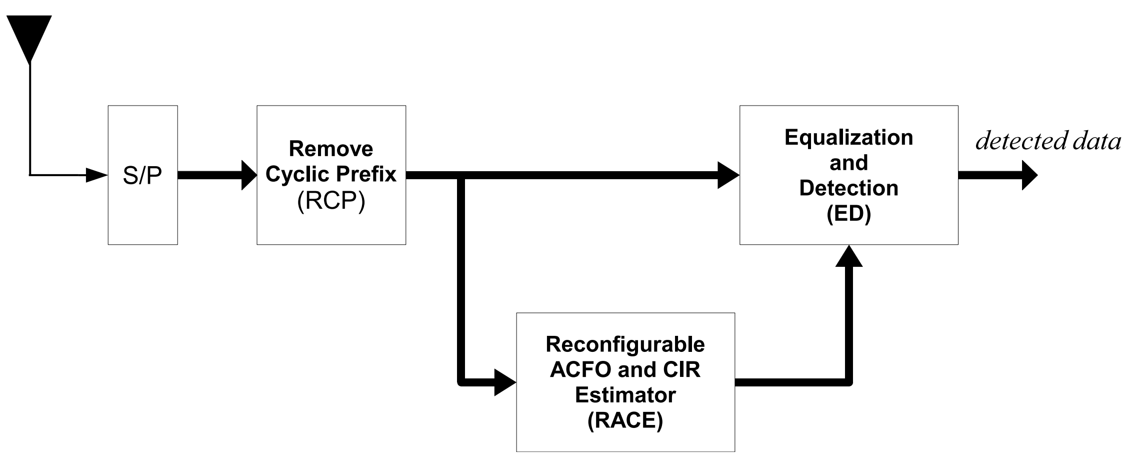

Fig. 8.2: Reconfigurable receiver.

Table 8.1: Block parameters for the reconfigurable transmitter.

System	SB $\{x_1\}$	S/P $\{x_2\}$	IB $\{\mathbf{A}_1\}$	TB $\{\mathbf{A}_2\}$	CP $\{\mathbf{A}_3\}$	P/S $\{x_3\}$
OFDM	1	N	$\mathbf{I}_N$	$\mathbf{W}_N^H$	$\mathbf{T}_{cp}$	$N+P$
DS-CDMA	G	G	$\mathbf{I}_G$	$\mathbf{I}_G$	$\mathbf{I}_G$	G
CP-CDMA	G	N	$\mathbf{I}_N$	$\mathbf{I}_N$	$\mathbf{T}_{cp}$	$N+P$
MC-CDMA	G	N	$\mathbf{\Pi}$	$\mathbf{W}_N^H$	$\mathbf{T}_{cp}$	$N+P$

Reconfigurable Receiver

The reconfigurable receiver consists of S/P, remove cyclic prefix (RCP), reconfigurable ACFO and CIR estimator (RACE) and equalization and detection (ED) blocks. The S/P block can be reconfigured according to the number of samples required for estimation and detection. RCP block, can be configured either to remove the cyclic prefix or remove the samples distorted due to ISI. It is to be noted that ACFO in OFDM can be estimated by utilizing the presence of virtual subcarriers as shown in [87] [89]. ACFO estimation using the presence of virtual carriers is based on the orthogonality between the data subcarriers and the null subcarriers. This orthogonality is similar to the orthogonality between the signal and the noise subspaces. In the ACFO estimation for CDMA systems, the determinant of a $(L \times L)$ positive semi-definite matrix is minimized, whereas for OFDM, a scalar polynomial is minimized. Thus by properly constructing the objective function to be minimized using the grid search, the ACFO estimator for CDMA and OFDM systems can be realized. Using the ACFO and CIR estimates from RACE and the knowledge of the signal structure, a subspace-based MMSE equalizer and detector can be formulated as shown in Appendix B.

Variations in Carrier Frequency Offset and Multipath Fading Channel

In the formulation of the proposed estimator, it was assumed that the users' CFO and CIR values do not vary during the frame duration. In practice, there could be small variations around the user's ACFO value due to slight displacement of the user or changes in the environment. These variations in ACFO can occur while the users' CIR remains unchanged. This scenario needs to be investigated and the two-stage ACFO estimator needs to be modified to track the variations in user's ACFO value.

In WiMAX [121] and future wireless communication systems, the objective is to provide higher data rate transmissions at vehicular speeds. At higher vehicular speeds, the multipath fading channel becomes time-varying. It has been shown that the time-varying multipath channel [122] lies in the span of a low dimensional subspace whose basis vectors can be obtained from Slepian expansion [123]-[125]. Using the Slepian basis expansion model, the proposed estimator can be formulated for time-varying multipath fading channels. The use of batch EVD/SVD method to estimate the signal and noise subspaces may not be accurate when the users' CIR is time-varying. Therefore, adaptive subspace estimation algorithms are essential to track the variations in signal and noise subspaces. The use of adaptive subspace algorithms along with the proposed estimator to obtain a fully adaptive time-varying multipath fading channel and CFO estimator is a challenging research problem which needs to be addressed. Furthermore, identifiability of the ACFO and CIR estimates obtained for the above scenario is another challenging field needing investigation.

Recently, there has been an immense interest in the study of the effects of sampling frequency offset (SFO) [126] and phase noise [49] in OFDM and DS-CDMA systems. The performance of the proposed estimator in the presence of SFO and phase noise and their impact on synchronization also needs to be investigated.

Appendix A

Cramer-Rao Lower Bound for Blind Joint ACFO and CIR Estimator

---

The Cramer-Rao Lower Bound (CRLB) for the proposed subspace-based blind joint ACFO and CIR estimator is derived using the following generalized $(N \times 1)$ received signal vector $\mathbf{r}(n)$ given by

$$\mathbf{r}(n) = \sum_{i=0}^{T-1} \sum_{k=0}^{Q-1} e^{j(n(N+P)+P)\phi_i} \mathbf{Z}_N(\phi_i) \widetilde{\mathbf{B}}_{i,k} \mathbf{h}_i s_i(nQ+k) + \mathbf{v}(n) \tag{A.1}$$

$$= \sum_{i=0}^{T-1} e^{j(n(N+P)+P)\phi_i} \mathbf{Z}_N(\phi_i) \breve{\mathbf{B}}_i \left(\mathbf{I}_Q \otimes \mathbf{h}_i\right) \mathbf{s}_i(n) + \mathbf{v}(n), \tag{A.2}$$

where $\mathbf{v}(n)$ is the AWGN noise vector with $E[\mathbf{v}(n)\mathbf{v}^H(n)] = \sigma^2 \mathbf{I}_N$ and $\mathbf{s}_i(n) = [s_i(nQ), s_i(nQ+1), \cdots, s_i(nQ+Q-1)]^T$. For DS-CDMA system, matrix $\breve{\mathbf{B}}_i$ is a $(N \times L)$ matrix, i.e., $\breve{\mathbf{B}}_i = \widetilde{\mathbf{B}}_i$. For CP-CDMA and MC-CDMA systems, matrix $\breve{\mathbf{B}}_i$

is a $(N \times QL)$ matrix given by $\breve{\mathbf{B}}_i = [\widetilde{\mathbf{B}}_{i,0}, \widetilde{\mathbf{B}}_{i,1}, \cdots, \widetilde{\mathbf{B}}_{i,Q-1}]$. Vector $\mathbf{r}(n)$ in (A.1) represents the received signal in the uplink transmission of DS-CDMA, CP-CDMA and MC-CDMA systems depending on the values for N, P, $\breve{\mathbf{B}}_i$ and $\widetilde{\mathbf{B}}_{i,k}$ as shown in Table A.1. It is assumed that B number of received signal vectors are used in

Table A.1: Generalized received signal parameters.

Parameter	DS-CDMA	CP-CDMA	MC-CDMA
Data Block size	1	Q	Q
N	$G - L + 1$	QG	QG
P	$L - 1$	$L - 1$	$L - 1$
Matrix $\breve{\mathbf{B}}_i$	$\widetilde{\mathbf{B}}_i$	$[\widetilde{\mathbf{B}}_{i,0}, \cdots, \widetilde{\mathbf{B}}_{i,Q-1}]$	$[\widetilde{\mathbf{B}}_{i,0}, \cdots, \widetilde{\mathbf{B}}_{i,Q-1}]$
Matrix $\widetilde{\mathbf{B}}_{i,k}$	Nil	Constructed from kth column vector of matrix $\mathbf{C}_i$.	Constructed from kth column vector of matrix $\mathbf{W}_N^H \mathbf{\Pi} \mathbf{C}_i$.

the computation of noise and signal subspaces. These vectors are stacked to form a $(BN \times 1)$ column vector $\breve{\mathbf{r}}(n)$ as shown below:

$$\breve{\mathbf{r}}(n) = \left[\mathbf{r}^T(n), \mathbf{r}^T(n+1), \cdots, \mathbf{r}^T(n+B-1)\right]^T \tag{A.3}$$

$$= \breve{\mathbf{H}}_B(n)\breve{\mathbf{s}}(n) + \breve{\mathbf{e}}(n), \tag{A.4}$$

where

$$\breve{\mathbf{s}}(n) = \underbrace{\left[\mathbf{s}_a^T(n), \mathbf{s}_a^T(n+1), \cdots, \mathbf{s}_a^T(n+B-1)\right]^T}_{BQT\times 1} \tag{A.5}$$

$$\mathbf{s}_a^T(n) = \underbrace{\left[\mathbf{s}_0^T(n), \mathbf{s}_1^T(n), \cdots, \mathbf{s}_{T-1}^T(n)\right]^T}_{QT\times 1} \tag{A.6}$$

$$\breve{\mathbf{H}}_B(n) = \underbrace{\begin{bmatrix} \overline{\mathbf{H}}(n) & \mathbf{0}_{N\times QT} & \cdots & \mathbf{0}_{N\times QT} \\ \mathbf{0}_{N\times QT} & \overline{\mathbf{H}}(n+1) & \vdots & \mathbf{0}_{N\times QT} \\ \vdots & & \ddots & \vdots \\ \mathbf{0}_{N\times QT} & \cdots & \mathbf{0}_{N\times QT} & \overline{\mathbf{H}}(n+B-1) \end{bmatrix}}_{BN\times BQT} \tag{A.7}$$

$$\overline{\mathbf{H}}(n) = \underbrace{\left[\bar{\mathbf{U}}_0(n), \bar{\mathbf{U}}_1(n), \cdots, \bar{\mathbf{U}}_{T-1}(n)\right]}_{N\times QT} \tag{A.8}$$

$$\bar{\mathbf{U}}_i(n) = e^{j(n(N+P)+P)\phi_i} \underbrace{\mathbf{Z}_N(\phi_i)\breve{\mathbf{B}}_i\left(\mathbf{I}_N \otimes \mathbf{h}_0\right)}_{N\times Q}, \quad \text{for } i = 0, 1, \cdots, T-1 \tag{A.9}$$

$$\breve{\mathbf{e}}(n) = \left[\mathbf{v}^T(n), \mathbf{v}^T(n+1), \cdots, \mathbf{v}^T(n+B-1)\right]^T. \tag{A.10}$$

The unknown parameters at the receiver are $\{\phi_i\}_{i=0}^{T-1}$, $\{\mathbf{h}_i\}_{i=0}^{T-1}$ and $\breve{\mathbf{s}}(n)$. CRLB is to be derived for the users' ACFO and CIR estimates obtained using (A.4) and the knowledge of the spreading codes. In blind subspace-based estimators, the estimated CIR always has a scalar phase ambiguity. In the presence of phase ambiguity, CRLB is derived by assuming that the phase information of the first channel tap is known for all users [75]. Thus, the first tap in the estimated CIR is real valued. The unknown parameters are stacked to form a $(2(BQ+L)T \times 1)$

vector $\mathbf{p}$ as follows[1]:

$$\mathbf{p} \;=\; \left[(\breve{\mathbf{s}}(n))_r^T, (\breve{\mathbf{s}}(n))_j^T, \mathbf{\Omega}^T\right]^T, \tag{A.11}$$

where

$$\begin{aligned}
\mathbf{\Omega} &= \left[\phi_0, \cdots, \phi_{T-1}, (\tilde{\mathbf{h}}_0)_r^T, \cdots, (\tilde{\mathbf{h}}_{T-1})_r^T, (\bar{\mathbf{h}}_0)_j^T, \cdots, (\bar{\mathbf{h}}_{T-1})_j^T\right]^T, && \text{(A.12)}\\
\tilde{\mathbf{h}}_i &= \left[h_i(0)e^{-j\angle h_i(0)}, h_i(1)e^{-j\angle h_i(0)}, \cdots, h_i(L-1)e^{-j\angle h_i(0)}\right] && \text{(A.13)}\\
&\quad \text{for } i = 0, 1, \cdots, T-1 \text{ and}\\
\bar{\mathbf{h}}_i &= \left[h_i(1)e^{-j\angle h_i(0)}, h_i(2)e^{-j\angle h_i(0)}, \cdots, h_i(L-1)e^{-j\angle h_i(0)}\right] && \text{(A.14)}\\
&\quad \text{for } i = 0, 1, \cdots, T-1.
\end{aligned}$$

Following the steps in [127] and [128], the $(BN \times 2(BQ+L)T)$ matrix $\mathbf{J}$ is obtained as

$$\mathbf{J} = \left[\frac{\partial \breve{\mathbf{r}}(n)}{\partial(\breve{\mathbf{s}}(n))_r^T}, \frac{\partial \breve{\mathbf{r}}(n)}{\partial(\breve{\mathbf{s}}(n))_j^T}, \frac{\partial \breve{\mathbf{r}}(n)}{\partial \mathbf{\Omega}^T}\right] = \left[\underbrace{\breve{\mathbf{H}}_B(n)}_{BN\times BQT}, \underbrace{j\breve{\mathbf{H}}_B(n)}_{BN\times BQT}, \underbrace{\boldsymbol{\beth}(n)}_{BN\times 2LT}\right]. \tag{A.15}$$

Matrix $\boldsymbol{\beth}(n)$ can be expressed as

$$\boldsymbol{\beth}(n) \;=\; \left[\widetilde{\boldsymbol{\beth}}^T(n), \widetilde{\boldsymbol{\beth}}^T(n+1), \cdots, \widetilde{\boldsymbol{\beth}}^T(n+B-1)\right]^T, \tag{A.16}$$

[1] The real and imaginary parts of a are denoted by $(a)_r$ and $(a)_j$, respectively.

where the $(N \times 2LT)$ matrix $\widetilde{\mathfrak{I}}(n)$ is given by

$$\begin{aligned}
\widetilde{\mathfrak{I}}(n) &= \frac{\partial \overline{\mathbf{H}}(n)\mathbf{s}_a(n)}{\partial \mathbf{\Omega}^T} && \text{(A.17)} \\
&= \left[\mathbf{g}_0(n), \mathbf{g}_1(n), \cdots, \mathbf{g}_{T-1}(n), \mathbf{K}_0(n), \cdots, \mathbf{K}_{T-1}(n), \widetilde{\mathbf{K}}_0(n), \cdots, \widetilde{\mathbf{K}}_{T-1}(n)\right], && \text{(A.18)}
\end{aligned}$$

and the $(N \times 1)$ vector $\mathbf{g}_i$ for $i = 0, 1, \cdots, T-1$ is defined as

$$\begin{aligned}
\mathbf{g}_i &= \left[\mathbf{O} + n(N+P)\mathbf{I}_N\right] \bar{\mathbf{U}}_i(n)\mathbf{s}_i(n) && \text{(A.19)} \\
\mathbf{O} &= diag\left([P, P+1, \cdots, P+N-1]^T\right). && \text{(A.20)}
\end{aligned}$$

The $(N \times L)$ matrix $\mathbf{K}_i(n)$ for $i = 0, 1, \cdots, T-1$ is obtained as follows:

$$\begin{aligned}
\mathbf{K}_i(n) &= \frac{\partial \overline{\mathbf{H}}(n)\mathbf{s}_a(n)}{(\partial \tilde{\mathbf{h}}_i)_r^T} && \text{(A.21)} \\
&= e^{j(n(N+P)+P)\phi_i} \mathbf{Z}_N(\phi_i)\breve{\mathbf{B}}_i \mathbf{N}\left(\mathbf{I}_L \otimes \mathbf{s}_i(n)\right), && \text{(A.22)}
\end{aligned}$$

where

$$\mathbf{N} = \left[(\mathbf{I}_Q \otimes \mathbf{I}_{L(:,1)}), (\mathbf{I}_Q \otimes \mathbf{I}_{L(:,2)}), \cdots, (\mathbf{I}_Q \otimes \mathbf{I}_{L(:,L)})\right]. \quad \text{(A.23)}$$

Using (A.22), the $(N \times T(L-1))$ matrix $\widetilde{\mathbf{K}}_i(n)$ is obtained from $\mathbf{K}_i(n)$ as given below:

$$\widetilde{\mathbf{K}}_i(n) = j\, \mathbf{K}_i(n)_{(:,2:L)}, \quad \text{(A.24)}$$

for $i = 0, 1, \cdots, T-1$. The CRLB for the desired parameters in $\mathbf{\Omega}$ is given by [128]

$$CRLB_{\mathbf{\Omega}} \;=\; \frac{\sigma^2}{2}\left[\left(\daleth^H(n)\,\Pi^{\perp}_{\breve{\mathbf{H}}_B(n)}\,\daleth(n)\right)_r\right]^{\dagger} \tag{A.25}$$

where

$$\Pi^{\perp}_{\breve{\mathbf{H}}_B(n)} \;=\; \mathbf{I}_{BN} - \breve{\mathbf{H}}_N(n)\left(\breve{\mathbf{H}}_B^H(n)\breve{\mathbf{H}}_B(n)\right)^{-1}\breve{\mathbf{H}}_B^H(n). \tag{A.26}$$

Substituting (A.7) and (A.16) into (A.25), the CRLB is simplified to

$$CRLB_{\mathbf{\Omega}} \;=\; \frac{\sigma^2}{2}\left[\left(\sum_{k=n}^{n+B-1}\widetilde{\daleth}^H(k)\,\Pi^{\perp}_{\overline{\mathbf{H}}(k)}\,\widetilde{\daleth}(k)\right)_r\right]^{\dagger}, \tag{A.27}$$

where

$$\Pi^{\perp}_{\overline{\mathbf{H}}(k)} \;=\; \mathbf{I}_N - \overline{\mathbf{H}}(k)\left(\overline{\mathbf{H}}^H(k)\overline{\mathbf{H}}(k)\right)^{-1}\overline{\mathbf{H}}^H(k). \tag{A.28}$$

The lth diagonal element of the $(2LT \times 2LT)$ matrix gives the minimum value for the MSE in estimating the lth element of vector $\mathbf{\Omega}$. Thus,

$$E\left[(\Delta\phi_i)^2\right] \;=\; [CRLB_{\mathbf{\Omega}}]_{(i+1,i+1)} \quad \text{for } i = 0, 1, \cdots, T-1 \tag{A.29}$$

$$\begin{aligned} E\left[|\Delta\mathbf{h}_i|^2\right] \;=\; & \sum_{l=1}^{L}[CRLB_{\mathbf{\Omega}}]_{(T+iL+l,T+iL+l)} \\ & + \sum_{l_1=1}^{L-1}[CRLB_{\mathbf{\Omega}}]_{(p_{i,l_1},p_{i,l_1})} \quad \text{for } i = 0, 1, \cdots, T-1, \end{aligned} \tag{A.30}$$

where $p_{i,l_1} = T(L+1) + i(L-1) + l_1$.

Appendix B

Subspace-based MMSE Detector

In this Appendix, a subspace-based MMSE detector for DS-CDMA system is formulated. The ISI free received signal vector in equation (3.14) is given by

$$\mathbf{r}(n) = \sum_{i=0}^{T-1} e^{(jnG+L-1)\phi_i} \mathbf{Z}_N(\phi_i) \widetilde{\mathbf{B}}_i \mathbf{h}_i s_i(n) + \mathbf{v}(n), \tag{B.1}$$

Following the steps in [131], the equalizer for the ith user can be written as

$$\gamma(n) = \mathbf{u}_i^H \mathbf{r}(n), \tag{B.2}$$

where

$$\mathbf{u}_i = \frac{1}{\mathbf{h}_i^H \widetilde{\mathbf{B}}_i^H \mathbf{Z}_N^H(\phi_i) \mathbf{U}_s \breve{\Lambda}_s^{-1} \mathbf{U}_s^H \mathbf{Z}_N(\phi_i) \widetilde{\mathbf{B}}_i \mathbf{h}_i} \mathbf{U}_s \breve{\Lambda}_s^{-1} \mathbf{U}_s^H \mathbf{Z}_N(\phi_i) \widetilde{\mathbf{B}}_i \mathbf{h}_i, \tag{B.3}$$

and $\breve{\Lambda}_s$ is a $(\mathcal{S} \times \mathcal{S})$ diagonal matrix containing the eigenvalues corresponding to the signal subspace. The soft output $\gamma(n)$ can then be used to detect the ith user's transmitted data symbol either through hard decision [5] [129] or through advanced iterative detection techniques [130]-[135].

The ith user's MMSE equalizer constructed using the estimated parameters is denoted by $\hat{\mathbf{u}}_i$. In the proposed estimator, the CIR is estimated as an eigenvector. Therefore, there is always a scalar phase ambiguity associated with the estimated CIR, i.e., $\hat{\mathbf{h}}_i = e^{j\varrho}\mathbf{h}_i$ where ϱ is a real-valued random variable. This phase ambiguity in the CIR estimate prevents the data symbols from being coherently detected. To circumvent this problem, the data symbols are differentially encoded [136] before spreading at the transmitter and differentially detected at the receiver. Let $s_i(n)$ denote the ith user's differentially encoded data symbol obtained from the data symbols $b_i(n-1)$ and $b_i(n)$. Thus, the differential detection is given by

$$\hat{b}_i(n) = detect\{\hat{\mathbf{u}}_i^H \mathbf{r}(n)\mathbf{r}^H(n-1)\hat{\mathbf{u}}_i e^{-jG\hat{\phi}_i}\}, \tag{B.4}$$

where the term $e^{-jG\hat{\phi}_i}$ in (B.4) is used to compensate for the accumulated phase value during differential detection.

Appendix C

Structure of Matrices in CP-CDMA System

Let the maximum order for the CIR of all users be $L-1=2$. Therefore

$$\mathbf{h}_i = [h_i(0), h_i(1), h_i(2)]^T, \tag{C.1}$$

and the length of cyclic prefix is $P=2$. Assuming the ith user's spreading code to be $\mathbf{c}_i = [c_i(0), c_i(1), c_i(2), c_i(3)]^T$ and the number of data symbols in a CP-CDMA symbol to be $Q=2$, the $(N \times Q)$ code matrix $\mathbf{C}_i$ can be written as

$$\begin{aligned} \mathbf{C}_i &= \mathbf{I}_2 \otimes \mathbf{c}_i \\ &= \begin{bmatrix} c_i(0) & c_i(1) & c_i(2) & c_i(3) & 0 & 0 & 0 & 0 \\ 0 & 0 & 0 & 0 & c_i(0) & c_i(1) & c_i(2) & c_i(3) \end{bmatrix}^T . \end{aligned} \tag{C.2}$$

Thus, the column vectors of matrix $\mathbf{C}_i$ are orthonormal by construction.

Now let us assume that $Q = 1$ and $G = 4$, therefore we have $N = QG = 4$. In this scenario, cyclic prefix is augmented for every spread data symbol. The structure of $((N + P) \times N)$ matrix $\mathbf{T}_{cp}$ and $(N \times (N + P))$ matrix $\mathbf{R}_{cp}$ are as follows:

$$\mathbf{T}_{cp} = \begin{bmatrix} 0 & 0 & 1 & 0 & 0 & 0 \\ 0 & 0 & 0 & 1 & 0 & 0 \\ 1 & 0 & 0 & 0 & 1 & 0 \\ 0 & 1 & 0 & 0 & 0 & 1 \end{bmatrix}^T ; \quad \mathbf{R}_{cp} = \begin{bmatrix} 0 & 0 & 1 & 0 & 0 & 0 \\ 0 & 0 & 0 & 1 & 0 & 0 \\ 0 & 0 & 0 & 0 & 1 & 0 \\ 0 & 0 & 0 & 0 & 0 & 1 \end{bmatrix}. \tag{C.3}$$

The $((N + P) \times (N + P))$ dimensional matrices $\widetilde{\mathbf{H}}_i$ and $\acute{\widetilde{\mathbf{H}}}_i$ for the ith user have the following structure:

$$\widetilde{\mathbf{H}}_i = \begin{bmatrix} h_i(0) & 0 & 0 & 0 & 0 & 0 \\ h_i(1) & h_i(0) & 0 & 0 & 0 & 0 \\ h_i(2) & h_i(1) & h_i(0) & 0 & 0 & 0 \\ 0 & h_i(2) & h_i(1) & h_i(0) & 0 & 0 \\ 0 & 0 & h_i(2) & h_i(1) & h_i(0) & 0 \\ 0 & 0 & 0 & h_i(2) & h_i(1) & h_i(0) \end{bmatrix}, \tag{C.4}$$

$$\acute{\widetilde{\mathbf{H}}}_i = \begin{bmatrix} 0 & 0 & 0 & 0 & h_i(2) & h_i(1) \\ 0 & 0 & 0 & 0 & 0 & h_i(2) \\ 0 & 0 & 0 & 0 & 0 & 0 \\ 0 & 0 & 0 & 0 & 0 & 0 \\ 0 & 0 & 0 & 0 & 0 & 0 \\ 0 & 0 & 0 & 0 & 0 & 0 \end{bmatrix}. \tag{C.5}$$

Using (C.3) and (C.5), it can be readily verified that

$$\mathbf{R}_{cp}\acute{\widetilde{\mathbf{H}}}_i\mathbf{T}_{cp} = \mathbf{0}_{N\times N}. \tag{C.6}$$

The $(N \times N)$ circulant channel matrix $\mathbf{H}_i$ is obtained as follows:

$$\begin{aligned} \mathbf{H}_i &= \mathbf{R}_{cp}\widetilde{\mathbf{H}}_i\mathbf{T}_{cp} \\ &= \begin{bmatrix} h_i(0) & 0 & h_i(2) & h_i(1) \\ h_i(1) & h_i(0) & 0 & h_i(2) \\ h_i(2) & h_i(1) & h_i(0) & 0 \\ 0 & h_i(2) & h_i(1) & h_i(0) \end{bmatrix}. \end{aligned} \tag{C.7}$$

Appendix D

Matrix $\mathbf{M}_c$ in MC-CDMA System

The $(N \times LQT)$ matrix $\mathbf{M}_c$ given by equation (5.54) in chapter 5 is analyzed in the following. The $(N \times LQT)$ matrix $\mathbf{W}_N\mathbf{M}_c$ can be written as (refer to equation (5.57))

$$\mathbf{W}_N\mathbf{M}_c = \left[[\mathbf{W}_N\mathbf{G}_0]^{(0)}, [\mathbf{W}_N\mathbf{G}_0]^{(1)}, \cdots, [\mathbf{W}_N\mathbf{G}_0]^{(Q-1)} \right], \tag{D.1}$$

where the $(N \times LT)$ matrix $\mathbf{W}_N\mathbf{G}_0$ is approximated as follows (refer to equation (5.56)):

$$\mathbf{W}_N\mathbf{G}_0 \approx \left[\left[\mathbf{W}_N\widetilde{\mathbf{B}}_{0,0}\right]^{(l_0)}, \left[\mathbf{W}_N\widetilde{\mathbf{B}}_{1,0}\right]^{(l_1)}, \cdots, \left[\mathbf{W}_N\widetilde{\mathbf{B}}_{T-1,0}\right]^{(l_{T-1})} \right], \tag{D.2}$$

and l_i is an integer such that $l_i \in [-N/2, N/2-1]$ for $i = 0, 1, \cdots, T-1$. Let the spreading gain be $G = 5$ and number of data symbols transmitted in one MC-CDMA symbol duration be $Q = 2$. Therefore, the number of subcarriers is $N = QG = 10$. The number of users is assumed be $T = 2$ and let the length of

CIR for all users be $L = 2$. The users' spreading codes are assumed to be

$$\mathbf{c}_0 = [p_0, p_1, p_2, p_3, p_4]^T \tag{D.3}$$

$$\mathbf{c}_1 = [q_0, q_1, q_2, q_3, q_4]^T. \tag{D.4}$$

From (5.24), (10×2) matrix $\mathbf{W}_N\widetilde{\mathbf{B}}_{i,0}$ can be written as

$$\mathbf{W}_N\widetilde{\mathbf{B}}_{i,0} = \left[\mathbf{Z}_{10}(0)\,\tilde{\mathbf{d}}_{i,0},\ \ \mathbf{Z}_{10}\left(-\frac{2\pi}{10}\right)\tilde{\mathbf{d}}_{i,0}\right] \quad \text{for } i = 0 \text{ and } 1, \tag{D.5}$$

where

$$\tilde{\mathbf{d}}_{i,0} = \mathbf{c}_i \otimes [1, \mathbf{0}_{1\times(Q-1)}]^T. \tag{D.6}$$

Thus, matrices $\{\mathbf{W}_N\widetilde{\mathbf{B}}_{i,0}\}_{i=0}^{2}$ are given by

$$\mathbf{W}_N\widetilde{\mathbf{B}}_{0,0} = \begin{bmatrix} p_0 & 0 & p_1 & 0 & p_2 & 0 & p_3 & 0 & p_4 & 0 \\ p_0 & 0 & p_1 e^{-j\frac{2\pi 2}{10}} & 0 & p_2 e^{-j\frac{2\pi 4}{10}} & 0 & p_3 e^{-j\frac{2\pi 6}{10}} & 0 & p_4 e^{-j\frac{2\pi 8}{10}} & 0 \end{bmatrix}^T$$

$$\mathbf{W}_N\widetilde{\mathbf{B}}_{1,0} = \begin{bmatrix} q_0 & 0 & q_1 & 0 & q_2 & 0 & q_3 & 0 & q_4 & 0 \\ q_0 & 0 & q_1 e^{-j\frac{2\pi 2}{10}} & 0 & q_2 e^{-j\frac{2\pi 4}{10}} & 0 & q_3 e^{-j\frac{2\pi 6}{10}} & 0 & q_4 e^{-j\frac{2\pi 8}{10}} & 0 \end{bmatrix}^T. \tag{D.7}$$

It is known that $l_i \in [-5, 4]$ for $i = 0$ and 1. Therefore, let it be assumed that $l_0 = 2$ and $l_1 = -3$. Using (D.1), (D.2), (D.7) and the above assumption, matrix

$\mathbf{W}_N\mathbf{M}_c$ for the above example is given by

$$\mathbf{W}_N\mathbf{M}_c = \begin{bmatrix} p_4 & p_4 e^{-j\frac{2\pi 8}{10}} & 0 & 0 & 0 & 0 & q_1 & q_1 e^{-j\frac{2\pi 2}{10}} \\ 0 & 0 & q_2 & q_2 e^{-j\frac{2\pi 4}{10}} & p_4 & p_4 e^{-j\frac{2\pi 8}{10}} & 0 & 0 \\ p_0 & p_0 & 0 & 0 & 0 & 0 & q_2 & q_2 e^{-j\frac{2\pi 4}{10}} \\ 0 & 0 & q_3 & q_3 e^{-j\frac{2\pi 6}{10}} & p_0 & p_0 & 0 & 0 \\ p_1 & p_1 e^{-j\frac{2\pi 2}{10}} & 0 & 0 & 0 & 0 & q_3 & q_3 e^{-j\frac{2\pi 6}{10}} \\ 0 & 0 & q_4 & q_4 e^{-j\frac{2\pi 8}{10}} & p_1 & p_1 e^{-j\frac{2\pi 2}{10}} & 0 & 0 \\ p_2 & p_2 e^{-j\frac{2\pi 4}{10}} & 0 & 0 & 0 & 0 & q_4 & q_4 e^{-j\frac{2\pi 8}{10}} \\ 0 & 0 & q_0 & q_0 & p_2 & p_2 e^{-j\frac{2\pi 4}{10}} & 0 & 0 \\ p_3 & p_3 e^{-j\frac{2\pi 6}{10}} & 0 & 0 & 0 & 0 & q_0 & q_0 \\ 0 & 0 & q_1 & q_1 e^{-j\frac{2\pi 2}{10}} & p_3 & p_3 e^{-j\frac{2\pi 6}{10}} & 0 & 0 \end{bmatrix}. \quad \text{(D.8)}$$

From (D.8), it is observed that for any combination of $\{l_0, l_1\} \in [-5, 4]$, there are only $LT = 4$ column vectors which are non-orthogonal. In the above example, the column vectors of matrix $\mathbf{W}_N\mathbf{M}_c$ can be divided into $Q = 2$ set with each set containing LT column vectors. The grouping of column vectors into Q different sets is done such that the column vectors in a set are orthogonal to the column vectors in other $Q-1$ sets. In the example in (D.8), column vectors $\{\mathbf{W}_N\mathbf{M}_c(:,1), \mathbf{W}_N\mathbf{M}_c(:,2), \mathbf{W}_N\mathbf{M}_c(:,7), \mathbf{W}_N\mathbf{M}_c(:,8)\}$ are orthogonal to the column vectors $\{\mathbf{W}_N\mathbf{M}_c(:,3), \mathbf{W}_N\mathbf{M}_c(:,4), \mathbf{W}_N\mathbf{M}_c(:,5), \mathbf{W}_N\mathbf{M}_c(:,6)\}$. Furthermore, it is to be noted that the column vectors in the set $\{\mathbf{W}_N\mathbf{M}_c(:,1), \mathbf{W}_N\mathbf{M}_c(:,2), \mathbf{W}_N\mathbf{M}_c(:,7), \mathbf{W}_N\mathbf{M}_c(:,8)\}$ can be expressed as column vectors of matrix $\left[\left[\mathbf{W}_N\widetilde{\mathbf{B}}_{0,0}\right]^{(2)}, \left[\mathbf{W}_N\widetilde{\mathbf{B}}_{1,0}\right]^{(-2)}\right]$, which is matrix $\mathbf{W}_N\mathbf{G}_0$ when $l_0 = 2$ and $l_1 = -2$. Similarly, column vectors in the set $\{\mathbf{W}_N\mathbf{M}_c(:,3), \mathbf{W}_N\mathbf{M}_c(:,4), \mathbf{W}_N\mathbf{M}_c(:,5), \mathbf{W}_N\mathbf{M}_c(:,6)\}$ are column vectors of matrix $\mathbf{W}_N\mathbf{G}_0$ when $l_0 = 3$ and $l_1 = -3$. Thus, if the $(N \times LT)$ matrix $\mathbf{W}_N\mathbf{G}_0$ is of full rank LT for all possible combinations of $\{l_0, l_1, \cdots, l_{T-1}\} \in [-N/2, N/2-1]$, then the $(N \times LQT)$ matrix $\mathbf{M}_c$ will be of full rank LQT.

Appendix E

Adjoint of a Polynomial Matrix

Matrix $\widetilde{\beth}_i(\phi)$ is a $(L \times L)$ polynomial matrix of order 2 (refer to equation (6.12)). Therefore, the adjoint of $\widetilde{\beth}_i(\phi)$ is also a $(L \times L)$ polynomial matrix of order $2(L-1)$ at most [117]. For small ACFO values around the true ACFO value ϕ_i, the adjoint of $\widetilde{\beth}_i(\phi)$ can be approximated as

$$adj(\widetilde{\beth}_i(\phi)) \approx \mathbf{F}_0 + (\phi - \phi_i)\mathbf{F}_1 + (\phi - \phi_i)^2\mathbf{F}_2, \tag{E.1}$$

where[1] $\mathbf{F}_0$, $\mathbf{F}_1$ and $\mathbf{F}_2$ are Hermitian matrices.

***Lemma* E.1.** Let $\mathbf{A}$ be a $(L \times L)$ Hermitian polynomial matrix in ϕ of order 2, i.e., $\mathbf{A} = \mathbf{A}_0 + \phi\mathbf{A}_1 + \phi^2\mathbf{A}_2$. If $\mathbf{A}$ is a positive semi-definite matrix, then $\mathbf{A}_0$ and $\mathbf{A}_2$ are also positive semi-definite.

Proof: *When $\phi = 0$, matrix $\boldsymbol{A} = \boldsymbol{A}_0$ and hence matrix $\boldsymbol{A}_0$ is positive semi-definite. For any $(L \times 1)$ column vector $\boldsymbol{x} \in \mathcal{C}^L$, it is known that $\boldsymbol{x}^H\boldsymbol{A}\boldsymbol{x} \geq 0$ as $\boldsymbol{A}$ is a positive*

---

[1] For notational convenience, the user index i is not tagged to matrices $\mathbf{F}_0$, $\mathbf{F}_1$ and $\mathbf{F}_2$.

semi-definite matrix. This implies that

$$\boldsymbol{x}^H \boldsymbol{A}_0 \boldsymbol{x} + \phi \boldsymbol{x}^H \boldsymbol{A}_1 \boldsymbol{x} + \phi^2 \boldsymbol{x}^H \boldsymbol{A}_2 \boldsymbol{x} \quad \geq \quad 0. \tag{E.2}$$

For the condition in (E.2) to be satisfied, we must have

$$(\boldsymbol{x}^H \boldsymbol{A}_1 \boldsymbol{x})^2 - 4(\boldsymbol{x}^H \boldsymbol{A}_0 \boldsymbol{x})(\boldsymbol{x}^H \boldsymbol{A}_2 \boldsymbol{x}) \quad \leq \quad 0. \tag{E.3}$$

As $(\boldsymbol{x}^H \boldsymbol{A}_1 \boldsymbol{x})^2 \geq 0$ *and* $\boldsymbol{x}^H \boldsymbol{A}_0 \boldsymbol{x} \geq 0$*, condition (E.3) will be satisfied if* $\boldsymbol{x}^H \boldsymbol{A}_2 \boldsymbol{x} \geq 0$*. Therefore, matrix* $\boldsymbol{A}_2$ *must be positive semi-definite.* $\square$

As $adj(\widetilde{\beth}_i(\phi))$ is an order 2 positive semi-definite polynomial matrix, Lemma E.1 implies that matrices $\mathbf{F}_0$ and $\mathbf{F}_2$ are positive semi-definite.

Bibliography

[1] T. S. Rappaport, “Wireless Communications Principles and Practice.” pp. 1, 13-21, 447-461, Pearson Education, 2002.

[2] S. Haykin and M. Moher, “Modern Wireless Communications.” pp. 18, 21, Pearson Education, 2005.

[3] R. Steele and L. Hanzo, “Mobile Radio Communications.” pp. 51-70, John Wiley & Sons, 1999.

[4] S. Glisic and B. Vucetic, “Spread Spectrum CDMA Systems for Wireless Communications.” pp. 234, 324, 329, Artech House, 1997.

[5] J. G. Proakis, “Digital Communications.” pp. 333, 561-565, 896-899, McGraw-Hill, 2001.

[6] P. W. Baier, “A critical review of CDMA,” *in Proc. 46th IEEE Vehicular Technology Conf.*, May 1996, pp. 6-10.

[7] K. S. Gilhousen and I. M. Jacobs and R. Padovani and A. J. Viterbi and A. Weaver and C. E. Wheatley, “On the capacity of a cellular CDMA system,” *IEEE Trans. Veh. Technol.*, vol. 40, pp. 301-311, May 1991.

[8] M. K. Varanasi and B. Aazhang, “Mulitstage detection in asynchronous code-division multiple-access communications,” *IEEE Trans. Commun.*, vol. 38, pp. 509-519, Apr. 1990.

[9] Y. Cho and J. H. Lee, “Analysis of an adaptive SIC for near-far resistant DS-CDMA,” *IEEE Trans. Commun.*, vol. 46, pp. 1429-1432, Nov. 1998.

[10] D. Koulakiotis and A. H. Aghvami, “ Evaluation of a DS/CDMA multiuser receiver employing a hybrid interference cancellation in Rayleigh-fading channels,” *IEEE Commun. Lett.*, vol. 2, pp. 61-63, Mar. 1998.

[11] P. Patel and J. Holtzman, “Analysis of a simple successive interference cancellation scheme in a DS/CDMA system,” *IEEE J. Sel. Areas Commun.*, vol. 12, pp. 796-807, June 1994.

[12] A. J. Viterbi, "CDMA: Principles of Spread Spectrum Communication." New York: Addison-Wesley, 1995.

[13] "Physical Layer Standard for CDMA2000 Standards for Spread Spectrum Systems – TIA/EIA/IS-2000.2-A.," TIA/EIA Interim Stand., Mar. 2000.

[14] "3GPP TS 25.2-Series (Physical Layer), Technical specification.", Mar. 2000.

[15] R. Prasad, "CDMA for Wireless Personal Communications." pp. 39, Artech House, 1996.

[16] L. Hanzo, L-L. Yang, E-L. Kuan and K. yen, "Single and Multi-Carrier DS-CDMA: Multi-User Detection, Space-Time Spreading, Synchronization and Standards." pp. 35-37, 46-52, John Wiley & Sons. 2003.

[17] S. Hara and R. Prasad, "Overview of multicarrier CDMA," *IEEE Commun. Mag.*, vol. 53, no. 12, pp. 126-133, Dec. 1997.

[18] A. Jamalipour, T. Wada, and T. Yamazato, "A tutorial on multiple access technologies for beyond 3G networks," *IEEE Commun. Mag.*, vol. 43, no. 2, pp. 110-117, Feb. 2005.

[19] Y. K. Kim and R. Prasad, *4G Roadmap and Engineering Communication Technologies.* Artech House, 2006.

[20] S. Chatterjee, W. A. C. Fernando, and M. K. Wasantha, "Adaptive modulation based MC-CDMA systems for 4G wireless consumer applications," *IEEE Trans. Consum. Electron.*, vol. 49, pp. 995-1003, Nov. 2003.

[21] M. Pursley, "Performance evaluation for phase-coded SSMA communication - part 1: System analysis," *IEEE Trans. Commun.*, vol. 25, pp. 795-799, Aug. 1977.

[22] S. Verdu, "Multiuser Detection." pp. 288-329, Cambridge University Press, 1999.

[23] A. J. Viterbi, A. M. Viterbi, and E. Zehavi, "Other-cell interference in cellular power-controlled CDMA," *IEEE Trans. Commun.*, vol. 42, pp. 1501-1504, Feb./Mar./Apr. 1994.

[24] A. M. Viterbi and A. J. Viterbi, "Erlang capacity of a power controlled CDMA system," *IEEE J. Sel. Areas Commun.*, vol. 11, pp. 892-899, Aug. 1993.

[25] K. L. Baum, T. A. Thomas, F. W. Vook and V. Nangia, "Cyclic-prefix CDMA: An improved transmission method for broadband DS-CDMA cellular systems," *in Proc. IEEE Wireless Communications and Networking Conf.*, Mar. 2002, pp. 183-188.

[26] D. D. Falconer, S. L. Ariyavisitakul, A. Benyamin-Seeyar, and B. Eidson, "Frequency domain equalization for single-carrier broadband wireless systems," *IEEE Commun. Mag.*, vol. 40, pp. 58-66, Apr. 2002.

[27] H. Sari, G. Karam, and I. Jeanclaude, "Transmission Techniques for Digital Terrestrial TV Broadcasting," *IEEE Commun. Mag.*, vol. 33, pp. 100-109, Feb. 1995.

[28] P. J. Davis, *Circulant Matrices.*, John Wiley & Sons, 1979.

[29] P.-H. Lin and T.-D. Chiueh, "Low complexity frequency-domain despreading for cyclic-prefix CDMA systems," *IEEE Commun. Lett.*, vol. 8, pp. 339-341, June 2004.

[30] Y. Li, S. McLaughlin, X. Wei, and D. G. M. Cruickshank, "Channel estimation and interference cancellation in CPCDMA systems," *IET Commun.*, vol. 1, pp. 106-112, Feb. 2001.

[31] N. Yee, J.-P. Linnartz, and G. Fettweis, "Multicarrier CDMA in indoor wireless radio networks," *in Proc. IEEE Int. Symp. Personal Indoor and Mobile Radio Communications*, Sept. 1993, pp. 109-113.

[32] R. W. Chang, "Synthesis of band-limited orthogonal signals for multichannel data transmission," *Bell Systems Technical Journal*, vol. 46, pp. 1775-1796, Dec. 1966.

[33] L. Hanzo and T. Keller, "OFDM and MC-CDMA: A Primer." pp. 21-102, John Wiley & Sons, 2006.

[34] S. L. Miller and B. J. Rainbolt, "MMSE detection of multicarrier CDMA," *IEEE J. Sel. Areas Commun.*, vol. 18, pp. 2356-2362, Nov. 2000.

[35] Z. Wang and G. B. Giannakis, "Wireless multicarrier communications," *IEEE Signal Process. Mag.*, vol. 17, pp. 29-48, May 2000.

[36] X. Gui and T.-S. Ng, "Performance of asynchronous orthogonal multicarrier CDMA system in frequency selective fading channel," *IEEE Trans. Commun.*, vol. 47, pp. 1084-1091, July 1999.

[37] H. Fazel and S. Kaiser, *Multi-Carrier Spread-Spectrum & Related Topics.* Kulwer 2000.

[38] B. Popovc. “Spreading sequences for multicarrier CDMA systems,” *IEEE Trans. Commun.*, vol. 47, pp. 918-926, June 1999.

[39] N. Yee, J.-P. Linnartz, and G. Fettweis, “Multi-carrier CDMA in indoor wireless radio networks,” *IEICE Trans. Commun.*, vol. E77-B, pp. 900-904, July 1994.

[40] J. Bingham, “Multicarrier modulation for data transmission; An idea whose time has come,” *IEEE Commun. Mag.*, vol. 28, pp. 982-989, May 1990.

[41] V. Tarokh and H. Jafarkhani, “On the computation and reduction of the peak-to-average power ratio in multicarrier communications,” *IEEE Trans. Commun.*, vol. 48, pp. 37-44, Jan. 2000.

[42] V. M. DaSilva and E. S. Sousa, “Multicarrier orthogonal CDMA signals for quasisynchronous communication systems,” *IEEE J. Sel. Areas Commun.*, vol. 12, pp. 842-852, June 1994.

[43] B. G. Lee and B.-H. Kim, “Scrambling Techniques for CDMA Communications.” pp. 173-176, Kluwer Academic Publishers, 2001.

[44] M.-O. Pun, M. Morelli, and C.-C. J. Kuo, “Iterative detection and frequency synchronization for OFDMA uplink transmissions,” *IEEE Trans. Wireless Commun.*, vol. 6, pp. 629-639, Feb. 2007.

[45] M. Septh, S. A. Fechtel, G. Fock, and H. Meyr, “Optimum receiver design for wireless broad-band using OFDM - Part I,” *IEEE Trans. Commun.*, vol. 47, pp. 1668-1677, Nov. 1999.

[46] P. Ciblat and V. Vandendrope, “Blind carrier frequency offset estimation for non-circular constellation based transmissions,” *IEEE Trans. Signal Process.*, vol. 51, pp. 1378-1389, May 2003.

[47] S. D. Rore, F. Horlin, and L. Van der Perre, “Impact and compensation of sample clock offset on up-link SC-CDMA,” *in Proc. Global Telecommunications Conf.*, vol. 6, Dec. 2005, pp. 3362-3366.

[48] D. D. Lin, R. A. Pacheco, T. J. Lim, and D. Hatzinakos, “Optimal OFDM channel estimation with carrier frequency offset and phase noise,” *in Proc. Wireless Communications and Networking Conf.*, volume 2, Apr. 2006, pp. 1050-1055.

[49] D. D. Lin and T. J. Lim, “The variational inference approach to joint data detection and phase noise estimation in OFDM,” *IEEE Trans. Signal Process.*, vol. 55, pp. 1862-1874, May 2007.

[50] S. J. Ko, K. H. Lee, and H. J. Choi, “Performance of coherent DS-SS/QPSK for mobile Communications in fast-fading multipath and high-frequency Offset,” *IEEE Trans. Veh. Technol.*, vol. 50, pp. 250-266, Jan. 2001.

[51] T. Pollet, M. Van Bladel, and M. Moeneclaey, “BER sensitivity of OFDM systems to carrier frequency offset and Wiener phase noise,” *IEEE Trans. Commun.*, vol. 43, pp. 191-193, Feb./Mar./Apr. 1995.

[52] L. Rugini and P. Banelli, “BER of OFDM systems impaired by carrier frequency offset in multipath fading channels,” *IEEE Trans. Wireless Commun.*, vol. 4, pp. 2279-2288, Sept. 2005

[53] H.-Q. Lai, W. P. Siriwongpairat, and K. J. R. Liu, “Performance analysis of multiband OFDM UWB systems with imperfect synchronization and intersymbol interference,” *IEEE J. Sel. Topics Signal Process.*, vol. 1, pp. 521-534, Oct. 2007.

[54] C.-H. Yih, “BER analysis of OFDM systems impaired by DC offset and carrier frequency offset in multipath fading channels,” *IEEE Commun. Lett.*, vol. 11, pp. 842-844, Nov. 2007.

[55] Y. Kim, K. Bang, S. Choi, C. You and D. Hong, “Effect of carrier frequency offset on performance of MC-CDMA systems,” *IEEE Electron. Lette.*, vol. 35, pp. 378-379, Mar. 1999.

[56] L. Tomba and W. A. Krzymien, “Sensitivity of the MC-CDMA access scheme to carrier phase noise and frequency offset,” *IEEE Trans. Veh. Technol.*, vol. 48, pp. 1657-1665, Sept. 1999.

[57] D. Kivanc and H. Liu, “Uplink performance of MC-CDMA in the presence of carrier frequency offset,” *in Proc. 50th IEEE Vehicular Technology Conf.*, Sept. 1999 Fall, pp. 2855-2859.

[58] L. Liu, P. Zhang, K. Hamaguchi and H. Wakana, “Impact of frequency offset on the spreading and despreading in broadband MC-CDMA systems,” *in Proc. 60th IEEE Vehicular Technology Conf.*, Sept. 2004 Fall, pp. 699-703.

[59] F.-T. Chien, C.-H. Hwang, and C.-C.J. Kuo, “Performance analysis of multicarrier CDMA systems with frequency offsets and random spreading under optimum combining,” *IEEE Trans. Commun.*, vol. 54, pp. 737-747, Apr. 2006.

[60] F. Horlin, S. De Rore, E. Lopez-Estraviz, F. Naessens, and L. Van der Perre, "Impact of frequency offsets and IQ imbalance on MC-CDMA reception based on channel tracking," *IEEE J. Sel. Areas Commun.*, vol. 24, pp. 1179-1188, June 2006.

[61] H. Liu and M. D. Zoltowski, "Blind equalization in antenna array CDMA systems," *IEEE Trans. Signal Process.*, vol. 45, pp. 161-172, Jan. 1997.

[62] R. Lupas and S. Verdu, "Linear multiuser detectors for synchronous code-division multiple-access channels", *IEEE Trans. Inf. Theory*, vol. 35, pp. 123-136, Jan. 1989.

[63] A. Tarighat, A. Subramanian, and A. H. Sayed, "An uplink DS-CDMA receiver using a robust post-correlation Kalman structure," *IEEE Trans. Wireless Commun.*, vol. 4, pp. 847-854, May 2005.

[64] D. G. Manolakis, V. K. Ingle, and S. M. Kogon, "Satistical and Adaptive Signal Processing - Spectral Estimation, Signal Modeling, Adaptive Filtering and Array Processing." pp. 378-387, McGraw-Hill, 2000.

[65] C. Carbonelli, A. A. D'Amico, U. Mengali, and M. Morelli, "Channel acquisition and tracking for DS-CDMA uplink transmissions," *IEEE Trans. Commun.*, vol. 53, pp. 1930-1939, Nov. 2005.

[66] L. Sanguinetti and M. Morelli, "Channel acquisition and tracking for MC-CDMA uplink transmissions", *IEEE Trans. Veh. Technol.* vol. 55, pp. 956-967, May 2006.

[67] P. Marques, A. Gameiro and J. Fernandes, "Vectorial channel estimation for uplink MC-CDMA in beyond 3G wireless systems," *in Proc. IEEE Int. Symp. Personal Indoor and Mobile Radio Communications*, Sept. 2003, pp. 984-988.

[68] K. Zheng, G. Zeng and W. Wang, "DFT-based uplink channel estimation in MC-CDMA systems," *in Proc. 8th IEEE Int. Symp. Spread Spectrum Techniques and Applications*, Aug.-Sept. 2004, pp. 570-574.

[69] H. Wang and L. Tongtong, "Channel tracking and signal detection for MC-CDMA in a time-varying environment," *IEEE Trans. Veh. Technol.*, vol. 56, pp. 3613-3620, Nov. 2007.

[70] Y. Li, S. Mclaughlin, X. Wei, and D. G. M. Cruickshank, "Channel estimation and interference cancellation in CP-CDMA systems," *IET Commun.*, vol. 1, pp. 106-112, Feb. 2007.

[71] A. A. D'Amico and M. Morelli, "Frequency estimation and timing acquisition in the uplink of a DS-CDMA system," *IEEE Trans. Commun.*, vol. 52, pp. 1809-1819, Oct. 2004.

[72] Y. Ma and R. Tafazolli, "Estimation of carrier frequency offset for multicarrier CDMA uplink," *IEEE Trans. Signal Process.*, vol. 55, pp. 2617-2627, June 2007.

[73] M. Torlak and G. Xu, "Blind multiuser channel estimation in asynchronous CDMA systems," *IEEE Trans. Signal Process.*, vol. 45, pp. 137-147, Jan. 1997.

[74] U. Tureli, D. Kivanc and H. Liu, "MC-CDMA uplink-blind carrier frequency offset estimation," *in Conf. Rec. 34th Asilomar Conf. Signals, Systems and Computers*, Nov. 2000, pp. 241-245.

[75] W. Kang and B. Champagne, "Subspace-based blind channel estimation: Generalization and performance analysis," *IEEE Trans. Signal Process.*, vol. 53, pp. 1151-1162, Mar. 2005.

[76] C. Li and S. Roy, "Subsapce-based blind channel estimation for OFDM by exploiting virtual carriers," *IEEE Trans. Wireless Commun.*, vol. 2, pp. 141-150, Jan. 2002.

[77] E. Aktas and U. Mitra, "Complexity reduction in subspace-based blind channel identification for DS/CDMA systems," *IEEE Trans. Commun.*, vol. 48, pp. 1392-1404, Aug. 2000.

[78] Z. Xu, "Low-complexity multiuser channel estimation with aperiodic spreading codes," *IEEE Trans. Signal Process.*, vol. 49, pp. 2813-2822, Nov. 2001.

[79] C.-Y. Chi, C.-H. Chen, and C.-Y. Chen, "Blind MAI and ISI suppression for DS/CDMA systems using HOS-based inverse filter criteria," *IEEE Trans. Signal Process.*, vol. 50, pp.1368-1381, June 2002.

[80] S. Lasaulce, P. Loubaton, and E. Moulines,"A semi-blind channel estimation technique based on second-order blind method for CDMA systems," *IEEE Trans. Signal Process.*, vol. 51, pp. 1894-1904, July 2003.

[81] H. Liu and G. Xu, "A subspace method for signature waveform estimation in synchronous CDMA systems," *IEEE Trans. Commun.*, vol. 44, pp. 1346-1354, Oct. 1996.

[82] X. G. Doukopoulos and G. V. Moustakides, "Adaptive power techniques for blind channel estimation in CDMA systems," *IEEE Trans. Signal Process.*, vol. 53, pp. 1110-1120, Mar. 2005.

[83] L. Tong, "Joint blind signal detection and carrier recovery over fading channel," *in Proc. IEEE Int. Conf. Acoustics, Speech, and Signal Processing*, May 1995, pp. 12051208.

[84] K. Li and H. Liu, "Joint channel and carrier offset estimation in CDMA communications," *IEEE Trans. Signal Process.*, vol. 47, pp. 1811-1822, July 1999.

[85] S. Attallah and H. Fu, "Joint channel and carrier offset estimation in a multiuser CDMA system," *IEEE Commun. Lett.*, vol. 6, pp. 428-430, Oct. 2002.

[86] G. H. Golub and C. F. Van Loan, "Matrix Computations." Baltimore, MD: Johns Hopkins Univ. Press, 1996.

[87] H. Liu and U. Tureli, "A high efficiency carrier estimation for OFDM communications," *IEEE Commun. Lett.*, vol.2, pp. 104-106, Apr. 1998.

[88] X. Ma, C. Tepedelenlioglu, G. B. Giannakis and S. Barbarossa, "Non-data-aided carrier offset estimators for OFDM with null subcarriers: Identifiability, algorithms and performance", *IEEE J. Sel. Areas Commun.*, vol. 19, pp. 2504-2515, Dec. 2001.

[89] U. Tureli, D. Kivanc and H. Liu, "Experimental and analytical studies on high-resolution OFDM carrier frequency offset estimator," *IEEE Trans. Veh. Technol.*, vol. 50, pp. 629-643, Mar. 2001.

[90] T. Roman, S. Visuri, and V. Koivunen, "Blind Frequency synchronization in OFDM via diagonality criterion," *IEEE Trans. Signal Process.*, vol. 54, pp. 3125-3135, Aug. 2006.

[91] Y. Yao and G. B. Giannakis,"Blind carrier frequency offset estimation in SISO, MIMO, and multiuser OFDM systems," *IEEE Trans. Commun.*, vol. 53, pp. 173-183, Jan. 2005.

[92] J. K. Tugnait, "Identification and deconvolution of multichannel linear non-Gaussian processes using higher-order statistics and inverse filter criteria," *IEEE Trans. Signal Process.*, vol. 45, pp. 658672, Mar. 1997.

[93] A. Feng, Q. Yin, J. Zhang and K. Deng, "Blind channel estimation in synchronous MC-CDMA system with consideration of carrier offset compensation", *in Proc. 55th IEEE Vehicular Technology Conf.*, May 2002 Spring, pp. 660-664.

[94] Y. Zhang, R. Hoshyar and R. Tafazolli, "Channel estimation for MC-CDMA with compensation of synchronization errors", *in Proc. 60th IEEE Vehicular Technology Conf.*, Sept. 2004 Fall, pp. 808-812.

[95] M. Guainazzo, M. Gandetto, C. Sacchi and C.S. Regazzoni, "Maximum likelihood estimation of carrier offset in a variable bit rate orthogonal multicarrier CDMA," *in Proc. 3rd Int. Symp. Image and Signal Processing and Analysis*, Sept. 2003, pp. 1181-1185.

[96] M. K. Tsatsanis, "Inverse filtering criteria for CDMA system," *IEEE Trans. Signal Process.*, vol. 45, pp. 102-112, Jan. 1997.

[97] K. Abed-Meraim, P. Loubaton and E. Moulines, "A subspace algorithm for certain blind identification problems," *IEEE Trans Inf. Theory*, vol. 43, pp. 499-511, Mar. 1997.

[98] P. Loubaton and E. Moulines, "On blind multiuser forward link channel estimation by the subspace method: Identifiability results," *IEEE Trans. Signal Process.*, vol. 48, pp. 2366-2376, Aug. 2000.

[99] S. H. Friedberg, A. J. Insel and L. E. Spence, "Linear Algebra." Prenctice-Hall, 1989.

[100] E. Kreyszig, "Advanced Engineering Mathematics." John Wiley & Sons, 1999.

[101] H. Start and Y. Yang, "Vector Space Projections: A Numerical Approach to Signal and Image Processing, Neural Nets and Optics." John Wiley & Sons, 1998.

[102] A. R. Gourlay & G. A. Watson, "Computational Methods for Matrix Eigenproblems."John Wiley & sons, 1973.

[103] A. Papoulis and S. U. Pillai, "Probability, Random Variables and Stochastic Processes." pp. 276, 532-537, Tata McGraw-Hill, 2002.

[104] V. C. Klema and A. J. Laub, "The singular value decomposition: Its computation and some applications," *IEEE Trans. Autom. control*, vol. 25, pp. 164-176, Apr. 1980.

[105] F. Li and R. J. Vaccaro, "Unified analysis for DOA estimation algorithms in array signal processing," *Signal Processing*, vol. 25, pp. 147-169, Nov. 1991.

[106] G. W. Stewart, "Error and perturbation bounds for subspaces associated with certain eigenvalue problems," *SIAM Rev.*, vol. 15, pp. 727-764, 1973.

[107] H. Fu and S. Attallah, "Fast blind channel and carrier offset estimation in multiuser CDMA," *IEE Proc. Commun.*, vol. 151, No.1, pp. 32-38, Feb. 2004.

[108] S. Attallah, L. B. Thiagarajan, H. Fu and Y.-C. Liang, "Joint channel and carrier offset estimation for synchronous uplink CDMA systems," *IEEE Trans. Veh. Technol.*, vol. 56, pp. 2769-2774, Sept. 2007.

[109] Jack L. Goldberg, "Matrix Theory with Applications." McGraw-Hill Inc., 1992.

[110] S. Attallah, "The generalized Rayleigh's quotient adaptive noise subspace algorithm: A householder transformation-based implementation," *IEEE Trans. Circuits Syst. II, Exp. Briefs*, vol. 53, pp. 3-7, Jan. 2006.

[111] K. Abed-Meraim, A. Chkeif, and Y. Hua, "Fast orthonormal PAST algorithm," *IEEE Signal Process. Lett.*, vol. 7, pp. 60-62, Mar. 2000.

[112] B. Yang, "Projection approximation subspace tracking," *IEEE Trans. Signal Proc.*, vol. 43, pp. 95-107, Jan. 1995.

[113] S. C. Douglas, S.-Y. Kung and S.-I. Amari, "A selfstabilized minor subspace rule," *IEEE Signal Process. Lett.*, vol. 5, pp. 328-330, Dec. 1998.

[114] G. Mathew, V. U. Reddy, and S. Dasgupta, "Adaptive estimation of eigensubspace," *IEEE Trans. Signal Process.*, vol. 43, pp. 401-411, Feb. 1995.

[115] A. V. Oppenheim, R. W. Schafer and J. R. Buck, *Discrete-Time Signal Processing*, 2^{nd} edition, Pearson Education, 2004.

[116] J. R. Magnus and H. Neudecker, *Matrix Differential Calculus with Applications in Statistics and Econometrics.*, John Wiley & Sons, 1999.

[117] P. Stefanidis, A. P. Paplinski and M. J. Gibbard, *Numerical Operations with Polynomial Matrices: Application to multi-variable dynamic compensator design*, Springer-Verlag, 1992.

[118] H. Neudecker, "A matrix trace inequality," *J. Math. Anal. Appl.*, vol. 166, pp. 302-303, 1992.

[119] V. Solo and X. Kong, *Adaptive Signal Processing Algorithms Stability and Performance.*, Prentice Hall, 1994.

[120] L. B. Thiagarajan, Y.-C. Liang and S. Attallah, "Reconfigurable transceivers for wireless broadband access schemes," *IEEE Wireless Commun. Magazine*, vol. 14, no. 3, June 2007.

[121] D. Pareek, *Wimax - Taking wireless to the MAX.* Auerbach Pulications, 2006.

[122] Y. R. Zheng and C. Xiao, "Improved models for the generation of multiple uncorrelated Rayleigh fading waveforms," *IEEE Commun. Lett.*, vol. 6, pp. 256-258, June 2002.

[123] T. Zemen, C. F. Mecklenbräuker, J. Wehinger and R. R. Müller, "Iterative joint time-variant channel estimation and multi-user detection for MC-CDMA," *IEEE Trans. Wireless Commun.*, vol. 5, pp. 1469-1478, June 2006.

[124] D. Slepian, "Prolate spheroidal wave functions, Fourier analysis and uncertainity – V: The discret case," *Bell Syste. Tech. J.*, vol. 57, no.5, pp. 1371-1430, May-Jun. 1978.

[125] T. Zemen and C. F. Mecklenbräuker, "Time-variant channel estimation using discrete prolate spheroidal sequences," *IEEE Trans. Signal Process.*, vol. 53, pp. 3597-3607, Sept. 2005.

[126] S. Gault, W. Hachem, and P. Ciblat, "Joint sampling clock offset and channel estimation for OFDM signals: Cramer-Rao bound and algorithms," *IEEE Trans. Signal Process.*, vol.54, pp. 1875-1884, May 2006.

[127] P. Stoica and E.G. Larsson, "Comments on "Linearization method for finding Cramer-Rao bounds in signal processing", *IEEE Trans. Signal Process.*, vol. 49, no. 12, pp. 3168-3169, Dec. 2001.

[128] E. de Carvalho, J. Cioffi and D. Slock, "Cramer-Rao bounds for blind multichannel estimation," *in Proc. IEEE Global Telecommunications Conf.*, Dec. 2000, pp. 1036-1040.

[129] M. Barkat, "Signal Detection and Estimation." pp. 533-572, Artech House, 2005.

[130] Y.-C. Liang, S. Sun, and C. K. Ho, "Block-iterative generalized decision feedback equalizers for large MIMO systems: Algorithm design and asymptotic performance analysis," *IEEE Trans. Signal Process.*, vol. 54, no. 6, pp. 2035-2048, June 2006.

[131] X. Wang and H. V. Poor, "Blind multiuser detection: A subspace approach," *IEEE Trans. Inf. Theory*, vol. 44, pp. 667-690, Mar. 1998.

[132] H. Li and H. V. Poor, "Reduced complexity joint iterative equalization and multiuser detection in dispersive DS-CDMA channels," *IEEE Trans. Wireless Commum.*, vol. 4, pp. 1234-1243, May 2005.

[133] X. Wang and H. V. Poor, "Iterative (turbo) soft interference cancellation and decoding for coded CDMA," *IEEE Trans. Commun.*, vol. 47, no. 7, pp. 1046-1061, July 1999.

[134] A. M. Chan and G.W.Wornell, "A class of block-iterative equalizers for intersymbol interference channels: Fixed channel results," *IEEE Trans. Commun.*, vol. 49, pp. 1966-1976, Nov. 2001.

[135] N. Benvenuto and S. Tomasin, "Block iterative DFE for single carrier modulation," *IEEE Electron. Lett.*, vol. 38, pp. 1144-1145, Sept. 2002.

[136] L. W. Couch II, "Digital and Analog Communication Systems." pp. 169-170, Prentice Hall, 2001.